AD NUMBER

AD916171

NEW LIMITATION CHANGE

TO

Approved for public release, distribution unlimited

FROM

Distribution authorized to U.S. Gov't. agencies only; Test and Evaluation; NOV 1973. Other requests shall be referred to Air Force Flight Dynamics Lab., Wright-Patterson AFB, OH 45433.

AUTHORITY

AFFDL ltr, 10 May 1976

AFFDL-TR-73-109

ANALYSIS FOR THE DETERMINATION OF SIGNIFICANT CHARACTERISTICS OF RUNWAY ROUGHNESS

ALAN P. BERENS
RONALD K. NEWMAN
UNIVERSITY OF DAYTON

TECHNICAL REPORT AFFDL-TR-73-109

NOVEMBER 1973

AIR FORCE FLIGHT DYNAMICS LABORATORY
AIR FORCE SYSTEMS COMMAND
WRIGHT-PATTERSON AIR FORCE BASE, OHIO 45433

NOTICE

When Government drawings, specifications, or other data are used for any purpose other than in connection with a definitely related Government procurement operation, the United States Government thereby incurs no responsibility nor any obligation whatsoever; and the fact that the government may have formulated, furnished, or in any way supplied the said drawings, specifications, or other data, is not to be regarded by implication or otherwise as in any manner licensing the holder or any other person or corporation, or conveying any rights or permission to manufacture, use, or sell any patented invention that may in any way be related thereto.

Copies of this report should not be returned unless return is required by security considerations, contractual obligations, or notice on a specific document.

AIR FORCE/56780/14 January 1974 — 100

ANALYSIS FOR THE DETERMINATION OF SIGNIFICANT CHARACTERISTICS OF RUNWAY ROUGHNESS

ALAN P. BERENS
RONALD K. NEWMAN

FOREWORD

This report was prepared by the Aerospace Mechanics Division of the University of Dayton Research Institute, Dayton, Ohio, for the Aerospace Dynamics Branch, Vehicle Dynamics Division, Air Force Flight Dynamics Laboratory, Wright-Patterson Air Force Base, Ohio, under Contract F33615-72-C-1346. This research program was conducted under Project 1370 "Dynamic Problems in Flight Vehicles," Task 137003 "Flight Vehicle Dynamic Load Problems." The project monitors were Mr. Bernard H. Groomes until 1 May 1973 and Mr. Daniel M. Sheets thereafter. This study was performed during the period of June 1972 to October 1973. Dr. Alan P. Berens of the University of Dayton Research Institute was the principal investigator.

The authors gratefully acknowledge the assistance of Messrs Groomes and Sheets of the Air Force Flight Dynamics Laboratory and Messrs Michael Hill and John Brick of the University of Dayton Research Institute.

Manuscript was released by the authors in August 1973.

This Technical Report has been reviewed and is approved.

Walter J. Mykytow

WALTER J. MYKYTOW
Asst. for Research & Technology
Vehicle Dynamics Division

ABSTRACT

To determine and evaluate significant characteristics of runway roughness, 40 runway elevation profiles from 14 runways were analyzed. Grade effects were removed by high-pass filtering at a maximum cutoff wavelength of 500 ft and the resulting profiles were shown to be both nonstationary and nongaussian. Since nonstationarity was caused by the long wavelength undulations, the profiles were again filtered at a maximum cutoff wavelength of 100 ft. These short wavelength profiles are shown to be sufficiently stationary for a compound characterization. The short wavelength components are modeled in the frequency domain while the long wavelength components are modeled by the distribution of relative maxima and minima per 1000 ft and the joint distribution of wavelength and amplitude of the maxima and minima. A method is presented for generating a simulated runway which has the characteristics of the real profiles used in the analysis.

TABLE OF CONTENTS

LIST OF ILLUSTRATIONS

LIST OF ILLUSTRATIONS (continued)

LIST OF ILLUSTRATIONS (continued)

LIST OF ILLUSTRATIONS (continued)

LIST OF ILLUSTRATIONS (continued)

LIST OF ILLUSTRATIONS (continued)

LIST OF ILLUSTRATIONS (concluded)

LIST OF TABLES

LIST OF SYMBOLS

Symbol	Description
d	Distance down runway (ft)
D. F.	Degrees of freedom
f_c	Cutoff frequency in low-pass filter
f_N	Nyquist frequency
f_s	Sampling rate (points/ft)
f(x)	Amplitude as function of increment down runway (in)
$F(\omega)$	Fourier transform of x(d)
FFT	Fast Fourier transform
FREQ	Frequency
h_n	Filter weight
H(f)	Fourier transform of filter weights
N	Number of data values in transform when computing PSD or the number of filter weight values
P { A }	Probability of A
PSD	Power spectral density
RMS	Root mean square
rad	Radian
x_d	Original runway elevations as function of distance
x^*_d	Low-pass filtered data
$\tilde{x}_d$	High-pass filtered data
Δd	Increment between samples (ft)
Δf	Roll-off frequency in low-pass filter
ϵ	Estimate of filter error
λ	Wavelength (ft)
λ_{max}	Cutoff wavelength in high-pass filter

LIST OF SYMBOLS (continued)

Symbol	Description
σ	Standard deviation
$\Phi(\Omega)$	Power spectral density as function of reduced frequency (in^2/rad ft)
$\Phi^*(\Omega)$	Normalized power spectral density as function of reduced frequency
$\phi(\omega)$	Power spectral density as function of frequency (cycles/ft)
ω	Frequency (cycles/ft)
Ω	Reduced frequency (rad/ft)

SECTION 1
INTRODUCTION

Runway roughness has long been recognized as a source of dynamic excitation for an aircraft. Changes in vertical runway profiles have been identified not only as major sources of fatigue damage for some aircraft types, but also as a potential cause of loss of control due to magnification of forces as they are transmitted through the aircraft structure to the cockpit. The effect of a runway-induced excitation obviously depends on the runway profile, the properties of the landing gear, and the dynamic characteristics of the aircraft.

Typically, at some stage in the development of an aircraft, a mathematical model is available to a designer or structural analyst which, when coupled with a given runway profile, is capable of providing a description of a response of interest. Thus, given the model and the runway profile, responses of interest can be predicted. Further, it can be assumed that the model can be transformed so that calculations can be performed in either the frequency or time domains. If these calculations are being performed in the design stages, changes in the landing gear are reflected by changes in the parameters or mathematical terms of the model. The effect of the change for the given runway can then be determined. However, the choice of the runway profile or profiles and the form of its mathematical description that should be used in the exercise of the model are quite difficult. No aircraft type will operate on only one runway and the roughness characteristics between runways exhibit significant variation that is important to aircraft response.

There are three dominant methods for analyzing the effectiveness of a landing gear system to runway excitation and these can be described as the discrete, statistical, and time history approaches. In the simplest of these analyses, the discrete approach, the runway is characterized as consisting

of a series of "1 - cos" bumps and depressions where the amplitudes and wavelengths of the disturbances are specified from an observed joint distribution of bump heights, depression depths and their corresponding wavelengths as determined from existing runway profiles. The aircraft response of interest is calculated for all relevant combinations of amplitude, wavelength and aircraft ground velocity. Since, in this analysis, each combination of amplitude and wavelength is treated separately, the possibility of existing dynamic conditions at the time of entry into the excitation is ignored. Further, the "1 - cos" shape of the bumps and depressions is not considered to be representative of actual runways and there exists considerable subjectivity in the determination of the joint distributions of amplitudes and wavelengths. For these reasons, the results of a discrete analysis are considered only as a preliminary indication of the adequacy of a landing gear system.

The statistical approach is centered on the concept that a runway can be considered as a stationary, gaussian excitation. In this mathematical framework, the characterization of the runways is performed in the frequency domain by modeling the power spectral densities (PSD) of available runway elevation profiles. Knowledge of the transfer function of the random dynamic excitation to a response of interest, coupled with known theory of time history analysis is then used to predict level crossing or peak distributions of the response parameter. This approach provides a more realistic prediction of response than does the discrete approach since the PSD and transfer function account for the continuously changing excitation. However, it has been found that the predicted response from the statistical approach is generally more severe than the actual when a given runway is analyzed. This lack of agreement is due to a violation of the assumptions of stationarity or gaussianness or to the nonlinearity of the system which is also a required assumption in the statistical approach.

The best method of predicting response to runway excitation is the time history approach. In this method a mathematical model relating a response of interest to the changes in elevation profiles is derived and the actual runway profiles are used as the input to the model. The time history of the response is then calculated and the accuracy of this prediction is dependent strictly on the mathematical model of the aircraft. The difficulty with this approach is that an actual runway profile is required as an input. If the response of a particular aircraft to a particular runway is desired, there is, of course, no problem. The elevation profile of the runway provides the input of interest. However, in the design stages of an aircraft, the choice of the runway profile that should be used is not clear since aircraft types respond differently to a specific runway. Currently, this problem is approached by specifying that the runway profile used in analysis must have a power spectral density which exceeds that given in specifications. Most runway profiles can be used in this procedure since by appropriately scaling the elevation measurements of a profile, the PSD can be raised or lowered to the specified limits. It can easily be seen, however, that this procedure can lead to an overdesign. It may well happen that to raise the power spectral density to the acceptable level at a noncritical wavelength, the power at a critical wavelength may be greater than can realistically be expected.

In specifying runway roughness design criteria, the above discussion leads to a dilemna. While runways can be characterized in terms of joint distributions of bump heights, depression depths and corresponding wavelengths and also in terms of power spectral densities, the methods of calculating response using these characterizations are unsatisfactory. On the other hand, the time history approach which provides the best method of predicting response requires a runway profile as input and the choice of the appropriate profile is not clear. This study represents an attempt to resolve the dilemna by achieving the following two objectives:

1) To determine and evaluate quantitative characteristics of runway profile elevations which are pertinent to aircraft ground loads analyses, and

2) To develop a method for synthesizing artificial runways which reflect the quantified characterization of the real runways which were used for analysis.

To achieve these objectives, 40 lines of profile elevations from 14 runways were analyzed. To make the profiles comparable and to remove grade effects of no dynamic interest, initially all lines were digitally, high-pass filtered at a cutoff wavelength of 500 ft. Power spectral densities and amplitude probability densities were obtained for each line. In order to investigate stationarity, power spectral densities were calculated for each third of each runway. Since, for some of the runways, the power spectral densities of the segments were significantly different, further study of the lack of stationarity was investigated by calculating the RMS value for each 512 ft section of each runway. These RMS values also displayed significant variation and it was determined that, generally, the significantly larger values were the result of long wavelength undulations in sections of the runways. It was concluded, therefore, that stationarity could not be assumed for the profiles filtered at 500 ft since they were not self-stationary. Further, the investigation of the amplitude probability densities could not generally be modeled by a gaussian distribution primarily because of an excess of values in the tails of the distribution. This excess of probability in the tails would also be a result of the long wavelength undulations.

The profiles were then high-pass filtered at a cutoff wavelength of 100 ft and it was concluded that for wavelengths less than 100 ft the assumptions of stationarity and gaussianness were far more reasonable. Therefore, a compound characterization was derived in which the wavelengths less than 100 ft were modeled by the PSD's, assuming stationarity and gaussianness, and the wavelengths between 100 ft and 500 ft were

modeled in a discrete fashion by determining the joint distributions of primary peaks, associated wavelength, and location on the runway from the profiles filtered at a cutoff wavelength of 500 ft. This compound characterization was then used to synthesize a simulated runway.

The details and results of these operations are presented in the following. First, the computational and data processing techniques are presented in Section 2. The results of the analysis of the data filtered at 500 ft and at 100 ft are presented in Section 3. And the method of synthesizing the simulated runway and a sample result are presented in Section 4. A brief summary and conclusions are contained in Section 5.

SECTION 2
DATA PROCESSING

The following is a description of the procedures used in the processing and analysis of the runway roughness data. Appendix I gives a more detailed description of the digital filtering techniques. All processing of the data was carried out on the CDC 6600 computer located at Wright-Patterson AFB.

2.1 DESCRIPTION OF RAW DATA

The raw data as received was in the form of runway elevations at intervals of either six inches or two feet. The data for Torrejon is the only data at two-foot intervals as measured by rod and level and punched on cards. All of the other data was measured and recorded at six-inch intervals by an automatic runway profile measuring instrument, profilometer, on magnetic tape and later punched on cards. The rod and level elevations were in feet, which were subsequently converted to inches, and the profilometer elevations in inches. All elevations are relative to some arbitrary starting point.

The description of the lines of survey and the total number of data points for each line is given in Table I.

2.2 FILTERING METHODS

The data from all of the runways contained a linear trend which biases the power spectral density considerably. This linear trend must be removed and digital filtering was considered the most reliable method to accomplish this. The digital filter that was designed, consisted of a two stage Martin-Graham low-pass filter, the results of which were subtracted from the original data so as to provide high-pass filtering of the data. A two stage filter was needed to provide a relatively short roll-off. The

TABLE I

IDENTIFICATION OF DATA ANALYZED

ID	Base	Runway	Line	No. Points
1	Altus	35	75L	26, 930
			CL	26, 910
			75R	25, 190
2	Bakalar	22	50L	10, 000
			CL	10, 000
			50R	9, 600
3	Carswell	17	13L	24, 060
			87L	24, 100
			13R	24, 060
4	Edwards	04	75L	28, 800
			CL	28, 800
			75R	28, 800
5	Ellsworth	30	CL	27, 120
6	Glasgow	10	75L	26, 960
			CL	27, 010
			75R	15, 030
7	Langley	7	50L	20, 040
			CL	20, 050
			50R	19, 010
9	McGuire	12	75L	14, 960
			CL	14, 950
			75R	15, 070
11	Shaw	04	50L	20, 070
			CL	18, 880
			50R	18, 000
12	Travis	21R	75L	22, 080
			CL	22, 040
			75R	22, 040
13	Torrejon	23	12L	26, 790*
			CL	26, 710*
			12R	26, 790*
14	Castle	30	75L	23, 650
			CL	23, 610
			75R	23, 660
15	George	3	50L	18, 260
			CL	18, 270
			50R	18, 000
16	Palmdale	7	50L	24, 030
			CL	24, 030
			50R	24, 030

*After interpolation to 6 inch intervals

filtering was performed with the following equation which is developed in Appendix I.

$$x^*_d = \sum_{n_2=-N_2}^{N_2} h_{n_2} \sum_{n_1=-N_1}^{N_1} h_{n_1} x_{(d+n_1\Delta d_1+n_2\Delta d_2)} \qquad (1)$$

The filter constants used are shown in Table II. The response of the high-pass filter is shown in Figure 1. The 500 ft wavelength cutoff was chosen because it was believed that greater wavelengths were of no interest. The roll-off was accomplished in as short a frequency span as practical. The data for each line of survey was filtered and plotted. Upon scanning these plots, numerous single point spikes were noticed. These were edited from the filtered data on the premise that they could not be real data if the amplitude was greater than 0.4 inches.

After some further analysis it was decided that the filter cutoff frequency would be increased to correspond to a wavelength of 100 ft. Filtering of all lines of survey was then accomplished using Equation (1) and constants in Table II which provide a high-pass filter with the response shown in Figure 2.

2.3 PSD COMPUTATION

The Power Spectral Density (PSD) of each line of survey was computed using the Fast Fourier Transform (FFT) on the filtered data. In order to get more degrees of freedom of the PSD estimates, the PSD values were computed for each 512 ft segment of a line of survey and these estimates averaged to obtain the PSD for the entire line. In order to make the most efficient use of the FFT to compute the PSD coefficients, it is necessary that the data array size be an integer power of 2. The array size chosen was 1024, which explains the previously mentioned 512 ft. The size of this array also sets the frequency resolution of the PSD output data:

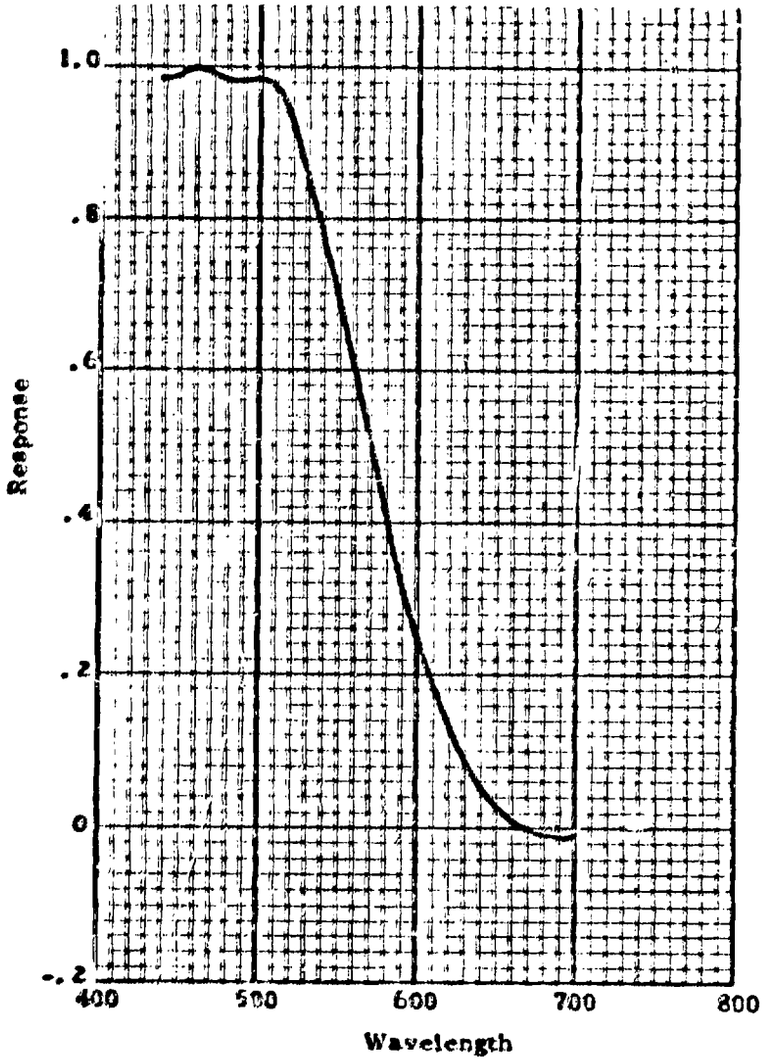

Figure 1 Response of 500 ft Cutoff Filter

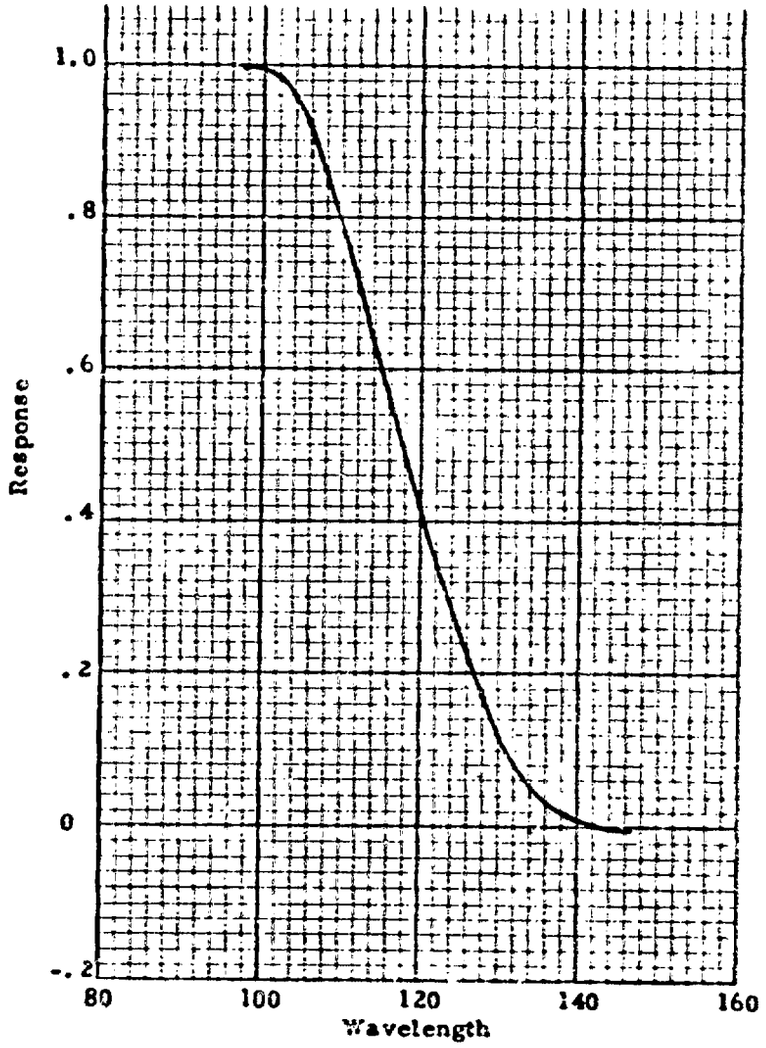

Figure 2 Response of 100 ft Cutoff Filter

TABLE II

FILTER CONSTANTS

	500 ft Cutoff		100 ft Cutoff	
	Preliminary	Final	Preliminary	Final
f_s	2	0.0667	2	0.2
Δd	0.5	15	0.5	5
f_c	0.0015	0.0015	0.007	0.007
Δf	0.030	0.0005	0.033	0.003
N	75	140	80	150

$$\Delta FREQ = \frac{\text{sample rate}}{\text{array size}} = \frac{2}{1024} = 0.001953 \text{ cycles/foot or } 0.01227 \text{ rad/foot}$$

The PSD coefficients were computed using the following equation:

$$\Phi(\Omega)_i = \frac{2|F(\omega)_i|^2 \Delta d}{2\pi(N-1)} \quad (2)$$

The 2 in the numerator of Equation (2) is required to distribute the total power over the positive frequencies only and the 2π in the denominator is to convert the value to reduced frequency. The units of the PSD values are in $in^2/(rad/ft)$. The number of degrees of freedom for each of the PSD's is equal to the number of 512 ft sections in the data times two. This number can vary by two on a given plot as a function of frequency since a PSD was computed for that portion of a line leftover after some integral multiple of 512 ft sections were used. For this last piece of data on each line, only the PSD's for frequencies having at least one full cycle were used in the averaging process. Therefore, a given line can have 2N degrees of freedom

up to some frequency and 2(N+1) degrees of freedom for higher frequency, where N is the number of integral multiples of 512 ft.

By breaking the line into 512 ft sections, the PSD's of various sections of the runway could be computed. Each of the lines was broken up into one-thirds and the PSD's computed for each third to determine if the ends of the runways were rougher than the centers. In order to have an equal number of degrees of freedom for each of the thirds, it was sometimes necessary to include adjacent 512 ft sections in two of the thirds.

To clarify any confusion that might arise on the use of the FFT to compute PSD's, a comparison was made between the PSD's computed by taking the transform of the autocovariance function with the PSD's obtained by use of the FFT. Since there was a program available to compute the PSD using the autocovariance function which also contained prewhitening and smoothing, the FFT method was reprogramed to include prewhitening and smoothing for comparison purposes. The results of this comparison are shown in Appendix II. The number of degrees of freedom associated with each PSD is shown on the plot. Confidence limits for the PSD plots are a function of the number of degrees of freedom on the estimates and can be determined from Table III. Using this table, it can be seen that for 50 degrees of freedom there is 80% confidence that the true value falls within 0.75 times the estimate and 1.26 times the estimate.

2.4 LONG WAVELENGTH DESCRIPTION

The term "long wavelength" is used here to describe all primary peaks and valleys greater than 100 ft wavelength. These peaks and valleys were extracted from the data after it had been filtered at the 500 ft cutoff. The method used selects the maximum excursion between crossings of the zero mean line. Only peaks with an amplitude greater than 0.25 inches were retained. These peaks were assigned a wavelength equal to twice the distance between mean crossings. Peaks were then tabulated by half

TABLE III

CONFIDENCE LIMIT FACTORS FOR SPECTRAL ESTIMATES

Degrees of Freedom	Exceeded by 90% of all values	Exceeded by 50% of all values	Exceeded by 10% of all values
10	0.49	0.93	1.60
20	0.62	0.96	1.42
30	0.69	0.98	1.34
40	0.73	0.98	1.30
50	0.75	0.99	1.26
100	0.82	0.99	1.18

wavelength and amplitude into two tables, one containing positive peaks and the other containing negative peaks. In the process of selecting the peaks, all wavelengths were retained.

It is thought that using primary peaks to define the long wavelengths in conjunction with the PSD representation of the shorter wavelengths is the most logical method of representing the runway profiles. It is believed that most of the data greater than 100 ft wavelength is in the form of primary peaks. An earlier attempt at selecting cyclic information from the data produced relatively large wavelengths that were known to have been removed from the data.

2.5 OTHER DESCRIPTORS

Amplitude probability densities were computed for all lines of survey. These were computed in the same program that computed PSD.

Root mean square (RMS) values were computed for each line of survey and for each 512 ft section of each line. The RMS values for each entire line of survey were computed in two ways. First, the RMS value

was computed on a point for point basis from the filtered data and was also computed as the square root of the area under the PSD curve. These agree to two significant figures in all cases. The RMS values for the 512 ft sections and for the profiles broken into thirds were computed from the square root of the area under the PSD curves only.

SECTION 3
DATA ANALYSIS

The basic rationale in the characterization of the available runway elevation profiles is that these data are a representative sample of all concrete runways which will be routinely traversed by Air Force aircraft during their lifetime. Any one runway, of course, provides a reasonable fixed dynamic excitation to an aircraft in that its elevation profile would be expected to change only slowly with time. But since at the design stages of an aircraft, it is not known which of the multitude of possible ground surfaces the aircraft will traverse, a statistical characterization of runway profiles becomes necessary. Thus, although all of the available elevation profiles have been resurfaced since the data were collected and although multiple lines were obtained from the same runways, it is assumed in the analysis that each line of data is representative of the population of possible inputs to an aircraft during takeoff and landing.

The original elevation measurements contain the long term grades exhibited by the runways (c.f. Reference 1). Assuming that any grade which has a wavelength greater than 500 ft would have no dynamic input to a modern aircraft, the long term grades for all lines of data were removed by a high-pass digital filter which essentially passed all wavelengths (λ) less than 500 ft and removed all wavelengths greater than 666 ft. Between 500 ft and 666 ft, the amplitudes were attenuated as described in Paragraph 2.2. The filtered profiles provided the basic data set which were then analyzed with particular emphasis on the statistical assumptions required for the power spectral density characterization. The results of this analysis are presented in Paragraph 3.1. Since it was found that, in general, the profiles filtered at $\lambda_{max} = 500$ ft are not stationary or gaussian, the profiles were again filtered with $\lambda_{max} = 100$ ft. The analysis of the profiles with the lower cutoff wavelength is presented in Paragraph 3.2

and the discrete characterization of the wavelengths between 100 and 500 ft is presented in Paragraph 3.3.

3.1 MAXIMUM WAVELENGTH OF 500 FEET

In determining the significant characteristics of runway roughness it is apparent that the most desirable characterization is that which requires the fewest parameters while retaining sufficient information for accurate ground loads analysis. Since from the response viewpoint the important roughness characteristics are the magnitude and corresponding wavelength of the surface undulations, the power spectral density characterization of the runways appears to provide a workable model. The rationale of this model is that each individual runway is a representation of a stationary, gaussian input and the family of power spectral densities can be modeled as a function of the RMS values of the elevation profiles and, perhaps, two or three other parameters. Past studies have indicated a similarity in shape of the power spectral densities from runway to runway, making such a model at least plausible. However, when the statistical response predicted by the power spectral density of a runway is compared to the response predicted by a time history analysis, the power spectral density generally overpredicts the magnitude of loads. Therefore, in the initial stages of this study considerable emphasis was placed on the power spectral density characterization of runway roughness with particular attention on the assumptions required by this approach.

Removing the grades present in the raw data by digitally filtering at the longest wavelength of interest (500 ft) results in an elevation profile of essentially zero mean. This permits comparison of amplitude probability densities across runways and allows a preliminary investigation of stationarity by determining if the RMS values of sections of one runway can be considered as constant. The following paragraphs are devoted to an analysis of the amplitude probability density function, the power spectral

densities of the profiles, and the study of stationarity for the profiles filtered at 500 ft.

3.1.1 Amplitude Probability Densities

An important element in the characterization of any time series is the distribution of the amplitude values about their mean value. In considering a runway profile to be a representative sample of random time series, the assumption of ergodicity is required. This assumption permits the estimation of statistical properties from a single time history as opposed to obtaining the estimates from an ensemble of time histories. The amplitude probability density can be obtained quite simply for any profile by counting the number of data points in defined ranges of deviation from the mean. The distribution thus obtained describes the amplitudes without regard to wavelength and can also be used to obtain the RMS value and other moments of the time history. Further, most of the available mathematics for the application of time theory methods to practical problems depends on the assumption that the amplitude probability density is gaussian.

In considering the amplitude probability densities of runway profiles it is easily seen that the definition of the mean value is critically important. For example, if grades present in the original profiles were not removed, the amplitude probability densities for some of the profiles would appear as a uniform distribution. Runway 35 at Altus AFB has an approximately linear grade of 350 inches over the length of the runway (c.f. Reference 1). The relatively smaller amplitudes which are important to aircraft would be completely lost if this grade (or nonrandom component) were not removed. Thus, if x_d represents the original profile, x_d^* represents the nonrandom or nonrelevant portion of the profile, the relevant portion is defined by

$$\tilde{x}_d = x_d - x_d^* \tag{3}$$

That is, x_d^* is the mean value about which the amplitude deviations are considered as important to roughness characterizations. As noted previously, this paragraph is devoted to the analysis of amplitudes about a mean defined as a result of a low-pass filtering operation in which all wavelengths less than 500 ft were removed.

Of prime concern in the investigation of these amplitudes is the applicability of one family of distributions (e.g., gaussian). That is, can one family be used to model the amplitude probability densities of all the profiles with the differences in the profiles being reflected by the values of the parameters of the family. Particular attention was given to the gaussian distribution because of the wealth of available theory for this distribution and because of the simplicity of synthesizing a time history with any given power spectral density when the amplitude probability densities are gaussian.

The amplitude probability densities for all lines of data were converted to cumulative distributions and plotted on normal probability paper. On this particular type of paper an exact gaussian distribution is represented by a straight line with the slope of the line being a function of the standard deviation and the abscissa of the 50th percentile being the mean. In general, the mid ranges of the distributions (between the 5th and 95th percentiles) were linear but deviations in tails were usually present. To provide an indication of the types of distributions observed, Figures 3, 4 and 5 present the cumulative distributions on normal probability paper for six of the 40 lines of data. The solid lines on those plots are those derived from the calculated means and standard deviations of the amplitudes as opposed to the best straight edge fit of data points.

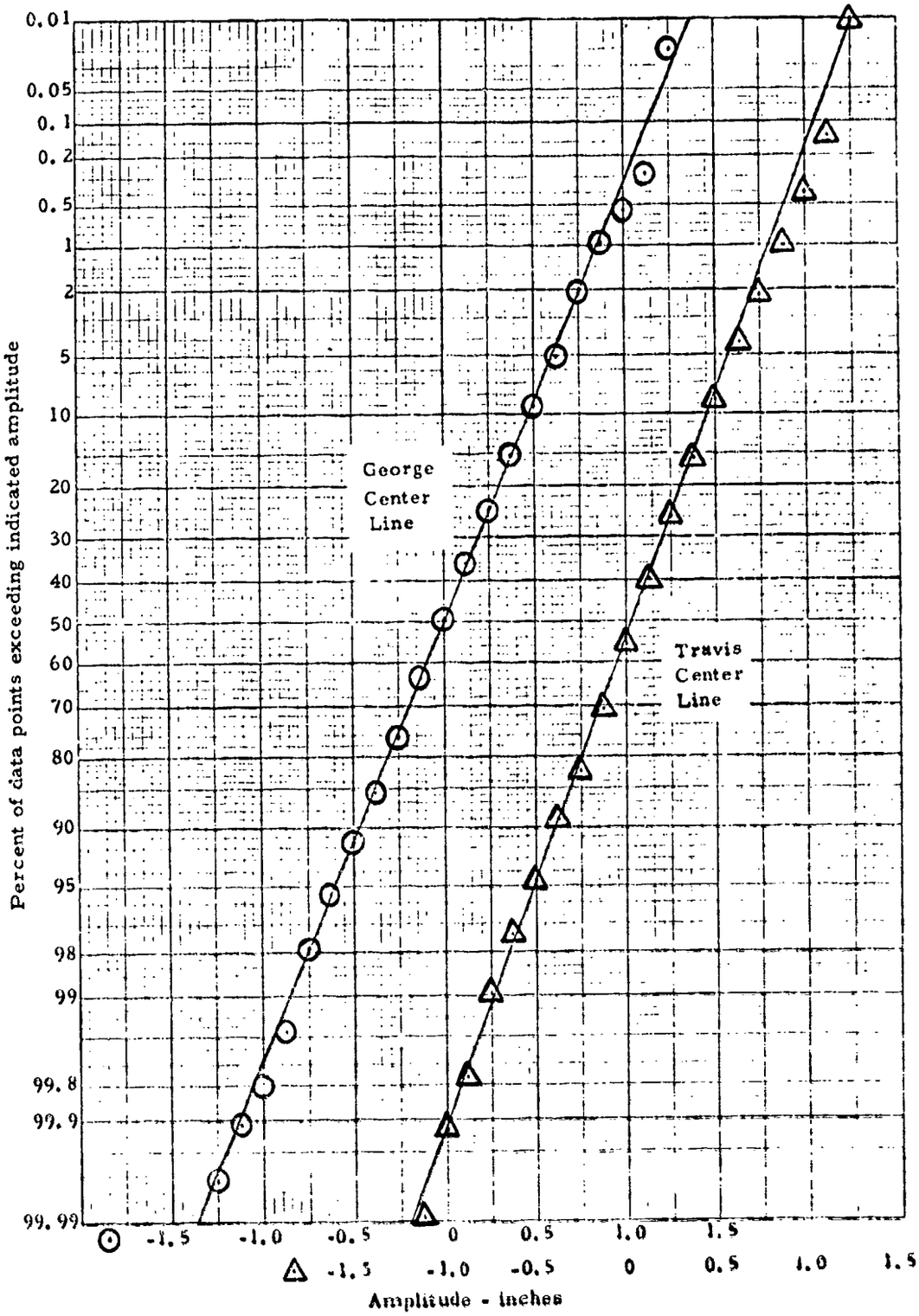

Figure 3 Cumulative Distributions of Amplitudes Filtered at 500 ft for Travis, Centerline, and George, Centerline

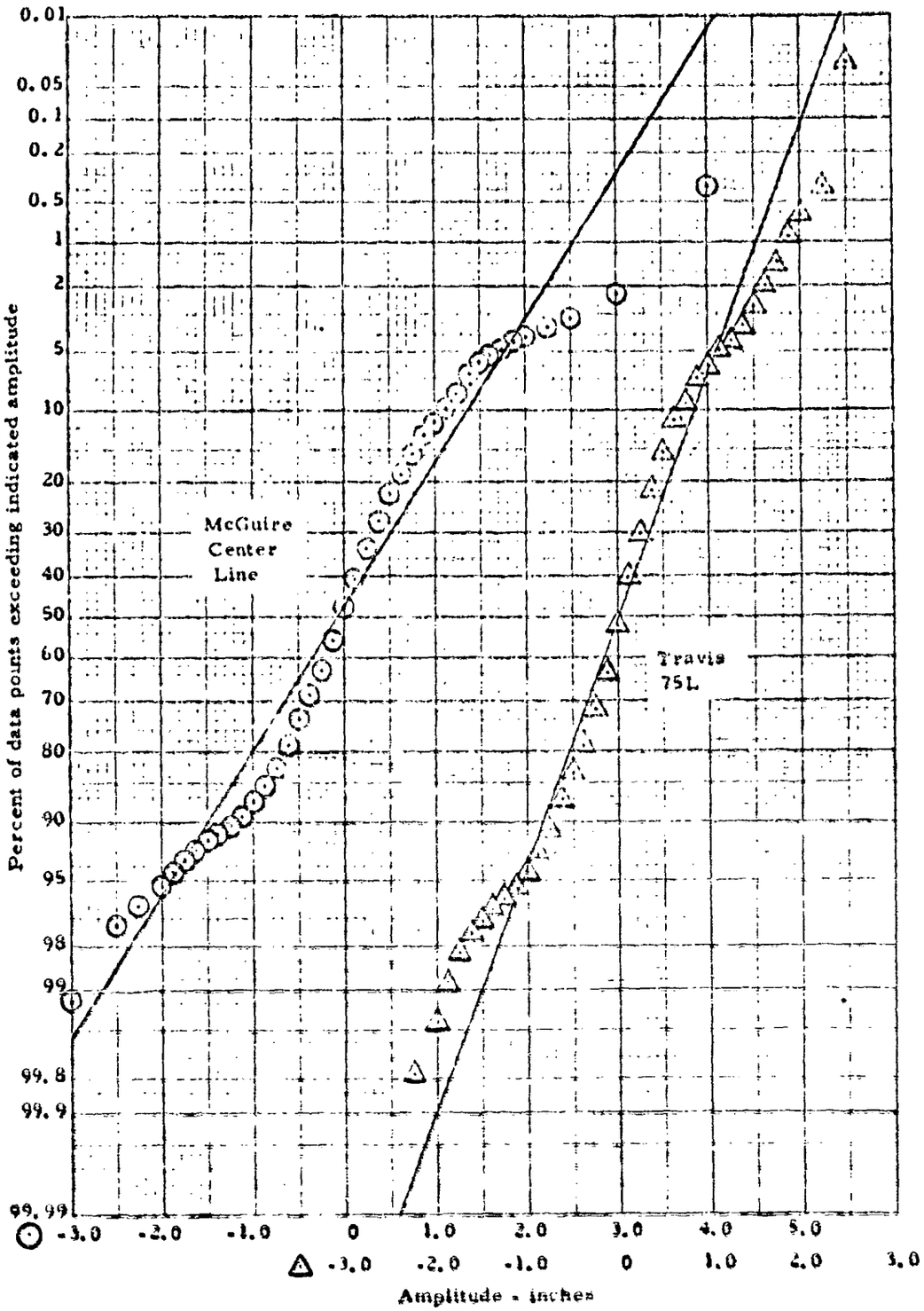

Figure 4 Cumulative Distributions of Amplitudes Filtered at 500 ft for McGuire, Centerline, and Travis, 75L

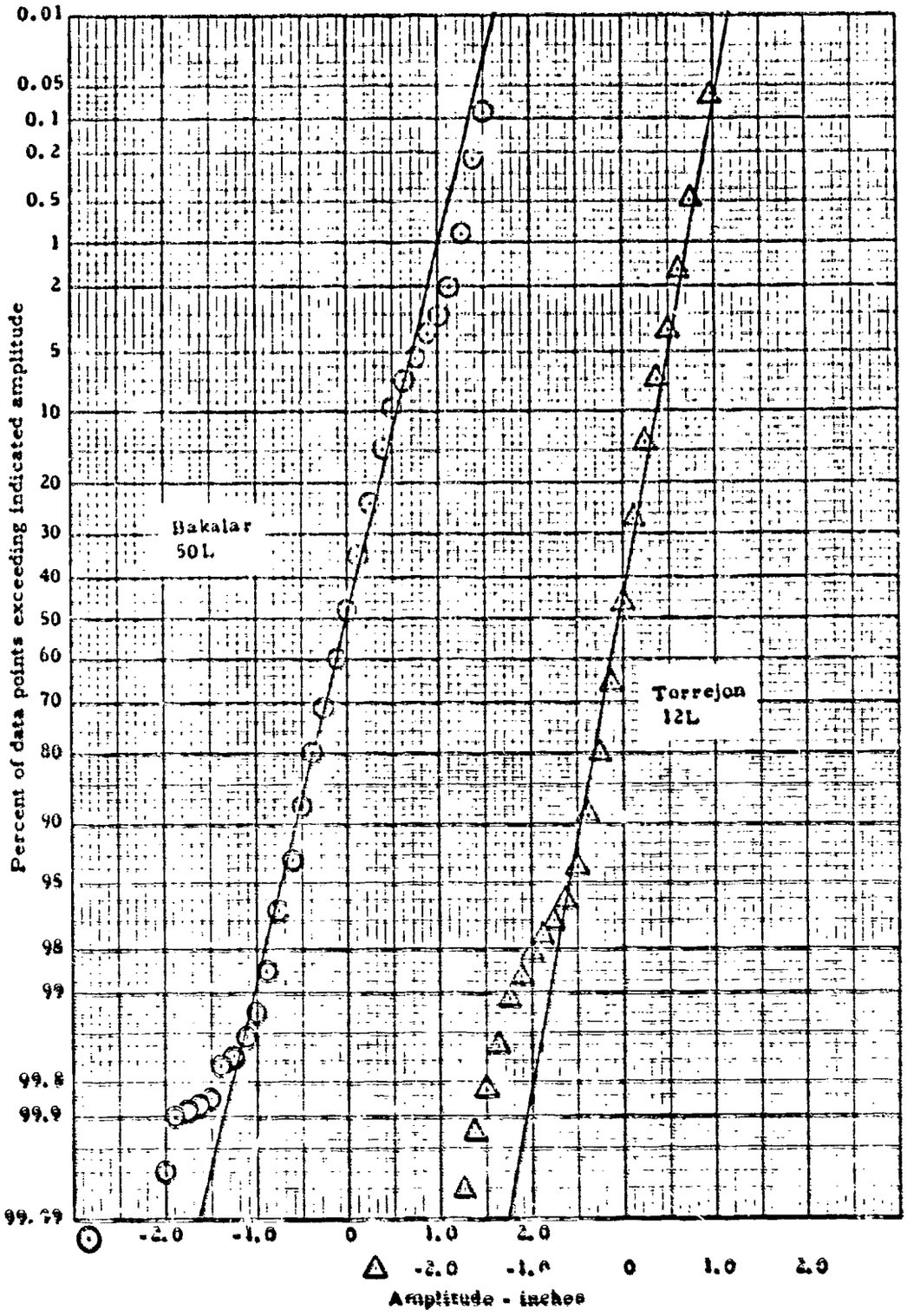

Figure 5 Cumulative Distributions of Amplitudes Filtered at 500 ft for Bakalar, 50L, and Torrejon, 12L

The distributions of Figure 3 indicate that the gaussian distribution provides an excellent model for the amplitude probability densities of these two lines of data. It should be noted there is no statistical test of the goodness of fit of these distributions since the amplitudes are not statistically independent. However, in view of the large number of data points involved, close agreement would be required for an acceptable fit. This degree of agreement between the sample distributions and the gaussian model, however, was uncommon among the 40 lines of data. Figure 4 displays the cumulative distributions of two lines for which the gaussian model provides an inadequate fit of the amplitude probability densities. Note in this figure that the gaussian distribution displays a marked disagreement at the mid values as well as in the tails. It may be of interest to note that one of the lines from Travis closely follows a gaussian distribution while another line from the same runway is not gaussian. The lines displayed in Figure 5 are considered representative of the majority of the amplitude distributions. They display reasonable agreement in the mid ranges and disagreement in the tails. The distribution for the runway from Bakalar is slightly skewed to the right while the distribution for the runway from Torrejon is slightly skewed to the left.

These figures display clearly that no single family of distributions would provide a good model for all of the available lines of data. They are both positively and negatively skewed indicating a change in the shape parameter of a distribution and although the gaussian model provides a good fit to a few of the lines, it does not provide a good fit for others. Therefore, at least two models would be required to describe all of the lines satisfactorily and the complexity introduced by multiple models is sufficiently great that fitting each line is unwarranted at present. If these amplitude probability densities must be modeled, the gaussian distribution would provide as good a fit as any other distributional model and, considering

the available theory for time history analysis for the gaussian model, would be recommended.

One other point regarding the amplitude probability densities should be noted at this time. The elevation profiles of the lines which are not gaussian each contain several cycles of high amplitude, long wavelength undulations that are not typical of the other sections of the runways. Conversely, the elevation profiles of the lines which have gaussian amplitude probability densities do not contain such cycles. This observation is taken as an indication that high amplitude, long wavelength cycles which are not consistently present in a runway profile tends to cause nongaussianness in the amplitude probability density. This contention is further supported by the realization that if, say, 20 percent of a runway profile consisted of high amplitude, long wavelength cycles while the remaining 80 percent consisted of a homogeneous mixture of lower amplitudes and wavelengths, the amplitude probability density would be distorted by the high values. Further, the RMS value for the entire runway would be representative of neither type of amplitudes. Therefore, the somewhat typical pattern observed in the amplitude distributions can be explained by the presence of high amplitude, long wavelength undulations of the profiles. In Paragraph 3.2.1, the amplitude probability densities of profiles filtered at a cutoff wavelength of 100 ft are discussed and it is shown that the gaussian distribution provides an acceptable model for these densities.

Since the RMS values for the elevation profiles provide a gross measure of the runway roughness, these values are presented in Table IV for each of the 40 lines of data. The histogram of the RMS values is presented in Figure 6 to display the distributional properties of this parameter. For this distribution the moment values are given by

mean	= 0.364
standard deviation	= 0.176
skewness	= 2.306
kurtosis	= 3.991

A Kolmogroff-Smirnov goodness of fit test rejects the hypothesis that the distribution is gaussian at a 99 percent level of confidence. Therefore, in view of this rejection and the large degree of skewness, the distribution of RMS values of elevation profiles filtered at 500 ft should not be considered as gaussian.

3.1.2 Power Spectral Densities

The power spectral density is a functional characterization of a time history which displays the contribution of each wavelength (or frequency) to the total RMS of the time history. Since the PSD not only accounts for changes in amplitude of a runway profile but also accounts for the wavelengths associated with the amplitude changes, such a characterization is important when a runway is considered as a dynamic excitation for an aircraft. For this reason the power spectral densities of all of the lines of data were obtained and these are presented in Appendix III.

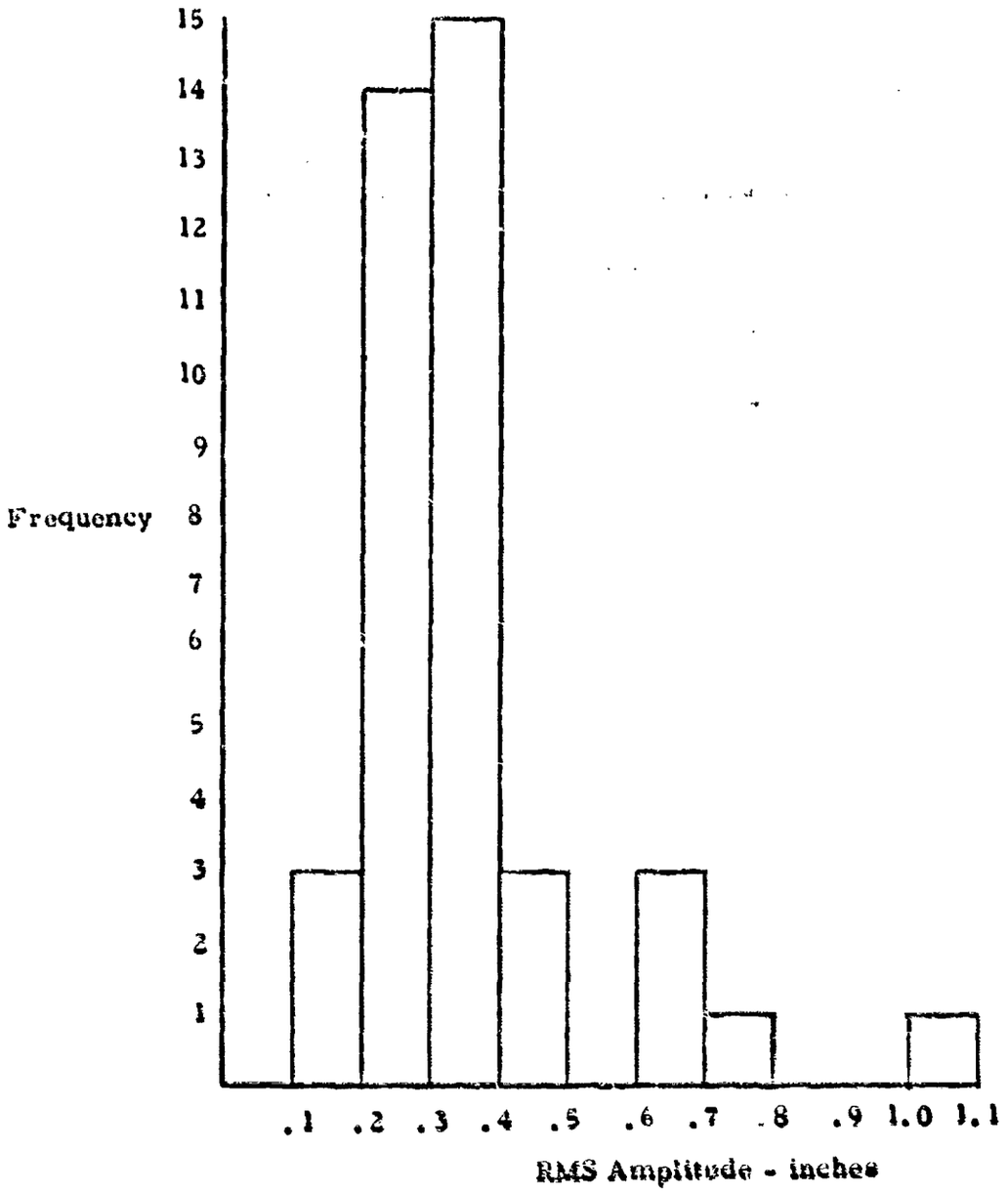

Figure 6 Histogram of RMS Values With Profile Filtered at 500 ft

TABLE IV

RMS VALUES FOR DATA FILTERED AT 500 FT

Base	Location							
	87L	75L	50L	13L or 12L	CL	13R or 12R	50R	75R
Altus		0.362			0.182			0.325
Bakalar			0.441		0.264		0.363	
Carswell	0.295			0.280		0.307		
Edwards		0.245			0.209			0.206
Ellsworth					0.274			
Glasgow		0.329			0.267			0.356
Langley			0.368		0.298		0.337	
McGuire		0.787			1.096			0.674
Shaw			0.252		0.183		0.188	
Travis		0.600			0.367			0.655
Torrejon				0.325	0.364	0.317		
Castle		0.469			0.262			0.468
George			0.311		0.337		0.336	
Palmdale			0.293		0.285		0.277	

Several comments are in order regarding these figures. Power spectral densities had been calculated and reported previously for these data (c. f. Reference 1). In these previous computations, the effect of grades in the profiles were removed by subtracting a linear mean as defined by a straight line between the first and the last points of the profile and the Fourier transform of the autocovariance function method was used to calculate the PSD. Since such a procedure could lead to a distortion in the long wavelength region, all PSD's were recalculated for the profiles digitally high-pass filtered at $\lambda = 500$ and also using the fast Fourier transform method of computation as described in Paragraph 2.3. In general, the PSD's of this program are in agreement with those formerly calculated except for the expected differences at the longest wavelengths. The differences for wavelengths less than 200 ft are considered negligible in view of the problem of finding a general model for all profiles at all wavelengths.

The PSD's for Torrejon are distorted for the small wavelengths. This is due to the fact that the profiles for this runway were taken by rod and transit at two-foot intervals rather than the six-inch intervals common to all of the other profiles. In order to use the same program to process all lines of data, intermediate points were calculated by linear interpolation. The resulting PSD is, of course, distorted for wavelengths less than four feet with possible distortion due to folding at higher wavelengths. It should also be noted that the RMS values listed on the figures of Appendix III are those obtained as the area under the power spectral density as opposed to those from the time histories that were discussed in the previous paragraph. For all practical purposes, the two sets of RMS values are in agreement.

The PSD's of the profiles display a reasonable commonality in shape. In the mid ranges of wavelengths, they are approximately linear (on a log-log scale) and they all flatten at the lowest wavelengths. The

behavior at the longest wavelengths is, however, erratic. Many of the profiles display relative maxima in the mid ranges and most have spikes at wavelengths less than five feet.

The flattening of the PSD's has generally been ignored in modeling runway profiles. It has been conjectured that this flattening is a result of aliasing from wavelengths less than one foot. To prove this hypothesis, a higher sampling rate than two measurements per foot would be required and such data are not available. Current specifications use a linear extrapolation from longer wavelengths to describe this region.

To investigate the gross commonality in shape of the spectral densities, the PSD values at 18 approximately equally spaced reduced frequencies were normalized by the respective mean square amplitude value for each of the 40 profiles. This approach assumes that the PSD is of the form

$$\Phi(\Omega) = \sigma^2 \Phi^*(\Omega) \tag{4}$$

where $\Phi^*(\Omega)$ is independent of σ^2 and is indicative of the common shape of all spectral densities. The resulting 18 normalized values for each of the 40 lines of data were analyzed by determining the average, 25th, 75th, minimum, and maximum values at each of the 18 reduced frequencies. These values are summarized in Figure 7. For reduced wavelengths less than 0.1 rad/ft, 50 percent of the normalized spectra are within a factor of 2. When engineering judgment was used to fit a straight line (on log-log paper) to the average normalized spectra, the equation of the line was given by

$$\Phi^*(\Omega) = 0.0125\ \Omega^{-2.00} \tag{5}$$

The scatter of the normalized spectral values is caused by the inability of Equation (4) to model the spectral densities and at least part of this inadequacy is the variation in the slopes of the spectral

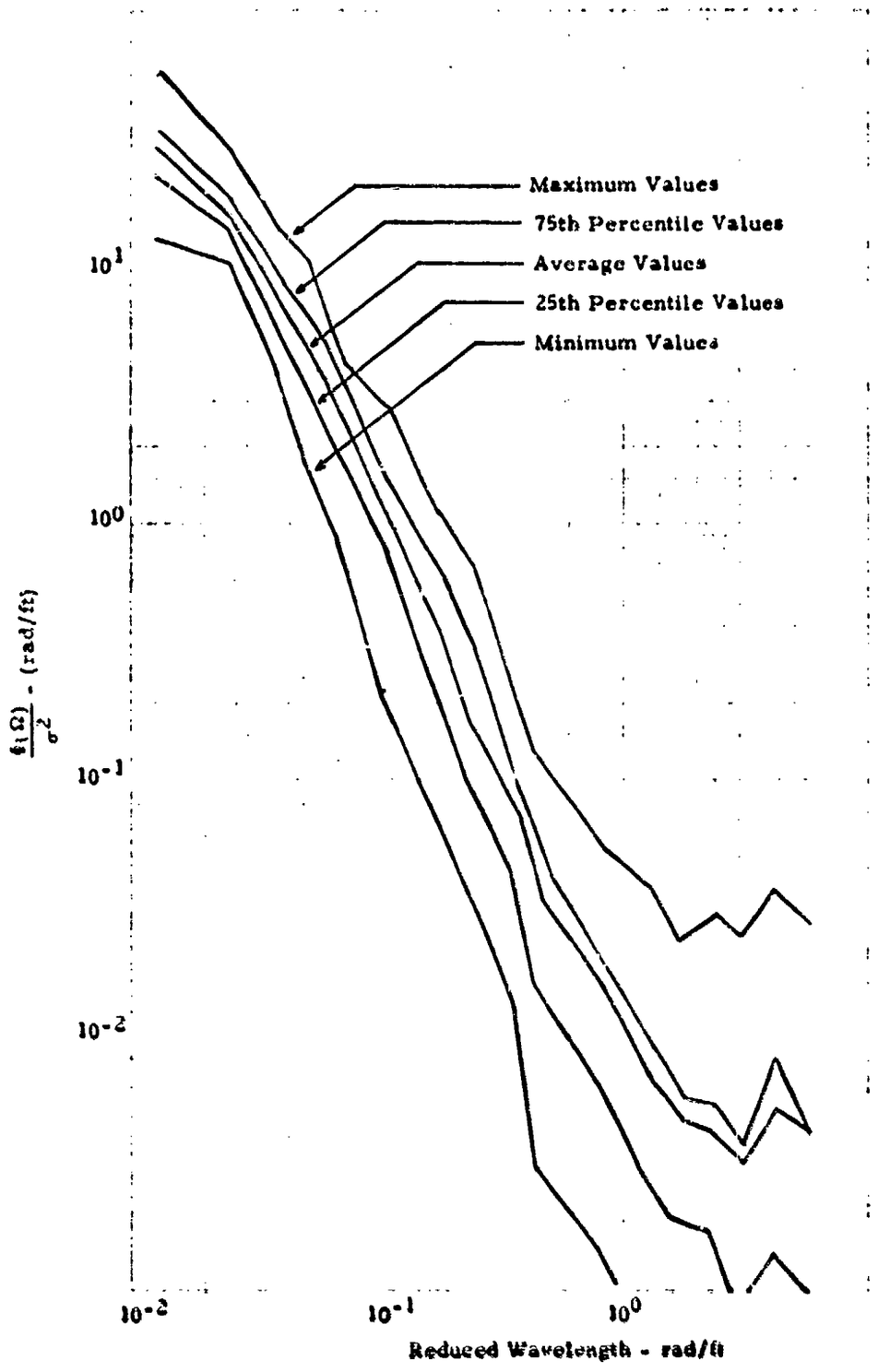

Figure 7 Summary Plot of Normalized Spectral Values

densities between profiles. To further investigate the slope variation, a straight line was fitted to the mid ranges of each PSD and the slope was determined for each of the fitted lines. Due to the engineering judgment involved, such slopes should be considered accurate to within ±10 percent. The histogram of the slope values thus obtained are presented in Figure 8. The mean and standard deviation of these values are 2.13 and 0.27, respectively. Thus, although the slopes do tend to cluster about a value of 2, there is significant variation in this parameter between runways. It is interesting to note the agreement between the average slopes of 2.13 and the slope calculated from the mean of the standardized values of 2.00 (c.f. Equation (5)).

The erratic behavior of the spectral densities in the long wavelength region can be attributed to the inconsistencies of the presence of long wavelength undulations present in some of the runway profiles. These will be discussed further in Paragraph 3.1.3.

To investigate the relative maxima apparent in the PSD's, each peak that was outside the 80 percent confidence limits of adjacent points was identified for all profiles. It must be admitted there is a degree of subjectivity involved in identifying peaks in this fashion but the process tends to miss peaks rather than include those which are insignificant. The peaks identified occurred at many distinct wavelengths up to 100 ft but there were clusters of peaks in certain wavelength ranges. These are summarized in Table V. According to Reference 1, the servo system characteristics of the profile instrumentation system coupled with a constant surveying speed produces spurious spectral peaks in the two to three foot wavelength region. It is speculated that the common peaks apparent at multiples of 2 and 2.5 ft wavelengths are due to higher harmonics of these spurious peaks. The common appearance of peaks at a wavelength of 25.6 ft is probably due to the tar strips or spalling between

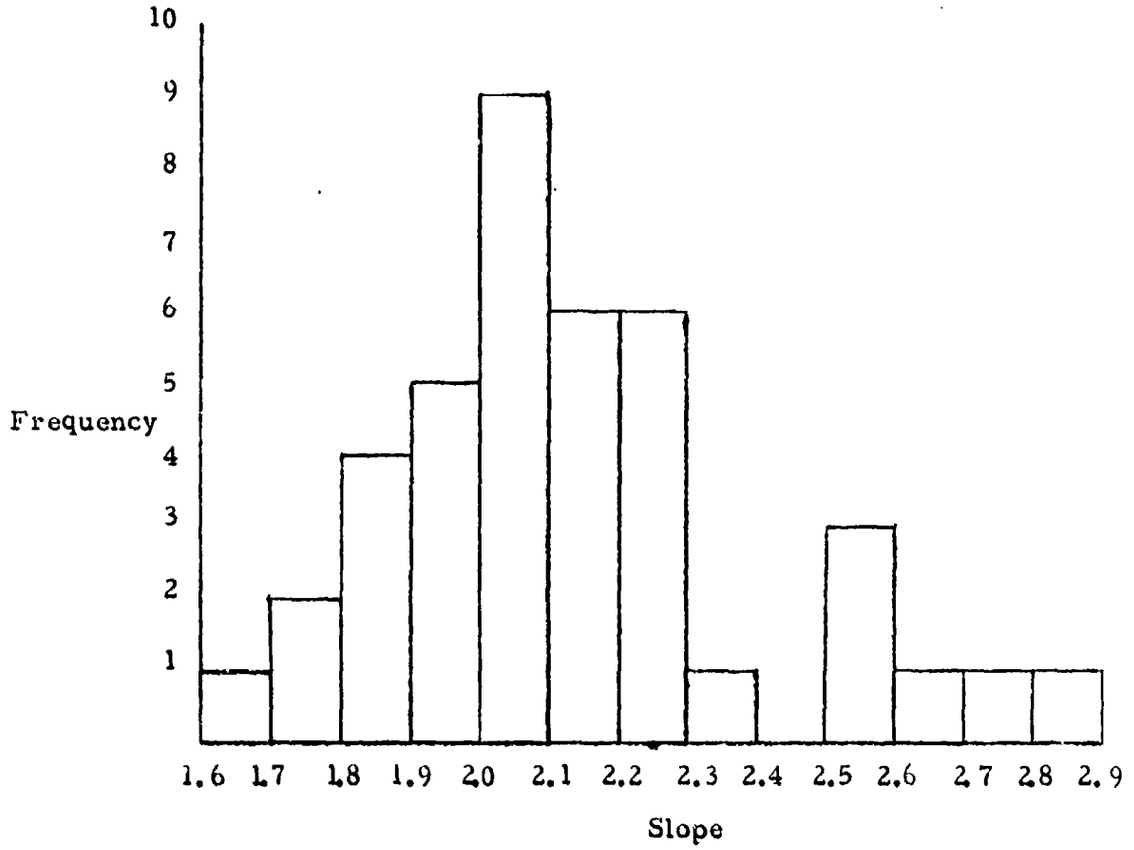

Figure 8 Histogram of PSD Mid Range Slopes

TABLE V

NUMBER OF PROFILES WITH RELATIVE MAXIMA OF PSD

AT INDICATED RANGES OF WAVELENGTH

Wavelength	Number of Profiles
51.2	4
25.6	16
15.1	10
12.5	9
10.0	8
8.4	9
7.5	7
5.0	6
4.0 - 4.2	32
2.4 - 2.6	18
2.0 - 2.1	36
1.3 - 1.4	42

the slabs of the pavement. If this is true, a general power spectral model should contain such a peak in this wavelength region.

Two other methods of considering the joint relationship of amplitude and wavelength were considered. Even though the results from these approaches were insignificant, they are described briefly in the following paragraphs.

The power spectral densities of the raw, unfiltered profiles were obtained and the anticipated results were apparent. The description of a ramp function in the frequency domain requires power at all wavelengths. Therefore, the long term grades in the original data distorted the spectral densities by distributing the much larger RMS values over all wavelengths to such an extent that peaks in the wavelengths of interest were often lost.

Figures 9 and 10 display the PSD's for Altus, Centerline, and Bakalar, Centerline. As shown in Reference 1, Altus, Centerline, has a linear grade the entire length of the runway with a total change in amplitude of approximately 350 inches. The PSD of this unfiltered profile is essentially a straight line. The PSD for Bakalar, Centerline, does show variation about a straight line and the linear grade for this profile extends only 22 inches over the length of the runway. It may be of interest to note that all of the power spectral densities of the unfiltered profiles could be modeled quite well with a straight line of -2 slope on the log-log plots.

The possibility of modeling the filtered profiles by a Fourier analysis was also briefly considered. In this approach, a profile was assumed to represent one cycle of length 2π and Fourier coefficients for wavelengths between 2 and 512 ft were obtained. The Fourier coefficients thus obtained displayed such tremendous variability (2 to 3 orders of magnitude) between runways that this characterization was abandoned.

3.1.3 Stationarity

An extremely important property in the analysis of time series is that of stationarity. This property is a necessary condition for obtaining statistical descriptions from a single time history. In essence a time series is considered stationary when the statistical characteristics do not change with time. Strictly speaking, this property can only be established by analysis of a collection of time histories but in practice this is often impossible. In the analysis of the runway elevation profiles, it is not sensible to attempt to establish stationarity by considering the 40 lines of data to be a representative sample of the ensemble since known differences exist in the profiles. For example, they have different RMS values. Therefore, the investigation of stationarity must be performed on the individual profiles. If the statistical properties do not change with distance down the runway, then the profile can be said to be self-stationary which is a necessary but not sufficient condition for stationarity.

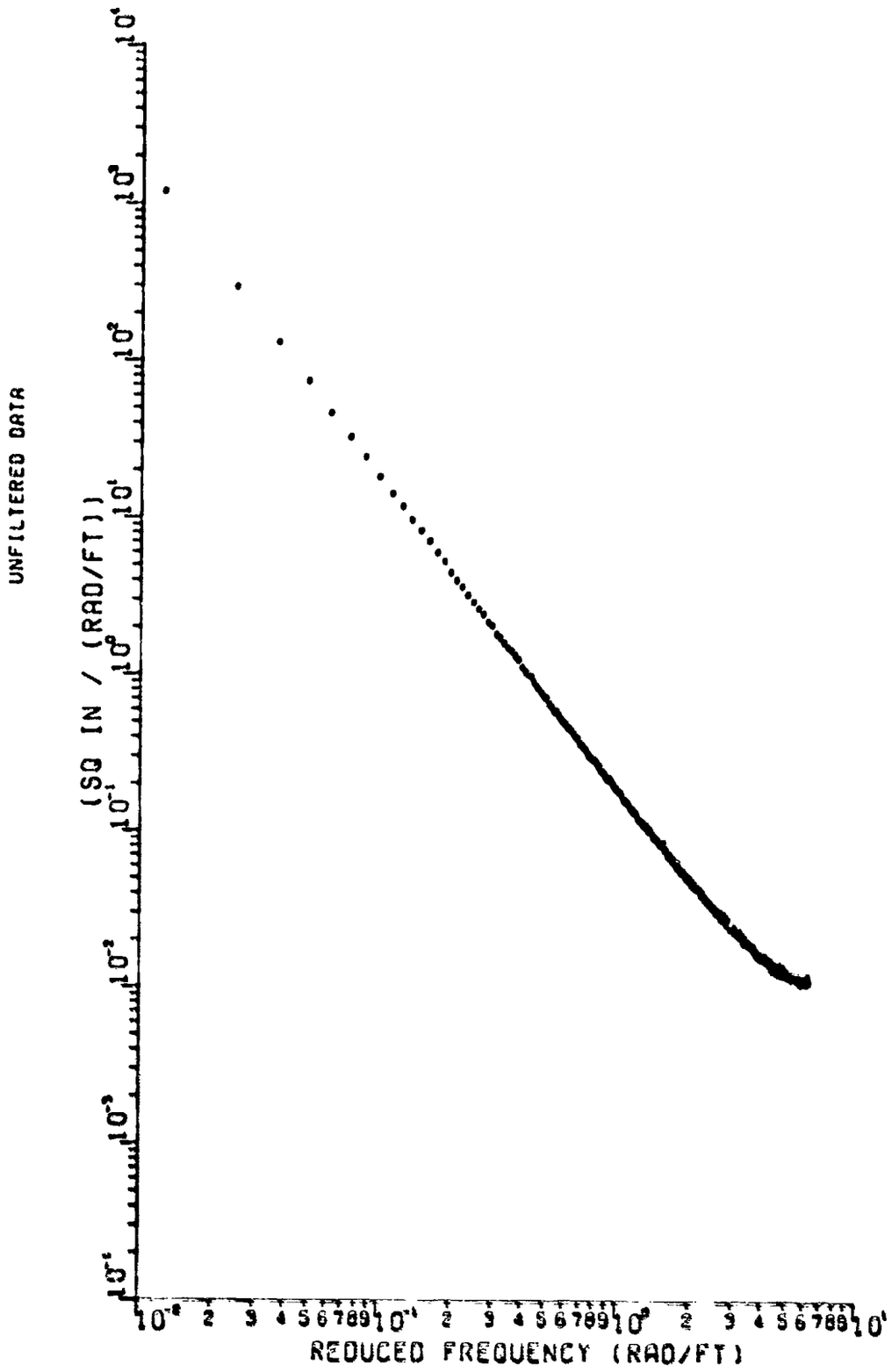

Figure 9 Power Spectral Density of Unfiltered Profile from Altus, Centerline

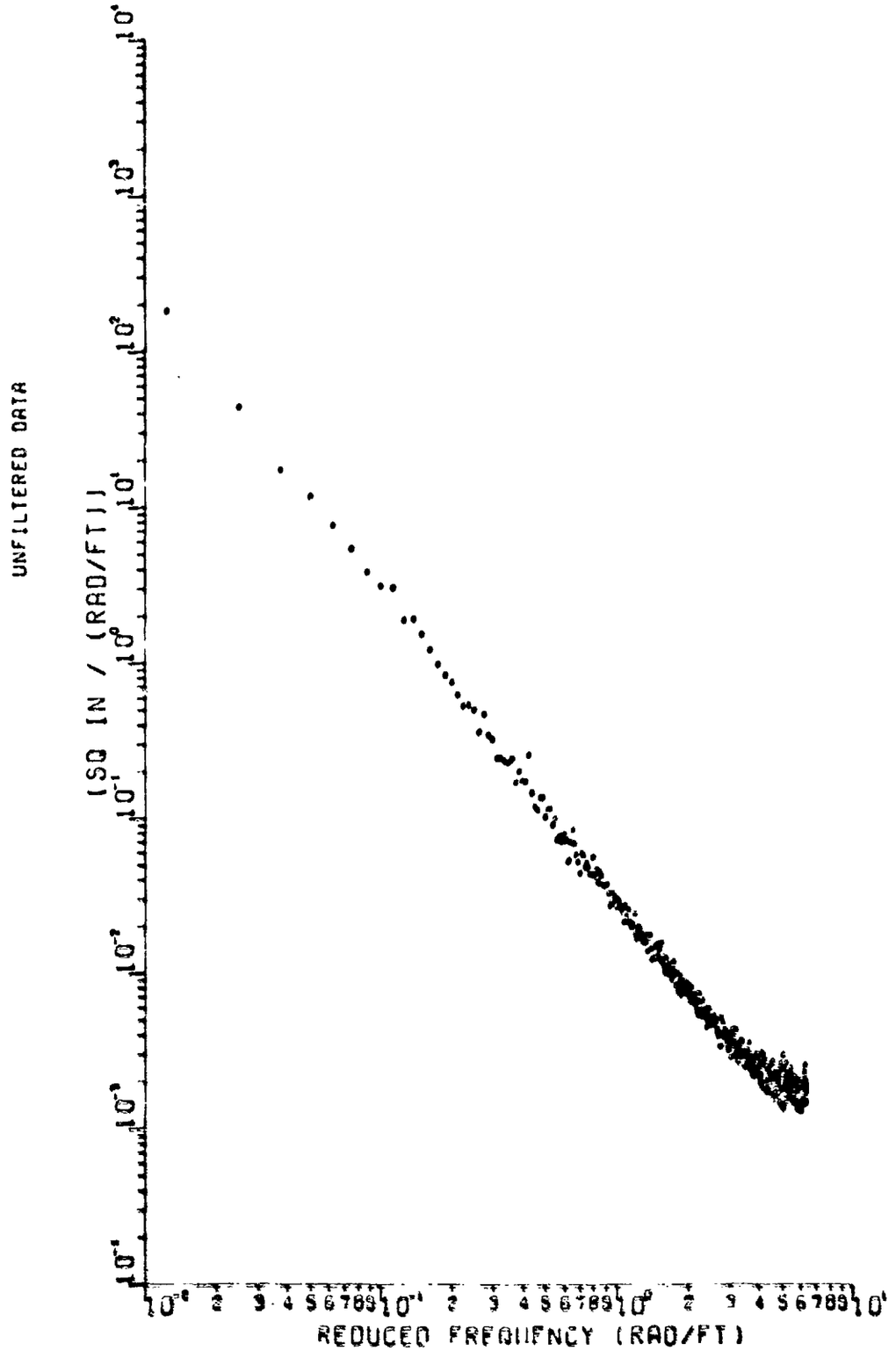

Figure 10 Power Spectral Density of Unfiltered Profile from Bakalar, Centerline

In practice, if a time history is shown to be self-stationary, it is treated as though it were stationary since quite often stationarity cannot be demonstrated and it is an extremely useful property.

The initial study of stationarity involved calculating the PSD of each third of each runway. If the profiles were self-stationary, the three PSD's for each would be approximately the same. Part of the motivation for this approach was the inability of the PSD method to yield an acceptable prediction of a response parameter. One hypothesis for the failure of the statistical approach to the analysis of response was that if different segments of a runway have different PSD's, then a PSD obtained from the total runway would not be representative of the individual segments.

For several of the runways, the three segments did have different PSD's. As the extreme example, Figures 11, 12 and 13 present the PSD's for the three segments of the McGuire, Centerline profile. The decrease in power at the long wavelengths is apparent even though there is general agreement in the shorter wavelengths. Note also the changing RMS values which decrease significantly between the first, second and third segments of the runway.

The changing intensity of the remaining runways are summarized in Table VI which displays the mean square value for each third and the composite of all three for most of the profiles. Mean square values are presented rather than RMS values since they more realistically reflect changes in the power spectral densities. It can be seen that segment mean square values can disagree with the composite mean squares by a factor of 8 and ratios of 2 to 1 are not uncommon. This observation led to a more detailed study of the RMS values.

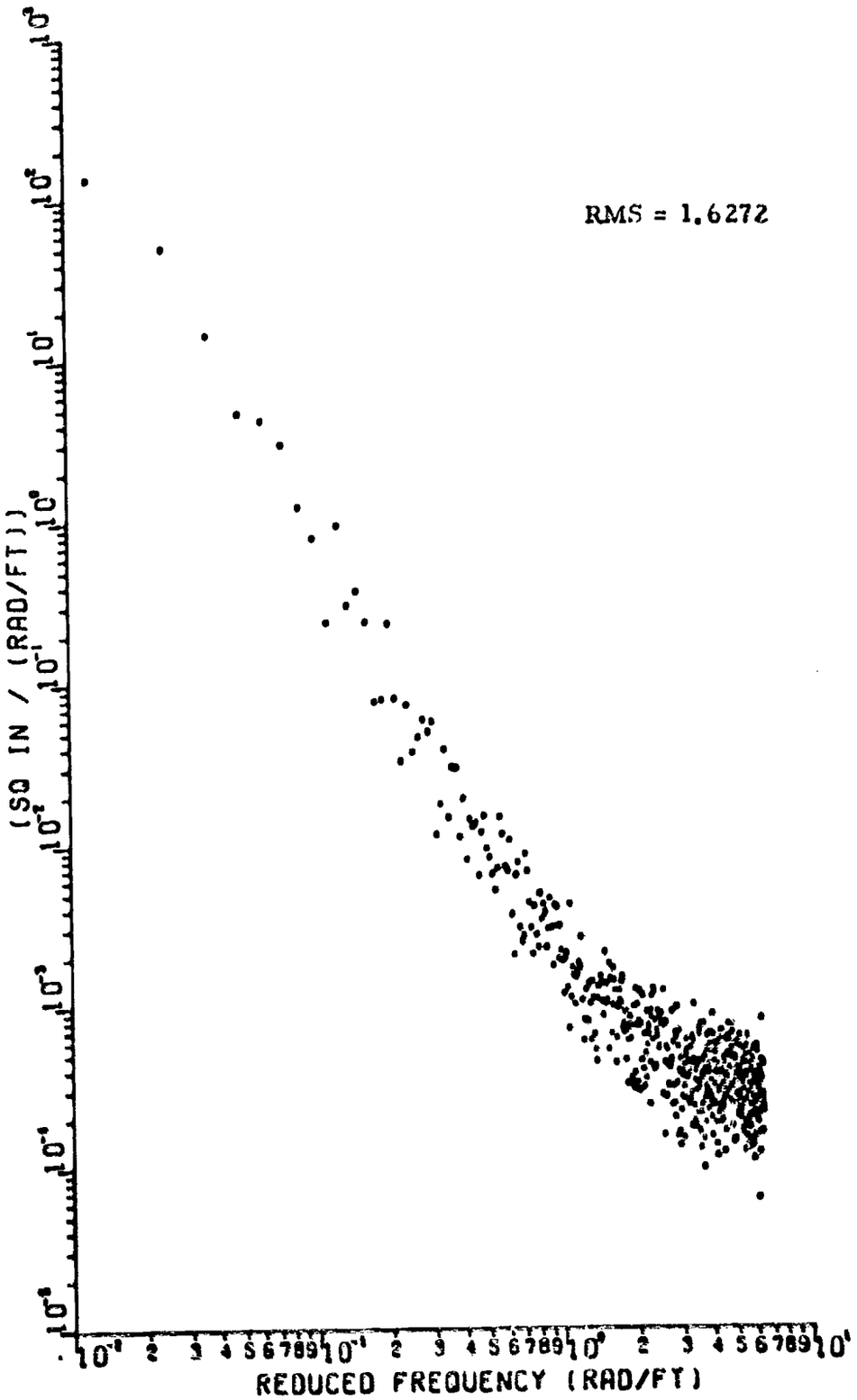

Figure 11 Power Spectral Density of First Third of McGuire, Centerline

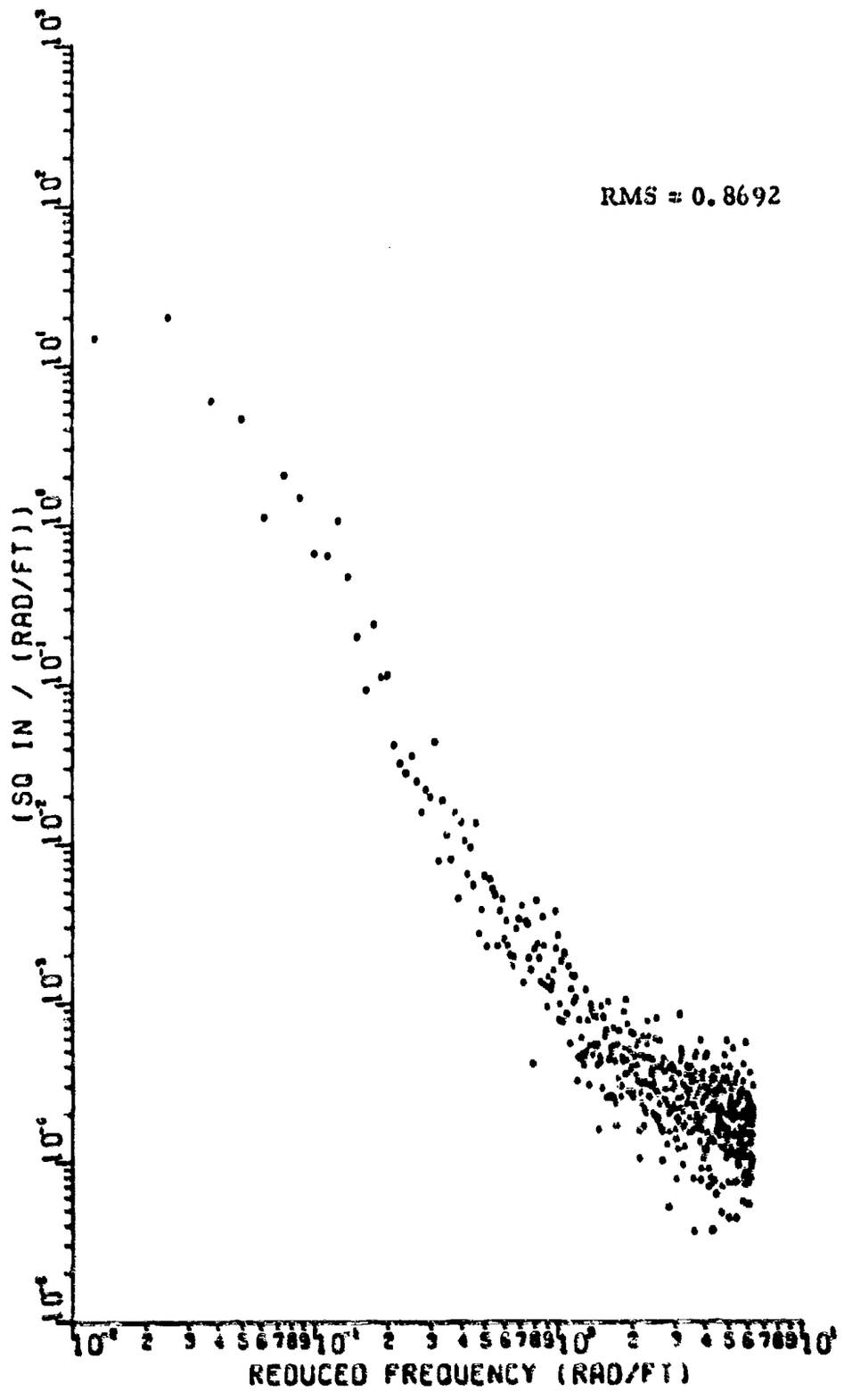

Figure 12 Power Spectral Density of Middle Third of McGuire, Centerline

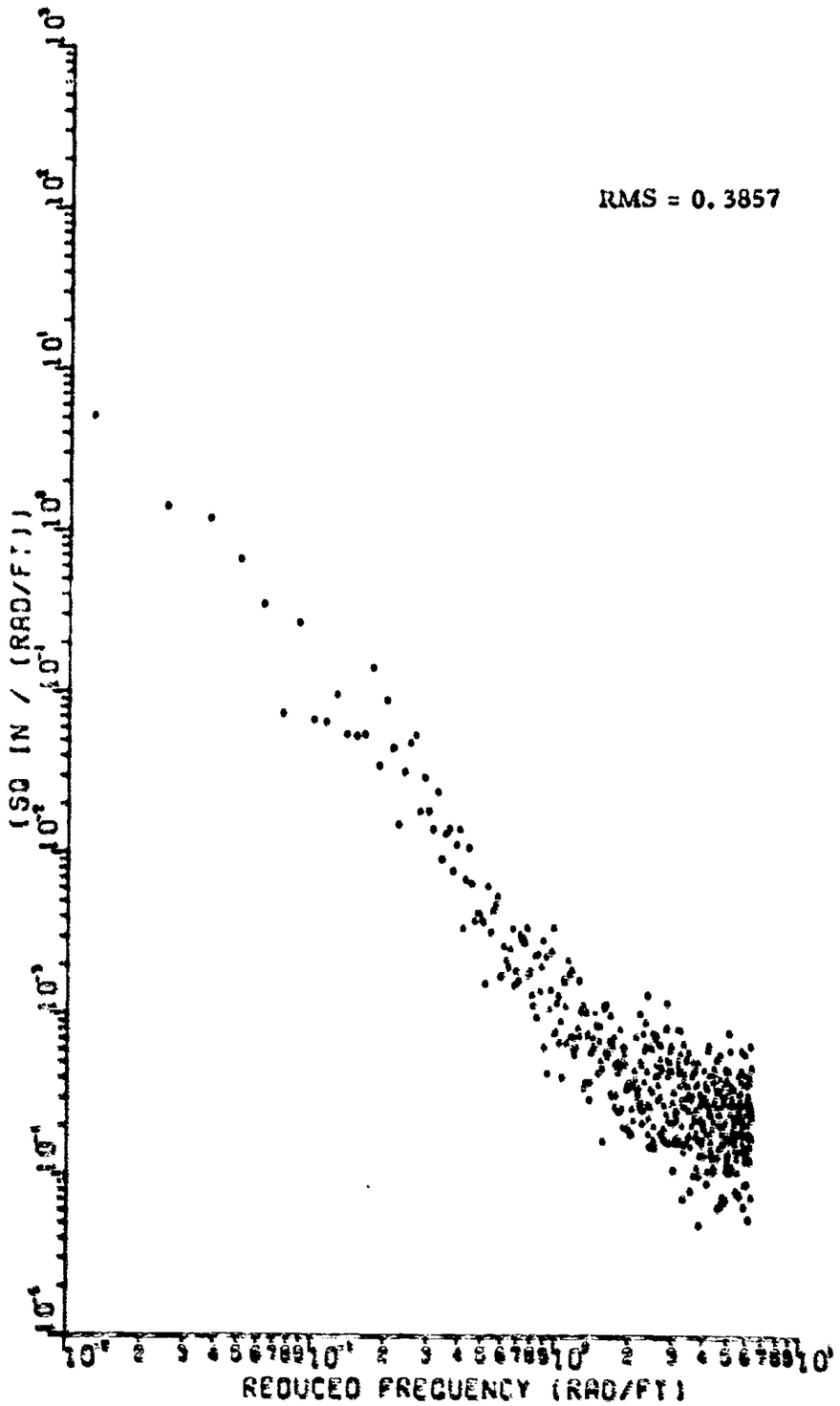

Figure 13 Power Spectral Density of Last Third of McGuire, Centerline

TABLE VI

MEAN SQUARE VALUES FOR SEGMENTS OF

PROFILES FILTERED AT 500 FT

Profile Identification		First Third	Middle Third	Last Third	Composite
Altus	75L	0.116	0.109	0.168	0.131
	CL	0.032	0.014	0.053	0.033
Bakalar	50L	0.150	0.196	0.209	0.195
	CL	0.060	0.066	0.079	0.070
Carswell	37L	0.117	0.114	0.033	0.087
	13L	0.130	0.081	0.028	0.078
	13R	0.153	0.096	0.039	0.095
Edwards	75L	0.087	0.047	0.044	0.060
	CL	0.041	0.045	0.045	0.044
	75R	0.054	0.038	0.036	0.043
Ellsworth	CL	0.039	0.073	0.122	0.076
Glasgow	75L	0.077	0.142	0.107	0.109
	CL	0.045	0.106	0.065	0.072
Langley	50L	0.077	0.165	0.172	0.136
	CL	0.070	0.123	0.084	0.089
McGuire	75L	1.168	0.543	0.140	0.620
	CL	2.648	0.756	0.149	1.201
	75R	0.574	0.610	0.202	0.454
Shaw	50L	0.031	0.060	0.105	0.064
Travis	75L	0.415	0.243	0.470	0.361
	CL	0.183	0.134	0.093	0.135
	75R	0.599	0.364	0.258	0.430
Torrejon	12L	0.201	0.084	0.032	0.106
	CL	0.236	0.093	0.069	0.132
	12R	0.175	0.082	0.047	0.101
Castle	75L	0.345	0.196	0.134	0.220
	CL	0.048	0.087	0.077	0.069
	75R	0.138	0.403	0.110	0.220
George	50L	0.121	0.072	0.105	0.097
	CL	0.115	0.101	0.133	0.115
Palmdale	50L	0.102	0.084	0.072	0.087
	CL	0.068	0.108	0.070	0.082
	50R	0.064	0.094	0.078	0.077

The RMS values for each 512 ft section of each profile were obtained and plotted as a function of distance down the runways. These RMS histories for all of the profiles are presented in Appendix IV and, as an example, the RMS histories for Altus and Bakalar are repeated as Figure 14. It is apparent that although some of the profiles display a consistency of RMS values over the entire length of the runway, many also display significant changes between segments. Therefore, it is concluded that the assumption of stationarity is not true in general even though some of the profiles are self-stationary.

To further investigate the high RMS regions of the profiles, the corresponding regions were identified on plots of the runway profiles. In every case, the high RMS values could be attributed to high amplitude, long wavelengths undulations as opposed to intense short wavelength regions of roughness. This observation leads naturally to the hypothesis that the long wavelength undulations are the cause of the nonstationarity.

3.2 MAXIMUM WAVELENGTH OF 100 FEET

Since the analysis of the profiles filtered at a maximum wavelength of 500 ft indicated that the long wavelength undulations are the possible cause of both nongaussianness and nonstationarity, the decision was reached to high-pass filter all profiles at a lower maximum wavelength and to analyze these different elevation profiles. Of course, the longer wavelengths are important as dynamic excitation to aircraft and they must be accounted for in the characterization of runway profiles. However, in the synthesis of a simulated runway, it would be most convenient if the shorter wavelengths could be modeled in the frequency domain. Since the previous analysis has shown that all wavelengths up to 500 ft cannot be modeled in the frequency domain, a compound characterization of runway roughness would be required. The long wavelengths would be modeled by a discrete description of amplitudes and wavelengths whereas the shorter wavelengths would be

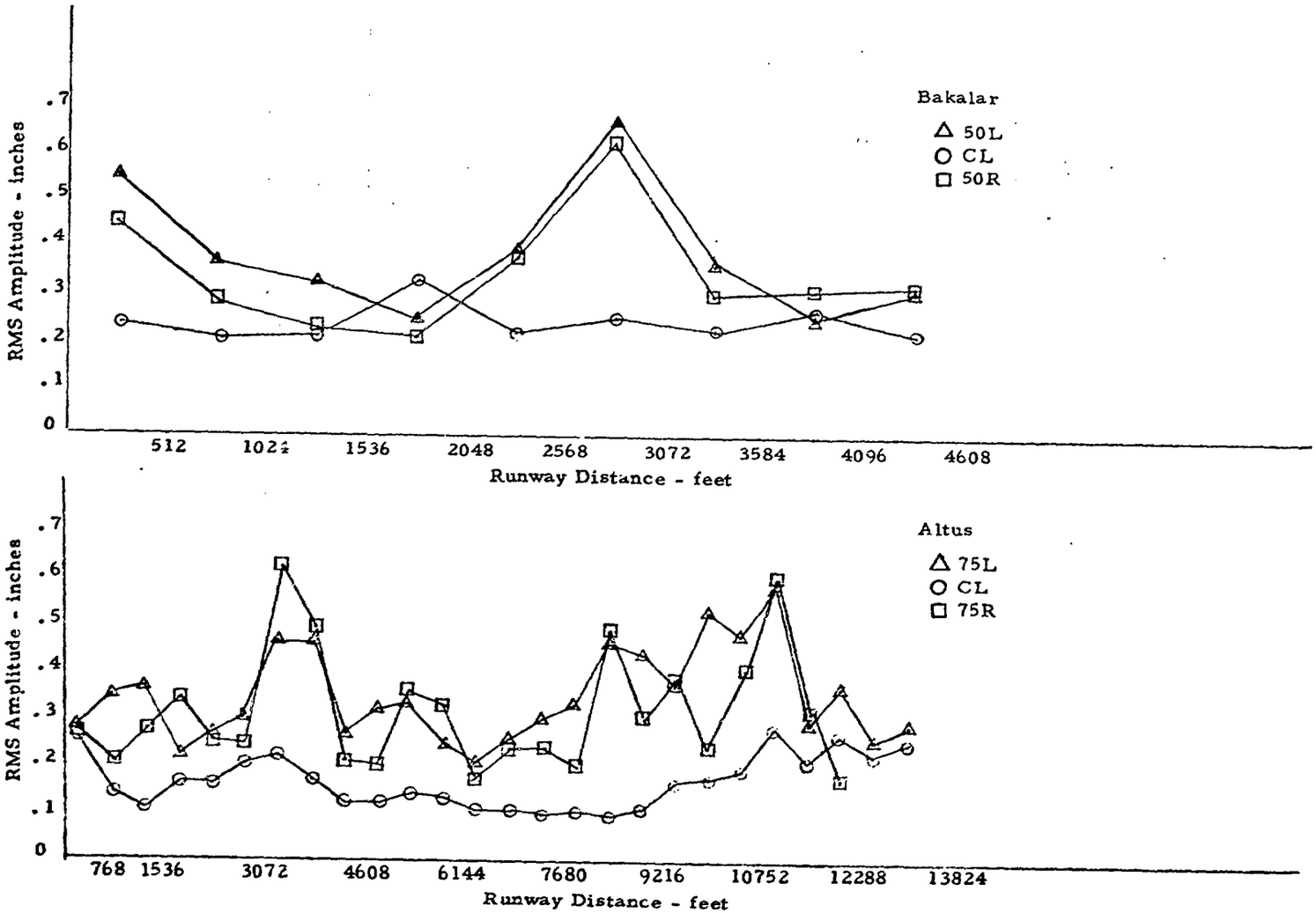

Figure 14 RMS Histories for Altus and Bakalar filtered at 500 ft

modeled by a gaussian, stationary time history with a PSD as determined by actual runway profiles.

Two considerations entered into the choice of the reduced maximum cutoff wavelength. For ease in modeling, it is desirable to have as large a maximum value as possible for which stationarity and gaussianness can be reasonably assumed. On the other hand, since the dominant excitation occurs at twice the gear spacing of the aircraft, the choice of the maximum wavelength for the short wavelength characterization should be such that it would contain wavelengths of twice the gear spacings of large aircraft. For these reasons, the initial choice of a reduced maximum wavelength was chosen at 100 ft with the intention of increasing this maximum if possible. As will be shown, however, stationarity and gaussianness are only marginally acceptable for all wavelengths less than 100 ft so that a larger maximum cutoff would lead to a higher degree of nonstationarity and non-gaussianness. Therefore, no other maximum wavelength was considered.

All profiles were digitally high-pass filtered by the methods described in Paragraph 2.2. All wavelengths less than 100 ft were passed unattenuated, all wavelengths greater than 140 ft were essentially eliminated, and between 100 and 140 ft the amplitudes were attenuated in accordance with the filter response of Figure 2. The analyses of Paragraph 3.1 were then repeated for these new profiles and the results of these analyses are presented in the following paragraphs.

3.2.1 Amplitude Probability Densities

The amplitude probability densities were obtained for each line of data filtered at a 100 ft maximum wavelength and, again, the cumulative distribution functions were plotted on gaussian probability paper. These comparisons for all lines of data are presented in Appendix V. Again, the solid line represents the gaussian fit as obtained from the mean and standard deviation of the amplitudes and not a best engineering judgment line through

the points. For all lines, the amplitude probability densities were more gaussian than those obtained from filtering at a maximum cutoff wavelength of 500 ft. However, discrepancies in the tails of the distributions are still present though less pronounced than before. Some of the extreme discrepancies may be explainable by noise spikes which passed the editing criteria of 0.4 inches described in Paragraph 2.1. The RMS values of the lines filtered at 100 ft are considerably smaller (average value of 0.16 in) than those filtered at 500 ft (average value of 0.36 in). Therefore, the effect of these spikes may have a greater effect in the distributions of amplitudes filtered at 100 ft. Again, the gaussian distribution would provide the best single family of distributions in modeling the amplitude probability density.

The RMS values of the lines filtered at 100 ft are presented in Table VII for each profile. These values are, of course, lower than the corresponding RMS value from the lines filtered at 500 ft. A histogram of the reduced RMS values is presented in Figure 15 from which it is easily seen that the scatter in the RMS values is also considerably reduced as compared to those from the profiles filtered at 500 ft. For these RMS values the mean, standard deviation, skewness and kurtosis are given by 0.156, 0.042, 1.992 and 6.916, respectively. A Kolmogoroff-Smirnov goodness of fit test rejects the hypothesis that these RMS values are from a normal distribution at the 99 percent level of confidence. It is not necessary for these RMS values to be normally distributed but if design criteria for intensity are set by the mean plus three standard deviations of the RMS distribution, there is no assurance that this value will be greater than 99.9 percent of the intensities to be encountered. Actually, the cause of the rejection of normality is the three large RMS values between 0.275 and 0.300 which came from the lines of data for McGuire.

TABLE VII

RMS VALUES FOR DATA FILTERED AT 100 FT

Identification	Location							
	87L	75L	50L	13L or 12L	CL	13R or 12R	50R	75R
Altus		0.151			0.096			0.139
Bakalar			0.181		0.182		0.180	
Carswell	0.134			0.149		0.147		
Edwards		0.138			0.117			0.114
Ellsworth					0.152			
Glasgow		0.139			0.119			0.153
Langley			0.150		0.141		0.144	
McGuire		0.291			0.282			0.283
Shaw			0.130		0.117		0.114	
Travis		0.134			0.149			0.145
Torrejon				0.136	0.168	0.130		
Castle		0.141			0.130			0.143
George			0.154		0.192		0.175	
Palmdale			0.158		0.171		0.168	

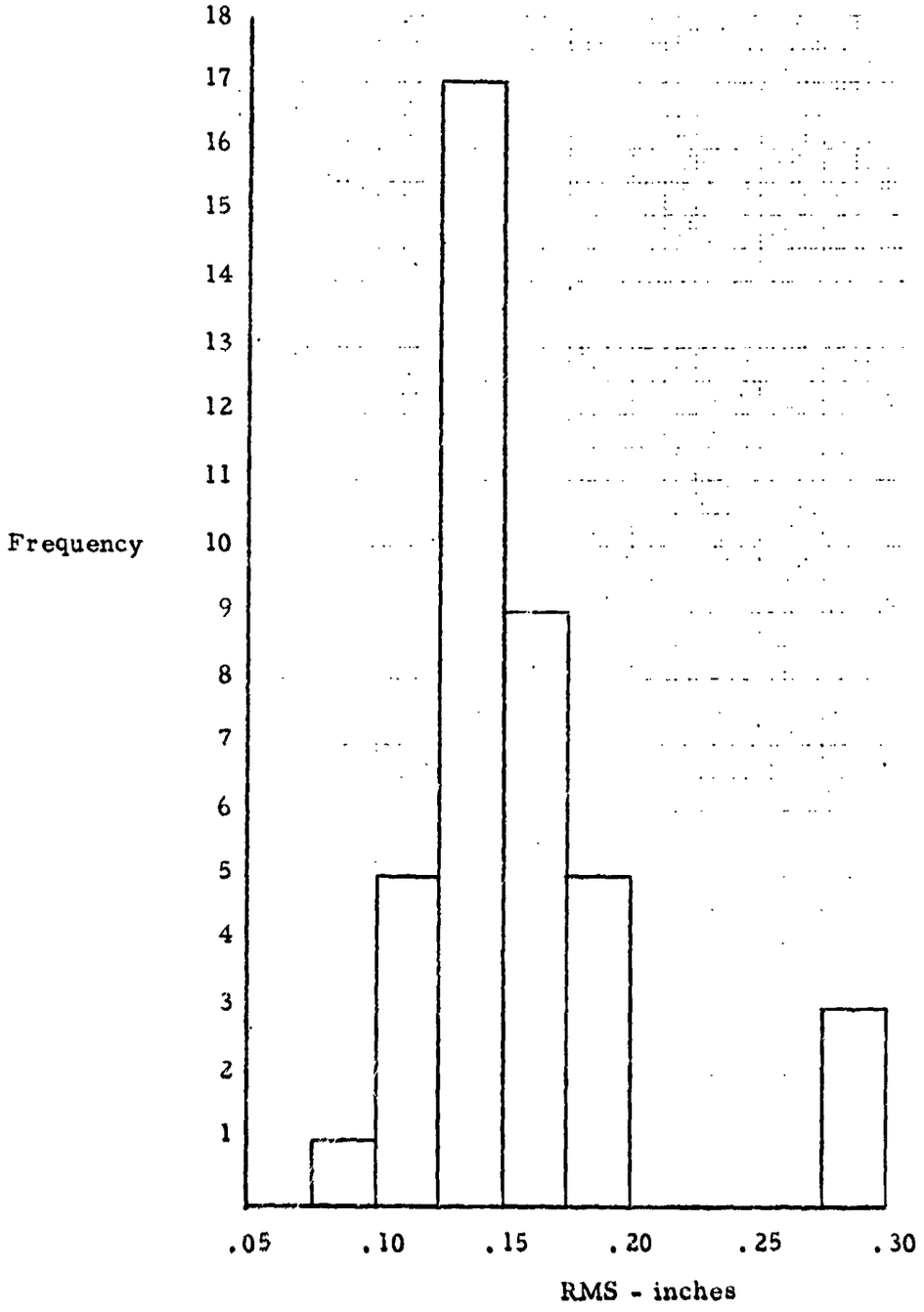

Figure 15 Histogram of RMS profiles filtered at Maximum Wavelengths of 100 ft

3.2.2 Power Spectral Densities

Theoretically, there should be no difference between the power spectral densities of profiles filtered at 100 ft and those filtered at 500 ft in the range of wavelengths less than 100 ft. To check this theoretical result, the PSD's were recomputed for all of the lines with the reduced cutoff wavelength. Since these PSD's agreed very closely for wavelengths less than 100 ft with those already presented in Appendix III, all of the comments of Paragraph 3.1.2 regarding analysis of the PSD's in the mid ranges of wavelength are directly applicable. Therefore, no further analysis is required. Perhaps it should be noted that the cutoff wavelength of 100 ft eliminates only the first four points of the spectra of Appendix III with a slight attenuation of the fifth point which is at a wavelength of 102 ft.

3.2.3 Stationarity

To investigate stationarity of the profiles filtered at 100 ft, RMS values were again calculated for each 512 ft section of each profile and plotted as a function of distance down the runway. These data are presented in Appendix VI and, for illustrative purposes, the RMS histories for Altus and Bakalar are repeated in Figure 16. It is apparent from these figures that the degree of self-stationarity, as indicated by RMS values, is much better for the profiles filtered at 100 ft than at 500 ft. Approximately half of the lines display erratic behavior in RMS and these generally have isolated sections of one RMS value considerably higher than the others. In most of the lines, however, the erratic behavior has been significantly reduced by the filtering at a lower cutoff wavelength. The three lines from McGuire again standout as being different from the remaining lines.

In the compound characterization of runway roughness, the degree of non-self-stationarity would have less effect in the synthesis of a simulated runway. This lessening of effect would be due to the reduced RMS values for the short wavelengths coupled with the independen

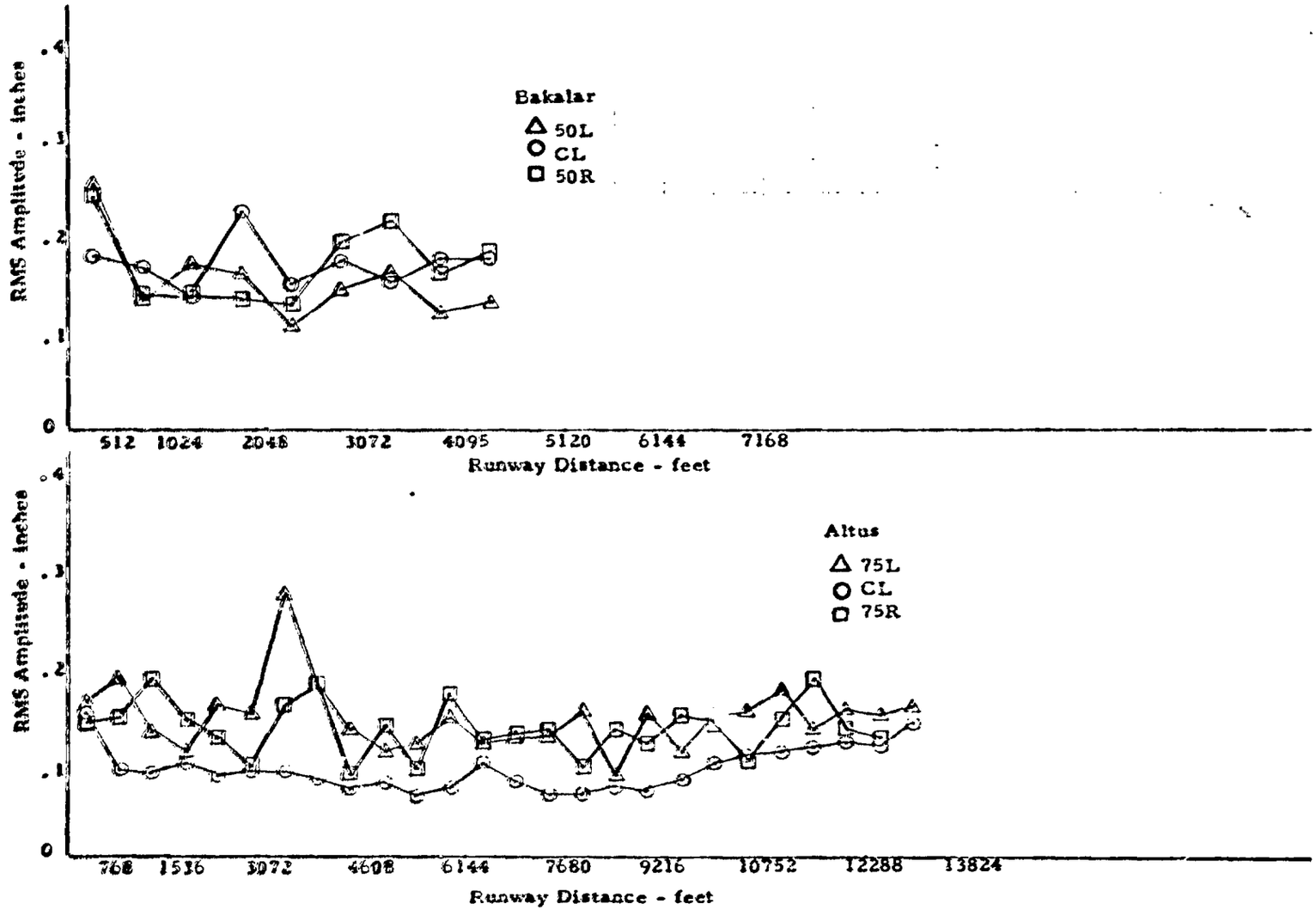

Figure 16 RMS Histories for Altus and Bakalar Filtered at 100 ft

introduction of the long wavelength, high amplitude cycles. Further, it was not considered practical to go to a maximum wavelength shorter than 100 ft. Therefore, even though there is evidence of nonstationarity, it was assumed in modeling the wavelengths less than 100 ft, that the short wavelength contribution to the simulated runways could be synthesized by using a theory dependent on the assumption of stationarity.

3.3 DISCRETE LONG WAVELENGTH DESCRIPTION

If a compound characterization of runway profiles is adopted wherein the wavelengths less than 100 ft are modeled in the frequency domain using available theory for stationary, gaussian time histories, the longer wavelength contribution to runway profiles must be independently characterized. Two methods of characterization of the long wavelengths components were given serious consideration. Initially, relative maxima and minima were paired by an algorithm with the distance between these peaks defined as the half wavelength and the difference in magnitudes defined as twice the amplitude. When the algorithm was applied to the profiles filtered at 500 ft, however, many of the peaks were described as having wavelengths greater than 500 ft. Since such a result is contradictory, this method of characterization was abandoned.

Study of the individual histories of the profiles, indicated that the long wavelength components are not generally superimposed. That is, when secondary peaks are present on a long wavelength undulation, these are due to cycles of less than 100 ft wavelength. Therefore, the method adopted for characterizing the long wavelength undulations was that of primary peaks of the profiles. Each maximum and each minimum between zero crossings was identified and associated with a half wavelength defined as the distance between zero crossings. All peaks with a half wavelength less than 50 ft were then dropped as these will be modeled by the short wavelengths component of runway profiles.

The characterization of the long wavelength undulations is then expressed in terms of the distribution of peaks per 1000 ft, the distribution of half wavelengths, and the joint distribution of half wavelengths and amplitudes. The method for using these distributions in deriving a simulated runway is presented in the next section.

Since the available runway profiles were of different lengths, and since it may be desirable to simulate runways of different lengths, the number of primary peaks in each profile was normalized by the length of the runway. The cumulative distribution of peaks per 1000 ft was then obtained and this distribution is presented in Figure 17 on normal probability paper. Although the hypothesis of normality could not be rejected by the Kolmogoroff-Smirnov test, the actual observed distribution was used in the runway simulation process rather than a normal distribution fit of data points. For the distribution of peaks per 1000 ft the mean and standard deviation are given by 5.26 and 0.89, respectively.

In this simulation process knowing the number of peaks per 1000 ft is not sufficient without knowledge of the manner in which these are distributed along the runway. As each peak was identified, its location on the runway was also noted. For each individual line of data, the number of peaks in 1000 ft increments down the runway was obtained. Each of these 40 distributions were tested against a uniform distribution for location of the peaks by a Kolmogoroff-Smirnov goodness of fit test at a level of confidence of 80 percent. The equality of the observed distribution of location of peaks to the uniform distribution was rejected in only three of the 40 tests. Since testing was performed at a level of confidence of 80 percent, the expected number of rejections in 40 tests is eight if the distribution of peak location is truly uniform. Therefore, these tests indicate that the peaks are uniformly distributed over the lengths of the runways.

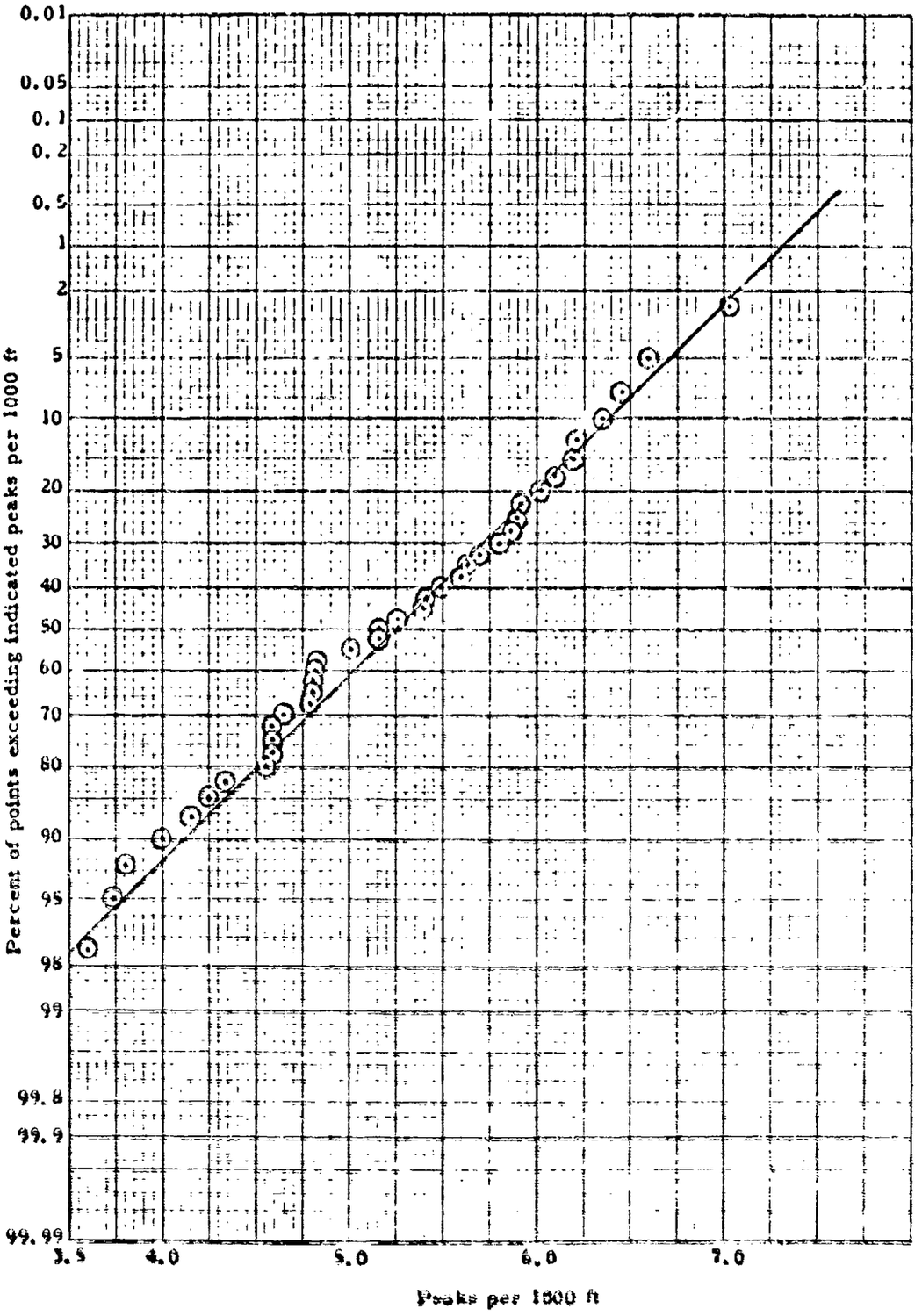

Figure 17 Cumulative Distribution of Primary Peaks per 1000 ft

The cumulative distribution of half wavelengths is presented in Figure 18 and the cumulative distributions of amplitudes for the half wavelength intervals are presented in Table VIII. In the generation of the simulated runway these observed distributions were directly used rather than fitting them with some family. The dependence of the amplitude distributions on half wavelength is apparent from Table VIII. Note, for example, the increasing median value with wavelength. Note also the increased proportion of high amplitude values at the long wavelength intervals. This dependence is accounted for in the simulation process by first drawing a wavelength at random from the cumulative distribution of Figure 18 and then drawing an amplitude at random from the appropriate cumulative distribution of Table VIII. This procedure is an application of the well-known law of probability that

$$P\{A \text{ and } B\} = P\{B\}\ P\{A \text{ given } B\}$$

where

A denotes a primary peak of given amplitude

B denotes a primary peak of given wavelength

This procedure insures a random selection of peaks with representative amplitudes and wavelengths.

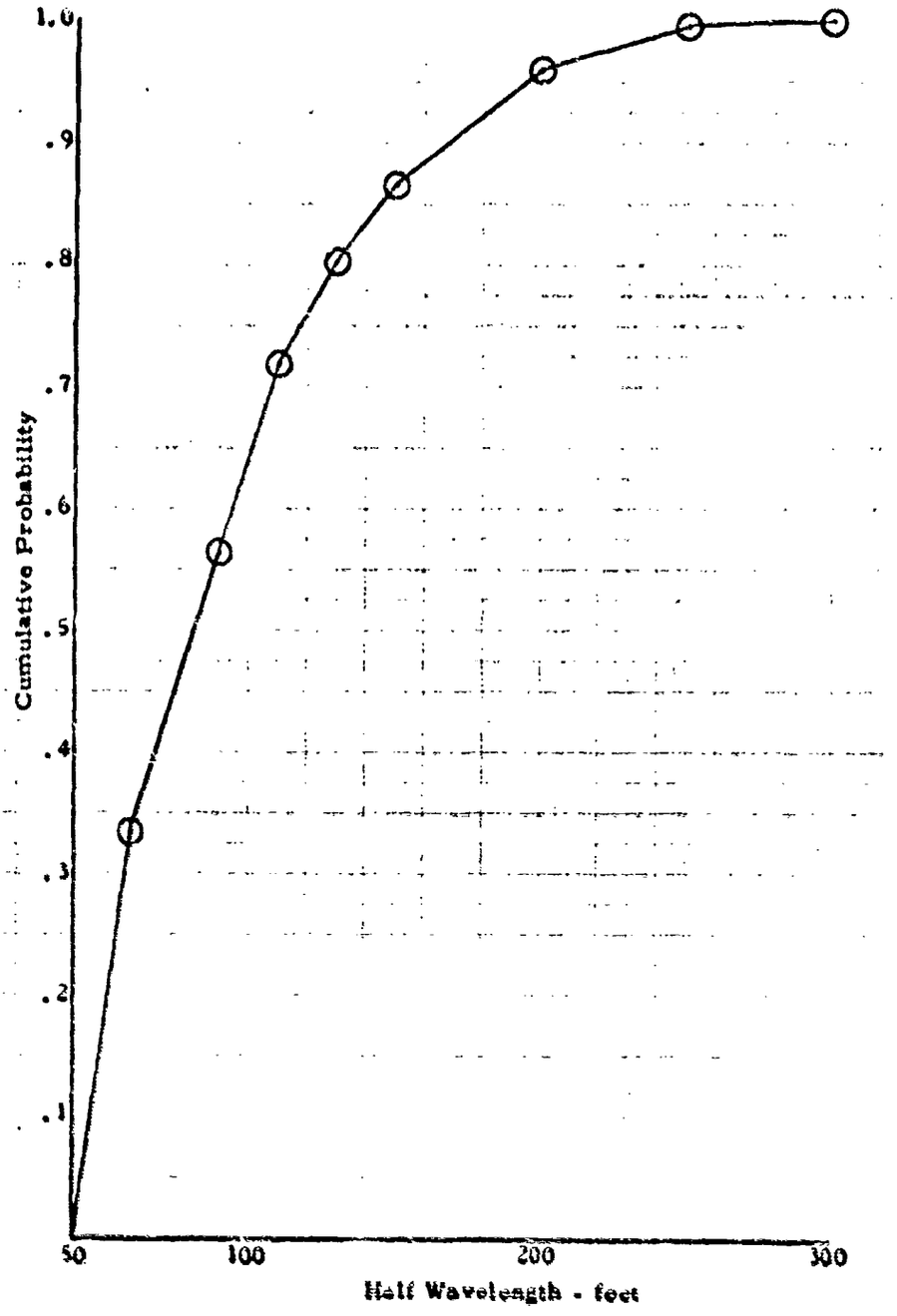

Figure 18 Cumulative Distribution of Half Wavelengths

TABLE VIII

CUMULATIVE DISTRIBUTIONS OF AMPLITUDES FOR HALF WAVELENGTH INTERVALS

Amplitude	Half Wavelength							
	50-70	70-90	90-110	110-130	130-150	150-200	200-250	250-300
0.375	1.000	1.000	1.000	1.000		1.000		
0.5	0.789	0.907	0.936	0.969	1.000	0.991	1.000	
0.625	0.455	0.623	0.758	0.850	0.938	0.912	0.915	
0.75	0.243	0.396	0.501	0.541	0.750	0.823	0.829	
0.875	0.131	0.216	0.298	0.407	0.514	0.637	0.720	
1.0	0.058	0.112	0.184	0.278	0.375	0.474	0.561	1.000
1.125	0.026	0.057	0.100	0.175	0.229	0.340	0.451	0.923
1.25	0.017	0.040	0.064	0.129	0.139	0.270	0.378	0.769
1.375	0.009	0.028	0.047	0.098	0.097	0.186	0.268	0.462
1.5	0.005	0.026	0.036	0.067	0.090	0.149	0.207	0.462
1.625	0.003	0.017	0.017	0.041	0.069	0.112	0.183	0.462
1.75	0.003	0.010	0.011	0.021	0.042	0.084	0.159	0.462
1.875	0.001	0.004	0.011	0.016	0.042	0.074	0.134	0.385
2.0	0.001	0.004	0.008	0.016	0.028	0.060	0.098	0.321
2.25	0.001	0.004	0.006	0.010	0.021	0.046	0.098	0.077
2.5		0.002	0.003	0.010	0.021	0.037	0.061	
3.0			0.003		0.007	0.019	0.061	
4.0			0.003		0.007	0.014	0.024	
5.0						0.005	0.012	

SECTION 4
SIMULATED RUNWAYS

A principal result of the analysis of the runway roughness data was to produce a simulated runway for use as design criteria. This simulated runway must have statistical properties similar to the sample of discrete runway data. A decision was made, during the analysis of the data, to represent the relatively high frequency (less than 100 ft wavelength) component in terms of a PSD and the low frequency data in terms of discrete peaks and valleys. Using the following equation (Reference 2) a time history can be computed from any PSD.

$$f(x) = \sqrt{2} \sum_{i=1}^{N} A_i \cos(x w_i - \theta_i) \qquad (6)$$

where

$f(x)$ is the amplitude at point x on the runway

$A_i = (\phi_i(w)\ \Delta w)^{1/2}$

$\phi_i(w)$ is the PSD as a function of frequency

w_i is the frequency

θ_i is a random angle between 0 and 2π

N is the number of points used to describe $\phi_i(w)$

Using Equation (6) a runway of any length can be created and it will have the desired PSD, hence the same RMS value. Large wavelength peaks and valleys can then be superimposed on this profile as desired.

4.1 SAMPLE RESULT

A computer program has been written to generate, at random, typical runways with the high frequency content described as:

$$\Phi(\Omega) = \frac{.0023}{\Omega^{2.007}} \tag{7}$$

where

$\Phi(\Omega)$ is the PSD ($in^2/(rad/ft)$)

Ω is the reduced frequency (rad/ft)

This equation was derived by fitting a straight line (on log-log paper) to the mean PSD of all lines of survey to obtain the slope and using the RMS value for which 90 percent of the lines of survey do not exceed.

The low frequency content was added to the runway by first randomly selecting the number of peaks to be added from Figure 17, which is the distribution of long wavelength peaks obtained from the runway profiles. This distribution contains the sum of the positive and negative peaks since it was found that there were an equal number. The rate drawn from the distribution is then multiplied by 10 for the 10,000 ft runway. Next, for each peak, which are alternately assigned positive and negative values, a half wavelength was randomly drawn from the cumulative distribution of half wavelengths (Figure 18) and an amplitude was randomly drawn from the cumulative distribution of amplitudes corresponding to the wavelength (Table VIII). The long wavelength peaks were determined to be uniformly distributed over the length of the runway, however, selecting a random place for the peaks becomes a matter for discussion. After some deliberation, it was decided that the peaks would be superimposed, as 1/2 sine waves, at the center of a randomly selected available segment of the runway. Therefore, the first peak selected is put in the center of the runway, leaving two, equal length available segments. The second peak

is then put in the center of one of the two available segments, which now leaves three available segments. This procedure is continued until all peaks have been superimposed on the runway. If at any time the randomly selected segment is too short to accept the peak, successive segments are examined until a long enough one is found, or if none are long enough a message is written by the program and the peak is not included.

Interpolation was performed in determination of the wavelength and amplitude of each peak, that is, the distributions were considered to be continuous from 50 ft to 300 ft in wavelength and from 0.25 inch to 5.0 inches in amplitude. The number of peaks per thousand feet of runway, however, was not interpolated since there are 36 entries in the table and the span when multiplied by 10 is only 35.

In order to prove that a runway generated in such a manner has the desired statistical properties, the simulated runway was then input to the program which extracts the primary peaks from the data. Tables IX and X show the peaks that were superimposed on the runway and the peak distributions that were extracted from the runway, respectively. The profile was then filtered using a 100 ft cutoff and the PSD was computed. A plot of this PSD is presented in Figure 19 and the corresponding amplitude probability density in Figure 20. The entire profile of the simulated runway is presented in graphical form in Figure 21 and in tabular form in Table XI.

TABLE IX

DISTRIBUTION OF LONG WAVELENGTH PEAKS
INPUT TO SIMULATED RUNWAY

Amplitude	Wavelength						
	70	90	110	130	150	200	250
0.375	6	2	2				
0.500	6	4	1				
0.625	6	1		2		1	
0.750	5	2	2	1	1	1	
0.875	1	1	1	1	1		1
1.000		1	2	2		1	
1.125		1					
1.250	1				1		
1.375							
1.500							
1.625							
1.750							
1.875							1
2.000							
2.250		1					

TABLE X

DISTRIBUTION OF LONG WAVELENGTH PEAKS
OUTPUT FROM SIMULATED RUNWAY

Amplitude	Wavelength						
	70	90	110	130	150	200	250
0.375							
0.500	1						
0.625	5						
0.750	1	1					
0.875	4	1			1		
1.000	1	3		3			
1.125	3	1	1	1			
1.250	2		2		1	2	
1.375			1	1			
1.500		3					
1.625							
1.750							
1.875							
2.000							
2.250			1				1

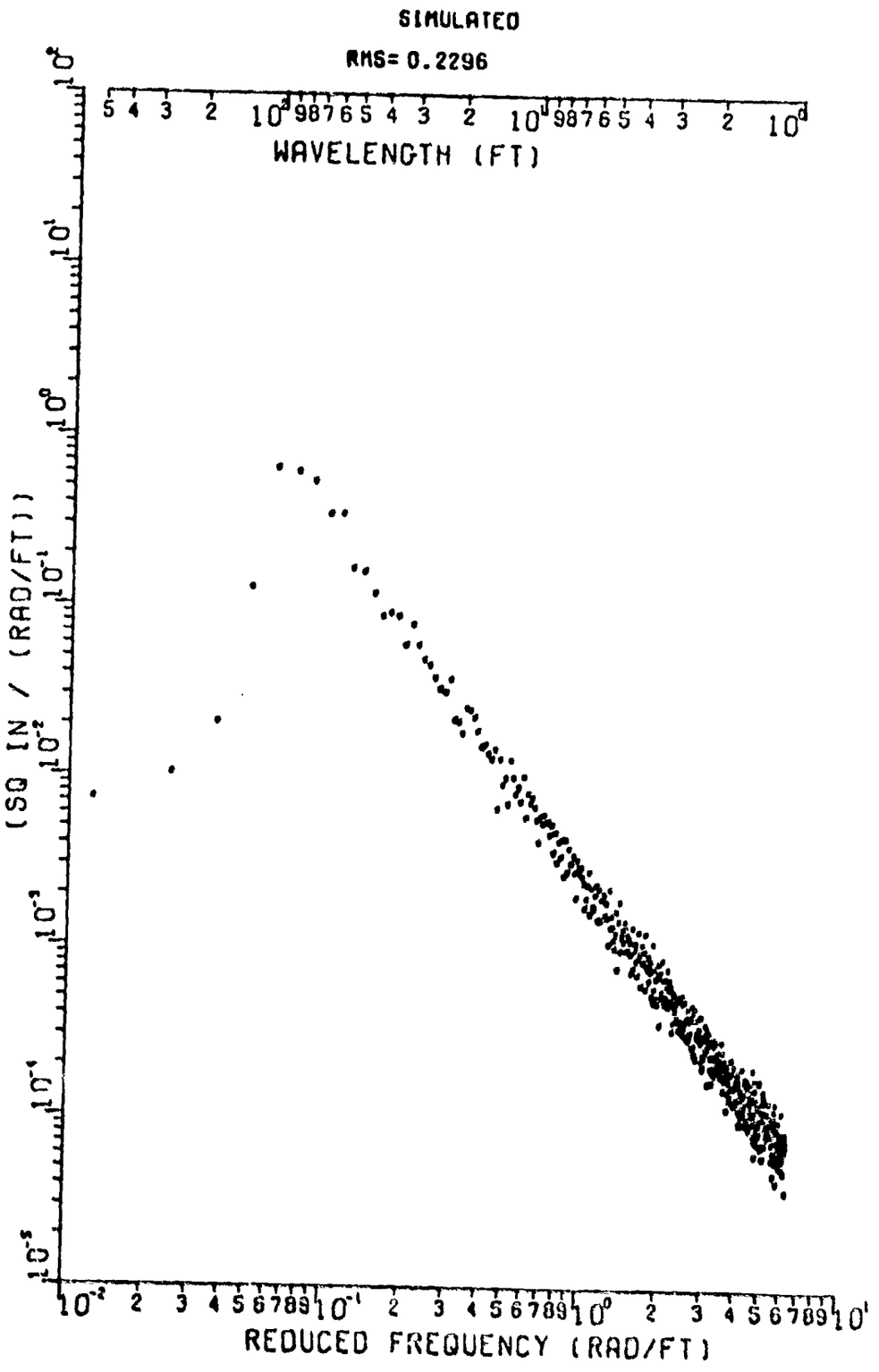

Figure 19 PSD from Simulated Runway

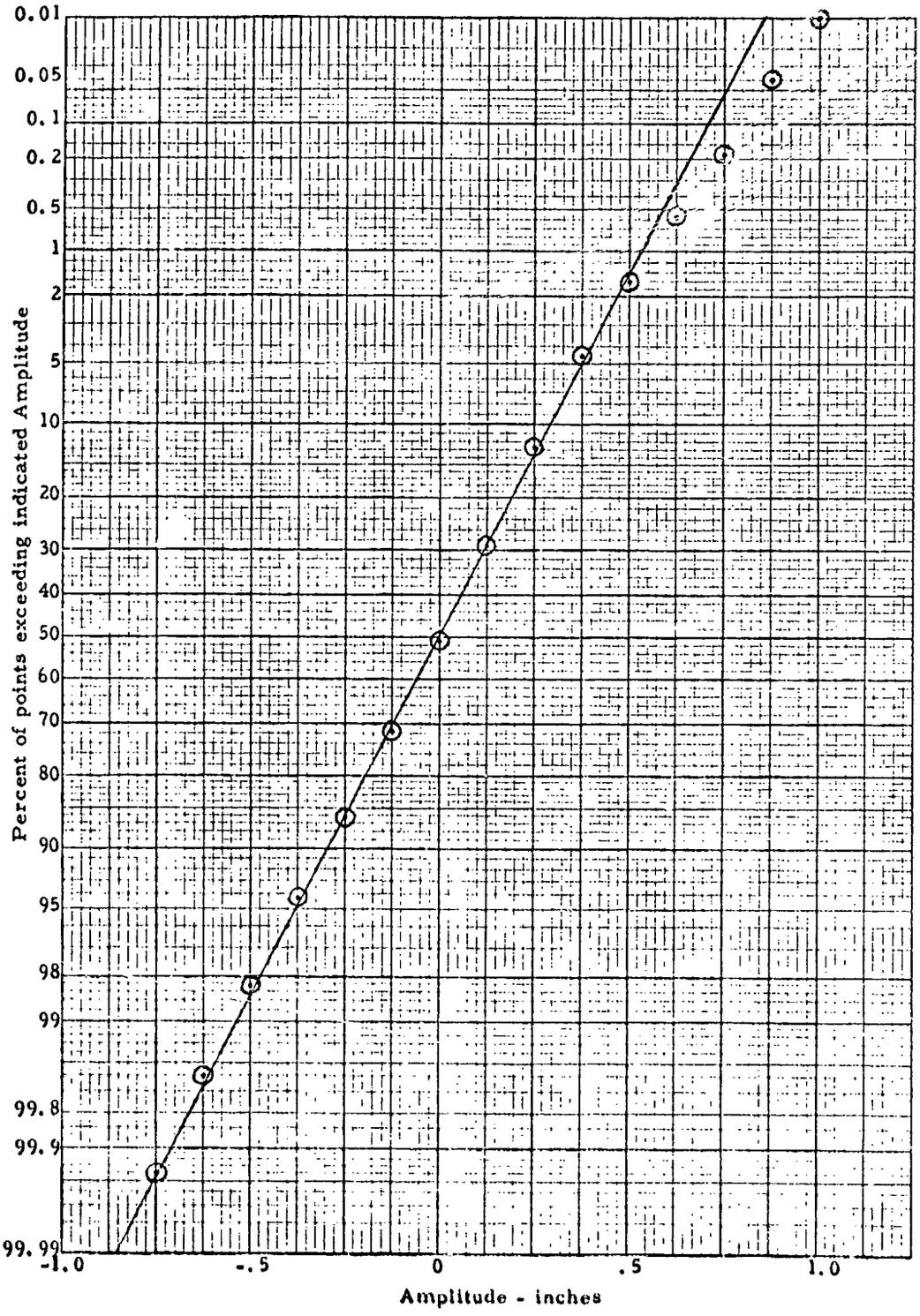

Figure 20 Amplitude Probability of Simulated Runway

(This blank page is included in order to comply with MIL-STD-847A ruling that foldouts must begin on a right-hand page.)

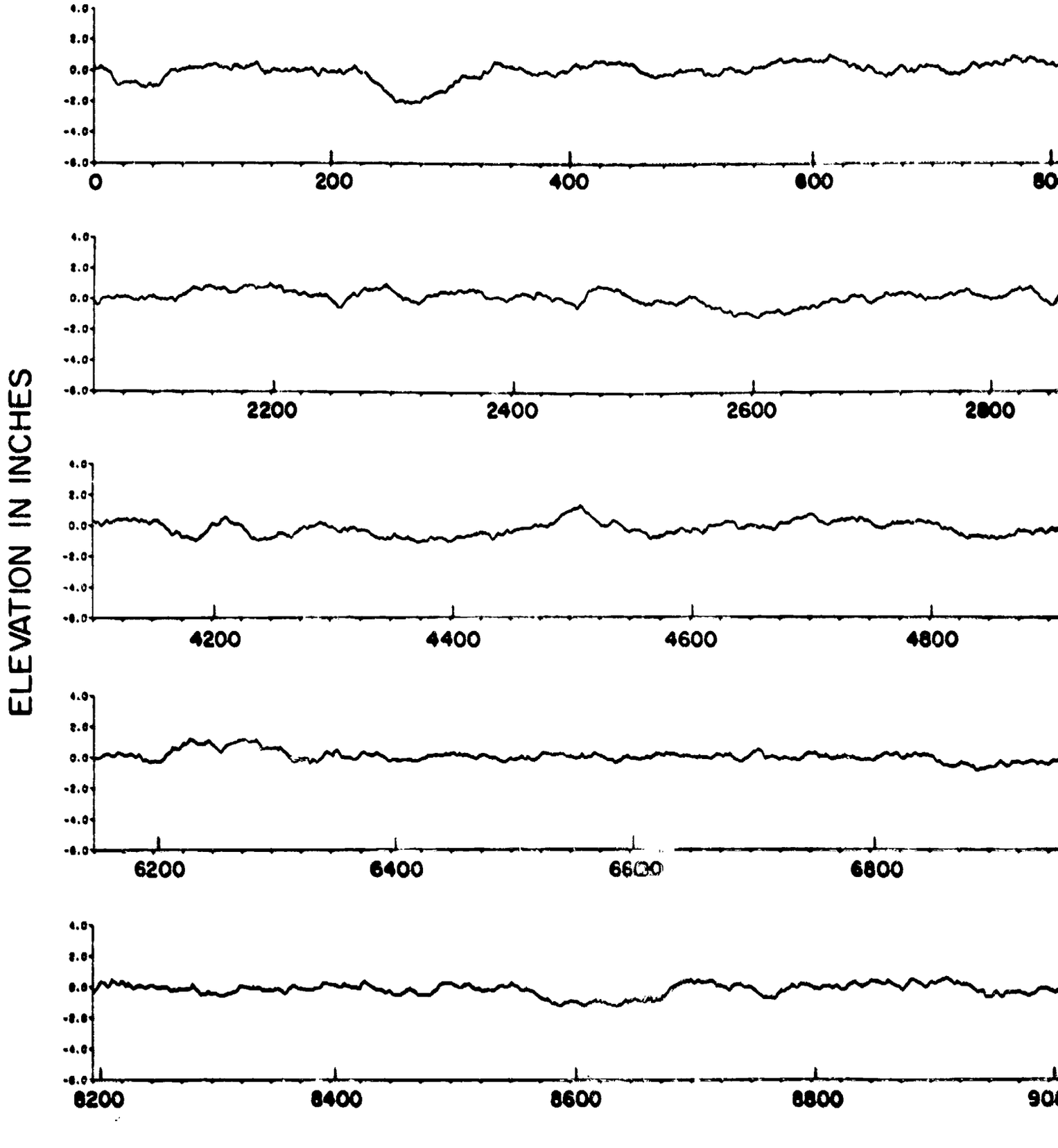

Figure 21 Profile of Simulated Runway

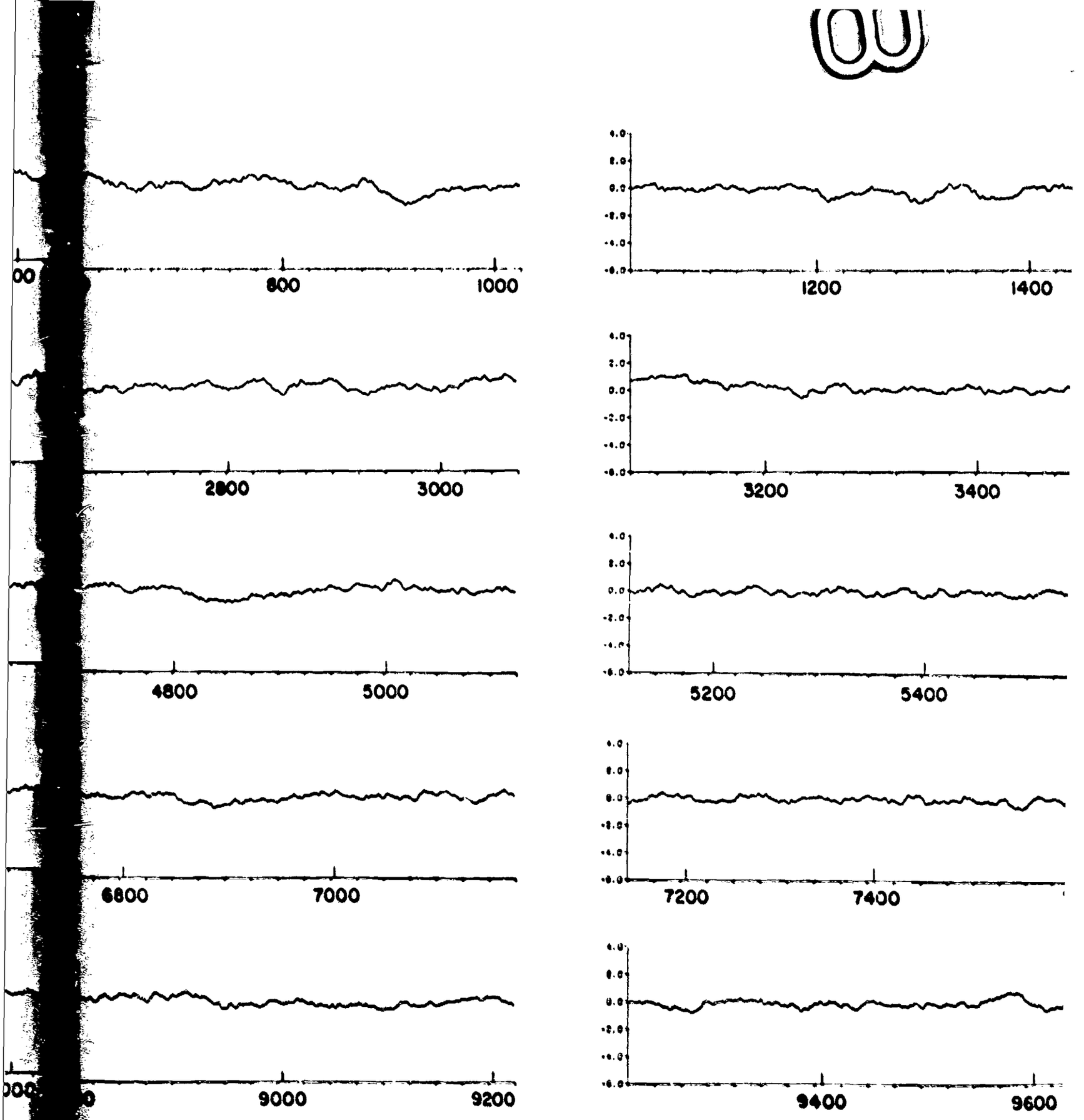

DISTANCE DOWN RUNWAY IN FEET

1200
1400
1600
1800
2000
3200
3400
3600
3800
4000
5400
5600
5800
6000
7400
7600
7800
8000
9400
9600
9800
10,000
FEET

TABLE XI

SIMULATED RUNWAY ELEVATIONS IN INCHES AT TWO-FOOT INTERVALS

NOTE: Read Data from Left to Right

.250	.110	.050	.150	.080	.090	-.100	-.150	-.500	-.710
-.960	-.910	-.790	-.770	-.760	-.810	-.780	-.750	-.810	-.940
-1.100	-.970	-1.130	-.930	-.870	-1.010	-.960	-1.000	-.810	-.620
-.360	-.190	.020	.030	.090	-.040	.090	.120	.060	.240
.100	.200	.220	.270	.250	.220	.200	.270	.390	.360
.410	.490	.530	.320	.240	.210	.250	.120	.030	.310
.180	.220	.270	.110	.320	.290	.390	.360	.500	.530
.230	.920	-.210	0.000	-.090	.110	.150	.030	.030	-.070
.010	.120	-.020	.060	.170	.120	.020	.010	.050	.120
.020	.150	.130	-.090	-.290	-.160	.110	.020	-.040	-.090
-.050	.010	-.130	.050	-.110	-.190	-.020	.030	.090	.220
.190	-.030	-.130	-.130	-.060	-.240	-.470	-.670	-.800	-.970
-.940	-1.100	-1.140	-1.420	-1.570	-1.620	-1.890	-2.060	-1.980	-1.960
-1.910	-2.120	-1.980	-2.070	-2.050	-2.010	-1.960	-2.050	-1.790	-1.650
-1.670	-1.650	-1.590	-1.430	-1.390	-1.360	-1.300	-1.410	-1.240	-1.000
-.950	-.810	-.660	-.660	-.420	-.240	-.320	-.400	-.380	-.350
-.420	-.420	-.460	-.160	.010	-.100	.020	.290	.590	.560
.520	.490	.510	.260	.300	.330	.190	.160	.170	.250
.140	0.000	-.050	-.070	-.250	-.160	-.210	-.060	-.150	-.050
-.060	-.130	-.200	-.270	-.310	-.060	.030	.060	.030	.030
.150	.340	.500	.390	.160	.370	.310	.310	.400	.460
.630	.640	.620	.720	.590	.520	.530	.570	.580	.520
.540	.520	.400	.550	.450	.500	.450	.350	.130	-.020
-.060	-.190	-.270	-.260	-.370	-.340	-.240	-.200	-.200	-.160
-.180	-.140	-.250	0.000	-.010	.150	.040	.020	.120	.100
.110	.070	.240	.090	.150	-.220	-.160	-.150	-.230	-.250
-.150	-.200	-.070	.170	.200	.190	.250	.150	-.030	.050
.040	-.050	-.100	-.020	.020	.290	.210	.220	.240	.300
.330	.310	.450	.610	.560	.590	.730	.780	.550	.600
.590	.700	.510	.680	.600	.720	.680	.730	.730	.840
.690	.660	.540	.690	.630	.780	.730	1.000	.930	.690
.900	.760	.700	.630	.540	.340	.350	.440	.330	.220
.130	.010	.000	.270	.220	.190	.010	-.140	-.140	-.170
-.240	-.390	-.190	-.340	-.170	.050	.150	.310	.270	.140

TABLE XI (continued)

-.070	-0.000	.050	-.060	.030	.320	.270	.220	.350	.300
.260	.240	.260	.270	-.020	.090	-.100	-.120	-.160	-.250
-.160	-.150	-.150	-.080	-.040	.080	.210	.470	.450	.310
.170	.330	.310	.400	.410	.330	.480	.560	.420	.350
.410	.630	.590	.640	.920	.680	.850	.790	.540	.570
.700	.810	.800	.730	.550	.550	.600	.550	.430	.360
.360	.450	.240	.250	.300	.080	-.020	-.150	-.150	-.170
-.160	-.040	-.030	.120	.010	0.000	.260	.260	.200	.170
.100	-.020	-.160	-.160	-.210	-.050	-.230	-.240	-.270	-.160
-.060	-.030	-.010	.090	.160	-.060	.270	.450	.620	.540
.300	.410	.360	.150	.020	-.160	-.330	-.390	-.360	-.480
-.930	-.620	-.370	-.230	-.970	-1.060	-1.070	-1.130	-1.390	-1.190
-1.250	-1.270	-1.150	-1.120	1.030	-.930	-.800	-.720	-.730	-.880
-.510	-.590	-.450	-.260	-.230	-.290	-.130	-.300	-.290	-.280
-.000	-.100	-.090	-.040	-.120	-.200	-.320	-.190	-.170	-.110
-.120	-.040	-.140	-.080	-.020	-.010	-.110	-.170	-.270	-.110
-.150	-.130	.000	.020	.020	.010	.010	.070	-.070	-0.000
.100	0.000	-.120	.010	.030	.050	.090	.060	.170	.200
.200	.230	.260	.350	.190	-.010	.020	.070	-.230	-.030
.020	-.070	.010	.080	-.020	.010	-.010	-.140	-.220	-.050
-.130	.070	-.220	-.190	-.290	-.050	-.080	-.170	.010	-.030
.020	.110	.210	.250	.250	.090	.050	-.010	-.020	.190
.220	.150	.040	-.030	-.110	-.060	-.150	-.230	-.370	-.170
-.100	-.130	-.060	.040	.070	.040	.010	.040	.100	-0.000
.000	.030	-.030	.150	.160	.240	.250	.290	.180	.170
.060	.050	.070	.000	.090	-.090	-.020	-.130	-.150	-.120
-.140	-.330	-.610	-.640	-.870	-1.010	-.790	-.690	-.630	-.660
-.700	-.560	-.610	-.530	-.450	-.370	-.320	-.470	-.430	-.430
-.430	-.650	-.300	-.200	-.170	.100	.040	-.120	-.110	-.130
-.160	-.150	-.140	-.200	-.290	-.150	-.380	-.390	-.300	-.310
-.250	-.320	-.520	-.700	-.930	-.800	-.850	-1.020	-1.110	-1.070
-.400	-.460	-.470	-.740	-.650	-.390	-.270	-.210	-.270	-.190
-.010	.040	.330	.130	.020	.040	.040	.230	.300	.260
.220	.100	-.000	-.260	-.180	-.430	-.620	-.680	-.570	-.750
-.770	-.750	-.590	-.660	-.820	-.710	-.730	-.760	-.780	-.690
-.000	-.650	-.710	-.500	-.500	-.380	-.220	-.050	.050	-.010

TABLE XI (continued)

.[illegible]	.100	.170	-.[illegible]	.080	.100	.150	.130	-.160	-.160
-.030	.170	.210	.130	.170	.280	.060	.020	.100	.010
.110	.010	-.050	-.030	.030	-.050	-.210	-.250	-.220	-.150
.220	-.020	.120	.060	.220	.140	.040	-.120	-.190	-.310
-.[illegible]	-.270	-.270	-.320	-.260	-.060	.300	.310	.510	.500
.530	.500	.590	.630	1.150	1.310	1.450	1.250	1.150	1.100
.980	.[illegible]	.690	.910	.980	1.100	1.280	1.110	1.050	.870
.950	.830	.930	.610	.670	.720	.630	.450	.470	.450
.230	.200	.180	.010	.120	.040	.060	.190	.250	.230
.050	.120	.200	.250	.2[illegible]	.340	.210	.120	.290	.400
.[illegible]10	.540	.440	.450	.500	.550	.690	.650	.680	.690
.[illegible]46	.[illegible]78	.[illegible]50	.520	1.060	1.040	1.260	1.130	1.160	1.190
1.450	1.510	1.360	1.360	1.670	1.760	1.720	1.550	1.630	1.580
1.570	1.561	1.[illegible]00	1.410	1.640	1.670	1.660	1.660	1.940	1.790
1.720	1.661	1.7[illegible]	1.750	1.970	1.920	1.930	2.020	2.050	1.980
1.950	2.090	1.9[illegible]	1.790	1.920	1.990	1.940	1.860	1.680	1.580
1.610	1.581	1.520	1.630	1.600	1.570	1.540	1.380	1.290	1.300
1.440	1.340	1.260	1.090	1.080	.800	.760	.880	.930	1.050
1.[illegible]0	1.021	.920	1.130	1.120	.860	.800	.730	.590	.520
.[illegible]00	.060	.020	-.160	-.080	.030	.030	.140	.170	.250
.[illegible]0[illegible]	.060	-.010	.030	.130	.180	.060	.090	.140	.030
-.[illegible]66	-.[illegible]40	-.570	-.510	-.360	-.600	-.960	-.690	-.780	-.850
-.770	-.620	-.710	-.[illegible]80	-.820	-.840	-.920	-.950	-.880	-1.030
-1.[illegible]50	-.[illegible]90	-1.070	-1.070	-.930	-.670	-.610	-.430	-.270	-.290
-.[illegible]20	-.[illegible]30	-.[illegible]10	-.210	-.110	.060	.200	.370	.110	.060
-.[illegible]00	.[illegible]50	.170	.[illegible]40	.090	-.170	-.210	-.190	.040	.090
.230	.210	.130	.090	.070	-.010	.100	-.120	-.090	-.020
-.[illegible]30	.[illegible]10	-.[illegible]10	-.[illegible]30	-.140	-.240	-.350	-.100	-.260	-.160
.[illegible]30	.[illegible]11	.[illegible]11	.380	.550	.760	.860	.610	1.130	1.270
1.[illegible]50	1.[illegible]	1.290	1.280	1.260	1.120	1.040	.960	.960	.860
.[illegible]10	1.[illegible]50	.[illegible]90	.670	.790	.590	.630	.620	.420	.230
.[illegible]10	.[illegible]41	.[illegible]60	.370	.250	.120	.250	.410	.440	.470
.230	.[illegible]55	.[illegible]20	.[illegible]10	-.250	-.370	-.330	.050	.100	.100
.170	.[illegible]40	.[illegible]50	.110	.200	.110	.130	.210	.090	.090
-.[illegible]10	-.[illegible]70	-.[illegible]70	.050	.150	-.[illegible]80	.090	.210	.210	.290
.[illegible]00	.[illegible]70	.[illegible]10	.030	.070	-.040	.050	.050	-.200	.070

TABLE XI (continued)

.200	.240	.360	.440	.530	.690	.840	.720	.640	.540
.720	.850	.780	.870	.800	.650	.660	.740	.770	.740
.630	.400	.410	.440	.510	.620	.700	.880	.930	.830
.930	.870	.750	.780	.780	.730	.780	.800	.950	.880
.640	.700	.880	.810	.430	.540	.490	.570	.470	.540
.340	.340	.440	.430	.280	.200	.190	.270	.320	.330
.200	.300	.340	.090	0.000	-.210	-.280	-.560	-.580	-.270
-.040	.130	.190	.440	.330	.260	.460	.620	.790	.670
.690	.640	.750	.750	.670	.780	.950	1.020	.770	.680
.540	.450	.250	.250	-.040	.120	.070	-.130	-.170	-.170
-.280	-.230	-.050	.090	.320	.360	.310	.410	.300	.490
.480	.510	.490	.480	.520	.420	.490	.690	.630	.510
.580	.610	.640	.750	.540	.680	.550	.460	.260	.180
.130	.140	.200	.220	.200	.120	.040	-.060	.090	.180
.280	.400	.290	.440	.540	.460	.350	.320	.230	.270
.630	.520	.370	.350	.320	.250	-.020	.150	.220	.220
.150	.020	-.050	-.140	-.140	-.210	-.320	-.400	-.180	0.000
.260	.630	.680	.810	.810	.920	.910	.930	.860	.900
.810	.790	.690	.830	.760	.580	.450	.470	.340	.270
.100	.110	.040	-.110	-.060	-.180	-.190	-.140	-.250	.020
.030	.060	.030	-.070	-.130	-.140	-.120	-.150	-.260	-.210
-.140	0.000	.130	.150	.280	.190	.210	.110	-.040	-.090
-.180	-.350	-.310	-.580	-.570	-.510	-.480	-.640	-.760	-.790
-.740	-.700	-1.020	-1.020	-.840	-.860	-.850	-.820	-.900	-.920
-1.060	-1.140	-1.150	-1.000	-.940	-.810	-.700	-.840	-.750	-.750
-.690	-.680	-.870	-.980	-.840	-.900	-.750	-.630	-.640	-.610
-.400	-.590	-.470	-.530	-.540	-.350	-.410	-.480	-.320	-.170
-.190	-.130	-.120	.080	.030	.010	-.170	-.170	-.110	-.080
.010	.220	.330	.180	.150	.270	.230	.130	-.190	-.200
-.220	-.070	.040	.100	.140	.260	.460	.300	.230	.350
.320	.390	.420	.450	.300	.450	.410	.340	.200	.100
.220	.140	-.010	.040	.050	.010	.100	.090	.100	.050
.110	.270	.310	.440	.300	.300	.450	.470	.490	.510
.640	.590	.420	.350	.290	.270	.190	.100	.120	.130
-.070	.100	.010	.090	.080	.140	.160	.280	.390	.590
.550	.590	.770	.630	.620	.670	.730	.710	.540	.380

TABLE XI (continued)

.330	-0.000	-.080	-.130	-.230	-.380	-.400	-.280	-.010	.230
.200	.360	.220	.320	.650	.550	.450	.320	.390	.360
.360	.400	.420	.470	.450	.690	.630	.670	.730	.730
.600	.620	.460	.310	.190	.050	-.140	-.160	-.010	-.020
-.030	-.070	-.130	-.250	-.320	-.410	-.460	-.180	-.200	-.220
-.170	-.020	.020	.010	.140	.290	.100	.300	.230	.280
.300	.440	.290	.330	.140	.010	.030	.100	.180	.370
.200	.140	.020	.040	-.070	-.030	-.140	.200	-0.000	-.010
-.270	-.140	-.160	.010	.200	.120	.140	.100	.070	.300
.230	.450	.650	.540	.700	.720	.840	.780	.740	.650
.890	.950	.770	.660	.630	.690	.730	.740	.820	.760
1.070	1.000	.890	.840	.670	.580	.680	.690	.800	.760
.890	.710	.800	.850	.840	.850	1.030	.940	.890	1.030
1.070	1.130	.970	.920	.990	.950	.930	.930	1.090	1.000
1.040	1.130	1.140	1.080	.700	.610	.490	.550	.620	.490
.650	.750	.750	.570	.550	.530	.550	.490	.410	.310
.130	.090	.070	.350	.350	.290	.410	.300	.240	.340
.340	.570	.540	.520	.470	.380	.300	.400	.260	.250
.180	.350	.220	.260	.320	.160	.100	.080	.030	.090
.130	.040	-.040	-.300	-.340	-.420	-.540	-.560	-.420	-.430
-.100	-.060	-.020	-.140	-.210	-.170	-.240	-.180	-.050	.230
.230	.330	.450	.490	.410	.260	.390	.370	.280	.060
-.130	-.230	-.240	-.180	-.010	-.080	-.270	-.080	-.080	.140
.090	.110	.030	.030	-.070	.030	-.020	.020	-.110	-.180
-.150	-.150	-.020	-.030	.090	.160	.060	.110	.260	.190
.040	-.080	.060	.090	.120	.010	-.010	.030	-.190	-.230
-.210	-.200	-.220	-.150	-.320	-.120	-.010	.100	.030	-.010
.040	.120	.120	.190	.380	.430	.230	.190	.150	.100
.250	.100	-.100	-.330	-.100	.020	-.080	-.030	-.190	-.240
-.290	-.110	0.000	-.170	-.040	.020	.110	.230	.110	.100
.160	.130	-.040	-.150	-.310	-.310	-.230	-.170	-.100	-.020
-.080	-.100	-.060	.060	.190	.030	-.040	-.020	-.100	-.010
-.110	.180	.340	.280	.300	.310	.240	.030	.030	.180
.280	.140	.030	.030	-.030	-.040	-.110	-.280	-.350	-.400
-.280	-.230	.400	-.230	-.010	-.090	-.130	.070	-.060	.130
.260	.060	.140	.060	.120	.010	-.130	-.240	-.280	-.070

TABLE XI (continued)

-.110	.070	-.090	.200	.220	.100	.170	.160	.090	.180
.210	.230	.250	.150	.050	-0.000	.140	.030	.060	.140
-.070	-.200	-.100	-.150	-.210	-.350	-.360	-.340	-.300	-.130
-.420	-.300	-.300	-.290	-.080	.020	-.040	.050	.050	.230
.270	.290	.170	.410	.490	.270	.060	.080	.130	.130
-.150	-.240	.050	-.010	.120	.050	-.080	.150	.250	.210
.150	.180	.040	-.030	-.010	.260	.030	.210	.170	.150
.150	.200	.120	.110	.150	.350	.340	.370	.380	.420
.430	.520	.590	.640	.740	.780	.850	.750	.770	.670
.680	.530	.750	.750	.890	.620	.820	.770	.750	.650
.560	.390	.290	.380	.300	.180	-.040	-.160	.010	.140
.340	.410	.310	.250	.280	.210	-.100	-.030	.160	.220
.280	.350	.110	-.020	-.190	-.280	-.110	-.160	.010	-.090
-.070	.020	.140	.120	.060	-.040	.010	.130	.050	.030
.190	.090	.100	-.060	-.130	-.210	-.220	-.250	-.110	-.080
-0.000	.130	.110	.040	-.150	-.120	-.110	-.100	-.160	-.090
-.220	-.280	-.250	-.310	-.480	-.450	-.610	-.650	-.740	-1.000
-.940	-.700	-.700	-.830	-.790	-.780	-1.020	-.850	-.640	-.800
-.740	-.630	-.620	-.550	-.440	-.300	-.030	.190	.090	.190
.240	.270	.250	.090	0.000	-.070	-.090	.060	.240	.210
.240	.250	.160	.170	.050	.050	.040	-.100	-.080	-.010
-.260	-.270	-.310	-.460	-.400	-.370	-.280	-.410	-.250	-.100
-.180	.070	.320	.290	.300	.140	.330	.210	.180	.230
.360	.380	.350	.480	.500	.600	.550	.640	.700	.640
.400	.350	.270	.500	.590	.510	.510	.490	.600	.650
.510	.590	.490	.320	.190	.150	.090	.040	-.230	-.300
-.320	-.220	-.210	-.110	.050	-.130	-.130	-.140	.310	.220
.230	-0.000	.080	.270	.320	.120	.200	.320	.390	.490
.410	.460	.390	.330	.390	.420	.360	.310	.320	.330
.260	.220	.100	.230	.380	.340	.210	.100	-.040	-.230
-.320	-.650	-.530	-.370	-.450	-.730	-.740	-.780	-.730	-.800
-.950	-1.000	-.900	-.800	-.690	-.520	-.410	-.110	.070	.070
.020	.050	.270	.380	.590	.430	.140	.170	-0.000	.070
.070	-.060	-.340	-.410	-.610	-.900	-.810	-.950	-.960	-.900
-.920	-.790	-.910	-.840	-.760	-.750	-.600	-.500	-.510	-.570
-.750	-.700	-.790	-.600	-.480	-.350	-.270	-.090	-.200	-.250

TABLE XI (continued)

-.110	-.120	-.030	.100	.140	.060	.070	-.090	-.150	-.120
-.300	-.390	-.470	-.300	-.210	-.400	-.230	-.210	-.110	-.260
-.370	-.360	-.360	-.340	-.420	-.590	-.640	-.840	-.920	-.860
-.860	-1.010	-.830	-.900	-.740	-.570	-.840	-.830	-.900	-.930
-.870	-.950	-.950	-.990	-1.140	-1.110	-1.100	-.980	-1.050	-.960
-.760	-.880	-.940	-.830	-.840	-.890	-1.030	-1.140	-1.090	-1.030
-.880	-.760	-.820	-.830	-.850	-.720	-.690	-.710	-.610	-.520
-.570	-.510	-.550	-.590	-.630	-.760	-.990	-.790	-.570	-.660
-.660	-.470	-.390	-.560	-.460	-.330	-.300	-.300	-.210	-.290
-.220	-.240	-.200	-.110	-.010	-.130	-.020	-.090	-.160	-.140
.080	.060	.130	.270	.490	.620	.710	.800	.830	.870
1.000	.990	1.080	1.120	.920	.700	.740	.560	.430	.280
.130	-.070	-.110	-.080	-.110	.020	.250	.150	.150	-.030
-.130	-.330	-.410	-.540	-.390	-.380	-.410	-.370	-.490	-.540
-.610	-.980	-.910	-.850	-.860	-.730	-.770	-.730	-.560	-.560
-.490	-.570	-.450	-.370	-.230	-.270	-.430	-.400	-.610	-.260
-.370	-.340	-.410	-.560	-.300	-.320	-.080	-.070	-.080	-.080
-.040	.020	.070	.170	.180	.100	.150	.030	-.260	-.260
-.210	-.220	-.070	.010	-.110	-.120	-.230	-.260	-.100	-.090
-.240	-.260	-.180	-.410	-.260	.010	.140	.060	.020	.020
.160	.290	.380	.460	.340	.370	.480	.500	.590	.620
.510	.340	.090	.160	-.020	-.050	-.020	.160	.180	.200
.250	.310	.360	.200	.370	.280	.390	.280	.190	.440
.410	.150	.230	.150	.030	-.080	-.110	-.240	-.210	-.190
-.070	-.130	.010	.100	.070	.100	.080	.130	.170	.150
.120	.060	.140	.250	.240	.200	.170	.070	.210	.030
.030	.050	.010	-.190	-.300	-.180	-.380	-.230	-.420	-.540
-.560	-.740	-.720	-.820	-.930	-.720	-.750	-.730	-.770	-.670
-.820	-.880	-.790	-.970	-.740	-.850	-.920	-.860	-.820	-.870
-.840	-.730	-.630	-.710	-.720	-.420	-.390	-.450	-.440	-.460
-.480	-.690	-.480	-.390	-.430	-.350	-.470	-.570	-.420	-.270
-.280	-.420	-.350	-.470	-.470	-.240	-.190	-.190	-.240	-.310
-.120	-.100	.030	.060	0.000	-.130	.040	.110	-.020	-.010
-.030	.120	.230	.250	.240	.210	.140	.220	.020	-.030
-.060	.010	.080	.260	.380	.430	.480	.370	.340	.280
.310	.320	.260	.200	.300	.200	.120	0.000	.170	.330

TABLE XI (continued)

.550	.420	.690	.750	.730	.630	.530	.220	.070	.180
.180	.270	.330	.300	.170	.150	.060	.200	.070	.070
.270	.130	.040	-.060	-.120	.070	-.050	-.110	.010	.020
.150	.040	-.120	-.200	.030	.210	.200	.050	-.180	-.230
-.240	-.240	-.100	-.090	-.030	-.040	.020	.010	-.030	-.050
.080	.230	.200	.200	.150	.310	.080	-.020	-.050	-.060
0.000	-.130	-.220	-.160	-.050	.070	-.070	.040	.210	.250
.060	.090	.240	.270	.420	.470	.290	.240	.200	.300
.360	.110	-.050	-.150	-.080	.090	-.030	-.260	-.330	-.370
-.390	-.320	-.150	-.270	-.080	-.050	.010	-.030	-0.000	.110
.140	-.030	-.110	-.270	-.160	-.130	-.070	.090	0.000	-.040
-.210	-.080	-.040	.100	.130	.300	.250	.220	.420	.400
.380	.280	.270	.150	.100	-.080	-.140	-.200	-.160	.020
.090	.120	.020	-.080	-.220	-.280	-.320	-.260	-.190	-.090
-.080	-.080	0.000	-.130	-.130	-.290	-.100	-.110	-.340	-.120
.060	.100	.160	.270	.040	.030	.140	.200	.460	.320
.300	.200	.040	.160	.200	.090	.090	.220	.040	-.060
-.210	-.360	-.280	-.250	-.180	-.110	.020	-.040	-.220	-.240
-.280	-.120	-.060	.050	.040	.060	.160	.250	.290	.350
.290	.310	.050	.050	.040	0.000	-.220	-.310	-.330	-.330
-.170	-.140	-.240	-.060	-.060	.220	.280	.260	.170	-.030
-.170	-.190	-.180	-.240	-.080	-.040	.210	.120	.090	.240
.210	.070	.050	.050	.050	.050	.160	0.000	-.070	.090
.010	-.090	.070	-.020	.090	.060	-.090	-.030	-.210	-.230
-.230	-.270	-.220	-.220	-.100	-.220	-.280	-.170	.040	.010
-.190	-.040	.030	.090	.090	.260	.260	.360	.360	.230
.270	.190	.130	.200	.170	0.000	.050	.020	.070	.010
.020	-.190	-.120	-.170	-.150	-.140	-.040	-.180	-.150	-.250
-.020	.080	.120	.240	.290	.550	.660	.650	.640	.630
.510	.370	.310	.510	.590	.590	.490	.670	.640	.580
.610	.590	.720	.910	.960	.900	.960	1.070	.850	.940
.990	1.030	1.080	.860	.770	.750	.280	.420	.260	.380
.500	.540	.330	.450	.560	.610	.520	.530	.600	.630
.510	.370	.230	.170	.150	.190	.030	.020	0.000	.010
-.040	-.190	-.330	-.260	-.380	-.400	-.320	-.350	-.330	-0.000
-.030	.020	.250	.380	.490	.490	.250	.250	.090	-.150

TABLE XI (continued)

.010	.040	.090	-.120	.010	-.080	-.090	-.150	-.250	-.300
-.200	-.020	.010	.180	.100	-.020	-.040	-.060	-.150	-.140
-.120	-.100	-.200	.050	-.070	.060	.130	.090	.130	.290
.480	.440	.200	.150	.080	.020	0.000	-.080	-.030	.250
.190	.030	-.030	-.180	-.280	-.330	-.140	-.060	-.220	-.140
-.140	-.090	.090	.080	-.070	-.050	-.140	-.200	-.330	-.270
-.120	-.150	-.160	-.080	-.080	.230	.120	.380	.360	.530
.520	.280	-.060	.020	.060	.040	.020	.060	-.050	-.130
-.010	.070	.110	.120	.040	.060	-.040	-.240	-.180	-.130
-.080	0.000	-.160	-.110	-.060	-.150	-.020	.010	-.050	-.120
-.040	.020	-.080	-.100	-0.000	-.140	-.210	-.180	.020	.210
.030	.050	-.060	-.050	.140	.120	.090	.060	.010	-.070
-.020	.180	.270	.300	.420	.260	.190	.130	.140	.190
.160	.130	.090	-.010	-.040	-.260	-.320	-.240	-.270	-.270
-.240	-.260	-.300	-.120	-.270	-.080	-.030	-.110	-.280	-.150
-.090	-.060	.060	.120	.150	-.050	.200	.170	.130	.180
.940	.090	.310	.320	.390	.370	.190	.140	-.020	-.040
-.030	-.040	.040	-.010	-.030	.180	.100	-.150	-.260	-.300
-.210	-.250	-.190	-.240	-.250	-.200	-.220	-.110	-.070	-0.000
-0.000	-.100	-.030	-.100	.030	.180	.240	.130	.110	-.180
-.220	-.060	-.140	.020	.050	-.010	.060	.300	.200	.290
.180	.270	-.140	-.080	-.090	.060	.210	.210	.250	.180
.130	.140	.310	.330	.190	.130	.210	.200	.210	.010
.100	.200	-.070	-.220	-.110	-.280	-.290	-.290	-.200	-.310
-.230	-.170	.090	.130	.310	.670	.550	.540	.540	.730
.330	.840	1.060	1.170	1.120	.910	.810	.890	.820	1.010
.970	1.020	.750	.720	.590	.390	.260	.600	.760	.830
.910	.940	.960	1.080	1.070	1.180	1.180	1.050	.980	.990
.990	1.020	.810	.510	.510	.510	.500	.550	.580	.580
.430	.610	.370	.280	.130	0.000	-.220	-.270	-.230	-.130
-.180	-.090	-.110	-.380	-.180	-.190	-.330	-.190	-.090	.130
.310	.280	.210	.220	.390	.420	.110	.010	-.040	-.020
.020	-.160	-.160	-.060	.120	.260	.320	.170	.200	.060
.070	.250	.130	.090	-.030	-.170	-.260	-.270	-.110	-.140
-.110	-.250	-.200	-.190	-.170	-.170	-.280	-.180	-.260	-.160
-.090	-.020	.050	.100	.140	.120	.130	.160	.060	.100

TABLE XI (continued)

.220	.110	.230	.250	.160	.110	.180	.050	.150	.090
.050	-.010	-.120	-.060	.090	.160	.110	.120	0.000	-.070
-.090	-.010	-.220	-.290	-.360	-.340	-.150	-.120	-.210	-.180
-.160	-.050	.020	-.210	-.010	-.090	-.210	-.230	-.080	.070
.220	.300	.160	.230	.220	.090	.150	.140	.260	.200
.090	.040	-.010	-.010	-.070	-.030	-.050	.180	-.100	-.040
.040	-0.000	.240	.190	.110	.060	-.040	-.140	-.230	-.210
-.250	-.460	-.310	-.220	0.000	0.000	.120	-.070	-.050	-.030
-.130	-.190	-.060	-.100	.070	-.050	-.020	.080	.270	.170
.160	.100	.230	.210	.120	.140	.140	.170	.060	.080
.140	.120	-.020	.020	0.000	-.100	.080	-.040	-.070	-.060
-.110	-.070	.050	.180	.150	.110	-0.000	.190	.090	.200
-.030	-.130	-.200	-.330	-.210	-.100	-.030	.130	.190	.300
.400	.420	.250	-.040	-.030	-.030	.020	.020	-.060	-.200
-.150	-.020	-.060	-.130	-.150	-.090	-.160	-.250	-.140	-.030
.140	.210	.230	.150	.250	.150	.030	-.030	.050	.040
-.050	-.190	-.060	-.120	.030	-.060	0.000	.150	-.050	-.050
0.000	-.180	-.120	-.130	-.230	-.150	-.190	-.120	-.220	-.150
.050	-.020	.140	.240	.280	.130	.120	.170	.320	.140
-.040	.020	-.010	.130	.090	.160	.270	.170	.080	.160
.240	.140	.010	.140	-.060	-.270	-.250	-.390	-.550	-.490
-.500	-.650	-.540	-.570	-.540	-.380	-.430	-.510	-.480	-.570
-.620	-.640	-.800	-.830	-.820	-.730	-.690	-.680	-.650	-.670
-.520	-.400	-.250	-.480	-.500	-.540	-.530	-.260	-.390	-.280
-.290	-.430	-.410	-.350	-.260	-.260	-.280	-.410	-.390	-.350
-.410	-.510	-.490	-.310	-.220	-.270	-.230	-.220	-.070	-.060
.110	-.140	-.180	-.200	-.150	.010	.030	-.020	.100	.180
.170	.140	.230	.310	.250	.090	-0.000	.080	.120	.320
.300	.230	.080	.030	.020	.020	-.070	0.000	-.030	-.140
-.140	-.290	-.230	-.180	.020	-.130	-.040	0.000	-.010	.010
.130	-.160	-.140	.090	.170	.060	0.000	-.060	-.100	-.100
-.260	-.100	-.010	-.090	-.090	-.240	-.350	-.370	-.130	.160
.190	.420	.320	.310	.260	.200	.120	.040	.160	.240
.310	.280	.340	.160	.090	.160	.020	-.010	-.270	-.270
-.190	-.220	-.400	-.330	-.500	-.570	-.460	-.340	-.340	-.150
-.130	.030	.100	.120	.190	.060	.210	.300	.380	.480

TABLE XI (continued)

.290	.120	.180	.130	-.300	-.340	-.200	-.150	-.210	-.240
-.220	-.170	-.120	-.180	.080	.210	.160	.100	.200	.340
.410	.340	.270	.160	.130	.080	.140	.210	.260	.050
.040	.140	.210	.220	.230	-.100	-.220	-.180	-.220	-.170
-.250	-.150	-.180	-.180	-.260	-.220	-.320	-.160	-.100	-.110
-.160	-.130	-.140	-.190	-.180	-0.000	.170	.330	.270	.150
.100	.120	.260	.270	.150	.250	.320	.230	.210	.390
.130	.110	-.070	-.160	-.120	-.270	-.150	-.200	-.110	-.250
-.300	-.020	-.220	-.180	-.060	.020	.080	.080	-.010	.040
.080	.110	.110	.140	.260	.120	.070	-.050	.040	-.100
-.150	-.120	-.190	-.280	-.360	-.170	.080	.020	-.060	.080
.070	-.100	-.040	-.080	.110	.150	.280	.280	.170	.080
.100	.070	.010	-.010	.010	.060	-.120	-.240	.030	-.140
-.140	-.310	-.340	-.280	-.010	.200	.320	.180	.220	.240
.270	.310	.140	-.020	-.330	-.210	-.260	-.220	-.030	-.190
-.210	-.140	-.100	-.090	-.230	-.200	-.030	-.010	-.040	-.070
-.140	-0.000	.260	.160	.110	.160	-.040	-.040	-.170	-.240
-.180	-.230	-.110	-.230	-.080	-.250	-.250	-.260	-.180	.020
.070	0.000	.100	-.110	-.330	-.370	-.540	-.650	-.500	-.630
-.700	-.500	-.470	-.210	-.140	.020	.110	.270	.210	.240
.090	.010	.020	.010	.100	.110	.050	.040	-.080	-.190
-.220	-.170	-.200	-.250	-.270	-.280	-.230	-.220	-.250	-.370
-.510	-.570	-.720	-.660	-.630	-.480	-.570	-.440	-.640	-.630
-.530	-.600	-.590	-.580	-.580	-.660	-.770	-.840	-1.030	-1.120
-1.030	-.950	-.900	-.810	-.870	-.930	-.810	-.820	-.750	-.960
-.900	-.730	-.750	-.570	-.520	-.590	-.420	-.470	-.380	-.310
-.910	-.910	-.910	-.690	-1.000	-1.090	-1.010	-.950	-.910	-.700
-.500	-.470	-.640	-.410	-.230	-.330	-.090	-.050	-.080	.090
.070	-0.000	-.030	.030	.120	.160	.310	.230	.300	.450
.960	.140	.180	.010	-.170	-.030	-.310	-.290	-.500	-.530
-.630	-.550	-.300	-.390	-.440	-.410	-.260	-.350	-.330	-.430
-.450	-.270	-.190	-.230	-.170	-.170	-.370	-.500	-.430	-.400
-.270	-.390	-.360	-.430	-.410	-.570	-.580	-.730	-.730	-.590
-.730	-.640	-.620	-.590	-.600	-.560	-.550	-.570	-.450	-.530
-.410	-.630	-.570	-.730	-.890	-.750	-.720	-.780	-.990	-.980
-.940	-.710	-.810	-.590	-.670	-.470	-.220	-.060	-.100	-.140

TABLE XI (continued)

-.140	-.120	-.170	-.070	.030	.120	.150	.050	.120	.070
.040	-.140	-.130	-.110	-.180	-.070	-.300	-.200	-.180	-.360
-.470	-.470	-.470	-.380	-.180	-.100	-.180	-.240	-.050	.030
-.230	-.480	-.510	-.470	-.280	-.230	-.210	-.190	-.080	.140
.030	.180	.240	.220	.160	.090	.050	.070	.190	.290
.290	.240	.170	.460	.470	.440	.520	.480	.390	.320
.380	.250	.410	.610	.690	.700	.790	.740	.850	.770
.510	.380	.230	-.080	.090	.010	.120	.090	.070	.030
.100	-.020	-.050	-.050	.020	.070	-.030	-.240	-.160	-.110
.060	.050	.100	-.030	-.120	-.090	-.010	-.060	-.010	-.010
.140	.020	.170	.170	.210	.110	.020	-.080	-.010	-.030
-0.000	-.070	-0.000	.050	.090	.160	.150	.010	.040	-.050
.120	.430	.520	.440	.500	.480	.470	.410	.350	.320
.350	.430	.360	.350	.200	.300	.180	.230	.380	.330
.350	.130	.060	.270	.260	.300	.070	.020	.060	-.100
-.160	-.230	-.170	-.110	0.000	.180	-.380	-.160	-0.000	.280
.250	.240	.040	.200	.500	.330	.260	.190	.350	.280
.050	.240	-0.000	-.060	.070	.030	.050	.040	-.090	.060
.110	.100	.100	-.080	-.120	.030	-.060	.010	-.160	-.200
-.140	-.270	-.070	-.170	-.120	-.130	-.150	-.130	.190	-.150
-.240	-.570	-.440	-.520	-.300	-.460	-.480	-.480	-.440	-.580
-.500	-.600	-.510	-.460	-.430	-.310	-.320	-.120	.050	.070
.010	-.020	-.060	-.140	-.120	-.080	-.020	-.170	-.160	-.190
-.170	-.160	-.220	-.130	-.080	-.240	-.280	-.400	-.230	-.050
.120	.140	-.030	-.120	-.120	-.110	-.160	-.170	-.220	-.090
-.060	-.050	-.030	.270	.220	.200	.190	.130	.140	.050
-.030	.140	.220	.060	.060	-.060	-.020	-.060	-.110	.210
.340	.310	.210	.060	-.030	-.130	-.190	-.160	-.240	-.400
-.280	-.260	-.500	-.520	-.530	-.530	-.410	-.350	-.180	-.060
-.250	-.210	-.400	-.550	-.550	-.450	-.530	-.470	-.490	-.290
-.210	.050	.200	.310	.200	.260	.250	.170	.050	.040
.050	.010	.210	.180	.220	-.060	-.140	-.130	-.080	-.300
-.180	-.190	-.140	-.250	-.300	-.110	.090	.100	.080	-.020
.030	.090	.190	.050	.050	-.130	-.230	-.190	-.040	-.170
-.270	-.320	-.520	-.620	-.720	-.860	-.850	-.860	-.990	-1.080
-1.030	-1.190	-1.220	-1.140	-1.000	-1.010	-.910	-.880	-1.010	-.980

TABLE XI (continued)

-1.050	-1.090	-1.230	-1.130	-1.020	-1.060	-.940	-.890	-.920	-.930
-.970	-1.030	-1.120	-1.170	-1.130	-1.250	-1.250	-1.140	-1.080	-.920
-.910	-1.020	-.990	-.850	-.840	-.960	-1.060	-.950	-.670	-.760
-1.040	-.880	-.760	-.870	-.660	-.610	-.510	-.300	-.050	-.010
.070	.190	.260	.370	.480	.410	.500	.320	.330	.380
.420	.320	.380	.310	.430	.480	.250	.040	.150	.060
-.030	-.070	-.250	.030	.110	.170	.140	.270	.050	-.060
0.000	-.050	-.170	-.250	-.460	-.560	-.640	-.640	-.610	-.700
-.690	-.710	-.520	-.350	-.180	-.300	-.140	-.130	.130	.040
-.030	.040	.240	.140	.210	.120	.060	-.020	-.040	-.090
-.080	-.010	.020	.040	.050	-.140	-.010	.090	-.020	-.180
-.150	-.010	.140	.210	.380	.270	.140	-.070	.060	.170
.150	.480	.410	.330	.400	.230	.190	.230	.490	.260
.190	.100	.060	-0.000	-.150	-.030	.200	.370	.520	.530
.370	.230	.270	.100	.020	.140	.310	.290	.240	.350
.410	.510	.450	.640	.460	.400	.190	.350	.210	.130
.210	.140	.190	.120	-.010	-.230	-.300	-.300	-.240	-.420
-.700	-.590	-.670	-.360	-.260	-.470	-.590	-.540	-.300	-.300
-.410	-.310	-.390	-.300	-.320	-.410	-.450	-.600	-.570	-.440
-.380	-.260	-.090	-.020	-.110	-.010	-.070	-.240	-.220	-.340
-.130	-.180	-.140	-.170	-.150	.050	.050	-.070	-.020	-.210
-.290	-.270	-.210	-.270	-.480	-.390	-.370	-.320	-.480	-.480
-.610	-.540	-.420	-.560	-.510	-.420	-.320	-.550	-.430	-.450
-.340	-.280	-.330	-.370	-.280	-.280	-.410	-.460	-.350	-.510
-.460	-.530	-.430	-.690	-.600	-.770	-.780	-.580	-.600	-.600
-.600	-.670	-.580	-.400	-.220	-.200	-.140	-.120	-.360	-.430
-.330	-.410	-.510	-.450	-.430	-.430	-.380	-.310	-.090	-.190
-.350	-.330	-.340	-.300	-.330	-.190	-.180	-.080	-.140	-.180
-.090	-.020	-.100	.110	.030	.090	0.000	.110	.160	.120
.210	.190	-.040	.050	.200	.230	.180	.210	.200	.210
.170	.150	-.130	-.110	-.110	-.250	-.280	-.300	-.040	-0.000
.010	-.050	-.080	-.030	-.030	-.210	-.050	-.010	-.010	0.000
-.040	-.140	-.140	-.260	-.340	-.420	-.380	-.470	-.590	-.490
-.290	-.430	-.560	-.550	-.570	-.590	-.600	-.670	-.810	-.680
-.620	-.500	-.410	-.280	-.090	.070	.010	-.100	-.190	-.040
-.900	.030	.040	.090	-0.000	.150	.190	.150	.080	.160

TABLE XI (concluded)

.150	.290	.090	.010	.040	.150	.210	.110	.110	-.010
.120	.150	-.200	-.150	-.030	-.090	-.120	-.020	-.040	-.090
-.300	-.200	-.160	-.330	-.150	-.130	-.240	-.390	-.440	-.690
-.540	-.450	-.550	-.390	-.310	-.170	-.100	-.130	.060	-.040
-.170	-.110	0.000	-.030	.040	.020	-.150	-.230	-.390	-.160
-.190	-.170	-.340	-.450	-.470	-.590	-.430	-.350	-.150	-.060
.070	.070	.100	.110	-.040	-.100	.010	-.100	-.160	-.170
-.200	-.240	-.130	-.250	-.180	-.140	-.270	-.370	-.270	-.360
-.180	-.220	-.090	-.100	-.140	-.220	-.410	-.260	-.030	-.030
-.090	-.140	-.130	-.230	-.250	-.250	-.190	-.150	-.110	-.120
-.150	-.230	-.170	.010	.080	.070	.070	-.310	-.280	-.210
-.270	-.280	-.280	-.160	.090	.030	.130	.140	.250	.270
.250	.360	.360	.360	.520	.520	.610	.740	.720	.660
.550	.760	.620	.620	.420	.170	.090	.020	-.130	-.230
-.080	-.310	-.180	-.330	-.480	-.640	-.570	-.550	-.470	-.540
-.310	-.320	-.350	-.360	-.230	-.430	-.710	-.880	-.710	-.730
-.700	-.840	-.920	-1.120	-1.230	-1.160	-1.220	-1.230	-1.160	-1.060
-1.050	-.900	-.880	-.550	-.720	-.890	-.860	-.680	-.720	-.700
-.720	-.440	-.260	-.160	.040	.080	.140	.410	.230	.320
.240	.120	-.170	-.420	-.540	-.770	-.600	-.670	-.760	-.720
-.630	-.570	-.540	-.660	-.590	-.660	-.740	-.770	-.880	-.700
-.560	-.190	-.120	-.010	.010	-.040	.050	.030	.090	.250
.310	.110	-.100	.080	-.190	-.100	-.150	-.250	-.160	-.250
-.450	-.450	-.440	-.280	-.190	-.390	.030	.040	.050	.020
.060	-.060	-.060	.170	.170	.220	.320	.170	.200	.280
.340	.330	.240	.190	220	.260	.180	.330	.160	-.010
.010	.080	0.000	-.160	-.230	-.230	-.270	-.060	.010	-.100
.030	.170	.420	.420	.480	.390	.340	.200	.310	.280
.300	.140	.140	.150	.130	.350	.370	.560	.420	.530
.420	.500	.360	.230	.080	.260	.220	.250	.200	.260
.390	.310	.130	.060	-.030	-.020	-.030	-.120	-.220	-.150
-.220	-.390	-.410	-.270	-.100	-.030	-.200	-.110	-.090	-.060
-.140	-.110	.100	.220	-.010	.070	.060	-.010	-.070	-.100
-.200	-.160	.090	.230	.350	.220	.010	.080	.190	-.100

4.2 OTHER USES OF SIMULATION PROGRAM

The program written to generate simulated runway profiles can be altered to perform simulations of many different types of runways. Any PSD may be input to that portion of the program which generates data from the PSD. The sample result uses a linear PSD to generate data with wavelengths of 100 ft down to one foot, however, this could easily be changed to: 1) cover a different band of wavelengths, 2) represent a PSD with a different slope or RMS, or 3) input any given PSD from cards. The method of generating discrete long wavelength peaks could also be altered to: 1) generate a given number of peaks, 2) generate a profile containing specific peaks at specific places on the profile, or 3) eliminate the generation of long wavelength peaks completely.

SECTION 5
SUMMARY AND CONCLUSIONS

Runway elevation profiles of 40 lines of data from 14 runways were analyzed to achieve two objectives: 1) to determine and evaluate significant characteristics of runway profiles with respect to their influence as dynamic excitation of aircraft and 2) to develop a method for generating simulated runways which have these significant characteristics. To achieve these joint objectives, runway elevation profiles of 40 lines of data from 14 runways were assumed to be a representative sample of the population of all runways of interest and analyzed with both objectives in view.

The grades present in the raw data were first removed by a digital high-pass filter with a maximum cutoff wavelength of 500 ft. The resulting profiles were shown to be both nonstationary and nongaussian. The failure of the profiles to meet these basic assumptions provides one explanation for the failure of the statistical approach to the prediction of the response and also precluded the possibility of generating a simulated runway by modeling in the frequency domain over all wavelengths less than 500 ft. Further analysis of the causes of nonstationarity and non-gaussianness indicated that to a large extent they are the result of the larger wavelength undulations of the profiles.

The data were again high-pass filtered with a reduced maximum wavelength of 100 ft and for these new profiles the degree of stationarity and gaussianness was significantly better than for the profiles filtered at 500 ft. Since the shorter wavelength profiles have a smaller intensity (RMS) than the longer wavelength profiles, the effects of nonstationarity and nongaussianness in a characterization of a runway with all wavelengths up to 500 ft would be minor. Therefore, a compound characterization was derived wherein the wavelengths less than 100 ft are modeled in frequency domain and the longer wavelengths are modeled in a discrete fashion by

means of the distributions of primary peaks per 1000 ft and the joint distribution of wavelengths and amplitudes of the primary peaks. Finally, a method is presented for generating a simulated runway which has the properties of the compound characterization of the actual profiles.

It should be stressed that the PSD plot shown in Figure 19 is for the filtered, simulated runway. As can be seen in this plot, the region greater than one hundred feet is greatly attenuated. The filter attenuates all amplitudes with a wavelength greater than one hundred feet and this PSD plot is only valid for wavelengths less than one hundred feet.

The runway profile elevations presented in Table XI merely demonstrates the use of the technique developed in this study and they are not intended for aircraft design purposes.

APPENDIX I

DIGITAL FILTERING CONCEPTS

The digital filtering process consisted of subtracting the low frequency mean, obtained by applying a low-pass filter to the original data, from the original data. This yields data which has been high-pass filtered and has a zero mean. The equation illustrating the high-pass filter operation is

$$\tilde{x}_d = x_d - x_d^* \tag{3}$$

where

x_d is the sampled input

x_d^* is the output of the low-pass filter

$\tilde{x}_d$ is the final high-pass filtered data

The low-pass filtering operation for equi-spaced intervals, Δd, is given as

$$x_d^* = \sum_{n=-N}^{N} h_n \, x_{(d+n\Delta d)} \tag{8}$$

where

h_n are the 2N+1 filter weights

$x_{(d+n\Delta d)}$ are the input data samples

x_d^* are the output data samples

Δd is the distance between samples

The filter shape chosen is attributed to Martin and Graham who developed it independently (References 3 and 4). The weights for this filter are computed from

$$h_n = \frac{1}{2\pi n\Delta d}\left(\frac{\sin 2\pi(f_c + \Delta f)n\Delta d + \sin 2\pi f_c n\Delta d}{1 - 4(\Delta f n\Delta d)^2}\right) \tag{9}$$

where

$n \pm 1, \pm 2, \ldots \pm N$

f_c is the cutoff frequency

Δf is the roll-off frequency

and $h_{n=0} = 2f_c + \Delta f$

Certain trends given as general polynomial forms and considered as desirable data components require constraints on the basic weights in order to pass without error. If the function does contain a polynomial content, it is not band limited and should be constrained so that the sample values of the polynomial content are passed without error. Therefore, to prevent trend type errors, constraints must be applied to the weighting function to satisfy

$$\frac{d^k H(f)}{df^k} = 0 \Big|_{f=0} \quad \text{for} \quad k \geq 1$$

$$= 1 \Big|_{f=0} \quad \text{for} \quad k = 0 \tag{10}$$

For $k = 0$ as in the case with the Martin-Graham filter, this is accomplished by normalizing the weights so that

$$\sum_{n=-N}^{N} h_n = 1 \tag{11}$$

Therefore, the normalized weights are computed from

$$\bar{h}_n = \frac{h_n}{\sum_{i=-N}^{N} h_i} \tag{12}$$

This forces the transfer function to have unity gain at zero frequency. It should be noted that $h_{-n} = h_n$, so that only weights for positive n need be computed.

Application of the digital filter involves the selection of f_c, Δf and N. Too small a Δf or too small a value of N will cause excessive overshoot at the filter corner frequencies. In extreme cases, this overshoot can carry through a wide range of the spectrum. The sampling frequency, $f_s = 1/\Delta d$, must be greater than twice the highest significant frequency present in the data to prevent aliasing. However, too large a value of f_s will reduce the distance width of the filter weighting function. The only remedy is to increase N, which is usually impractical, or to decrease f_s. This is accomplished by pre-filtering the data through a low-pass filter that has

$$f_{c_1} \geq f_{c_2}$$

$$f_{s_2}/2 \geq (f_{c_1} + \Delta f_1)/2 + (f_{c_2} + \Delta f_2) \tag{13}$$

where

f_{c_1} = cutoff frequency of the preliminary low-pass filter

f_{c_2} = cutoff frequency of the final low-pass filter

Δf_1 = the prelininary filter roll-off

f_{s_2} = the sampling frequency of the data to the final low-pass filter

Δf_2 = the final filter roll-off

The requirements of the initial filter were that the frequencies to be passed by the final low-pass filter remain unchanged and that the gain of the filter transfer function be zero at $f_{s_2} \geq (f_{c_2} + \Delta f_2)$. The zero gain requirement is necessary so that there is no significant frequencies present above the Nyquist frequency which would introduce aliasing.

$$f_{N_2} = \frac{1}{2\Delta d_2} = \frac{f_{s_2}}{2} \tag{14}$$

where f_{N_2} is the Nyquist frequency.

Aliases that occur at frequencies in the output of the preliminary filter greater than $f_{c_2} + \Delta f_2$ are of no concern since they will be filtered out by the final low-pass filter. The expression for the double filter is

$$x_d^* = \sum_{n_2=-N_2}^{N_2}{}' h_{n_2} \sum_{n_1=-N_1}^{N_1}{}' h_{n_1} x(d+n_1\Delta d_1+n_2\Delta d_2) \tag{1}$$

Filtered high-pass data is obtained by linear interpolation between samples of the low-pass data with sampling frequency f_{s_2} and subtracting from the original data with sampling frequency f_{s_1}. Consequently, to keep interpolation errors to a minimum, f_{s_2} must be chosen large enough to reconstruct the highest frequency passed by the low-pass filter. The following guidelines are used to determine f_s, Δf and N, given f_c, for a resultant overshoot ≤ 1 percent and an interpolation error ≤ 1 percent.

$$\begin{aligned} f_s &\geq 20(f_c + \Delta f) \\ \Delta f &\geq 0.015\, f_s \\ N &\geq \frac{1.05 f_s}{\Delta f} \end{aligned} \tag{15}$$

One additional guideline must also be fulfilled in order to avoid a limit condition in the computation of the filter weights. This is $0.5/\Delta f\Delta d$ may not be an integer value < N. The empirical error bound for the Martin-Graham filter in terms of N, Δf and Δd is given as

$$\epsilon \approx \frac{1}{5\pi} \ln \frac{4N^2(\Delta f\Delta d)^2}{4N^2(\Delta f\Delta d)^2 - 1} \tag{16}$$

An indication of just how well the two stage filters designed for filtering the runway profile data fulfilled the suggested guidelines and the estimates of the error associated with the filters can be found in Table XII.

TABLE XII

FILTER GUIDELINES

Guideline	500 ft Cutoff		100 ft Cutoff	
	Preliminary Filter	Final Filter	Preliminary Filter	Final Filter
$f_s \geq 20(f_c + \Delta f)$	0.63 (2)	0.04 (0.0667)	0.8 (2)	0.2 (0.2)
$\Delta f \geq 0.015 f_s$	0.03 (0.03)	0.001 (0.0005)	0.03 (0.033)	0.003 (0.003)
$N \geq 1.05 f_s/\Delta f$	70 (75)	140 (140)	64 (80)	70 (150)
ϵ	1.4%	1.6%	1.0%	0.3%

NOTE: Values in parentheses are the actual values of f_s, Δf and N used.

In the actual application of the low-pass filters, two different computer programs were written. The first, for the 500 ft cutoff, applied the preliminary filter in the distance domain. This makes a quite complex program in which the filter constants cannot be changed by much without restructuring the program. The final stage was then applied in the frequency domain by making use of the Fast Fourier Transform and the convolution theorem which states that

$$Y(z) = W(z)X(z) \tag{17}$$

The interpretation of this expression is that the Fourier transform of the filtered output is equal to the product of the Fourier transforms of the filter transfer function and the input function. Therefore, the second stage

weights were computed using Equations (9) and (12) and then transformed. The output of the first stage filter was then transformed, the complex product of the two transforms was formed and the inverse transform was made resulting in the final low-pass filtered data.

The advantage of applying the first stage filter in the distance domain is that it takes less computer time since it is only necessary to compute the output for every 30th point.

When it was decided that the data should be filtered with a shorter wavelength cutoff, a new filter program was written to make use of the FFT in both stages of the filter. By doing this, a more general filter program, in which the filter constants could easily be varied, was obtained. The time increase of approximately 15 percent for this program was of little significance.

The only additional aspect of the filtering procedure not yet discussed is that of folding the data at the beginning and end of the runway profile. When data are filtered, N values are lost from the beginning and end of the series. Several schemes are available to extend the data so that the output is the same length as the input. The choice of scheme to use is dependent upon the predominant data trend of the original data series, particularly in the first and last N values. Since the low frequency trend in most of the lines of survey was near linear, the data was folded and inverted. This tends to continue any linear trend present in the beginning and end of the data and appeared to introduce the minimum error at the beginning and end of the data.

APPENDIX II

POWER SPECTRAL DENSITIES FOR TWO METHODS OF COMPUTATION

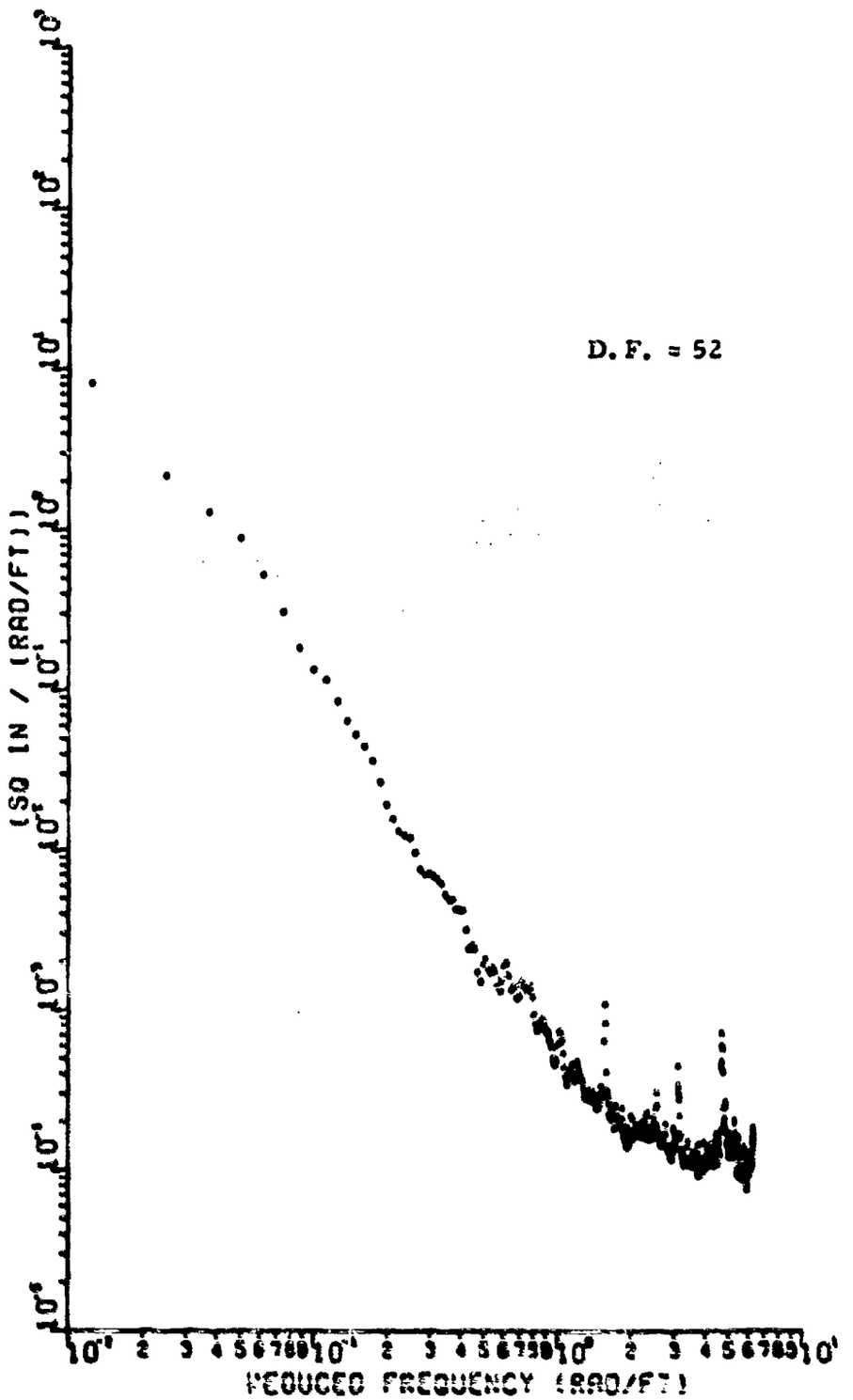

Figure 22 PSD Altus 75L (FFT - Prewhitened and smoothed)

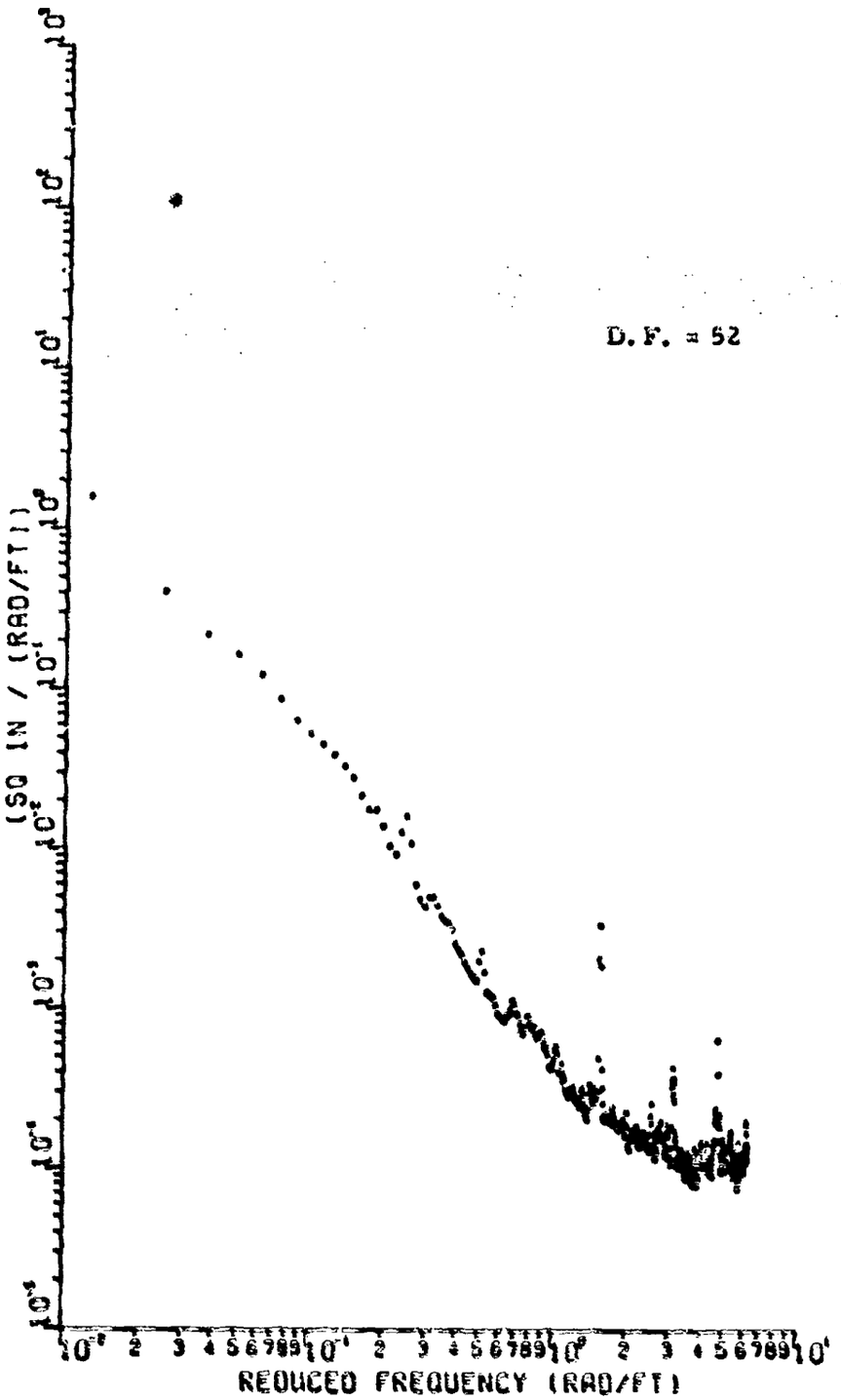

Figure 23 PSD Altus CL (FFT - Prewhitened and smoothed)

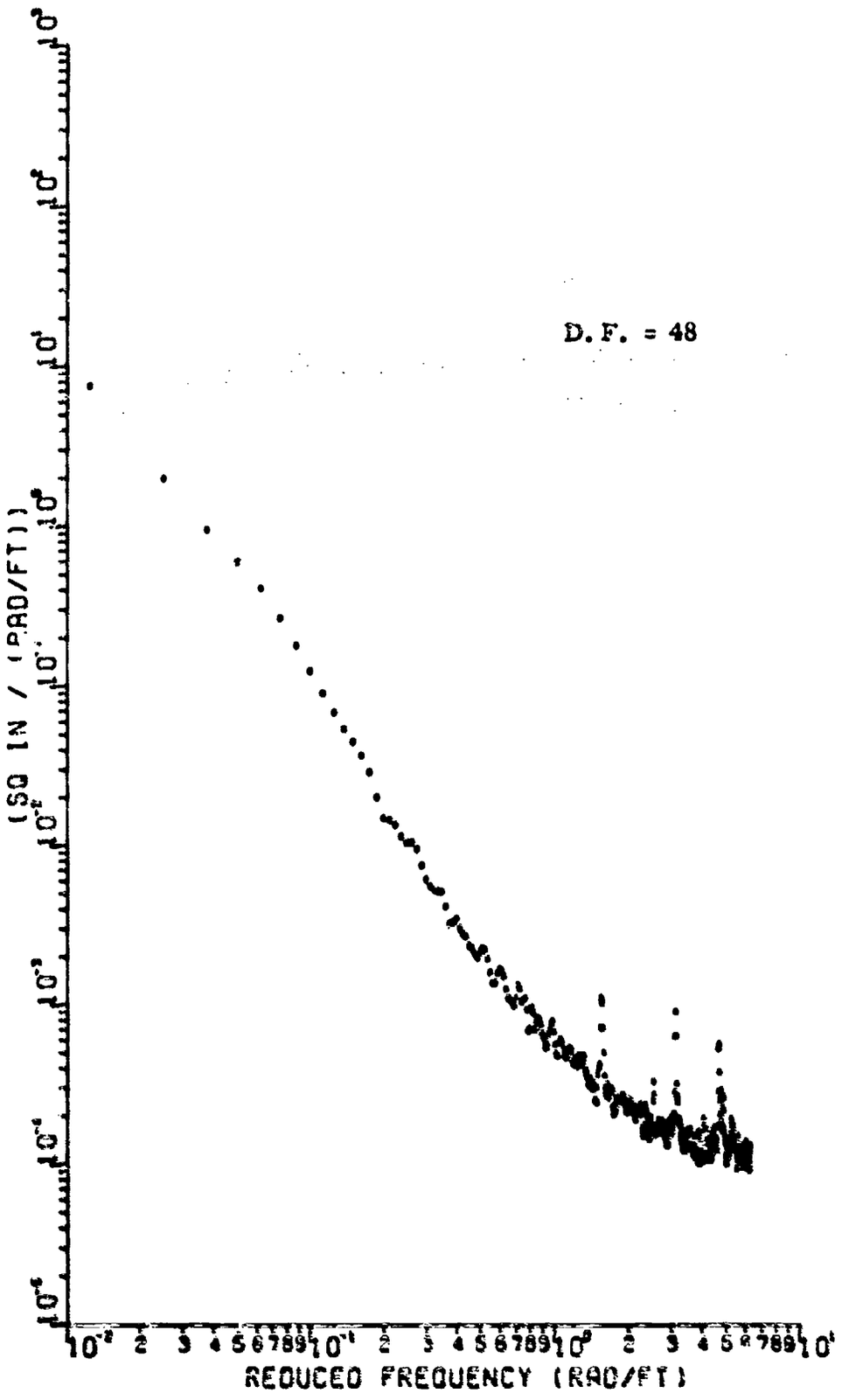

Figure 24 PSD Altus 75R (FFT - Prewhitened and smoothed)

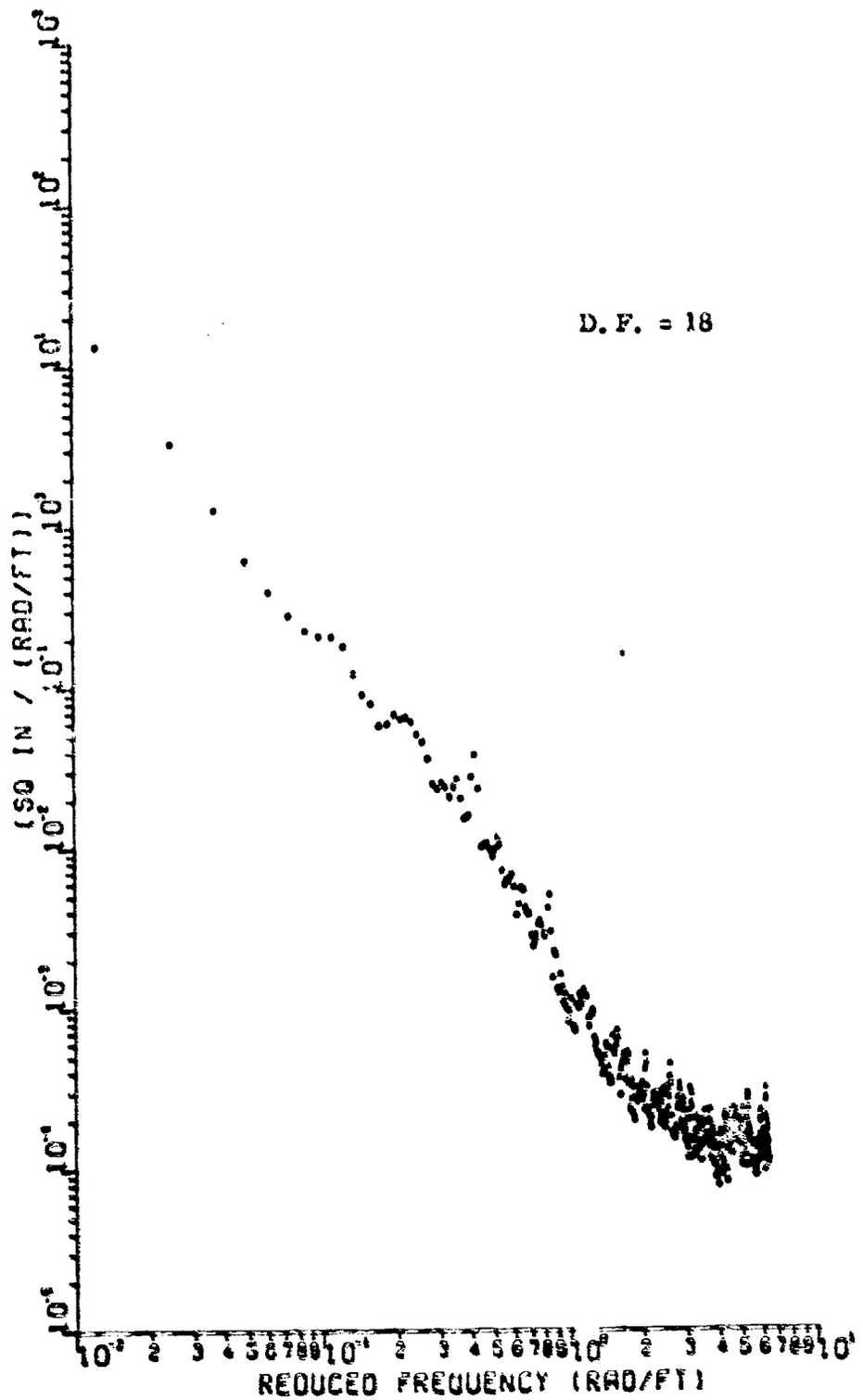

Figure 28 PSD Bakalar SOL (FFT - Prewhitened and smoothed)

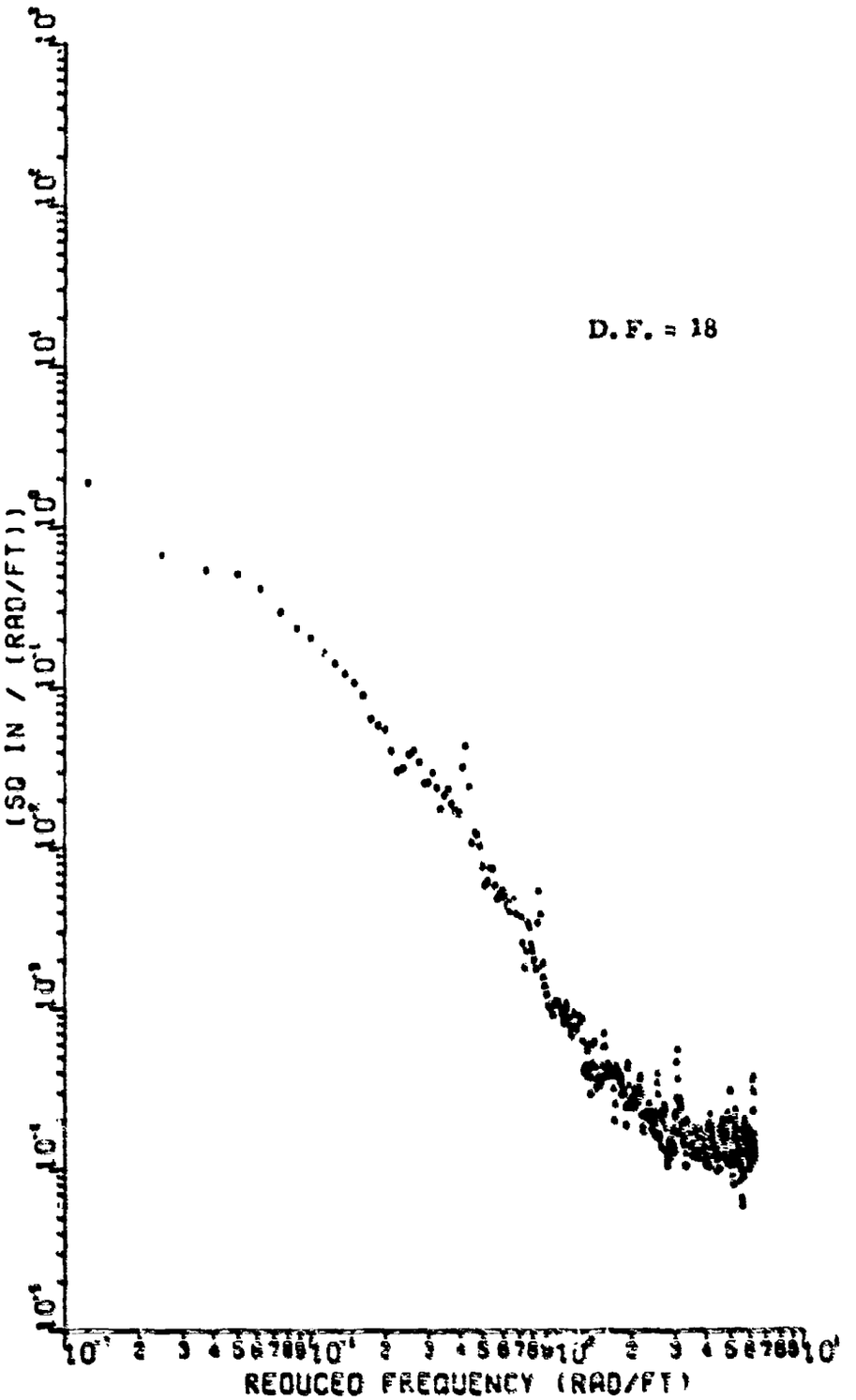

Figure 26 PSD Bataler CL (FFT - Prewhitened and smoothed)

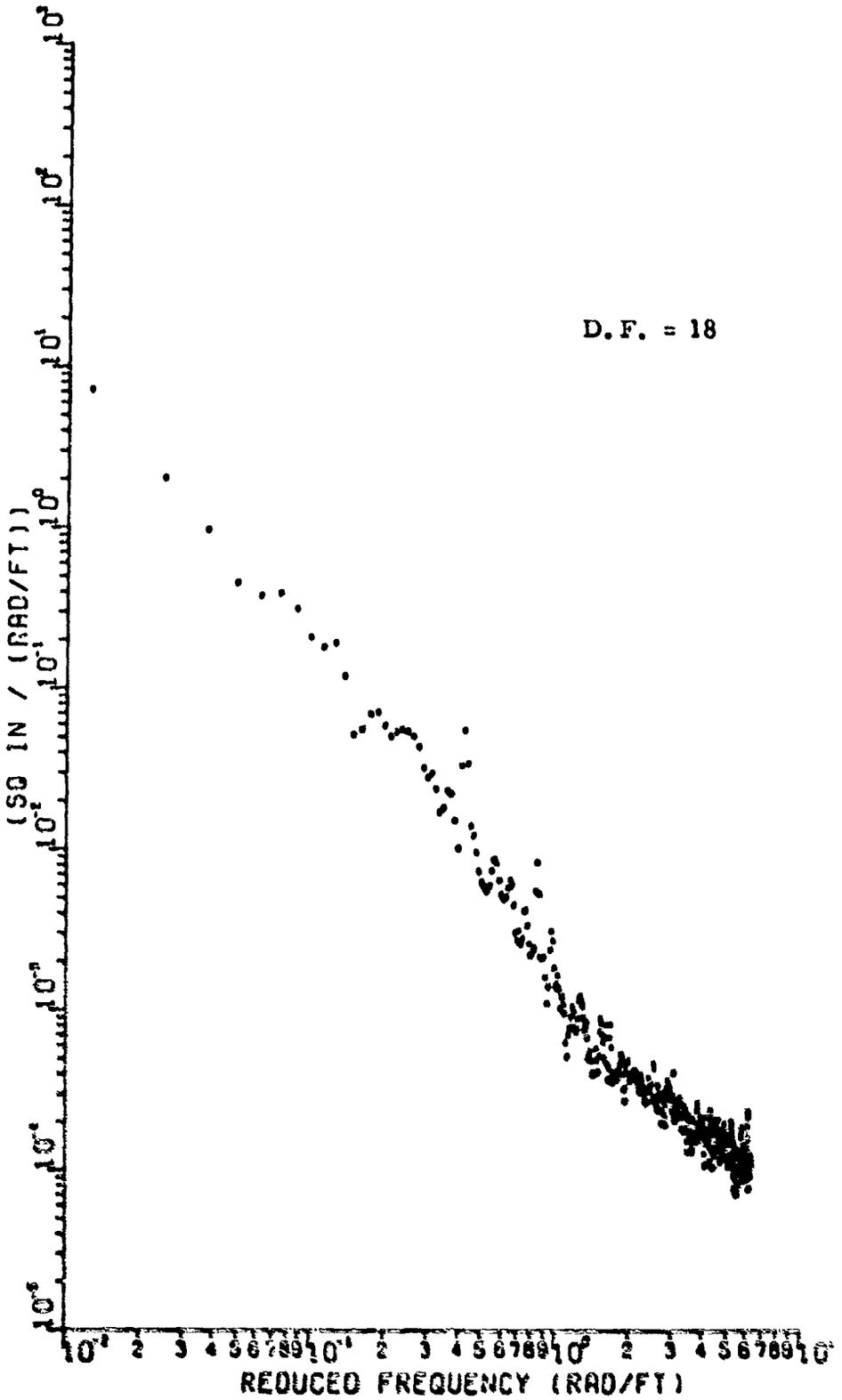

Figure 27 PSD Bakalar 50R (FFT - Prewhitened and smoothed)

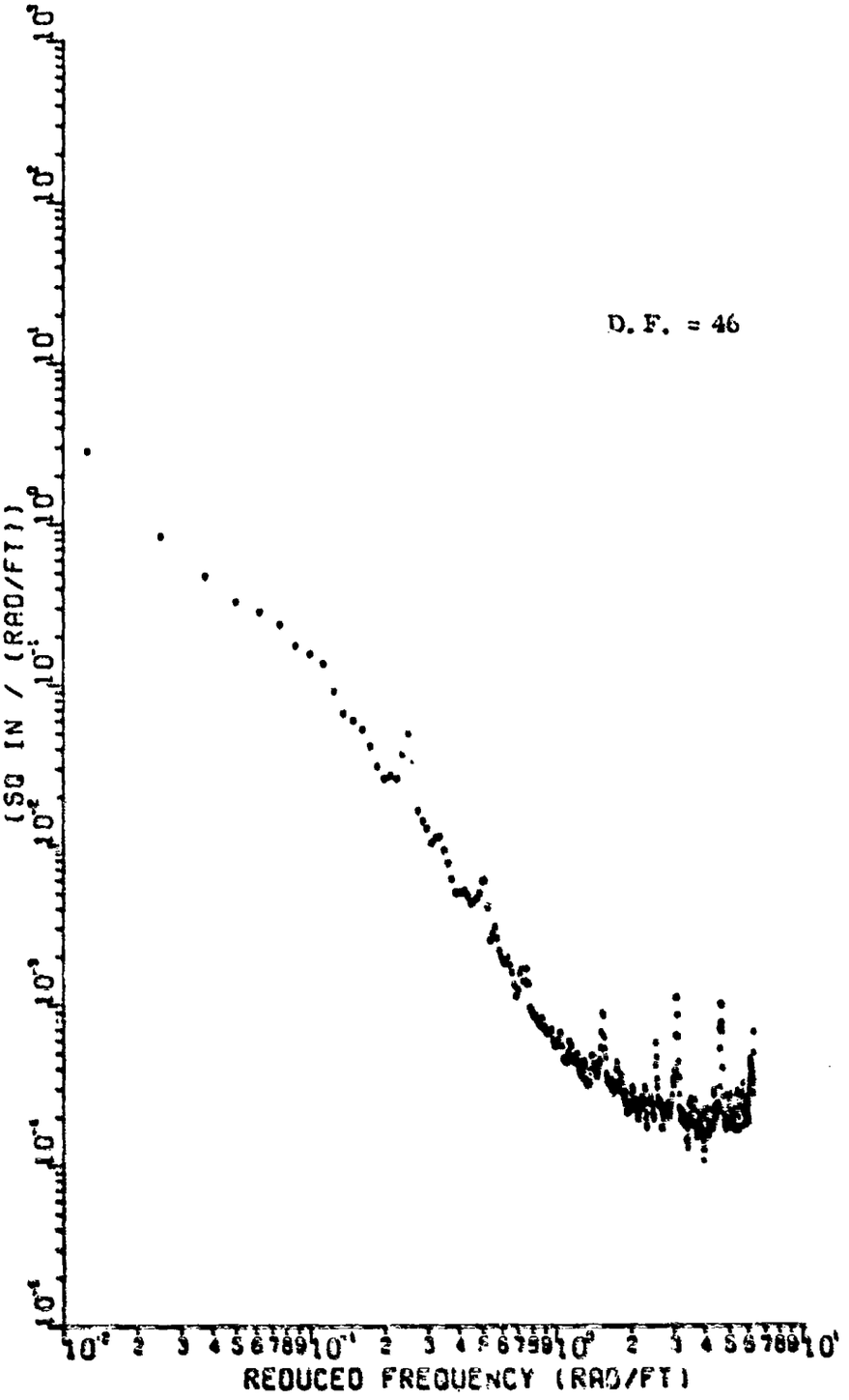

Figure 28 PSD Carswell 13L (FFT - Prewhitened and smoothed)

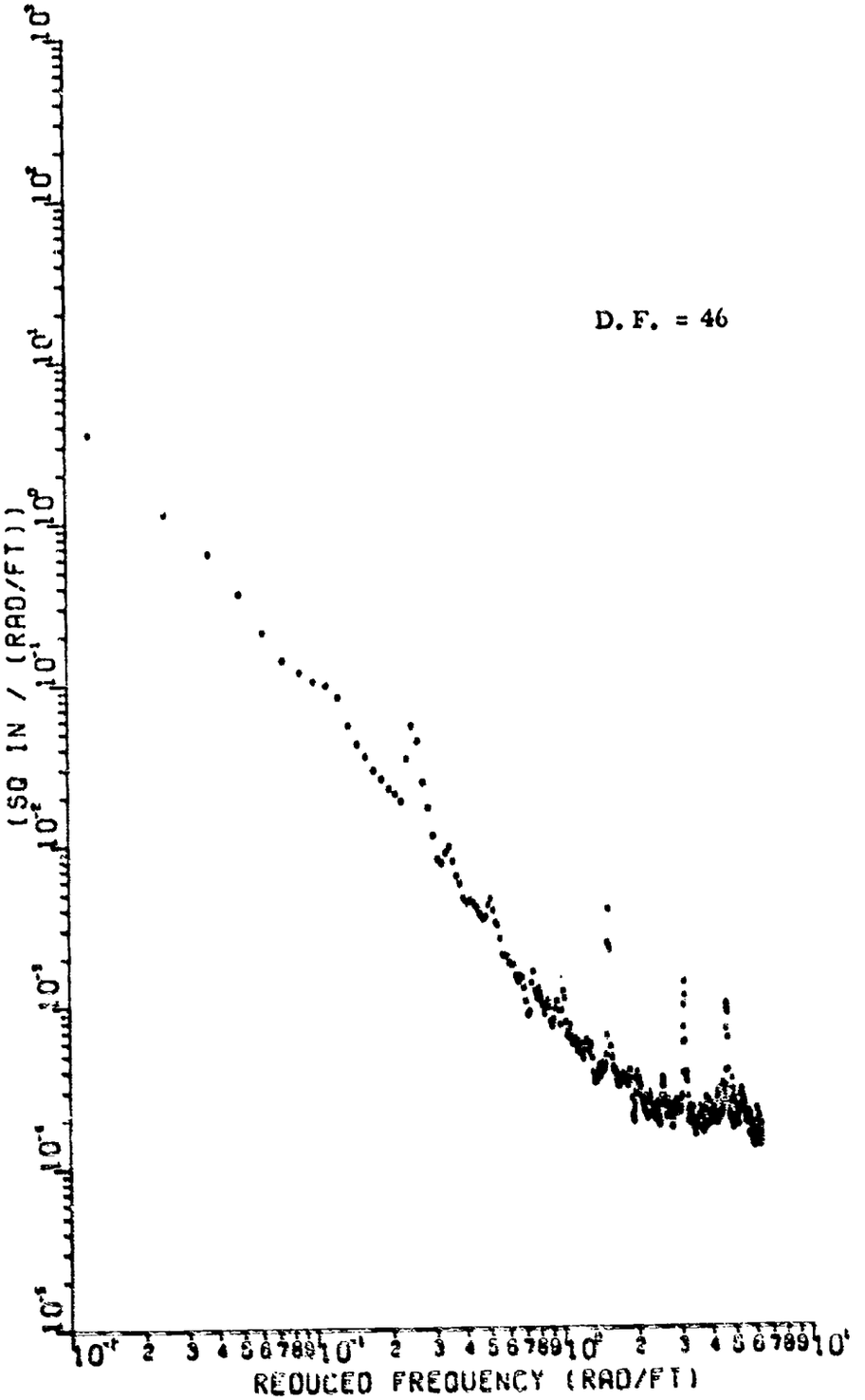

Figure 29 PSD Carnwell 87L (FFT - Prewhitened and smoothed)

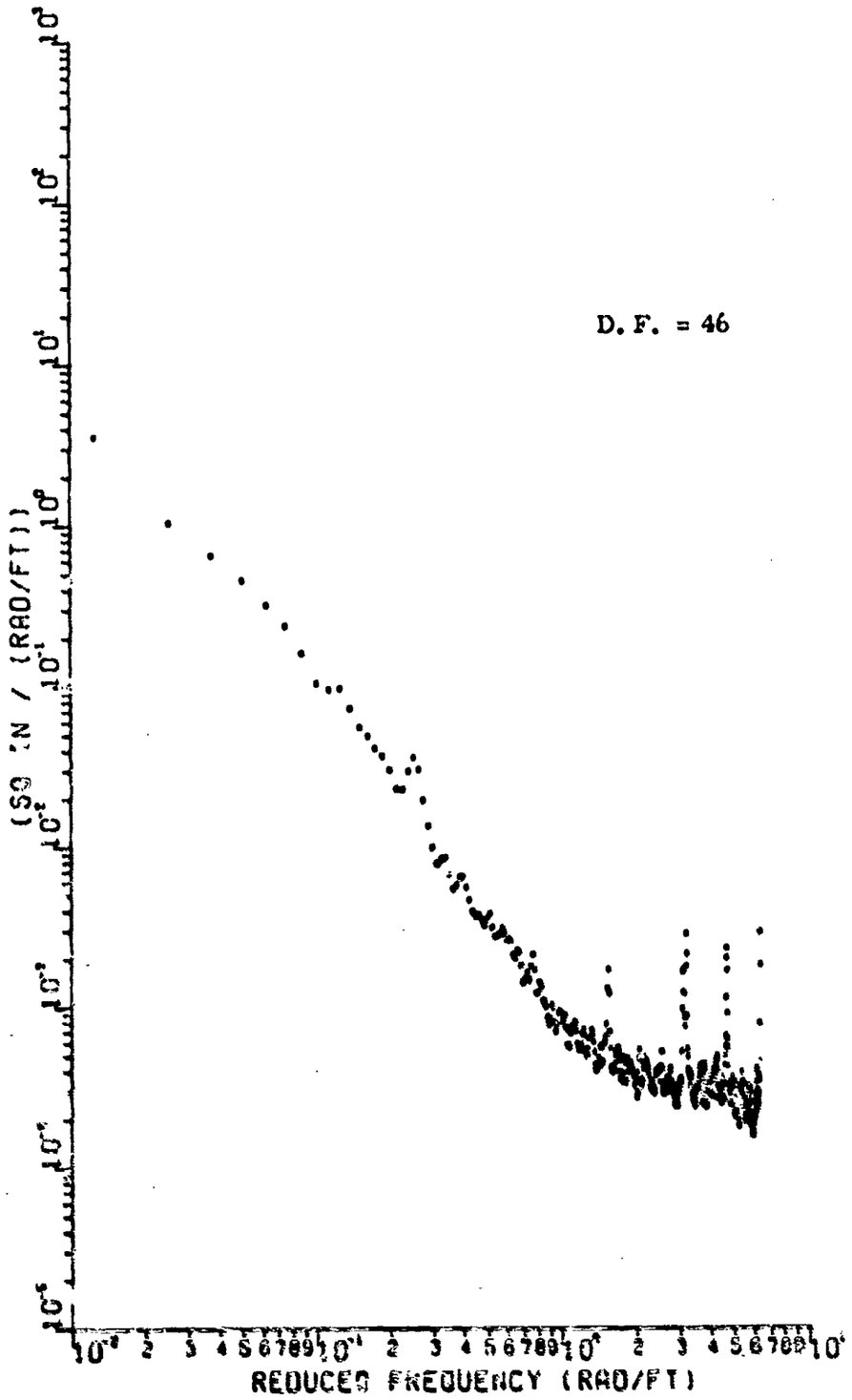

Figure 30 PSD Carewell 15R (FFT - Prewhitened and smoothed)

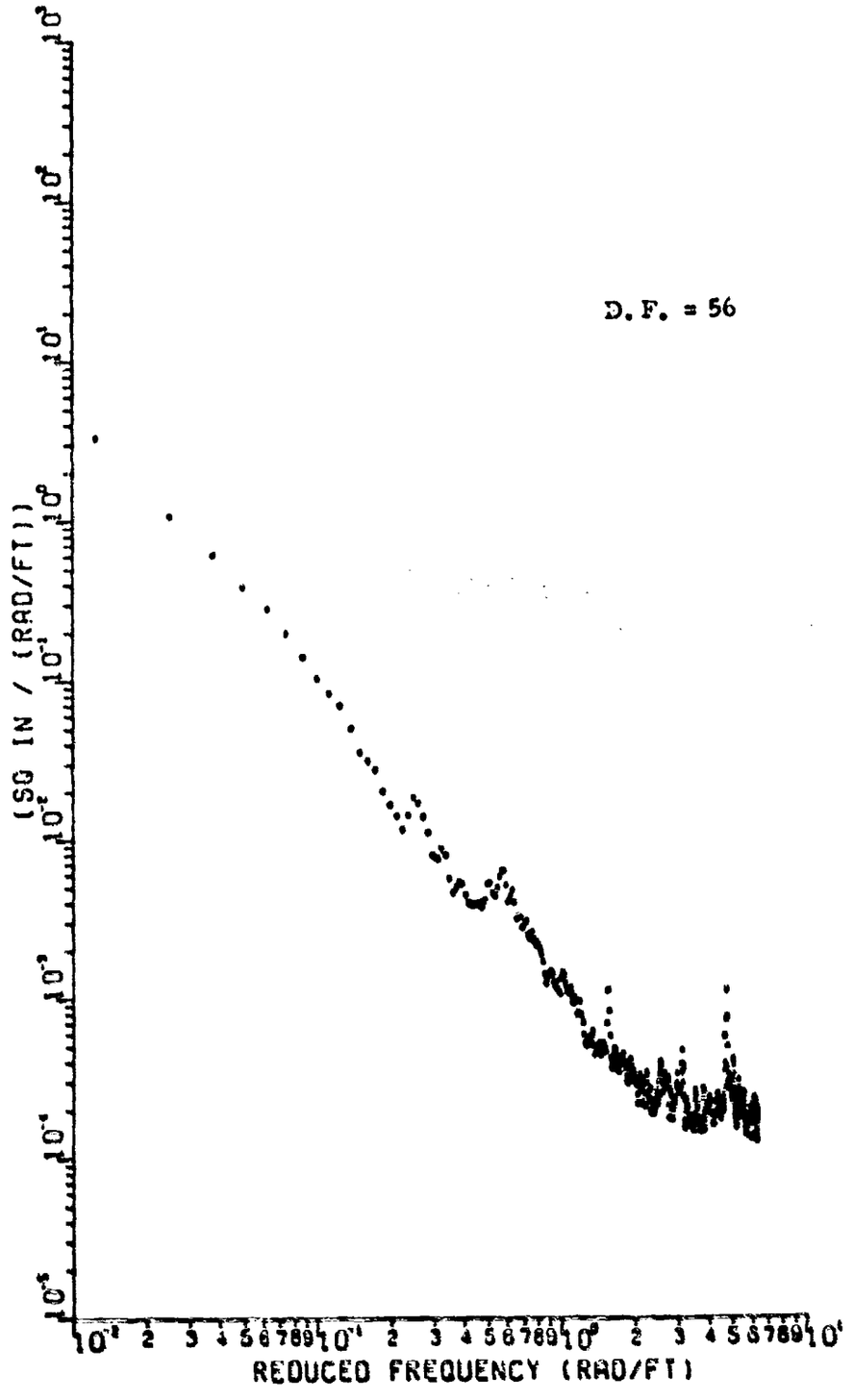

Figure 31 PSD Edwards 75L (FFT - Prewhitened and smoothed)

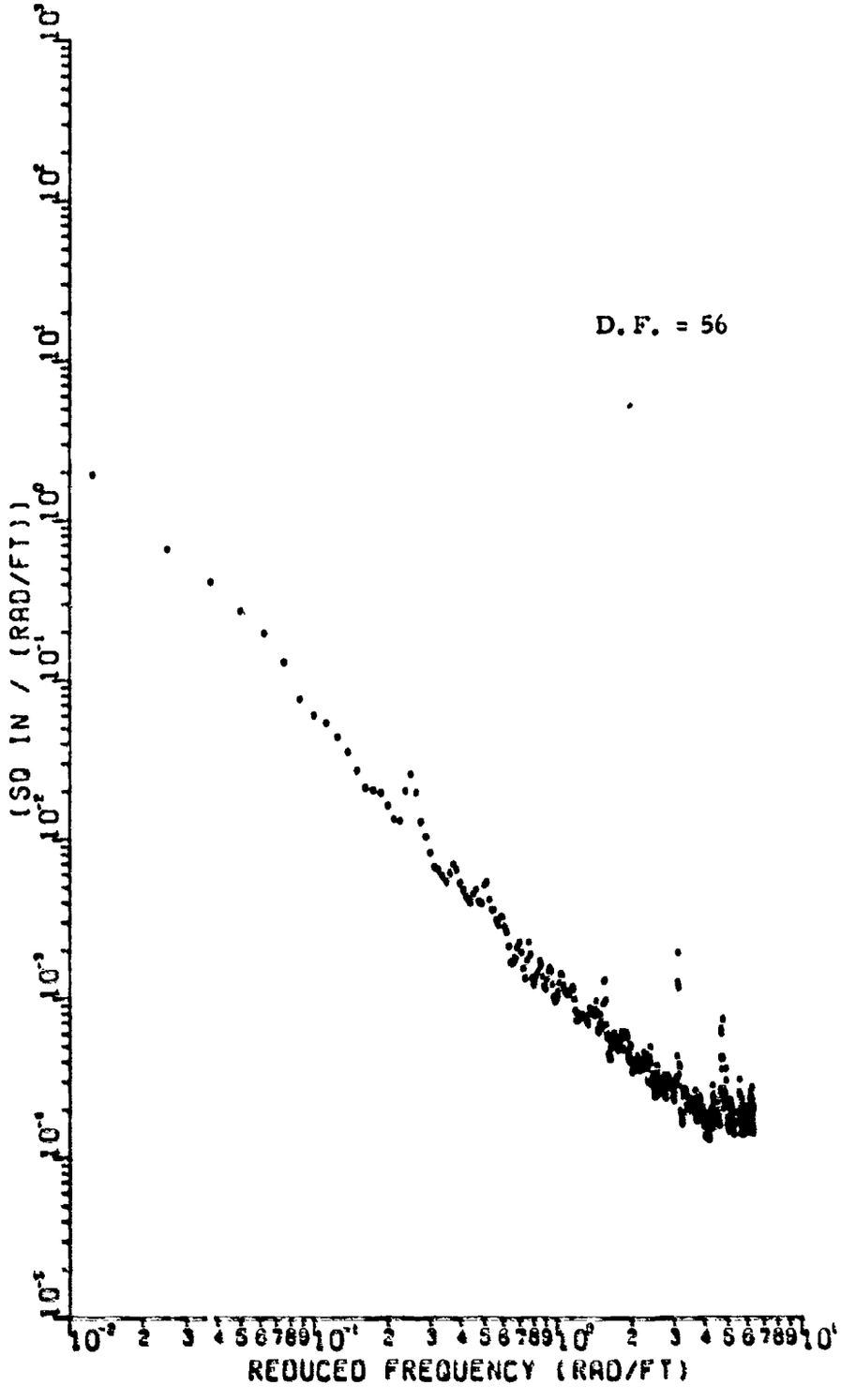

Figure 32 PSD Edwards CL (FFT - Prewhitened and smoothed)

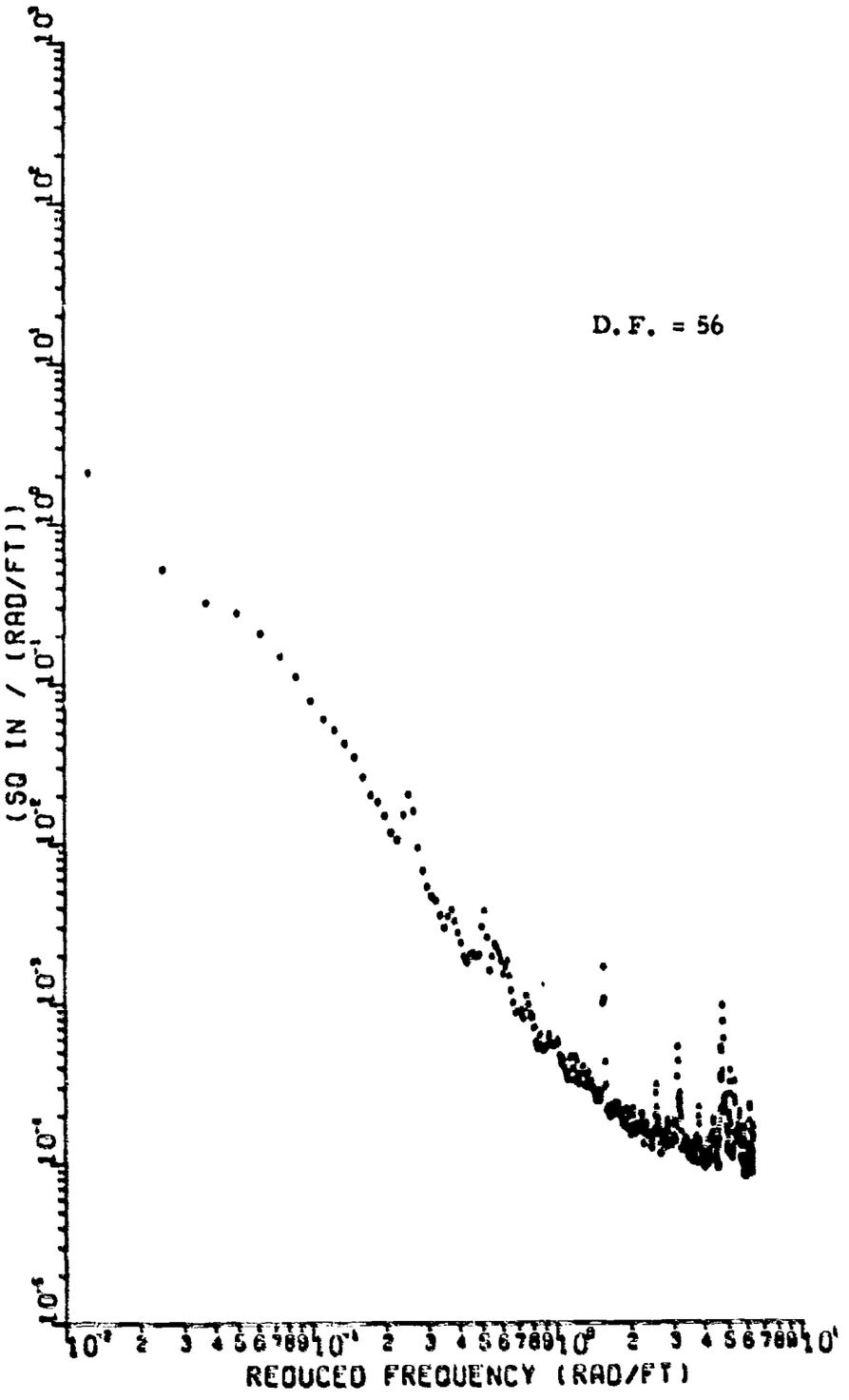

Figure 33 PSD Edwards 75R (FFT - Prewhitened and smoothed)

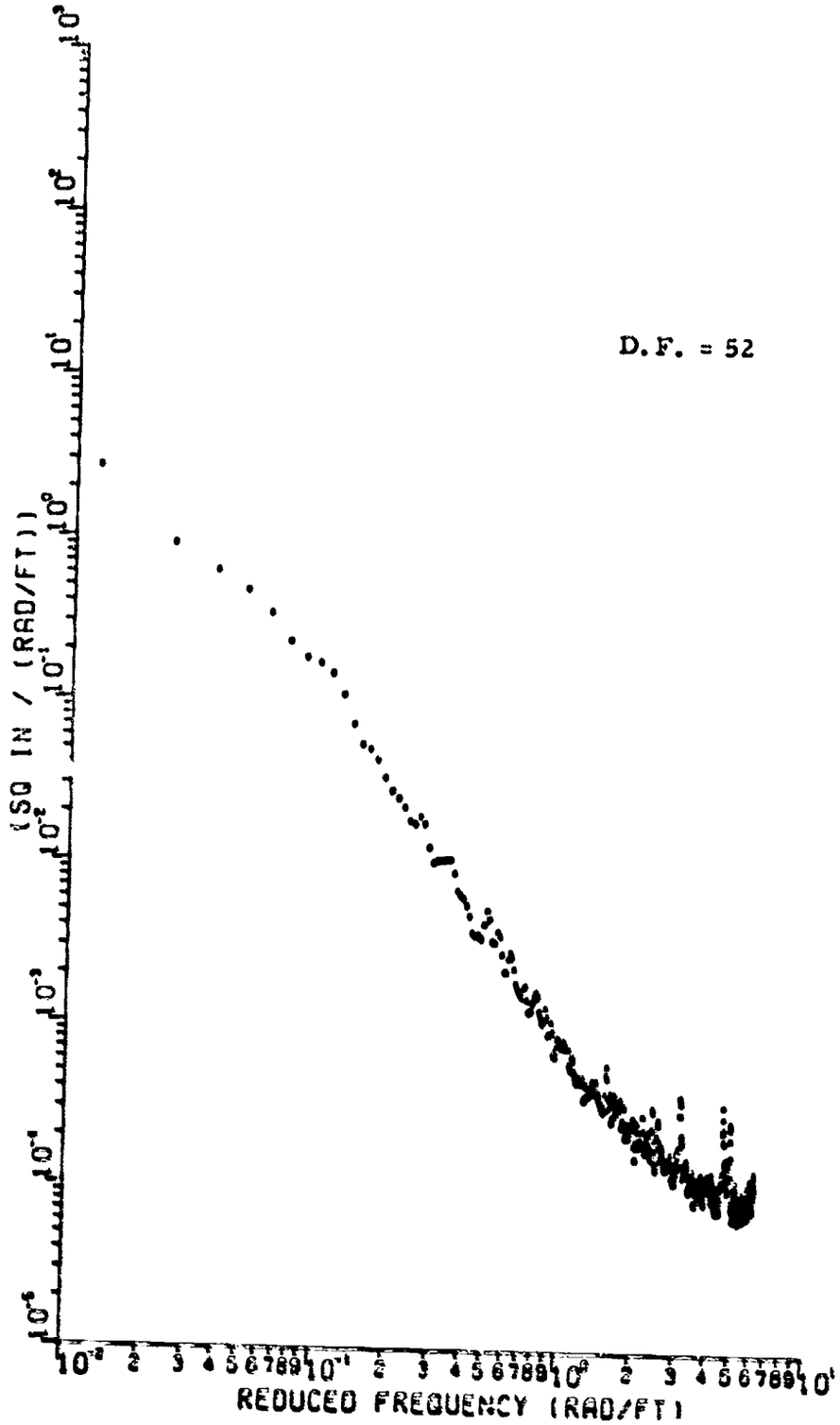

Figure 34 PSD Ellsworth CL (FFT - Prewhitened and smoothed)

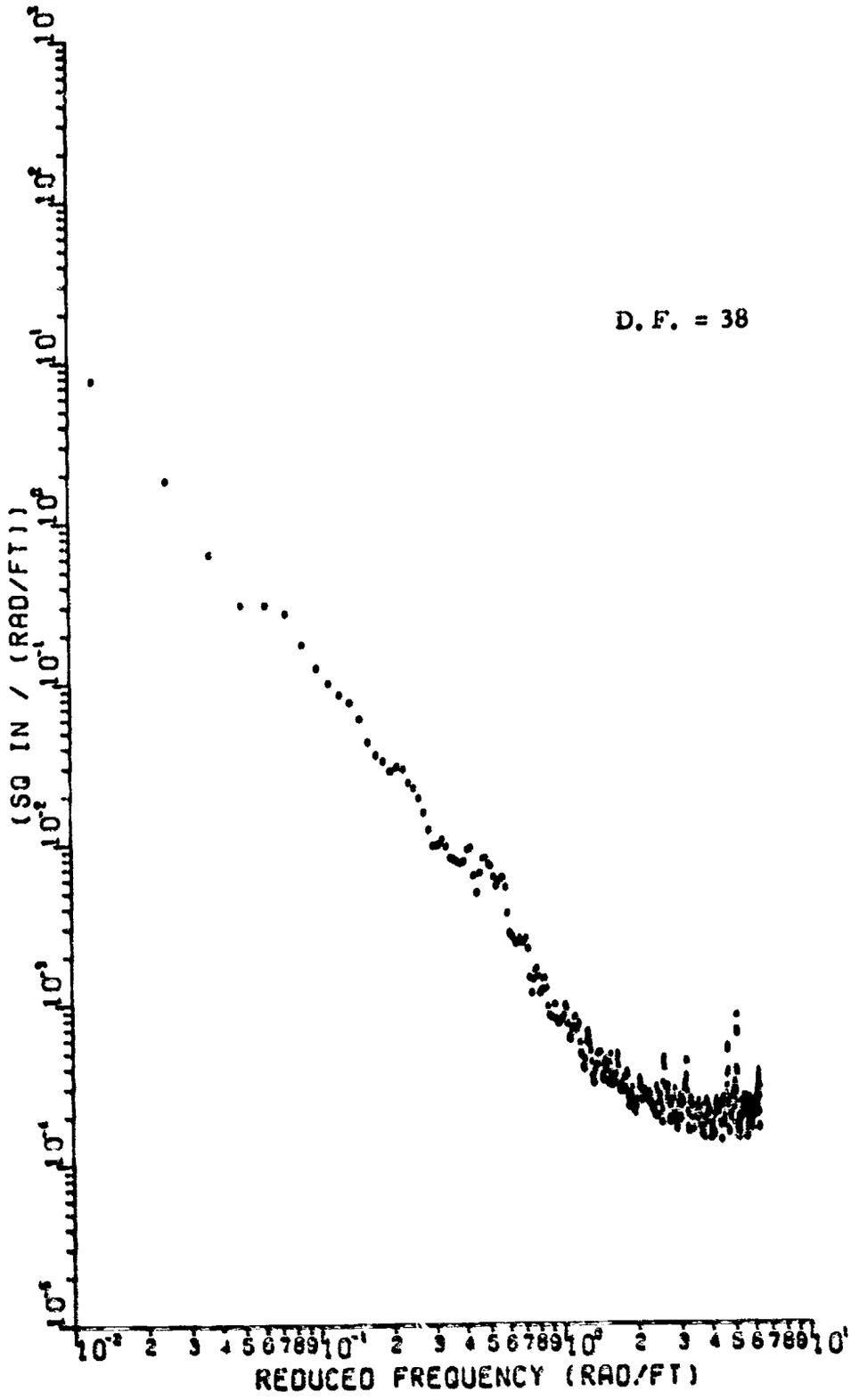

Figure 35 PSD Langley 50L (FFT - Prewhitened and smoothed)

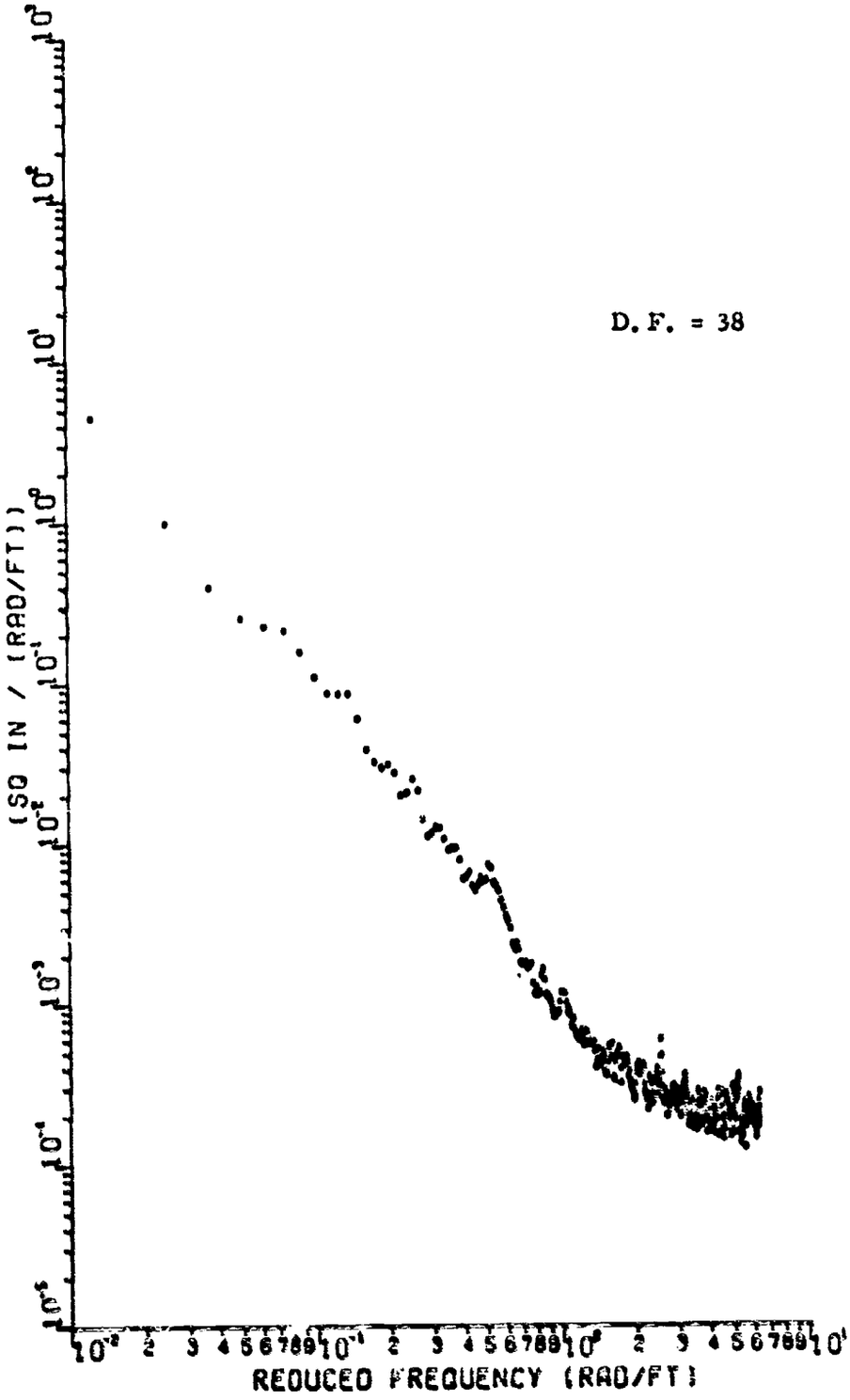

Figure 36 PSD Langley CL (FFT - Prewhitened and smoothed)

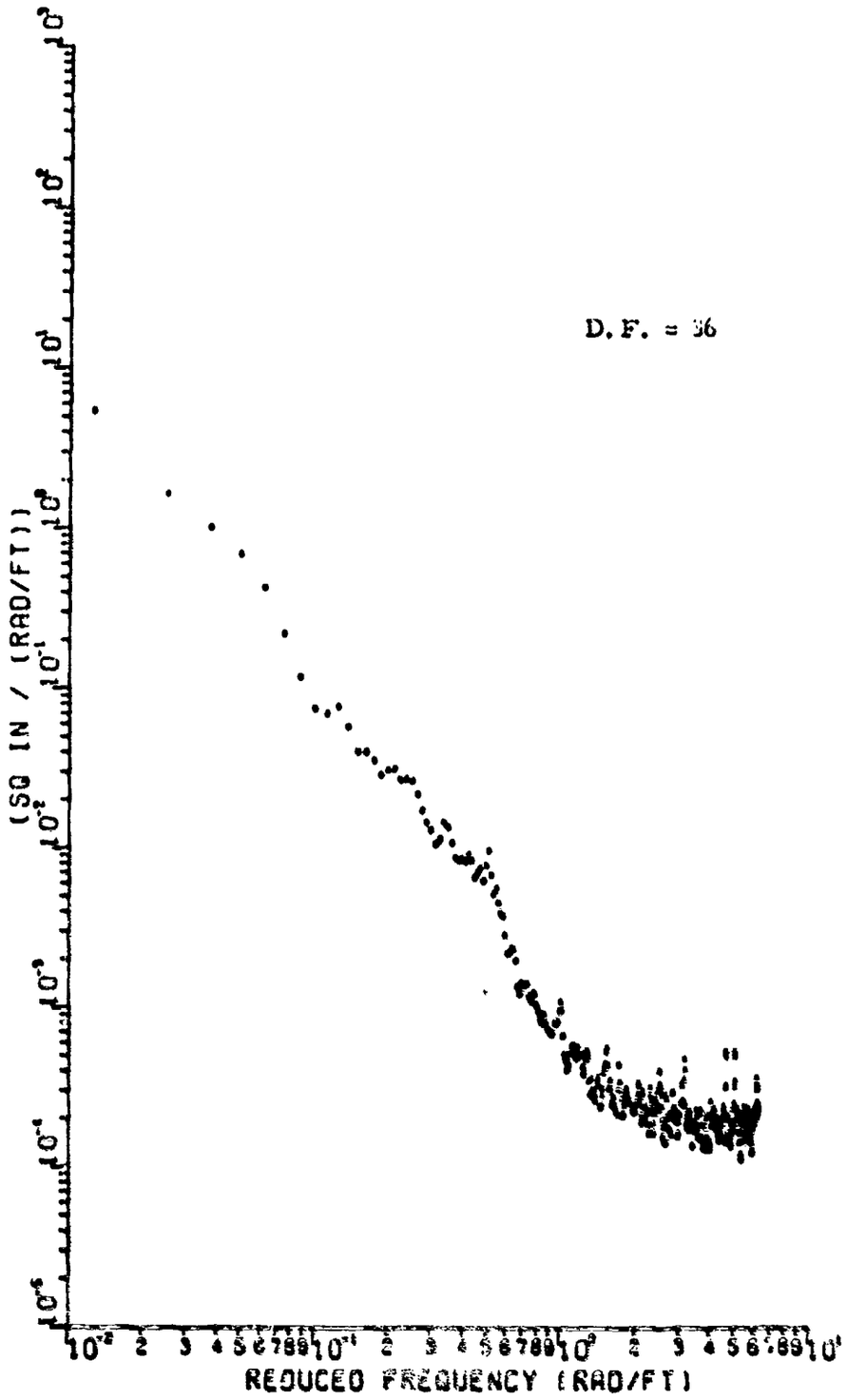

Figure 37 PSD Langley 50R (FFT - Prewhitened and smoothed)

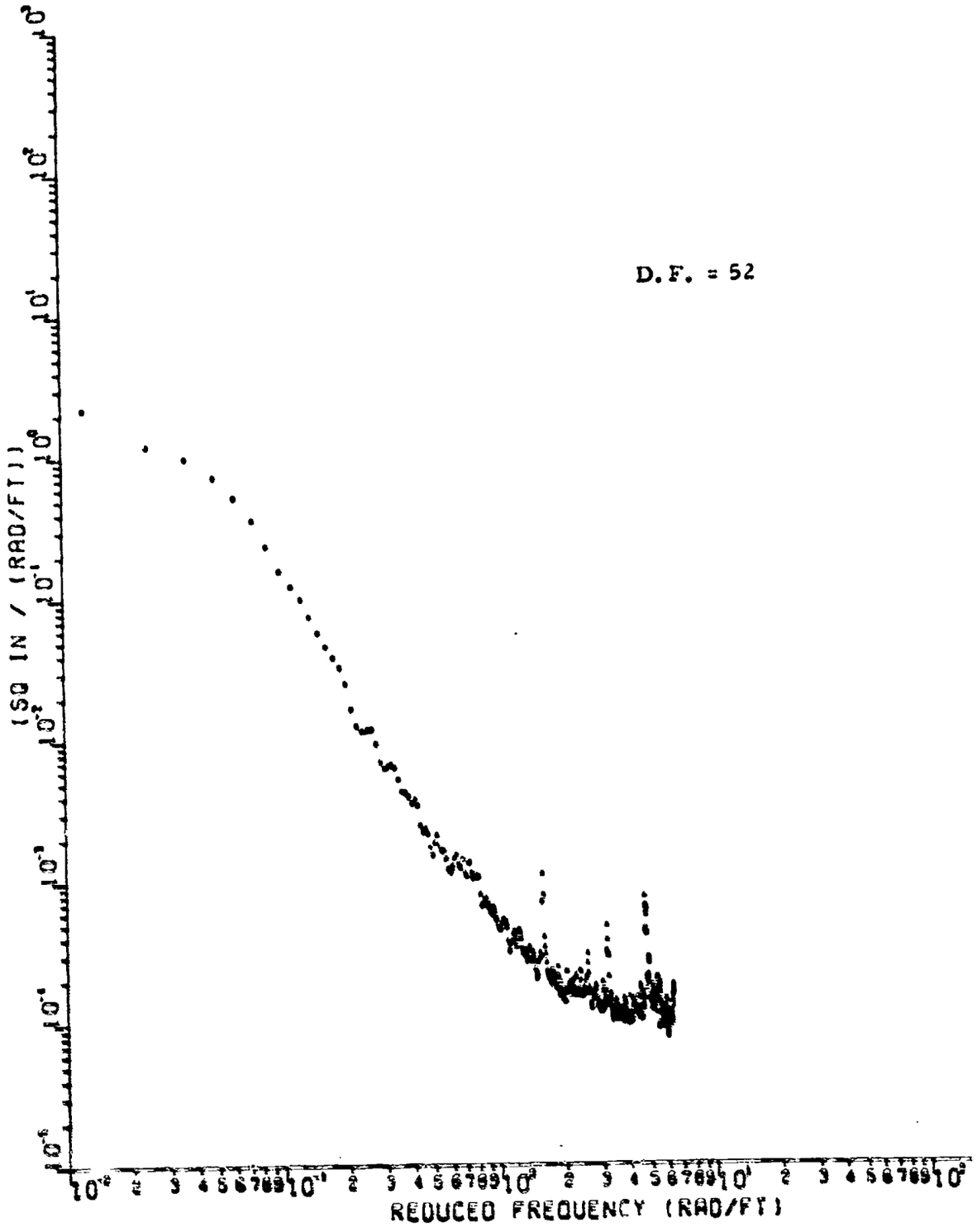

Figure 38 PSD Altus 75L (Autocorrelation - Prewhitened and smoothed)

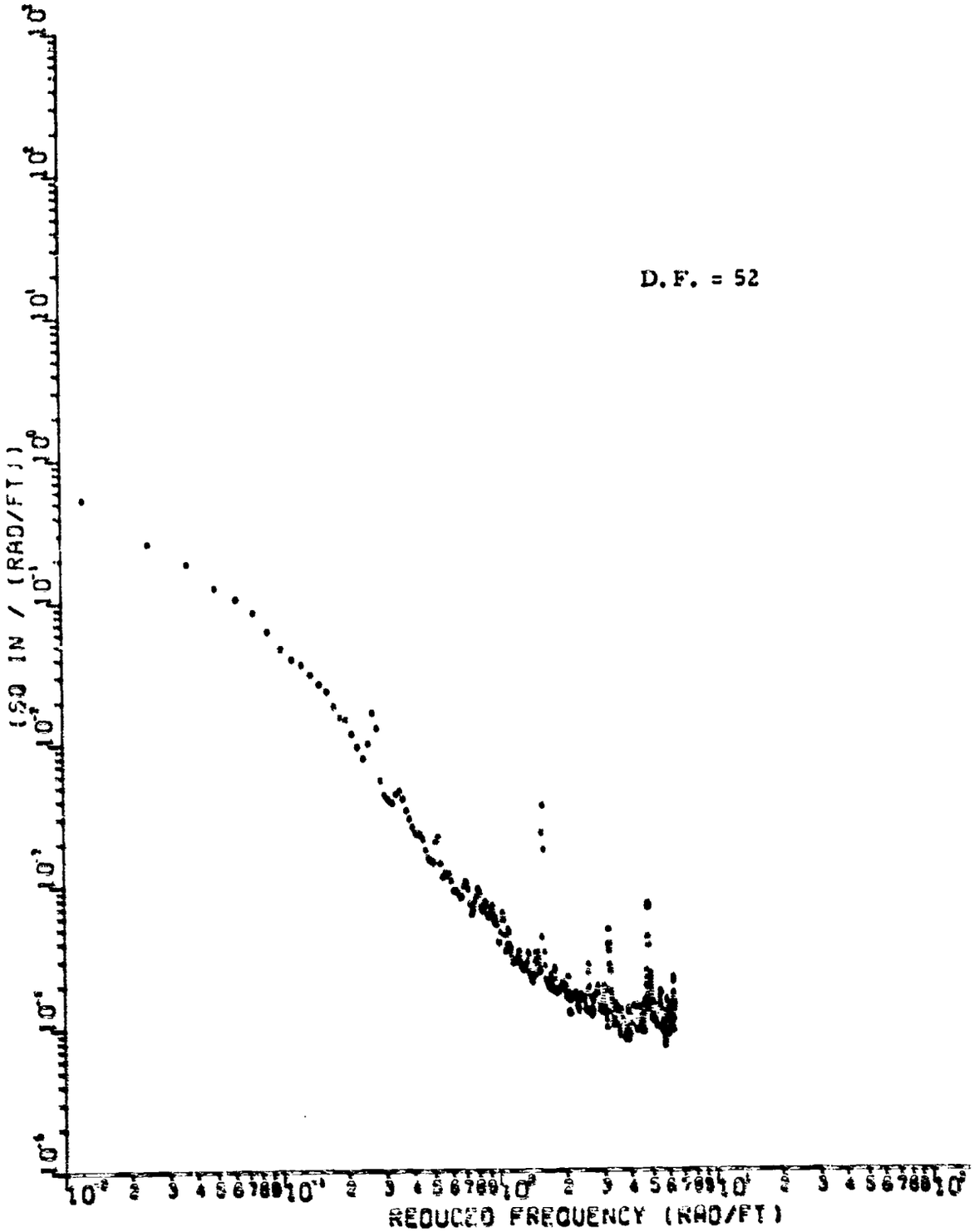

Figure 39 PSD Altus CL (Autocorrelation - Prewhitened and smoothed)

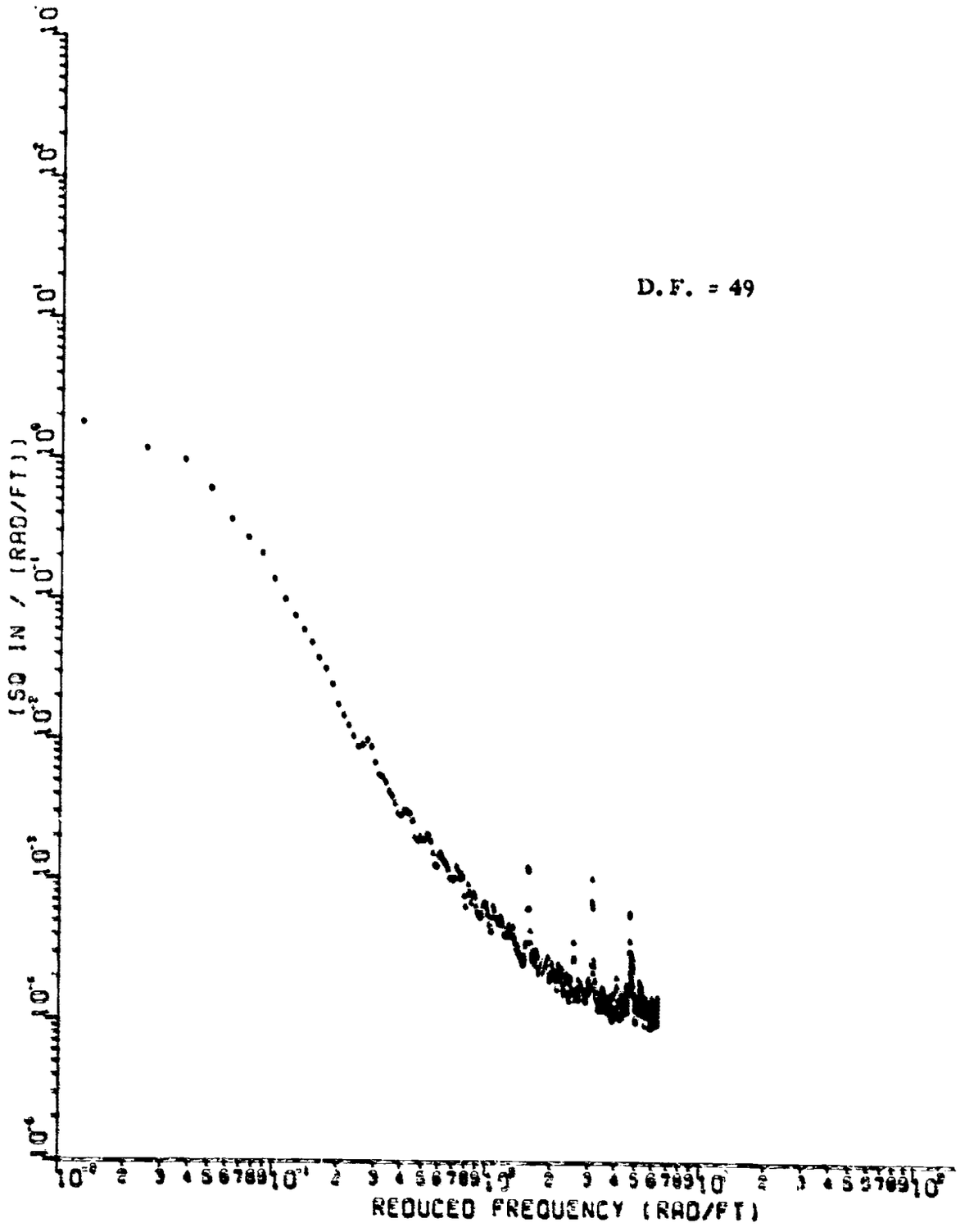

Figure 40 PSD Altus 75R (Autocorrelation - Prewhitened and smoothed)

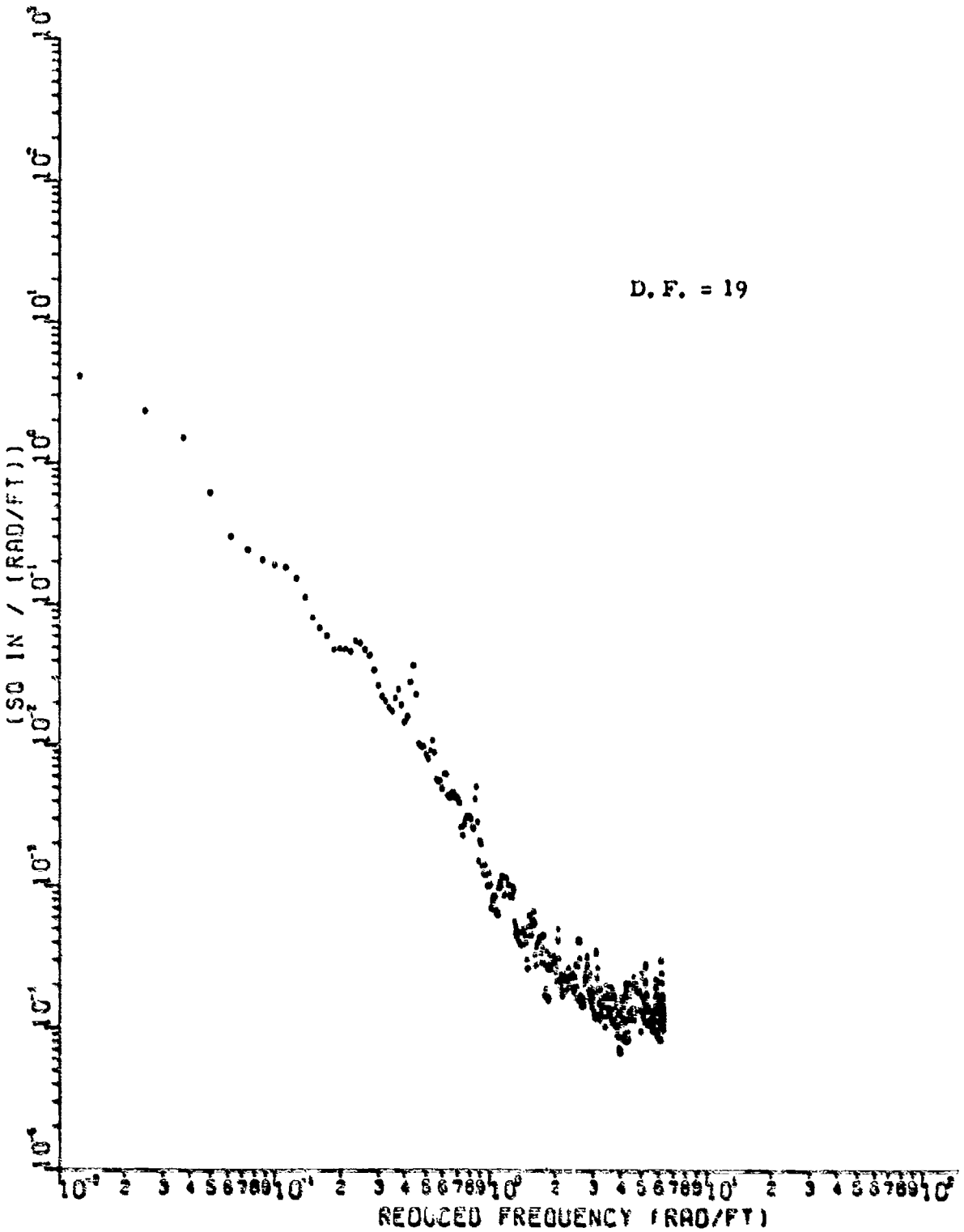

Figure 41 PSD Bakalar 50L (Autocorrelation - Prewhitened and smoothed)

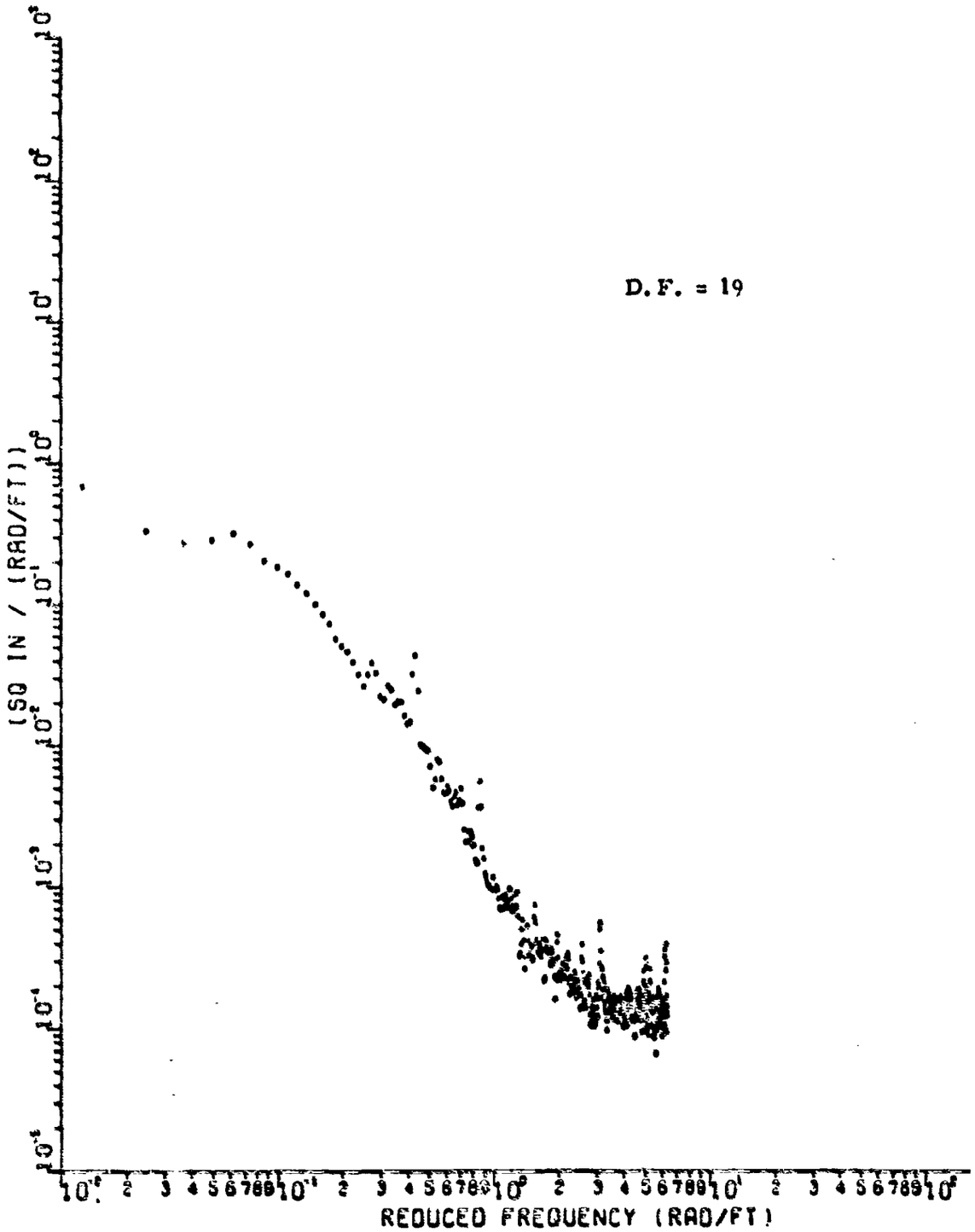

Figure 42 PSD Bakalar CL (Autocorrelation - Prewhitened and smoothed)

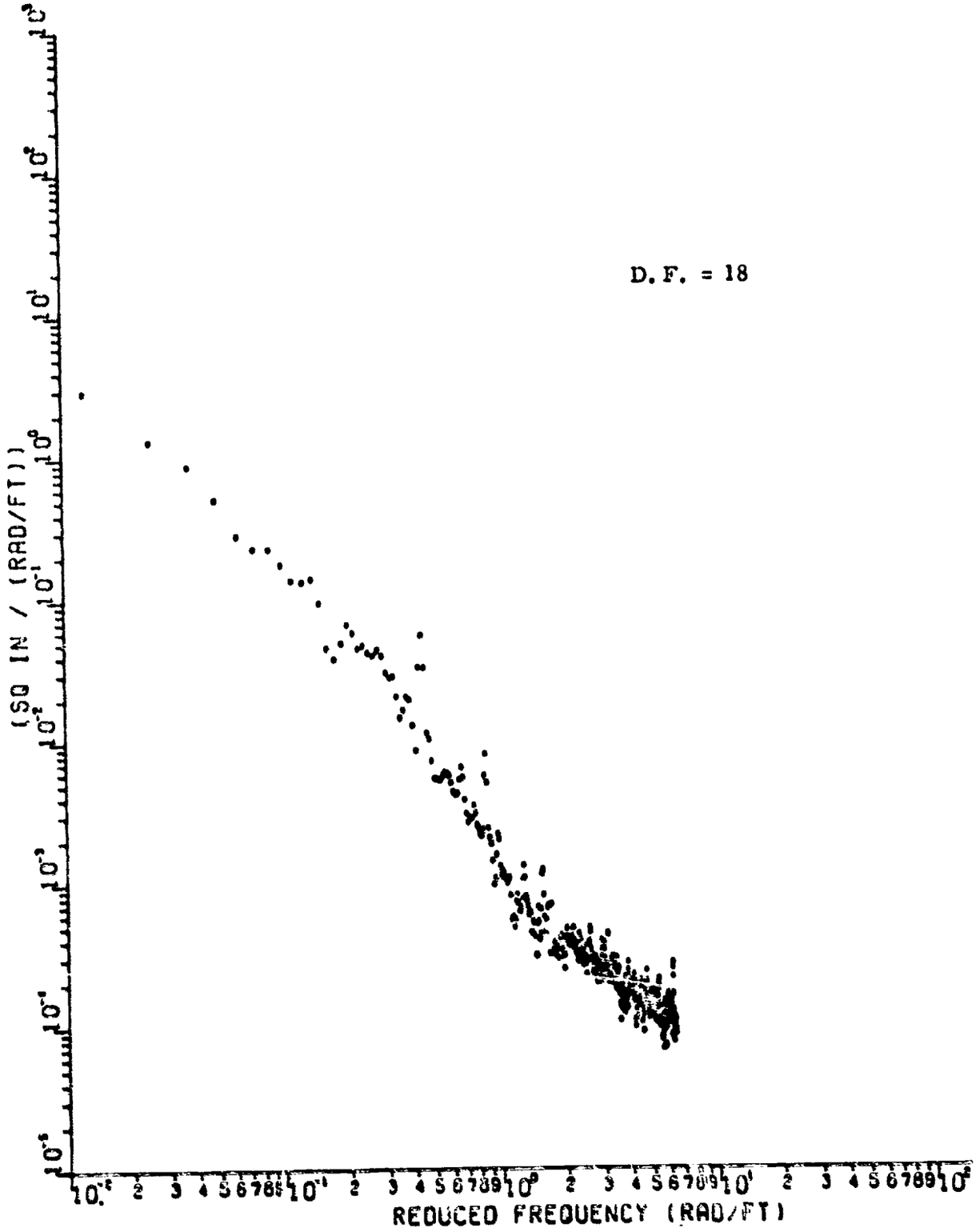

Figure 43 PSD Bakalar 50R (Autocorrelation - Prewhitened and smoothed)

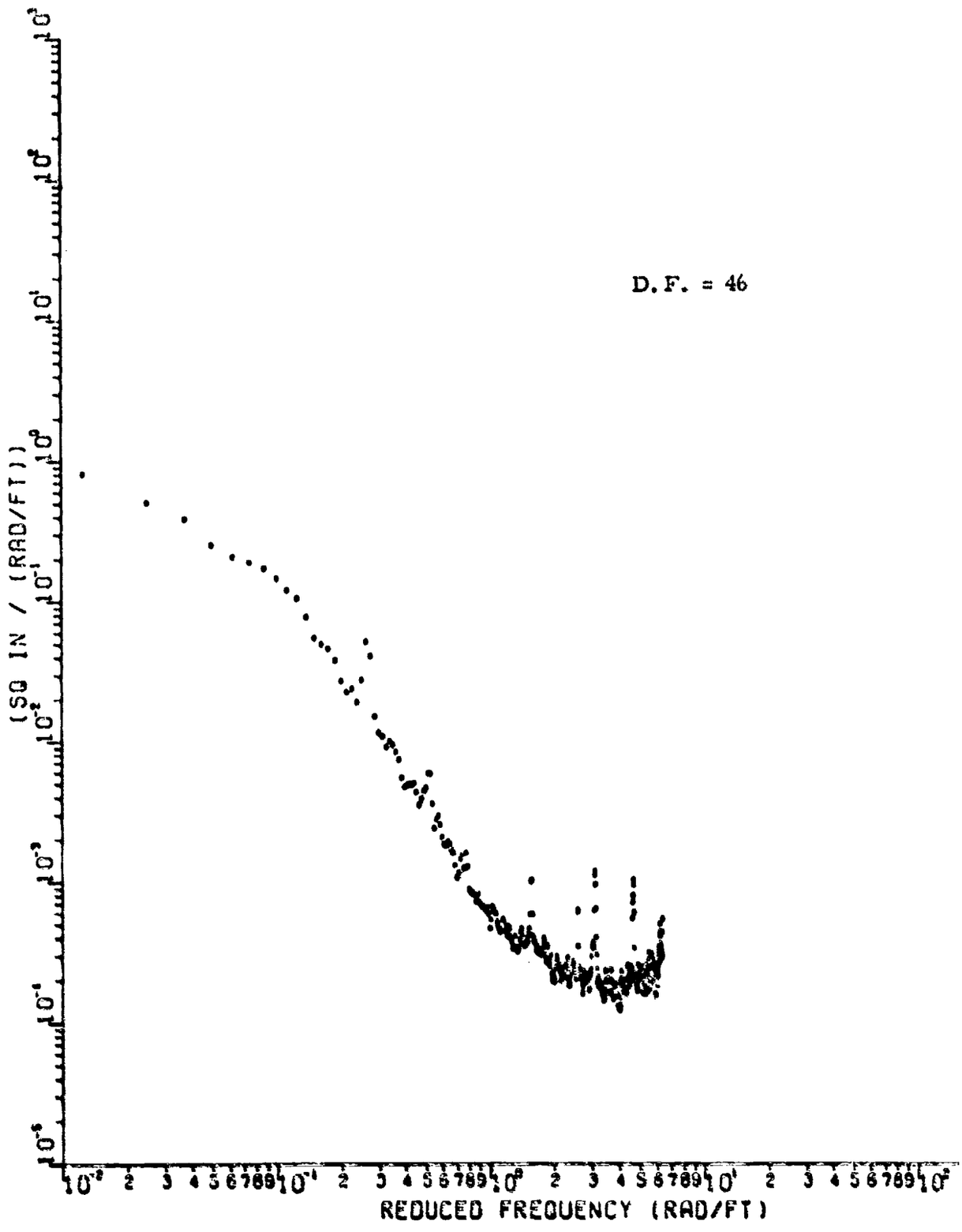

Figure 44 PSD Carswell 13L (Autocorrelation - Prewhitened and smoothed)

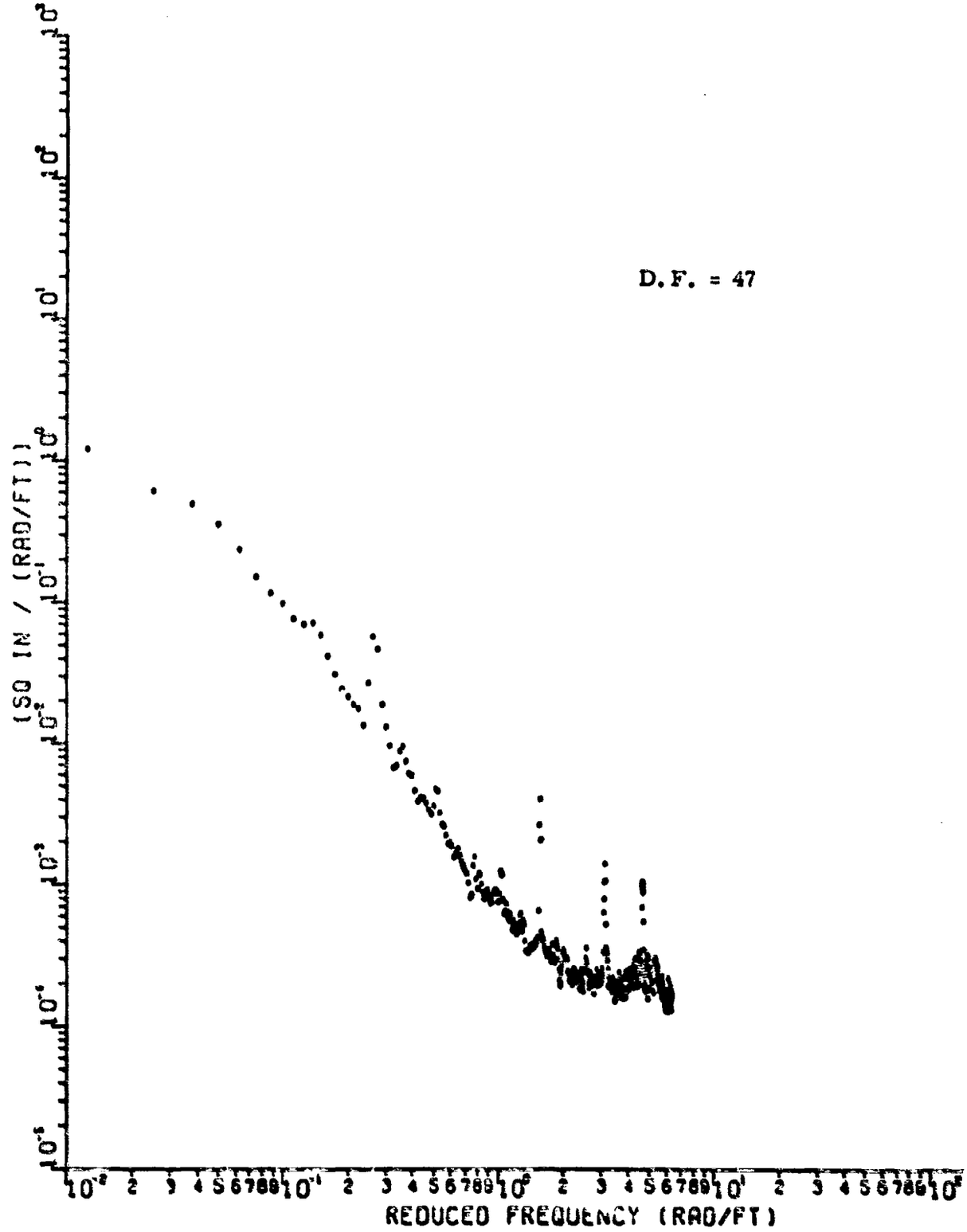

Figure 45 PSD Carswell 87L (Autocorrelation - Prewhitened and smoothed)

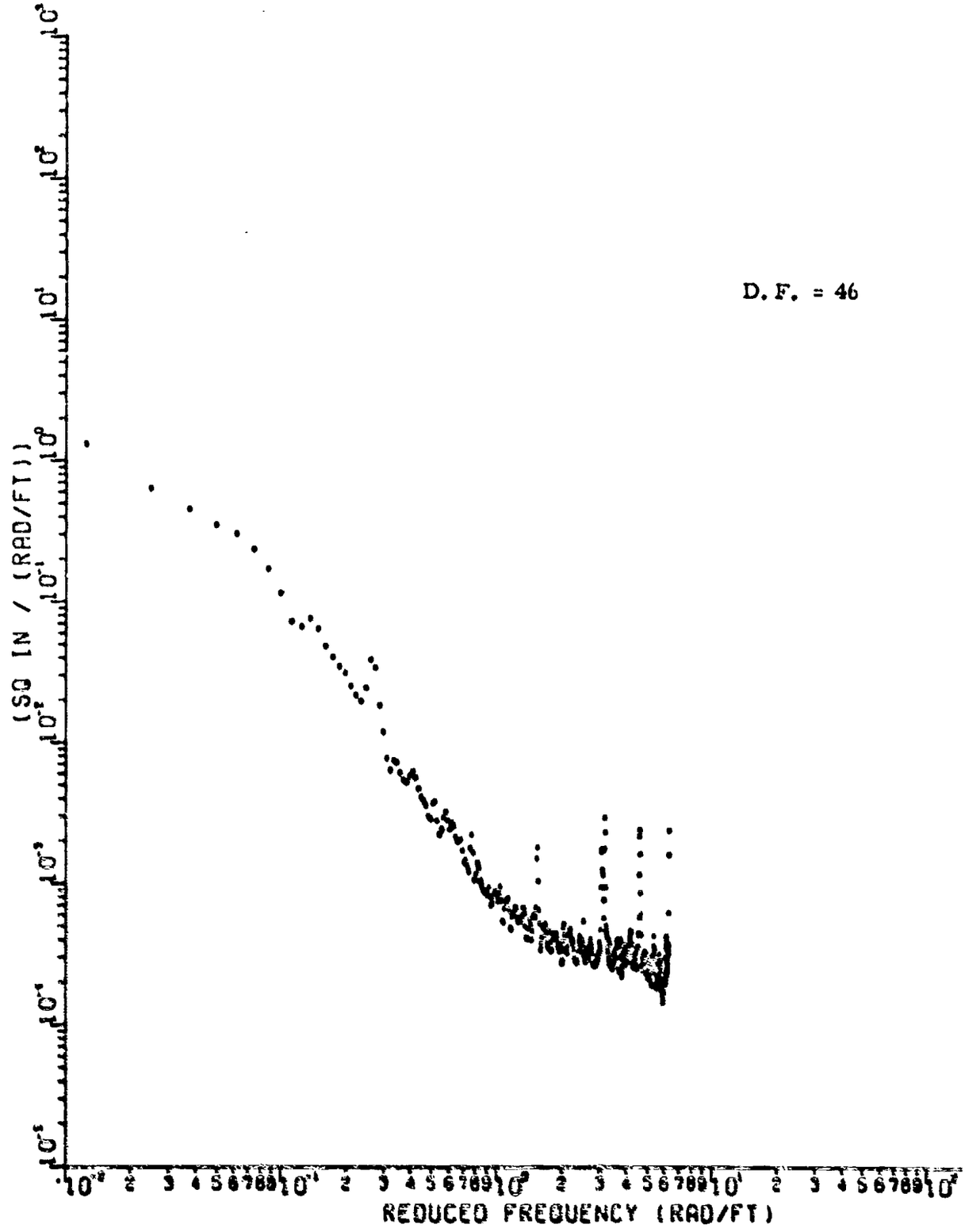

Figure 46 PSD Carswell 13L (Autocorrelation - Prewhitened and smoothed)

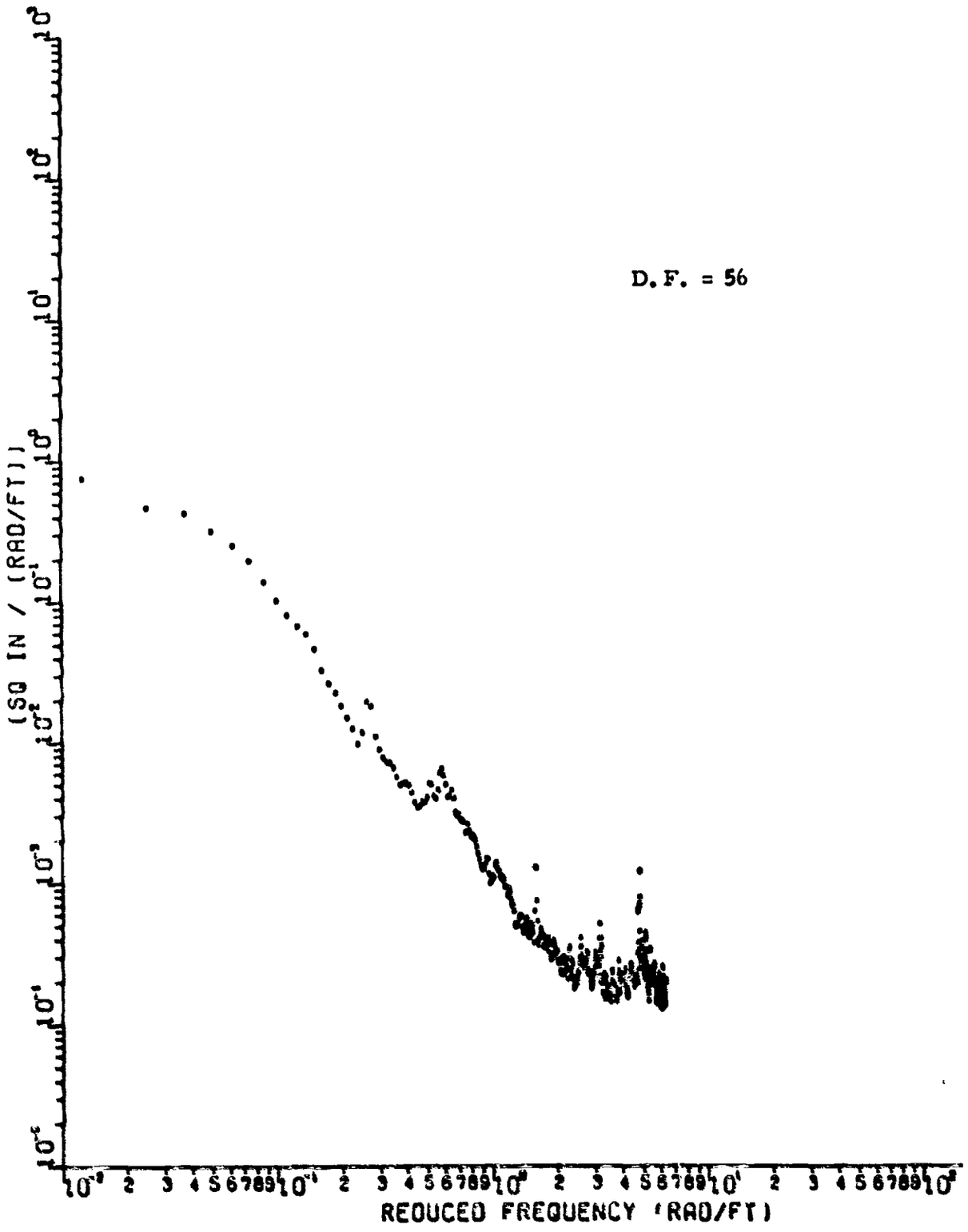

Figure 47 PSD Edwards 75L (Autocorrelation - Prewhitened and smoothed)

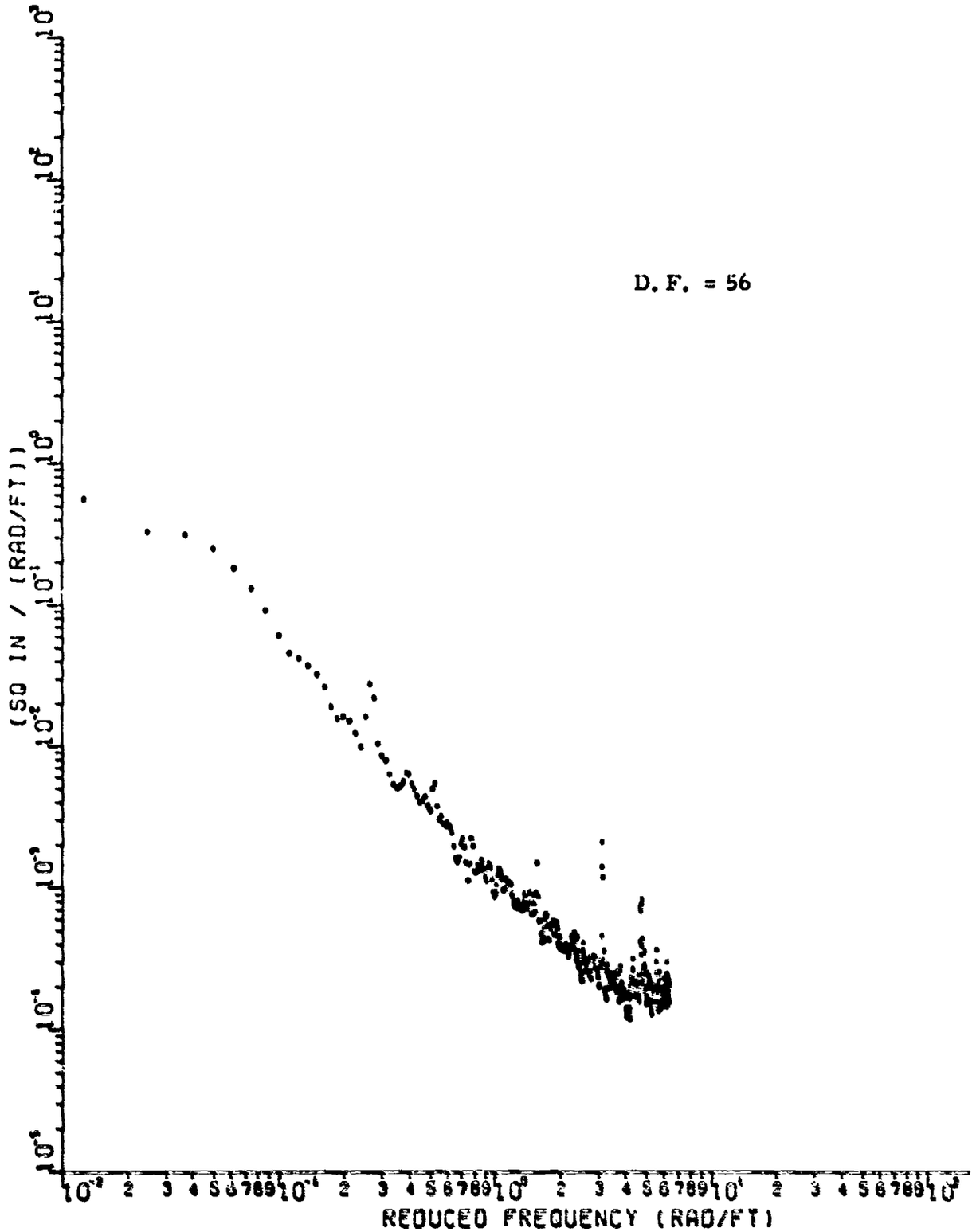

Figure 48 PSD Edwards CL (Autocorrelation - Prewhitened and smoothed)

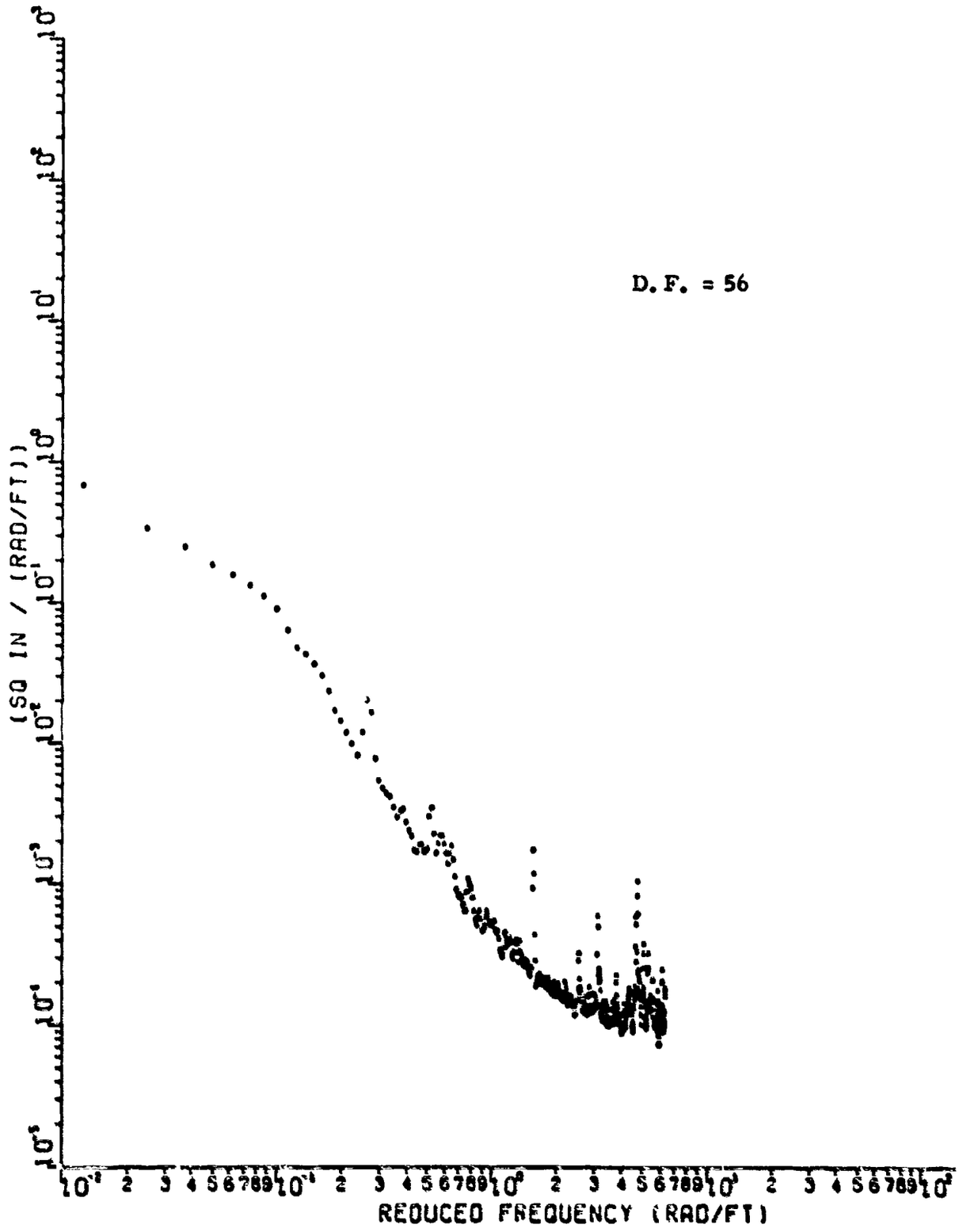

Figure 49 PSD Edwards 75R (Autocorrelation - Prewhitened and smoothed)

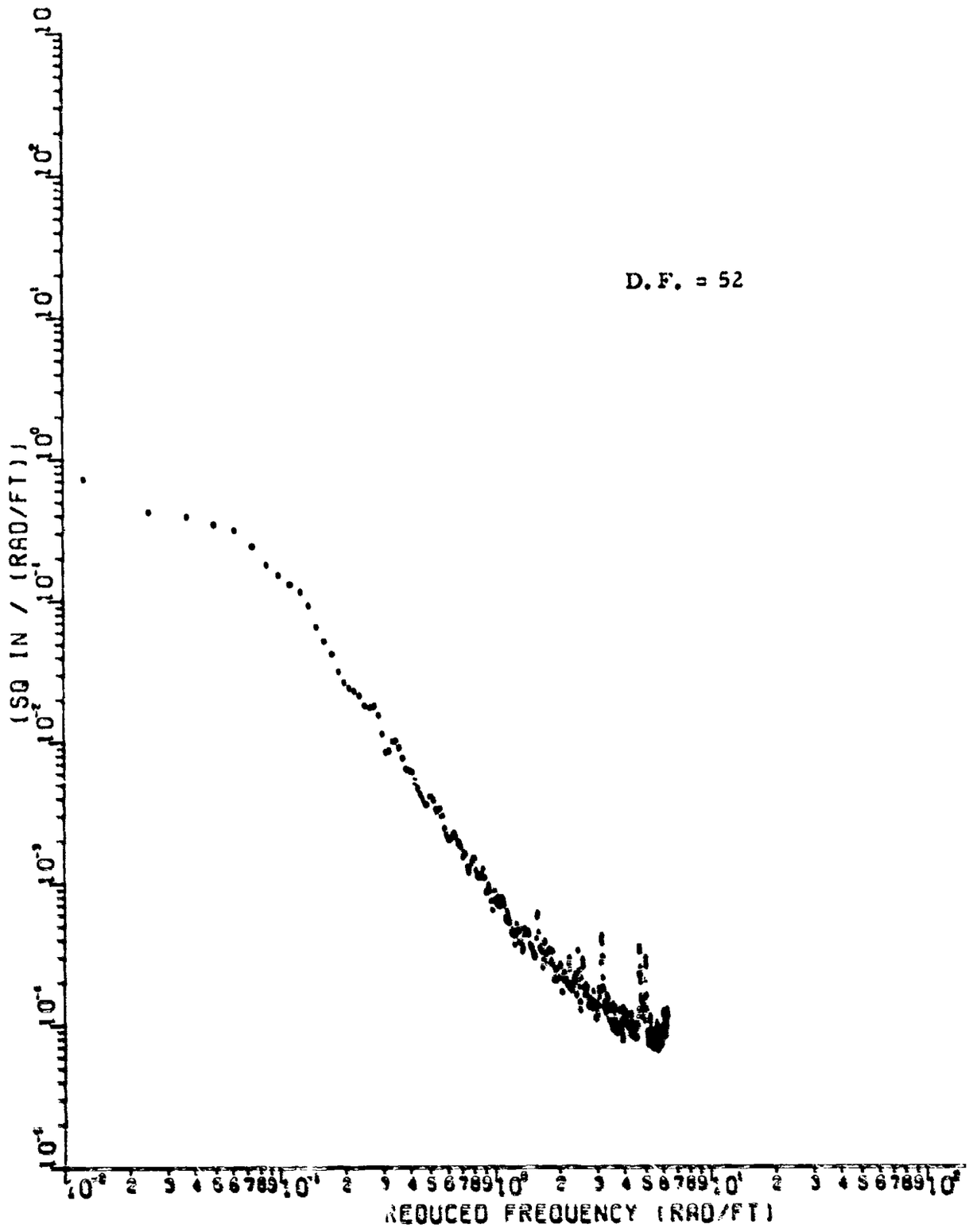

Figure 50 PSD Ellsworth CL (Autocorrelation - Prewhitened and smoothed)

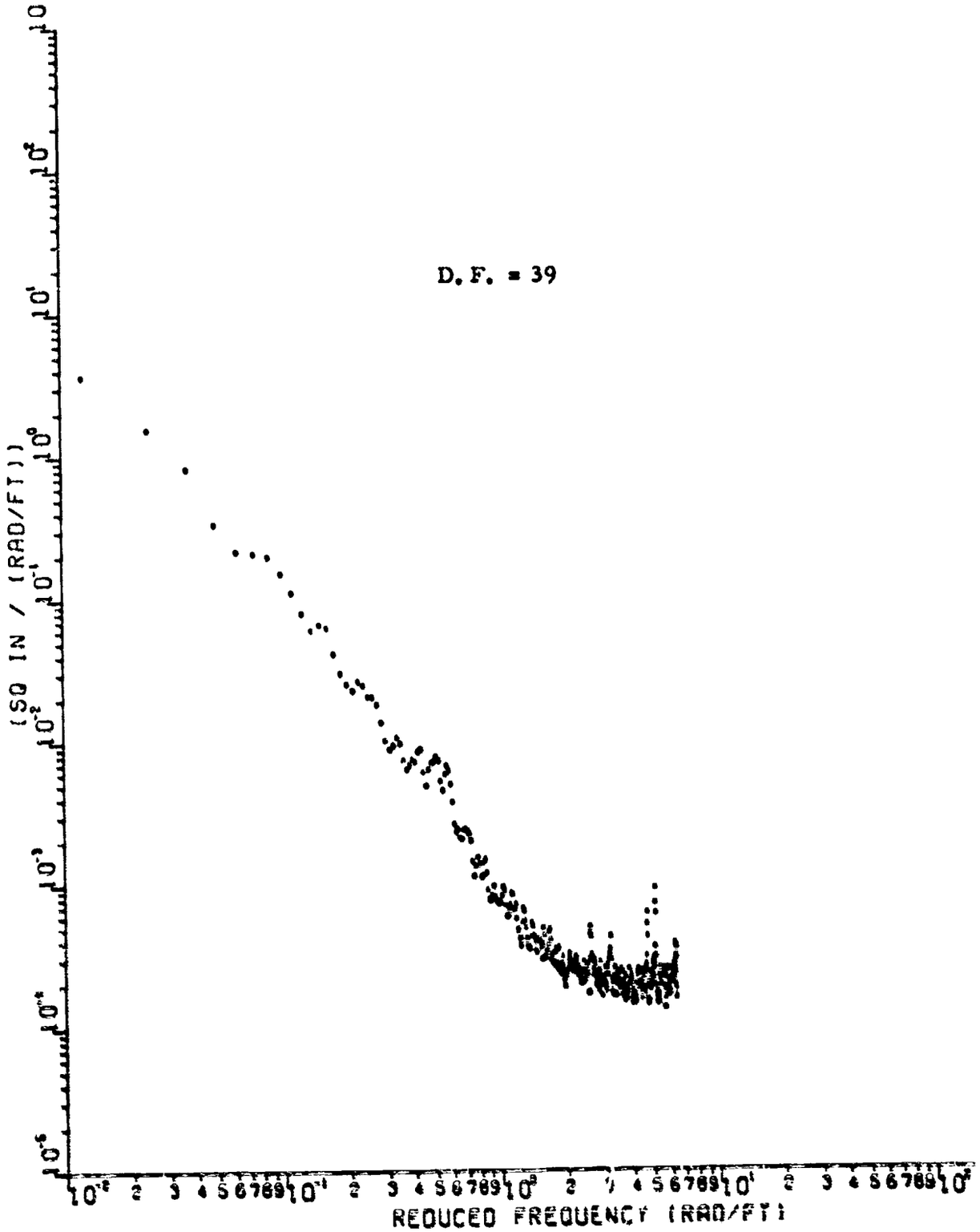

Figure 51 PSD Langley 50L (Autocorrelation - Prewhitened and smoothed)

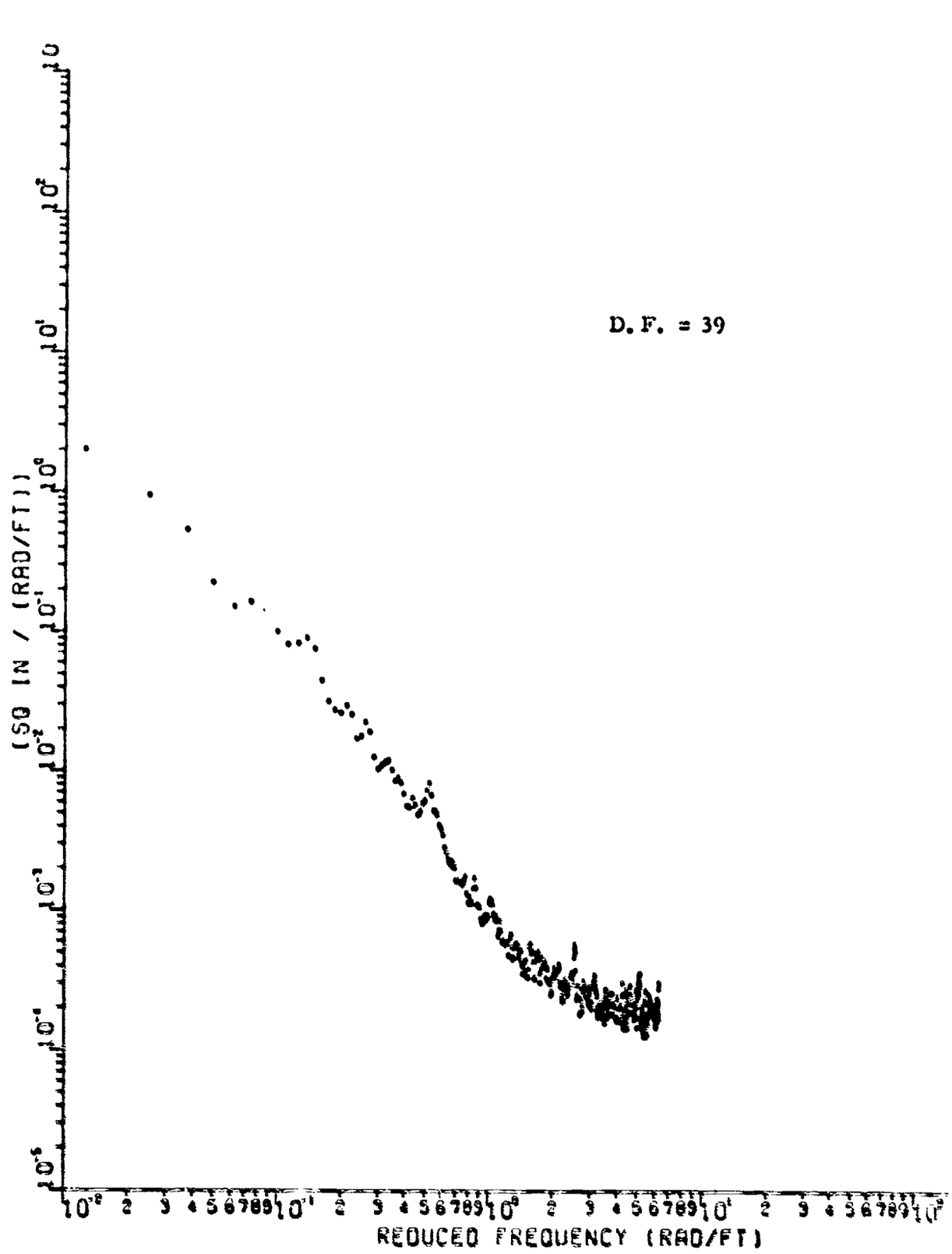

Figure 52 PSD Langley CL (Autocorrelation - Prewhitened and smoothed)

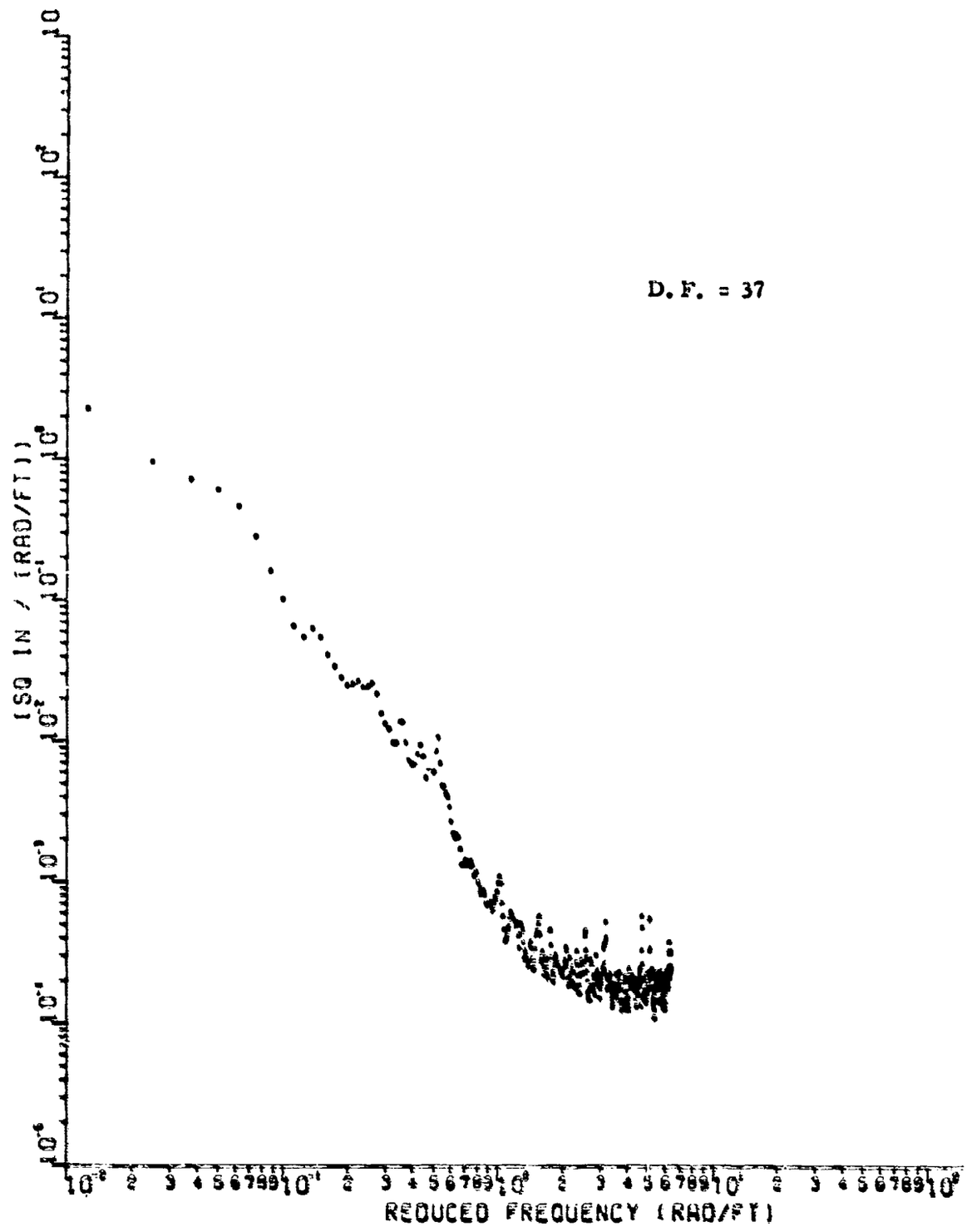

Figure 53 PSD Langley 50R (Autocorrelation - Prewhitened and smoothed)

APPENDIX III

POWER SPECTRAL DENSITIES

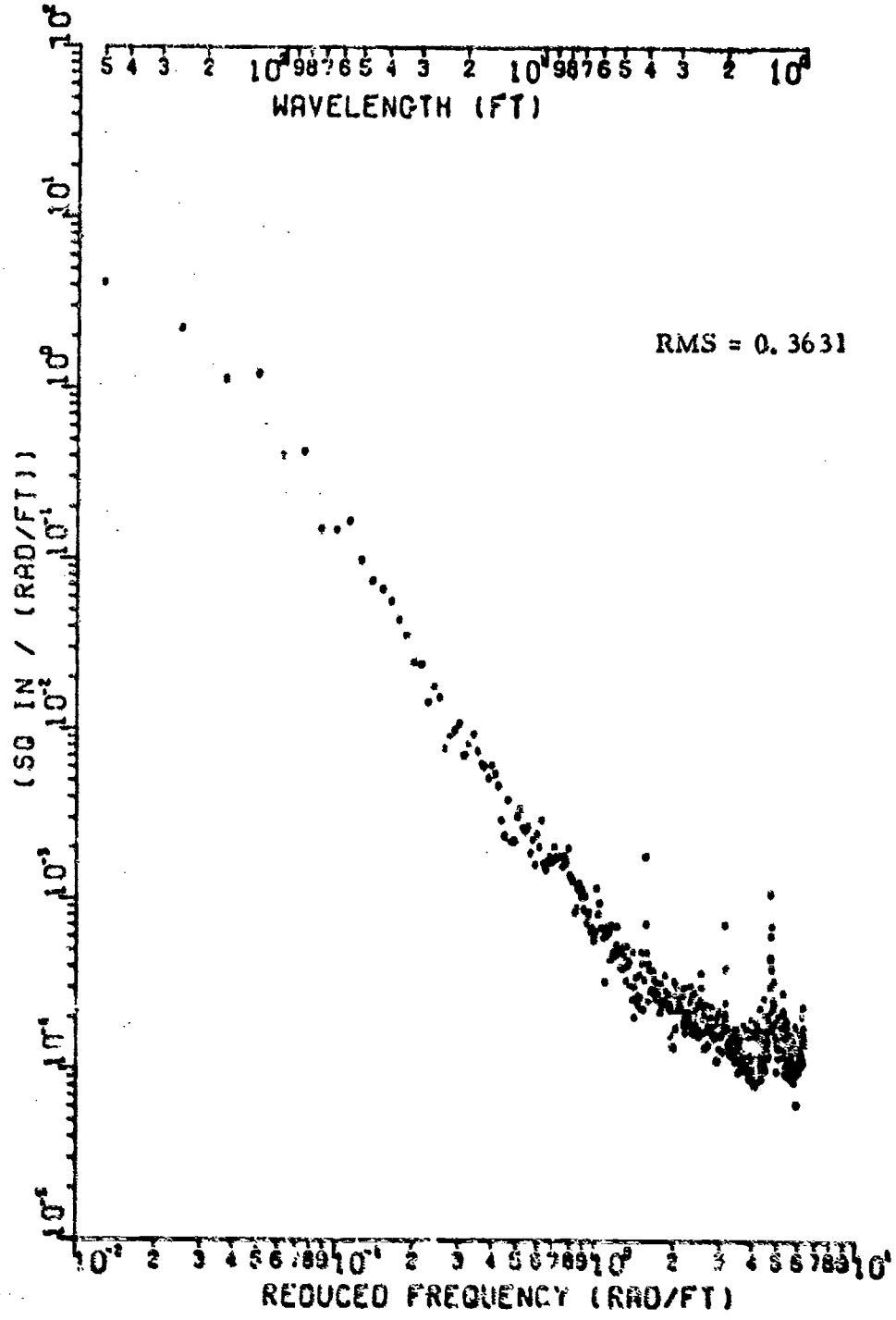

Figure 54 Power Spectral Density of Altus, 75L, filtered at 500 ft

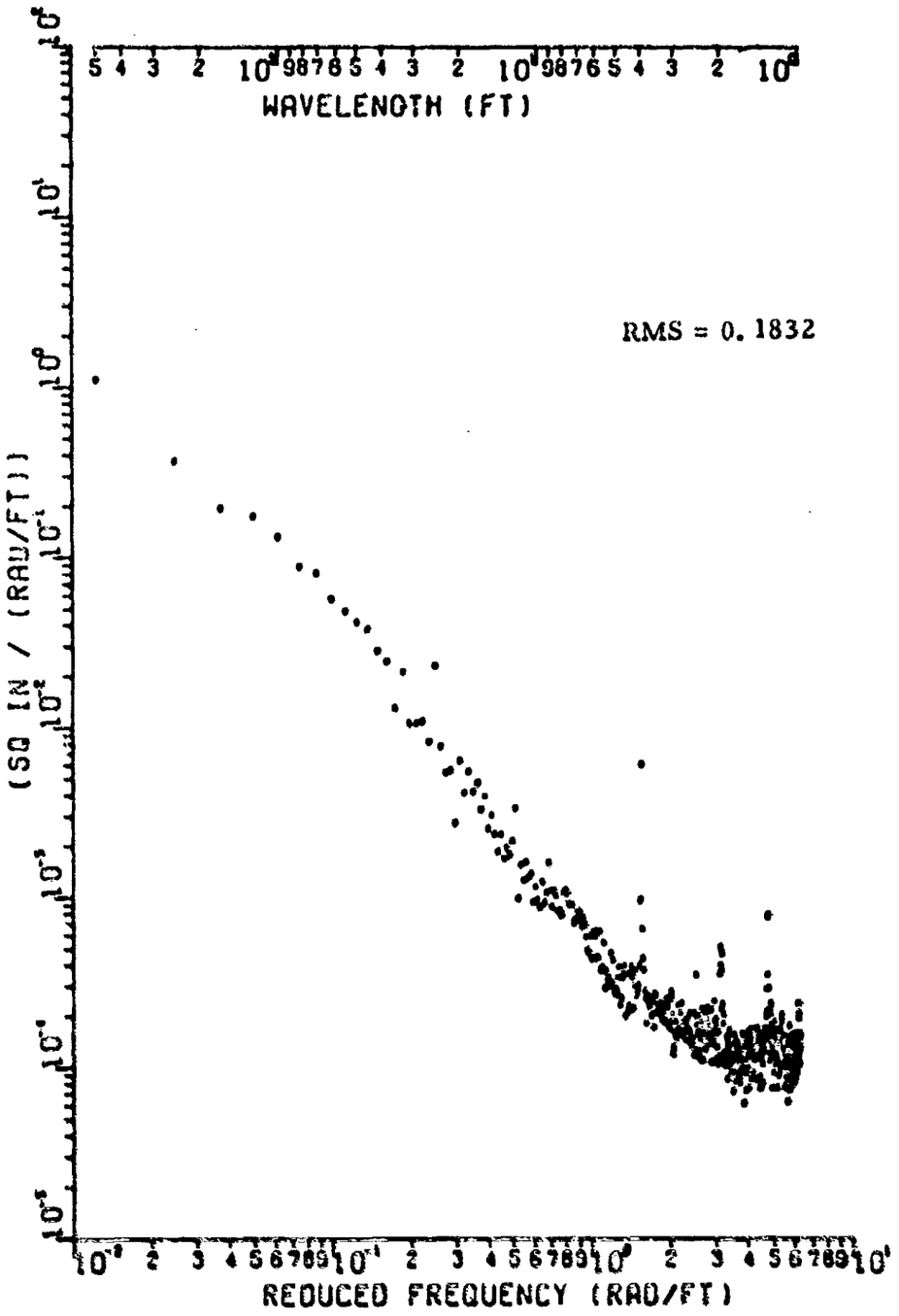

Figure 55 Power Spectral Density of Altus, Center, filtered at 500 ft

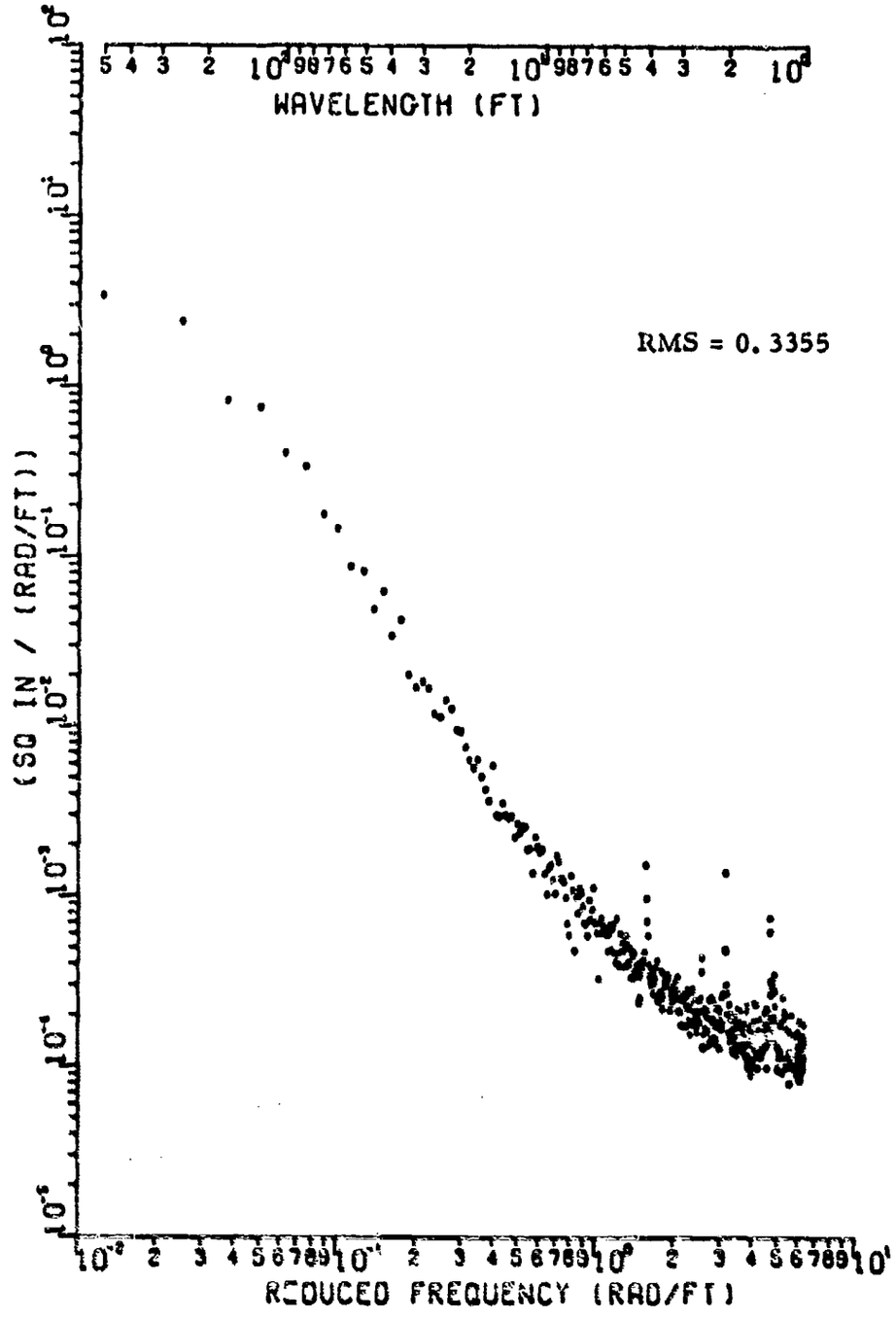

Figure 66 Power Spectral Density of Altus, 75R, filtered at 500 ft

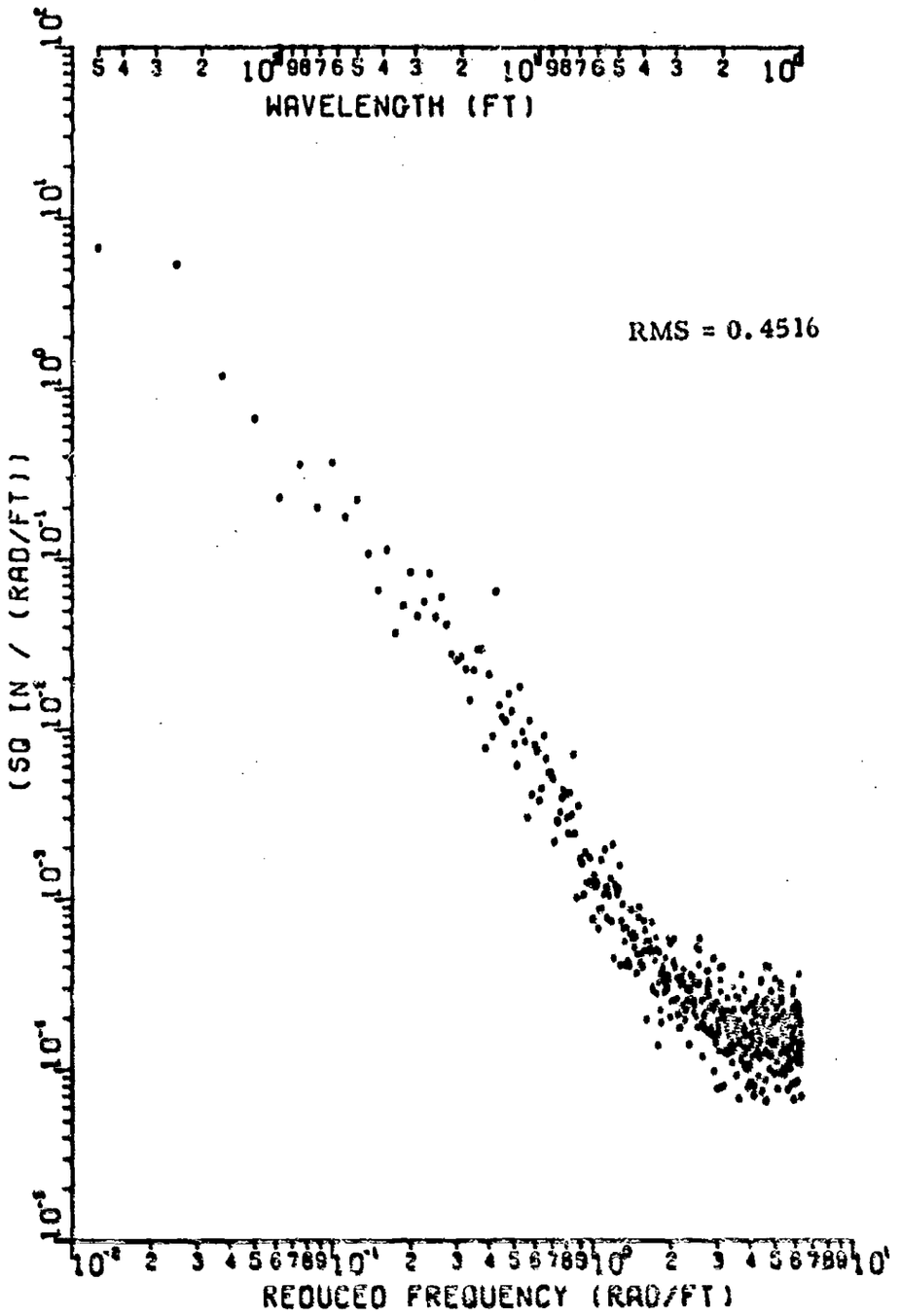

Figure 57 Power Spectral Density of Bakalar, 50 L, filtered at 500 ft

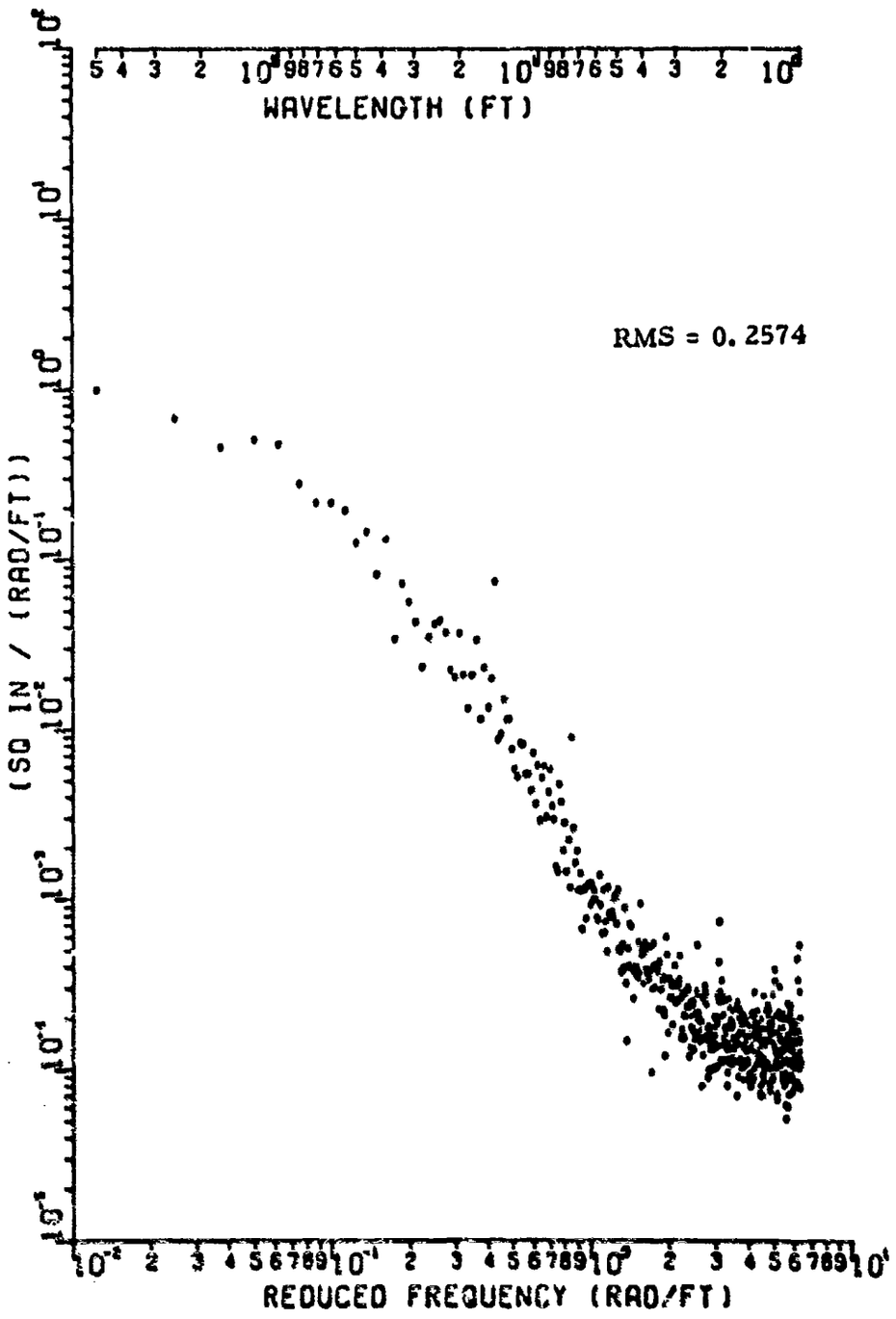

Figure 58 Power Spectral Density of Bakalar, Center, filtered at 500 ft

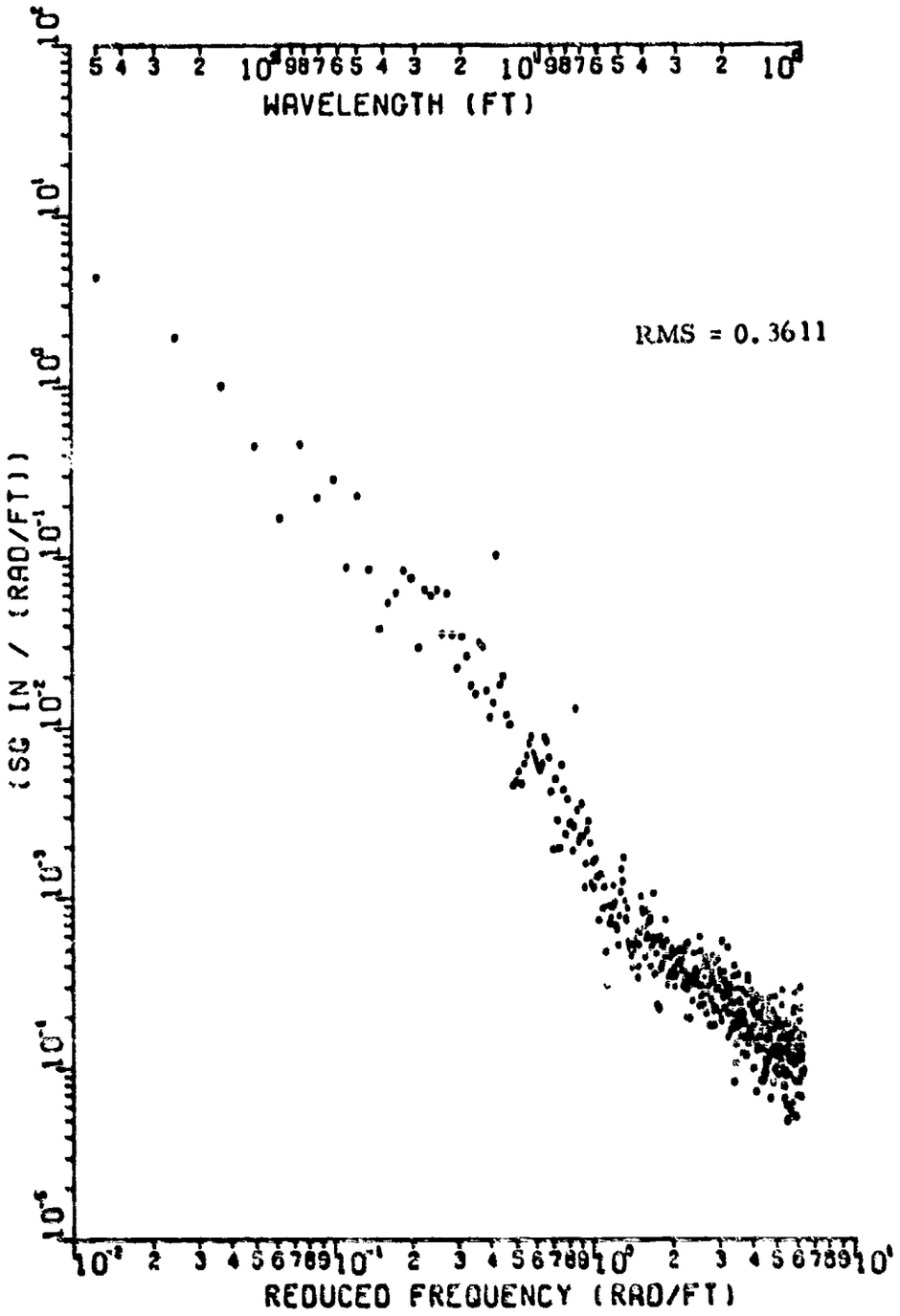

Figure 59 Power Spectral Density of Bakalar, 50 K, filtered at 500 ft

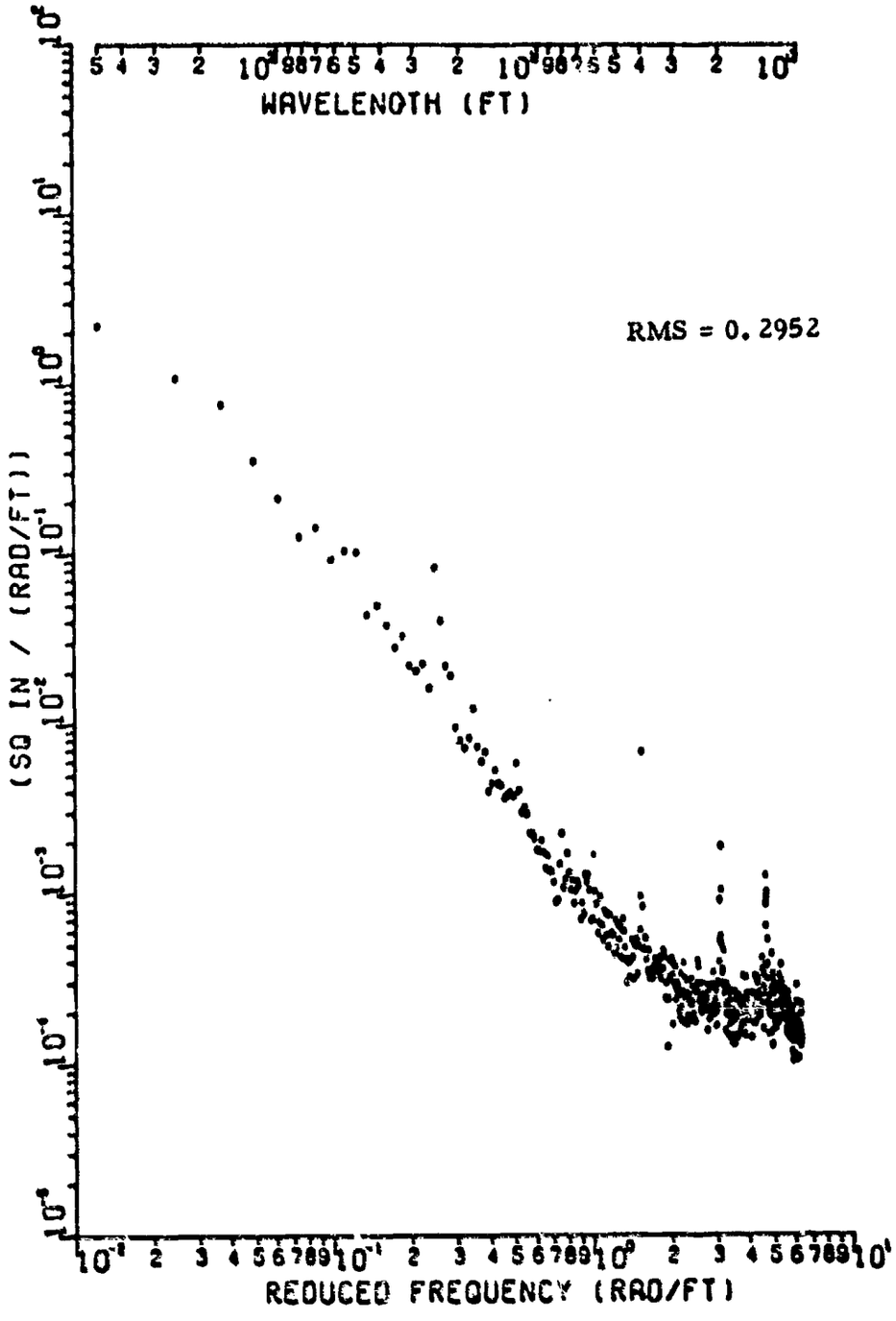

Figure 60 Power Spectral Density of Carswell, 87L, filtered at 500 ft

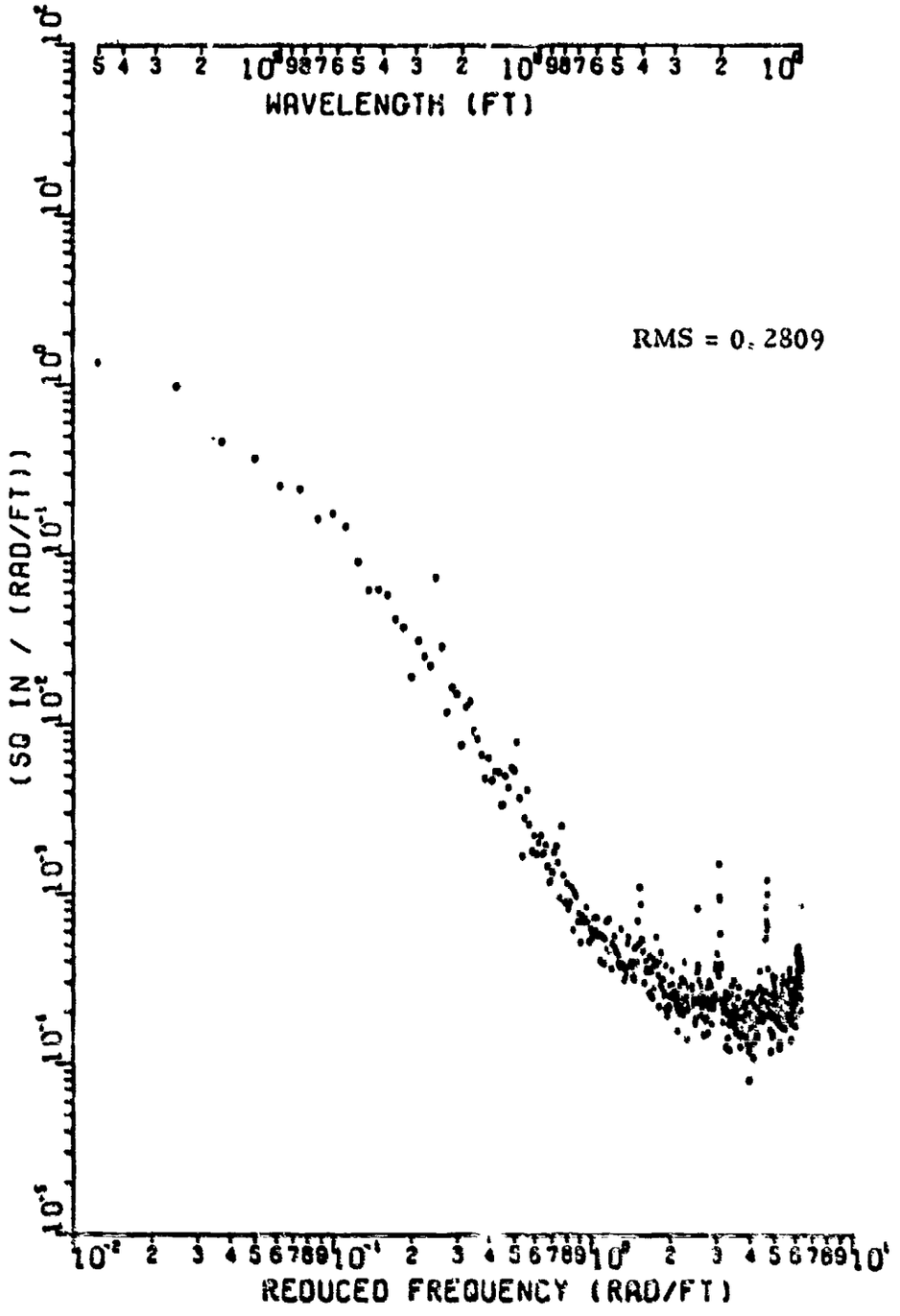

Figure 61 Power Spectral Density of Carswell, 13L, filtered at 500 ft

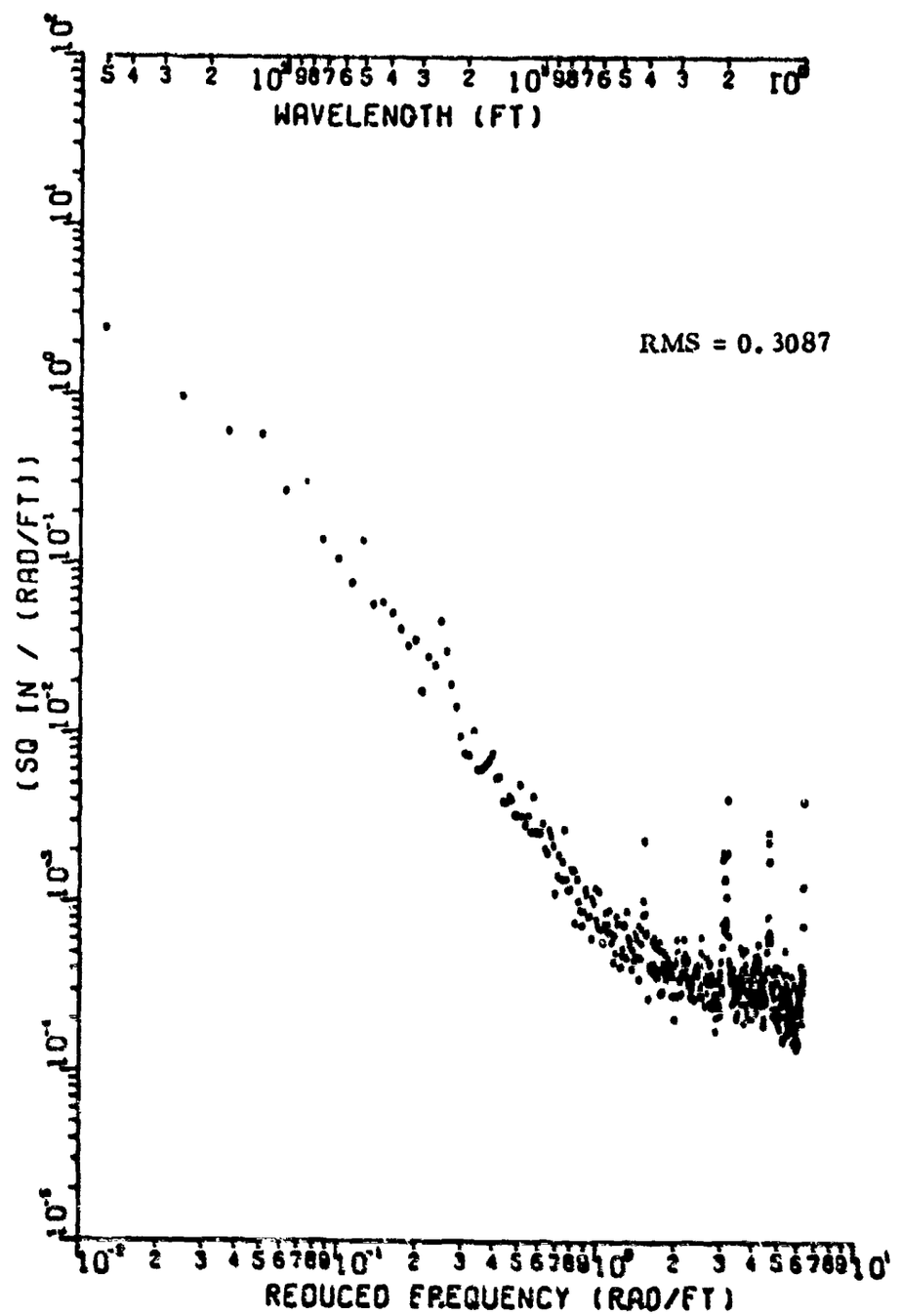

Figure 62 Power Spectral Density of Carswell, 13R, filtered at 500 ft

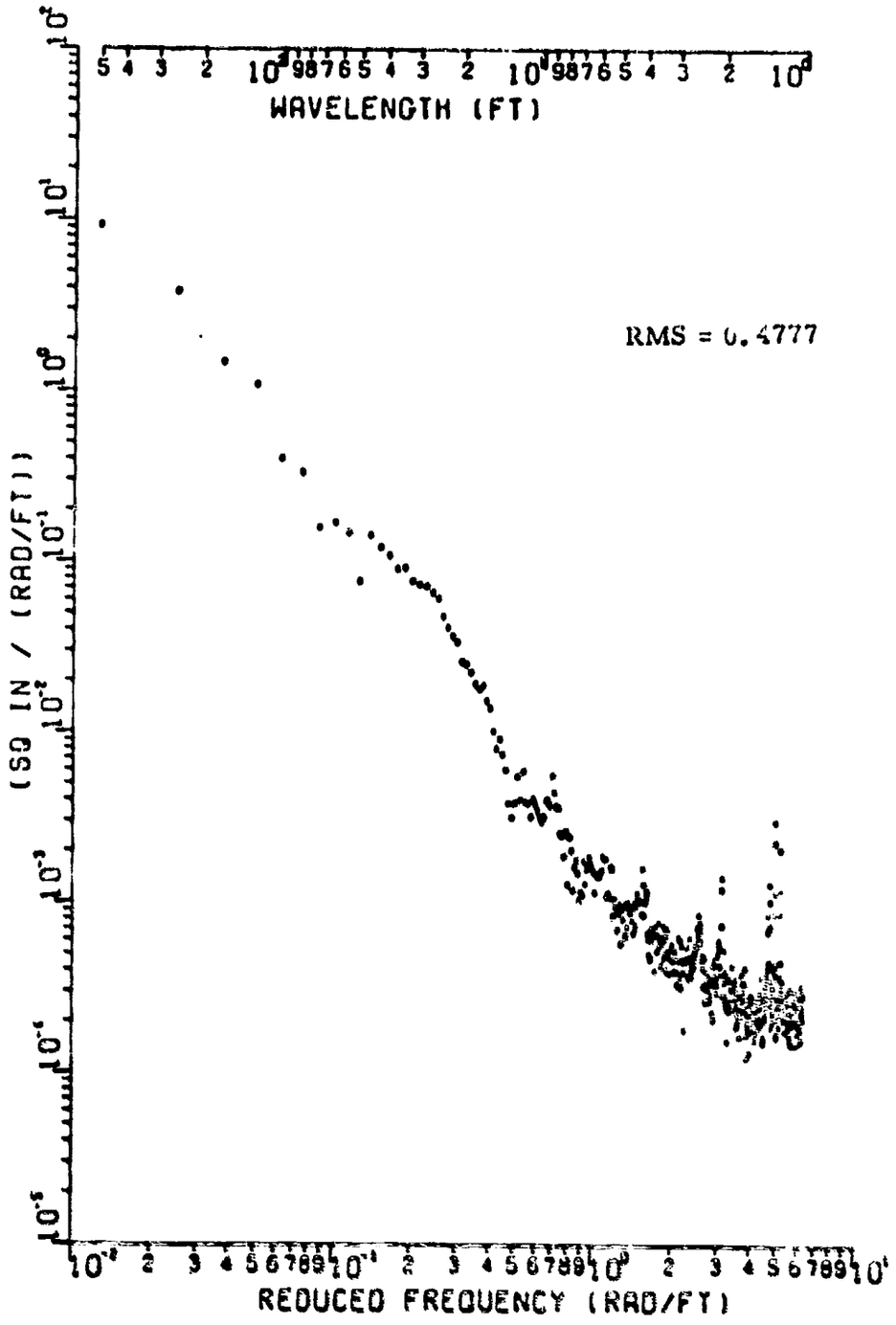

Figure 63 Power Spectral Density of Castle, 75L, filtered at 500 ft

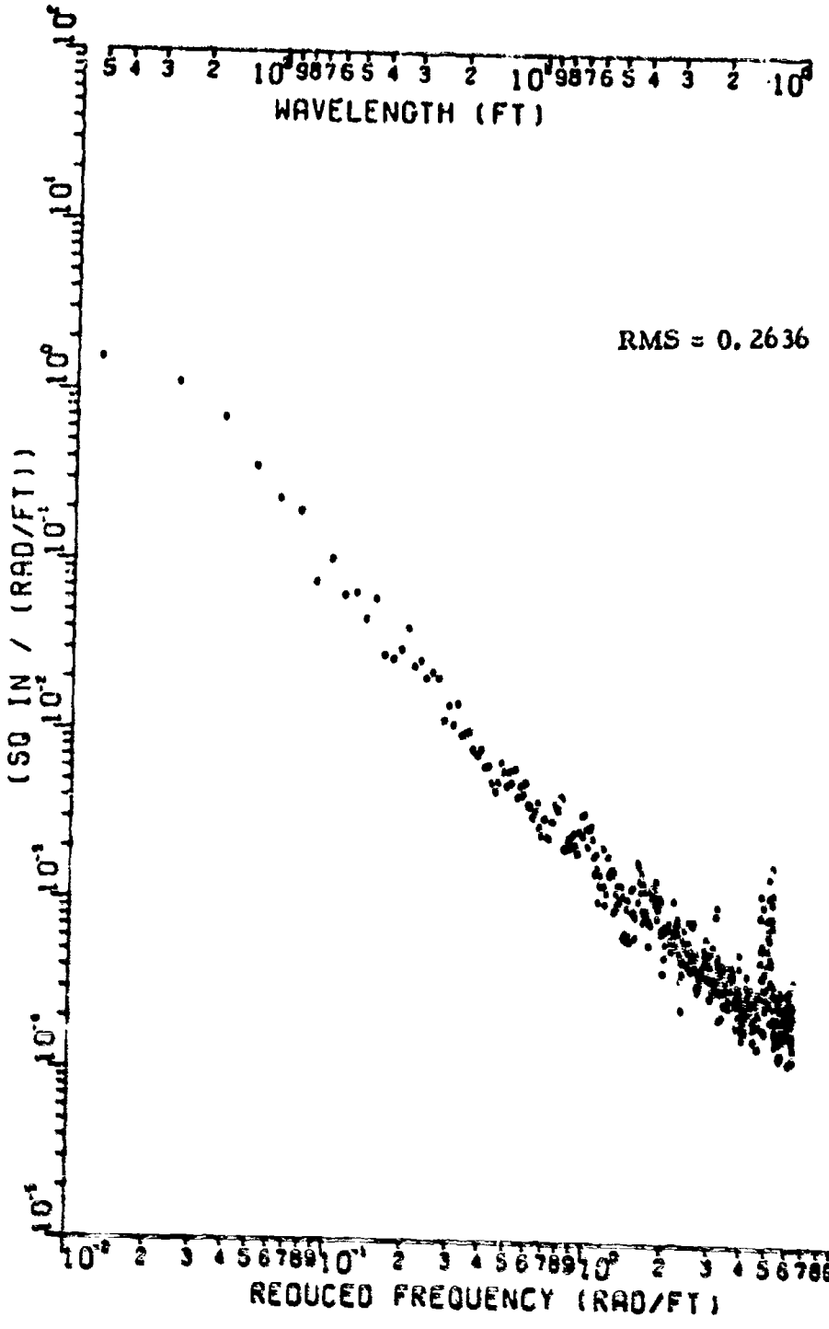

Figure 64 Power Spectral Density of Castle, Center, filtered at 500 ft

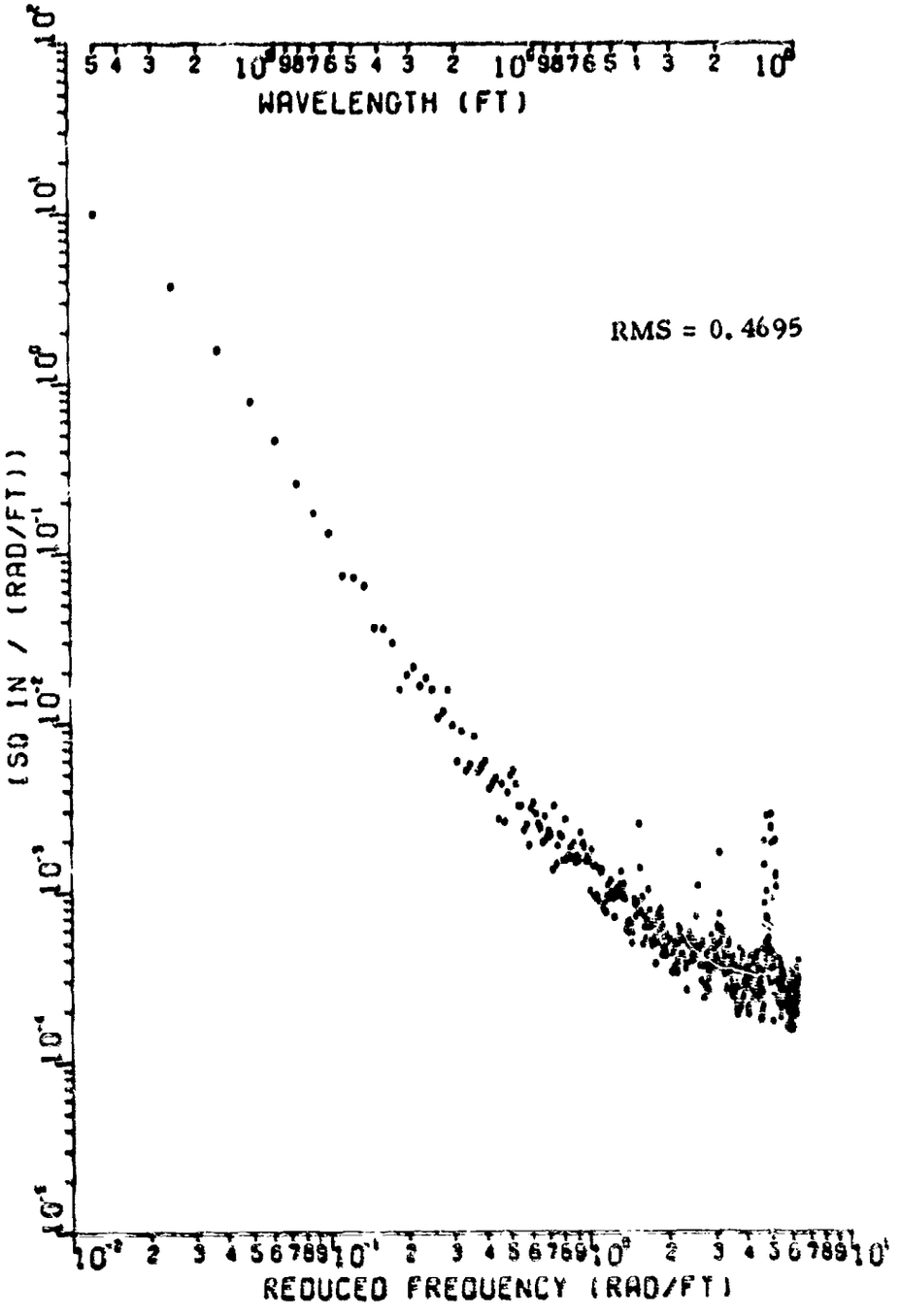

Figure 65 Power Spectral Density of Castle, 75R, filtered at 500 ft

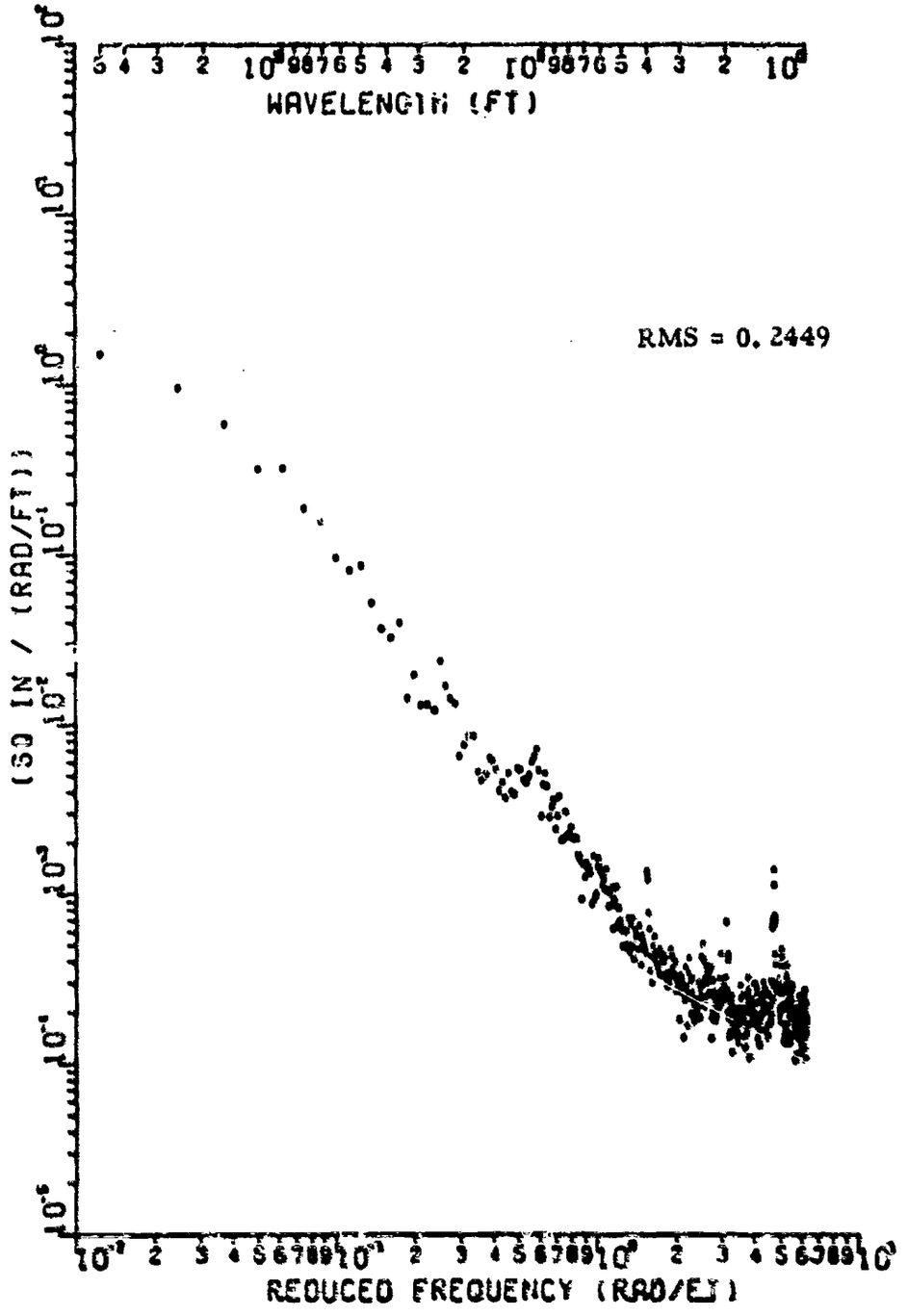

Figure 66 Power Spectral Density at Edwards, 75L, filtered at 500 ft

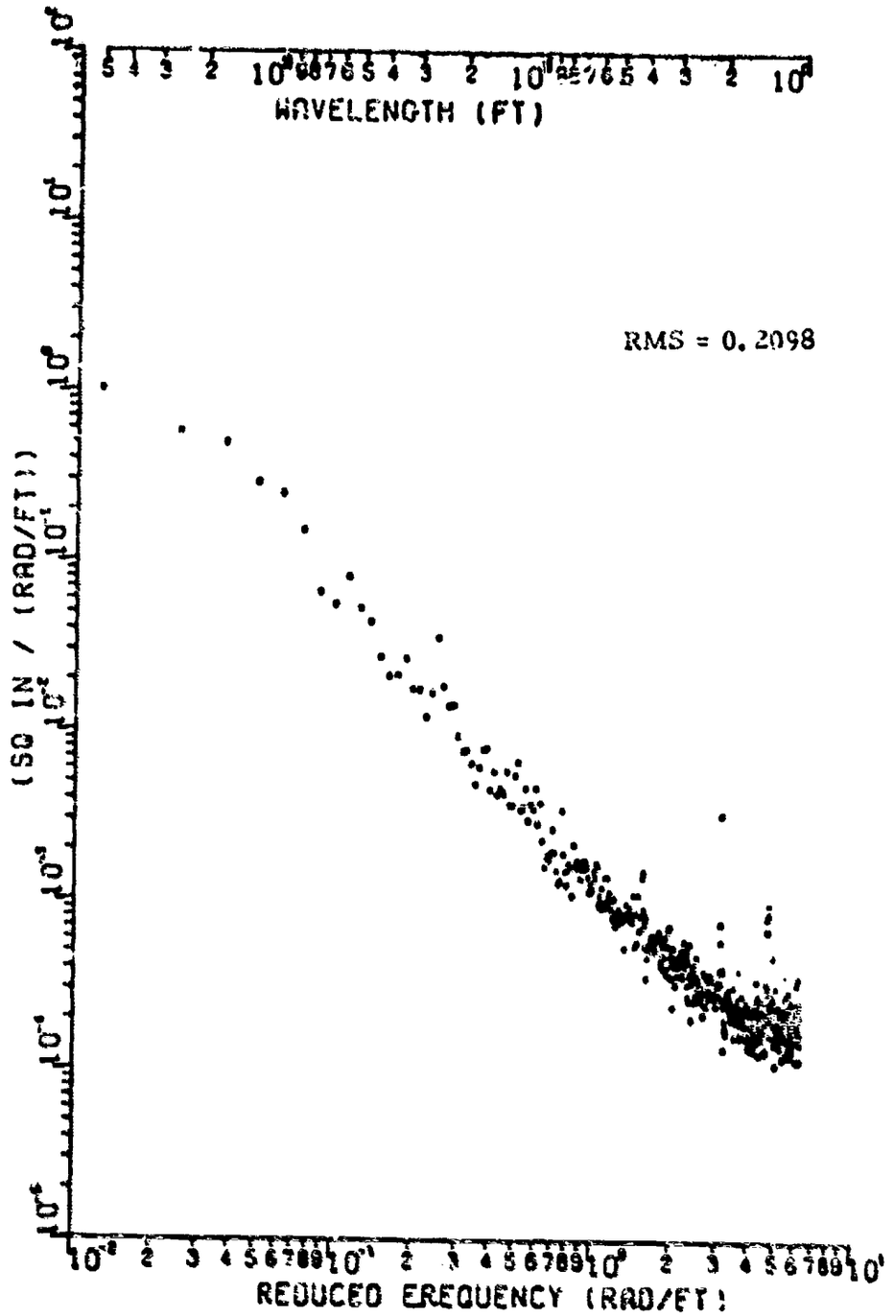

Figure 67 Power Spectral Density of Edwards, Center, filtered at 500 ft

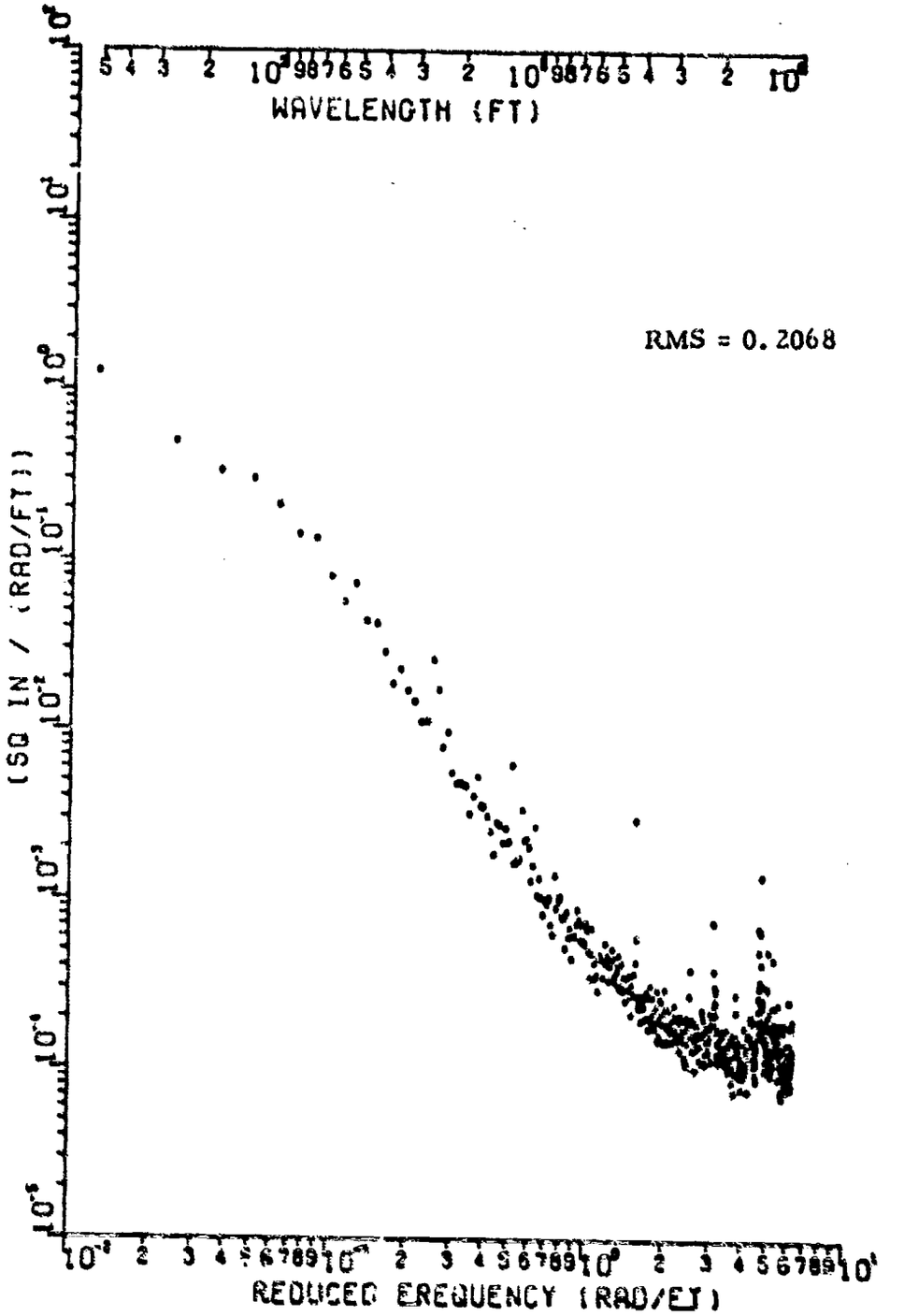

Figure 68 Power Spectral Density of Edwards, 75R, filtered at 500 ft

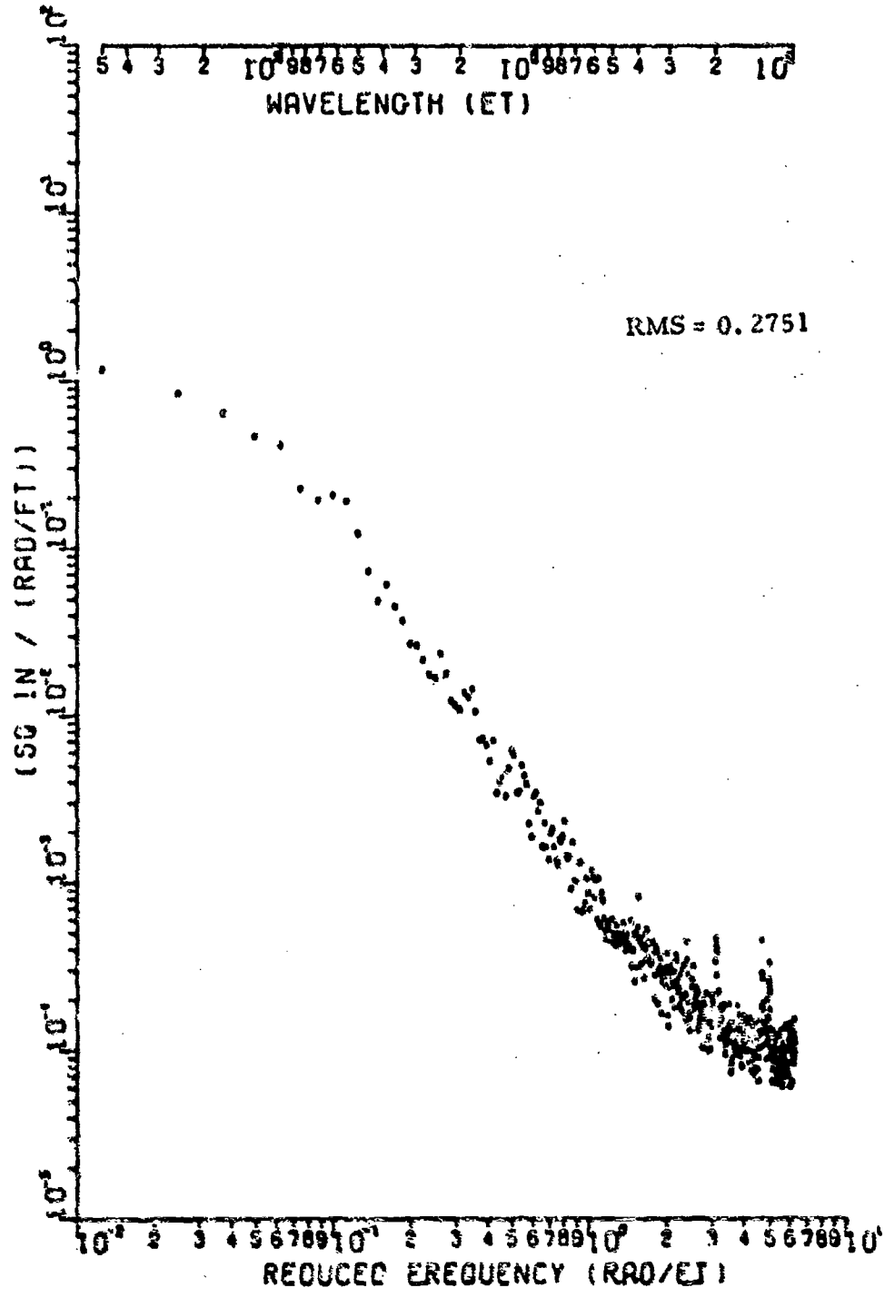

Figure 69 Power Spectral Density of Ellsworth, Center, filtered at 500 ft

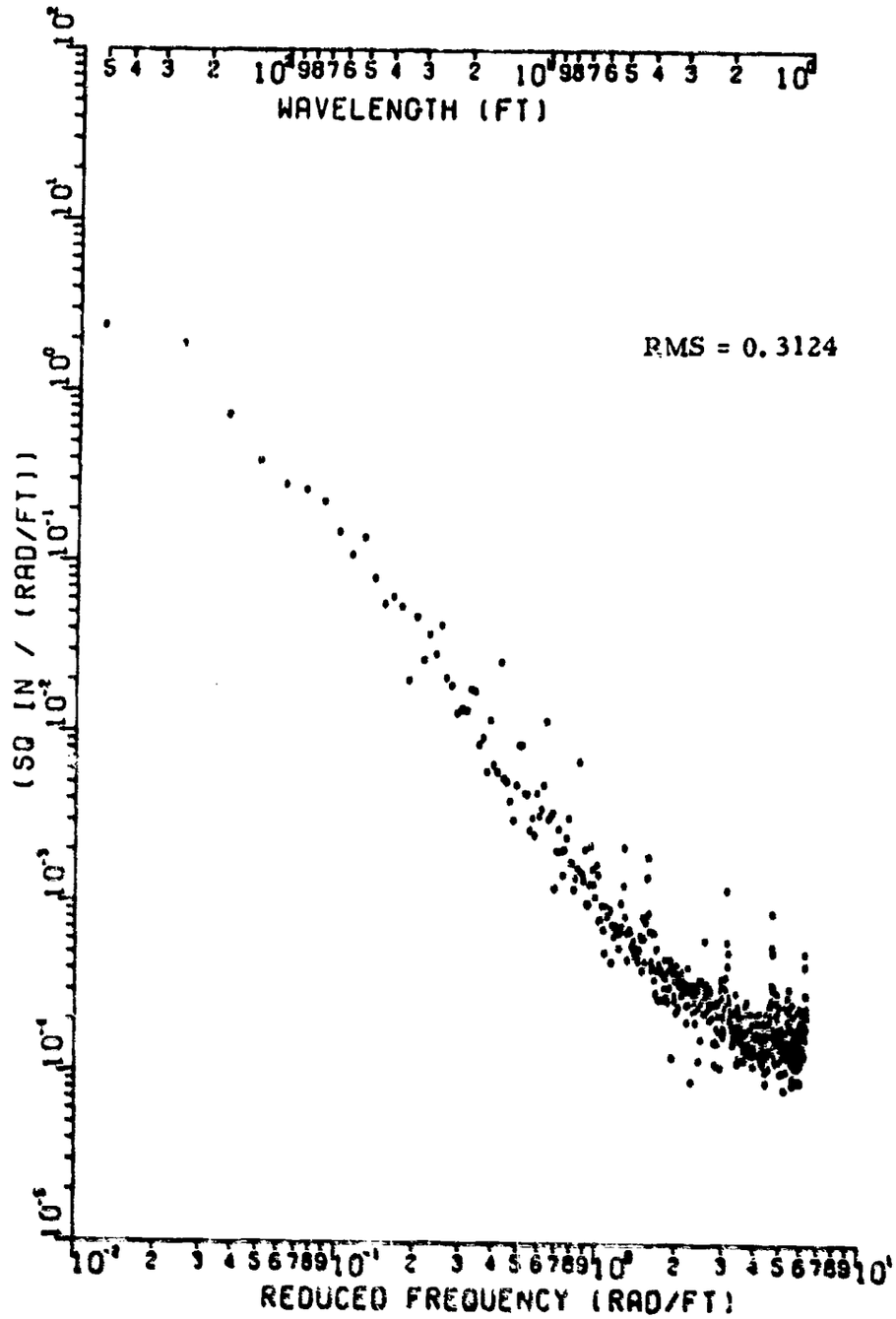

Figure 70 Power Spectral Density of George, 50 L, filtered at 500 ft

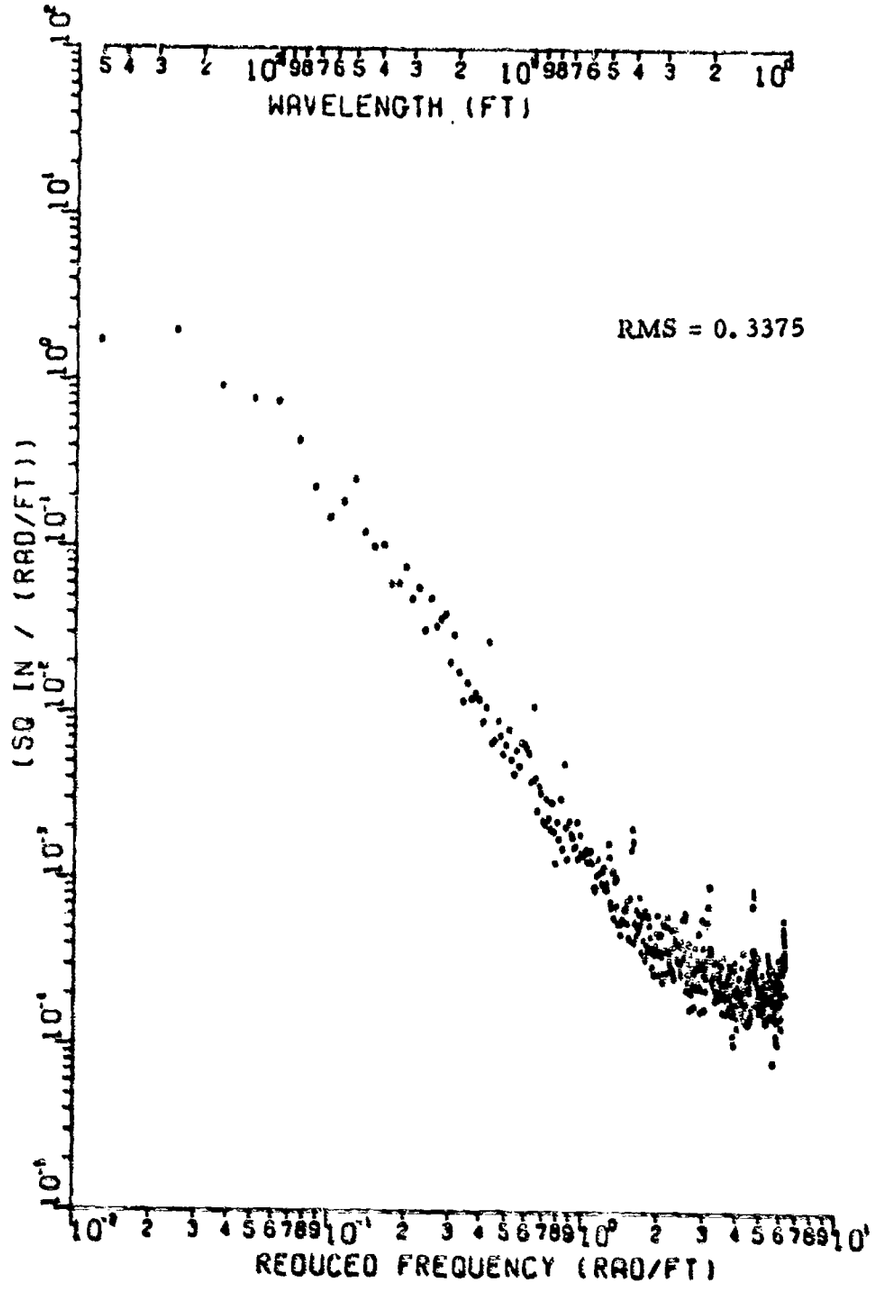

Figure 71 Power Spectral Density of George, Center, filtered at 500 ft

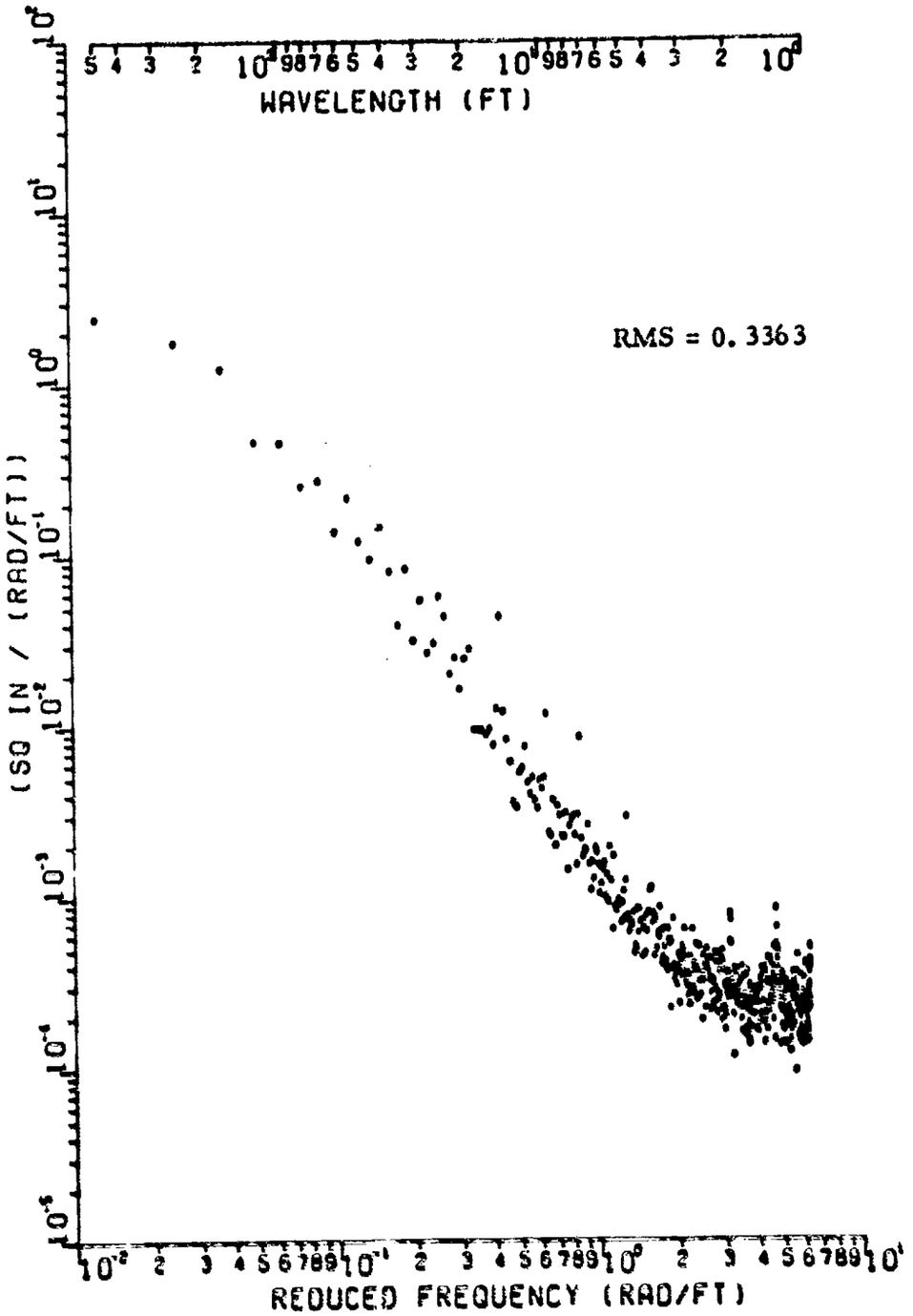

Figure 72 Power Spectral Density of George, 50 R, filtered at 500 ft

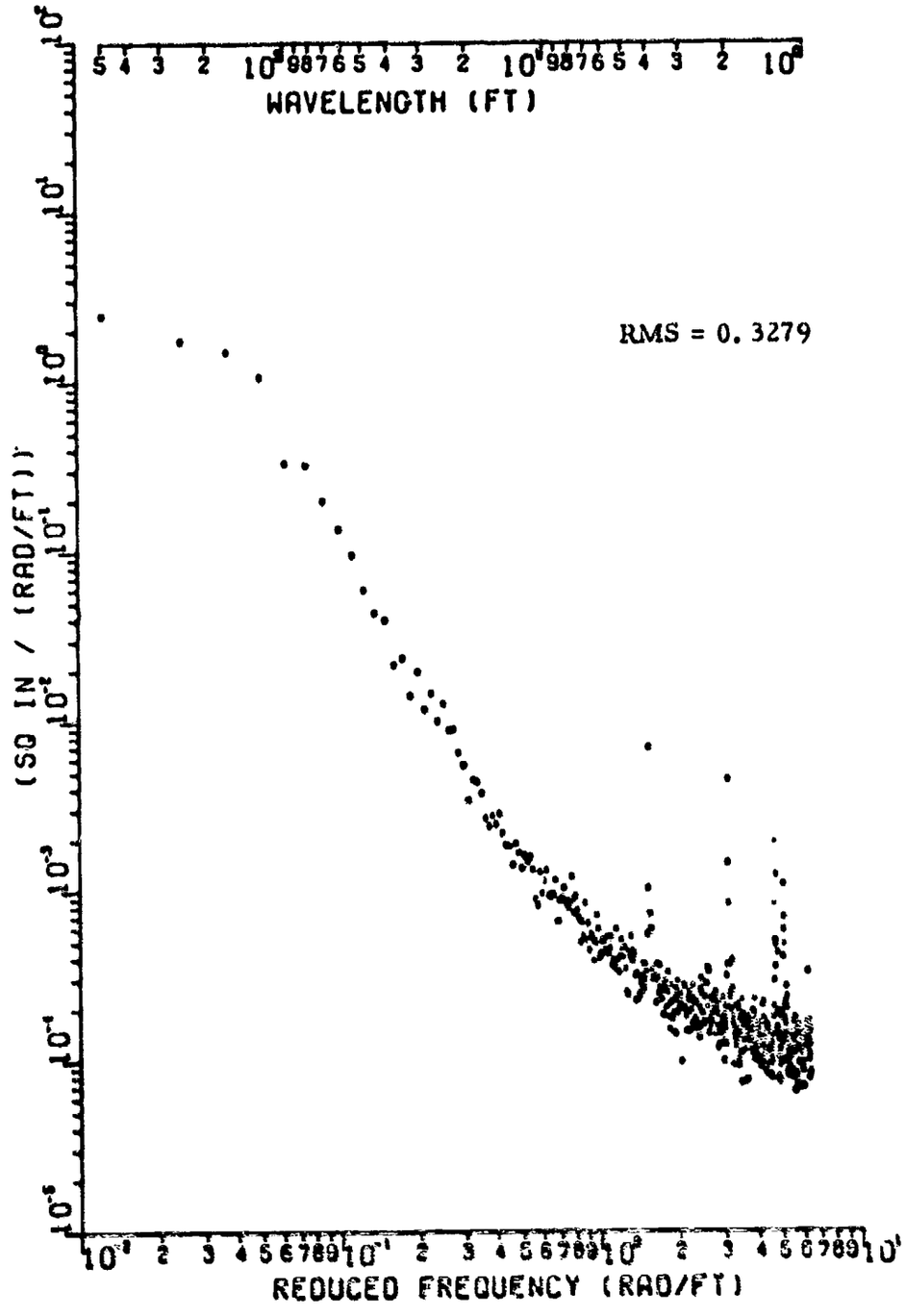

Figure 73 Power Spectral Density of Glasgow, 75L, filtered at 500 ft

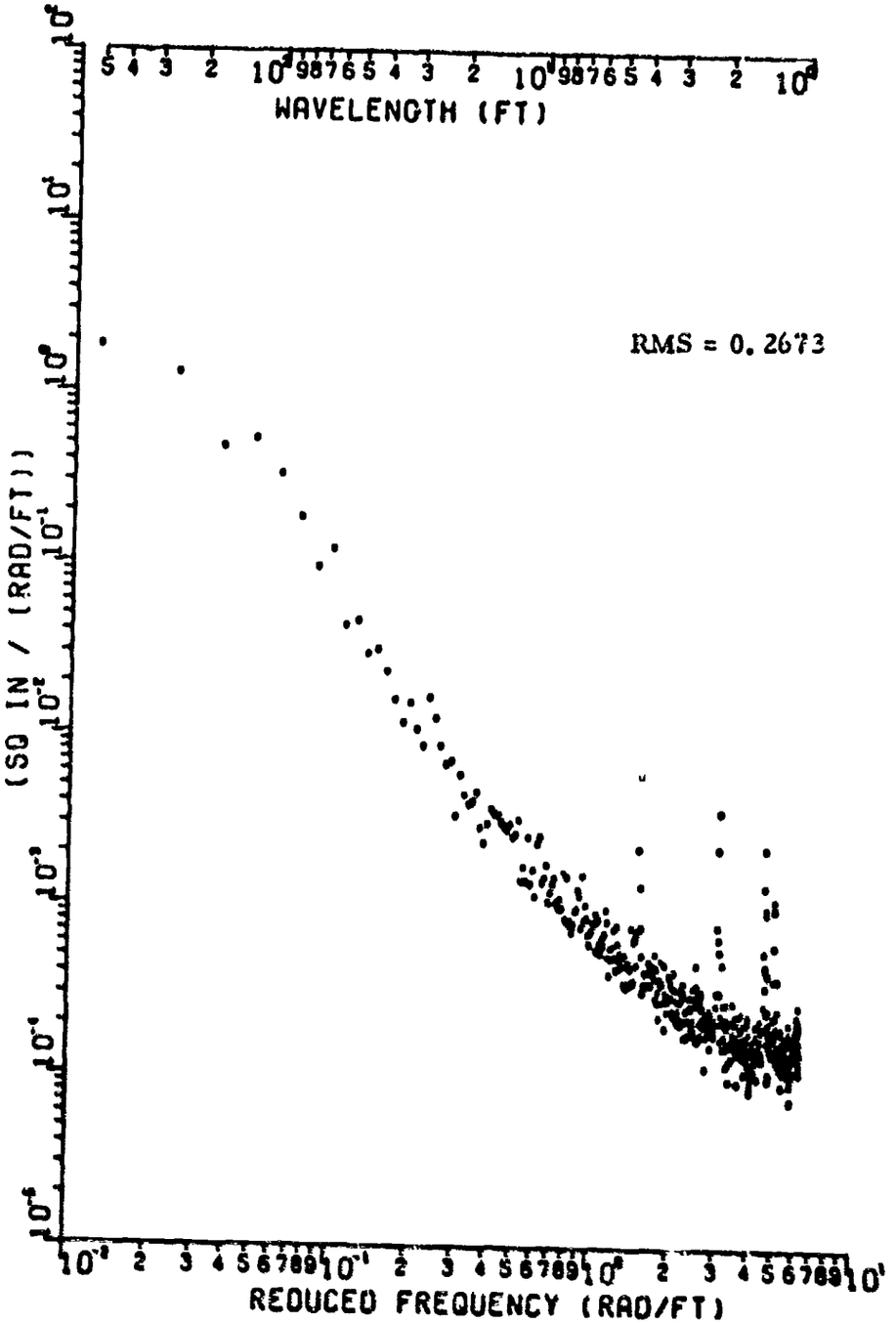

Figure 74 Power Spectral Density of Glasgow, Center, filtered at 500 ft

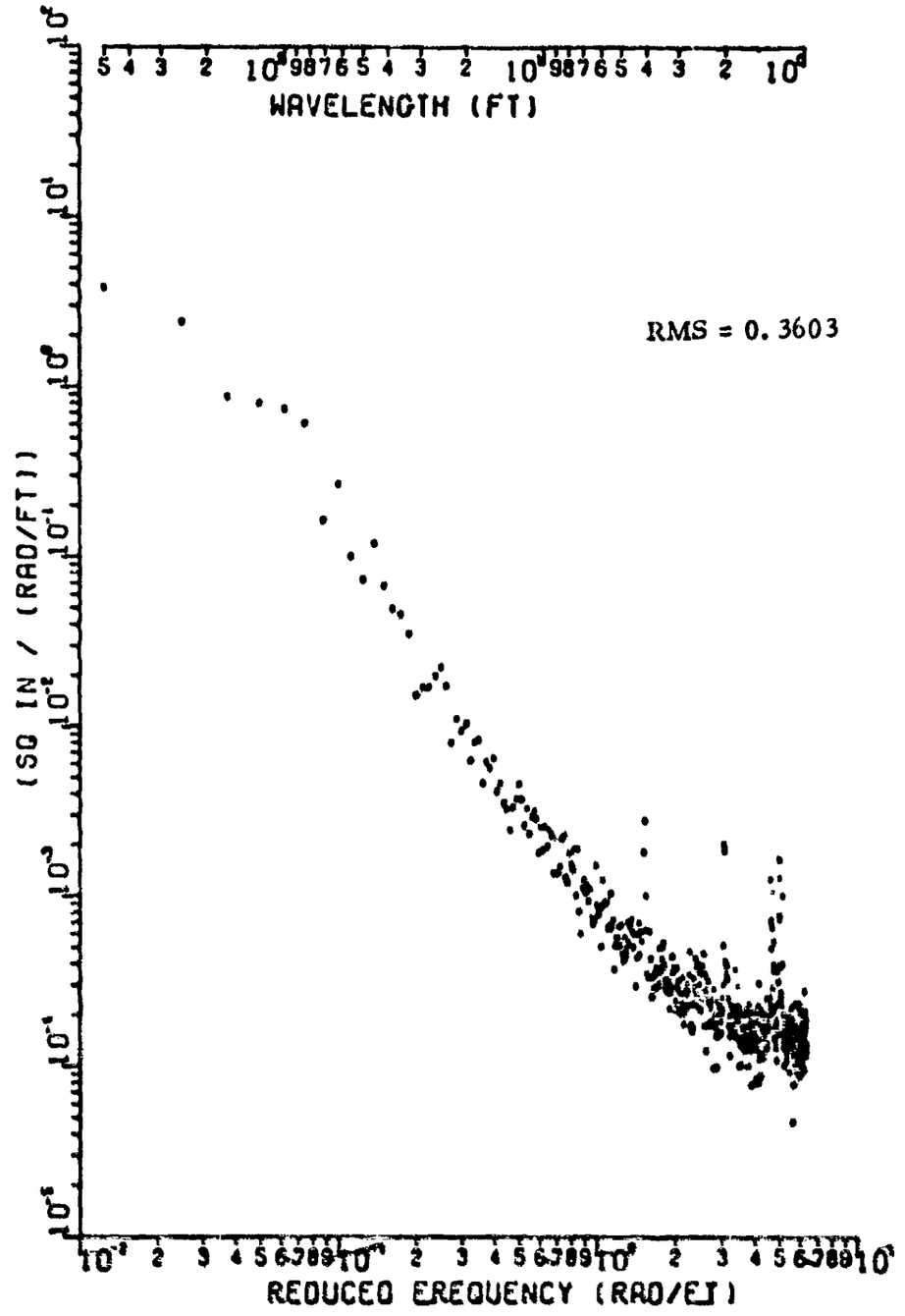

Figure 75 Power Spectral Density of Glasgow, 75R, filtered at 500 ft

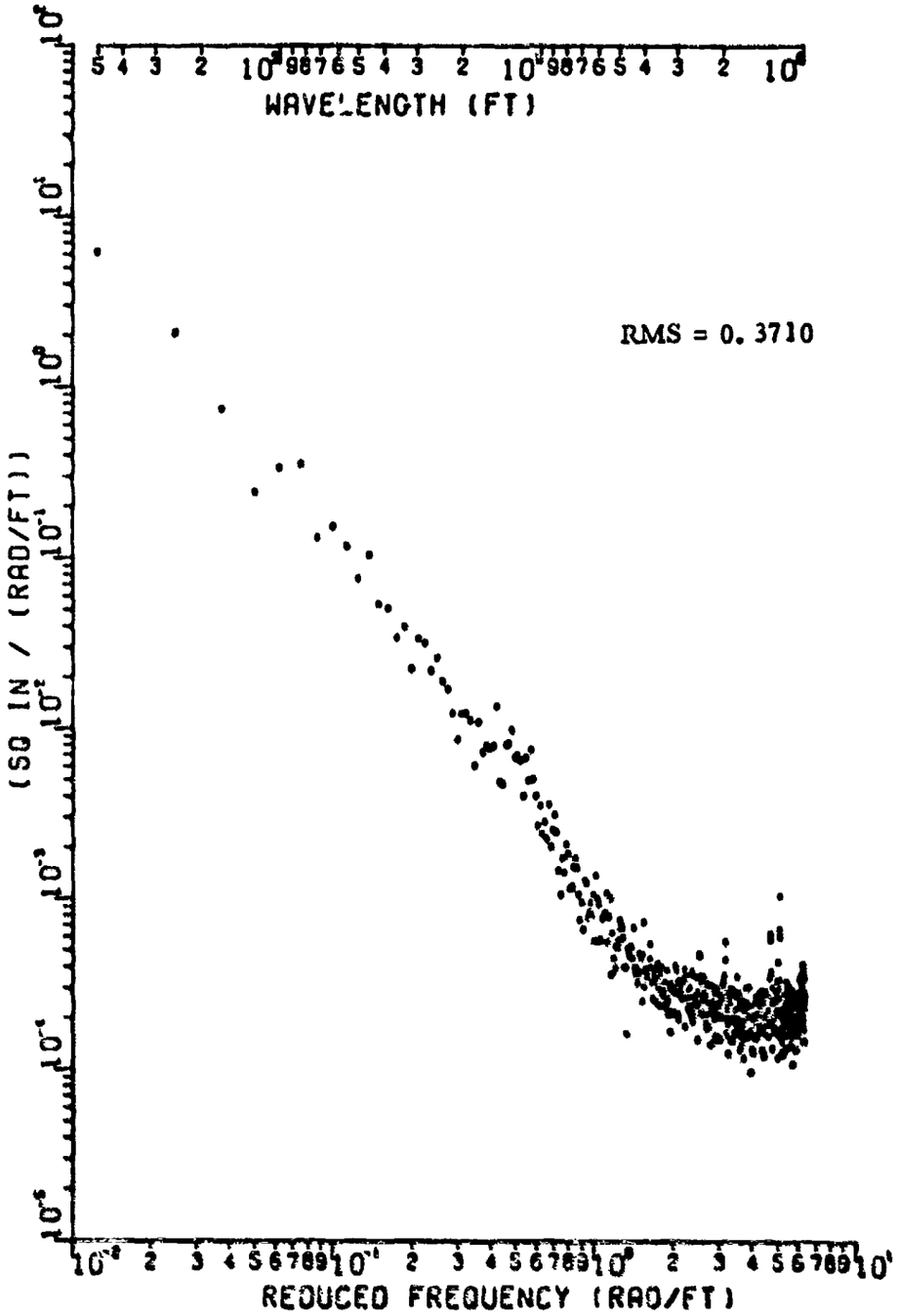

Figure 76 Power Spectral Density of Langley, 50L, filtered at 500 ft

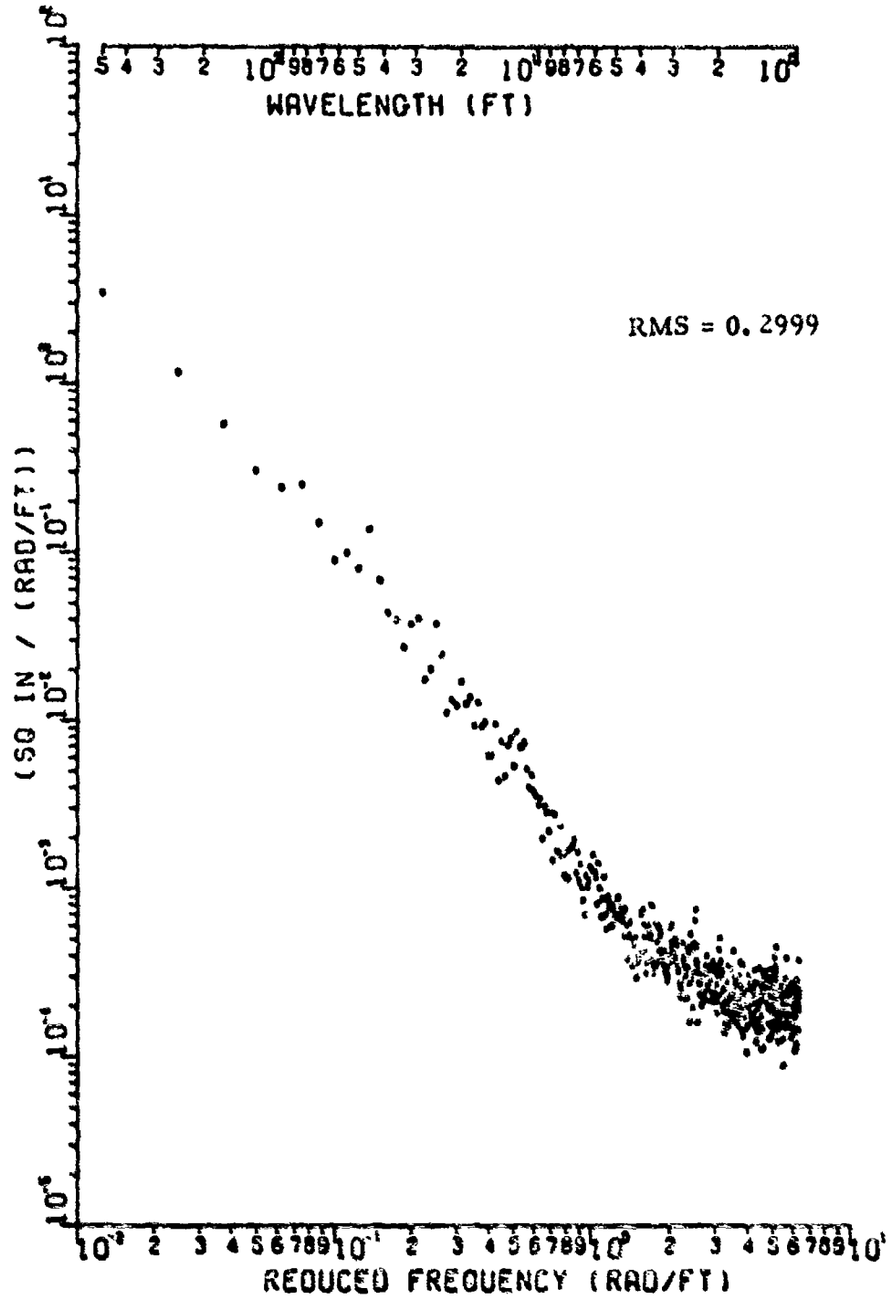

Figure 77 Power Spectral Density of Langley, Center, filtered at 500 ft

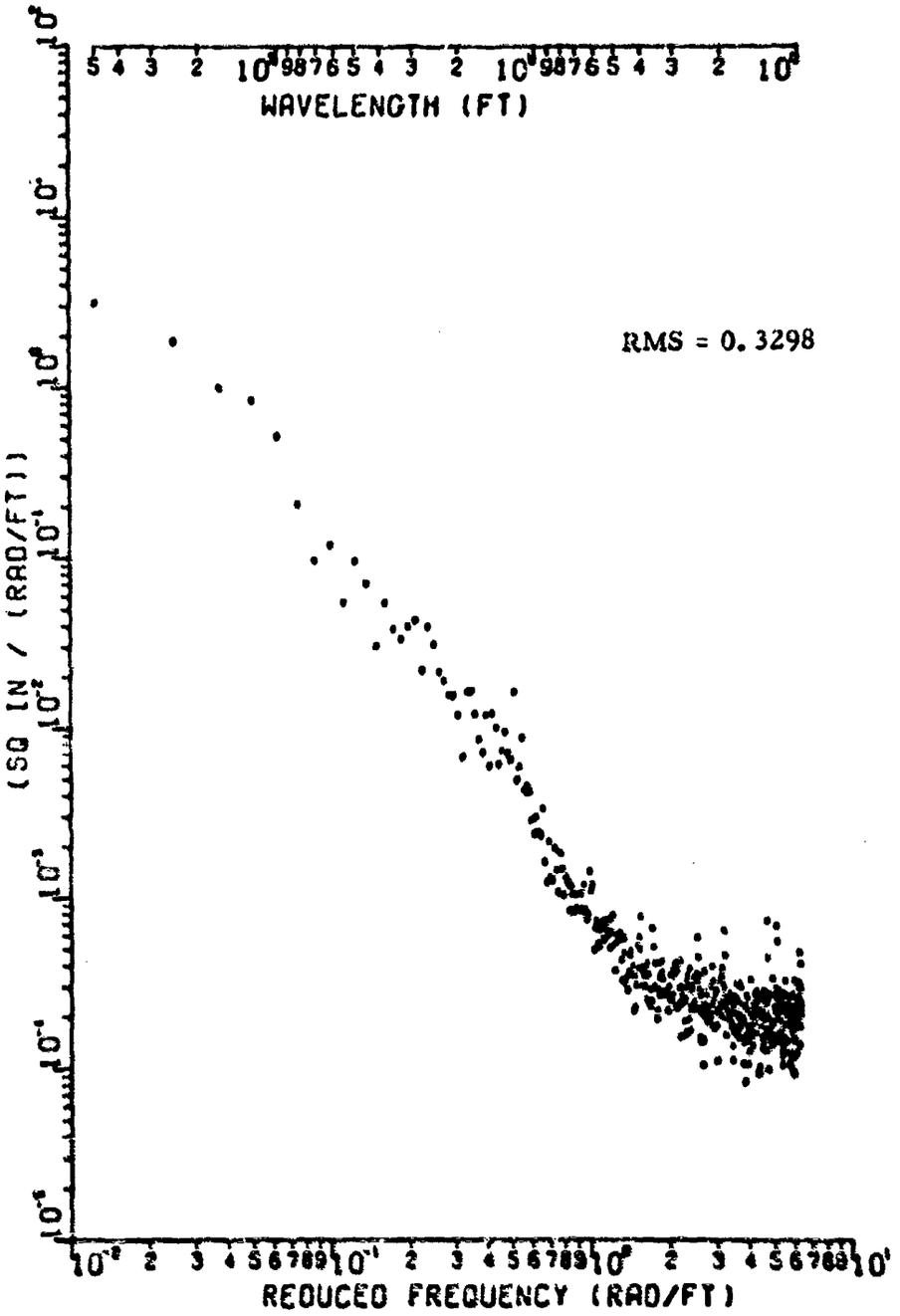

Figure 78 Power Spectral Density of Langley, 50R, filtered at 500 ft

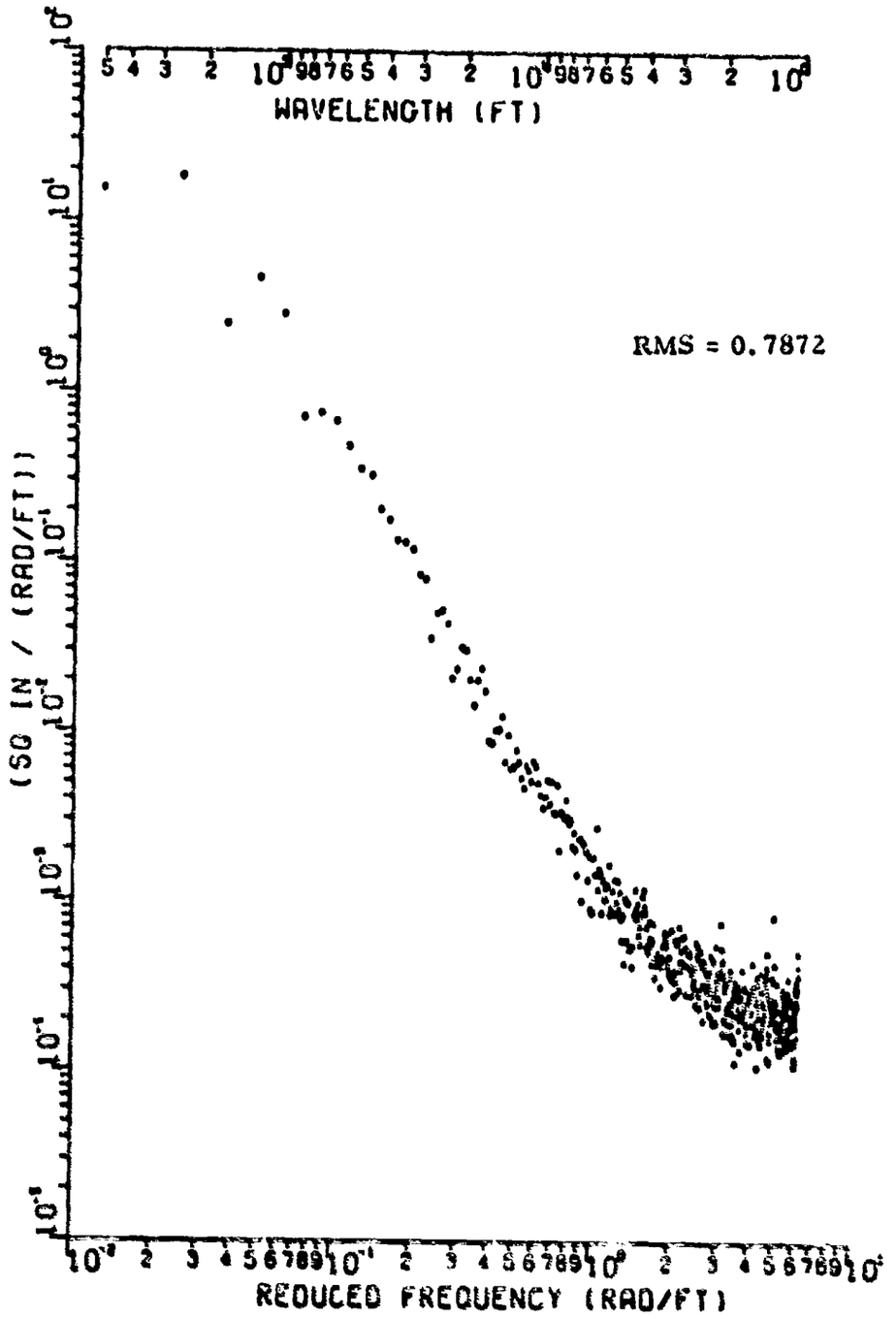

Figure 79 Power Spectral Density of McGuire, 7SL, filtered at 500 ft

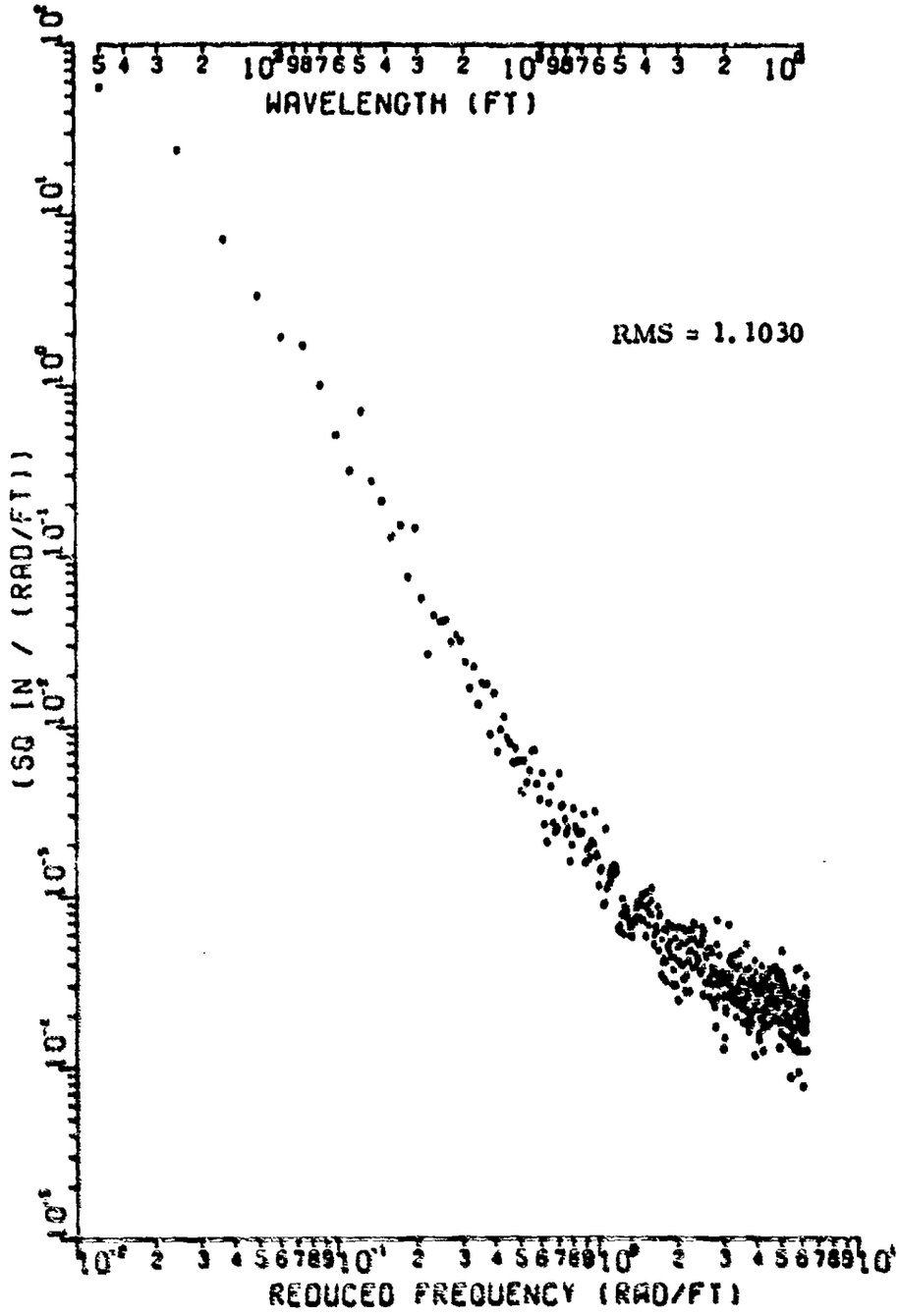

Figure 60 Power Spectral Density of McGuire, Center, filtered at 500 ft

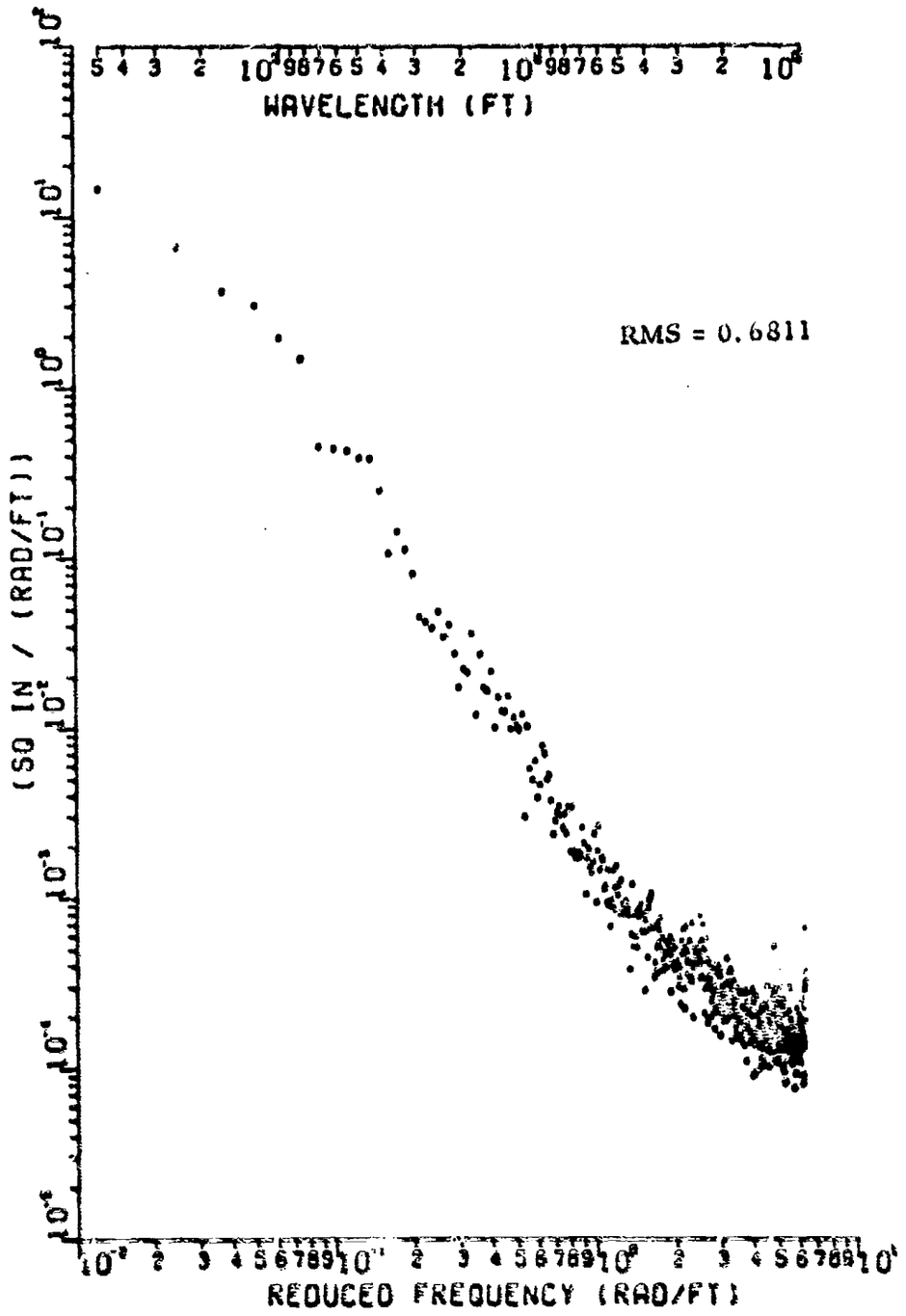

Figure 81 Power Spectral Density of McGuire, 75R, filtered at 500 ft

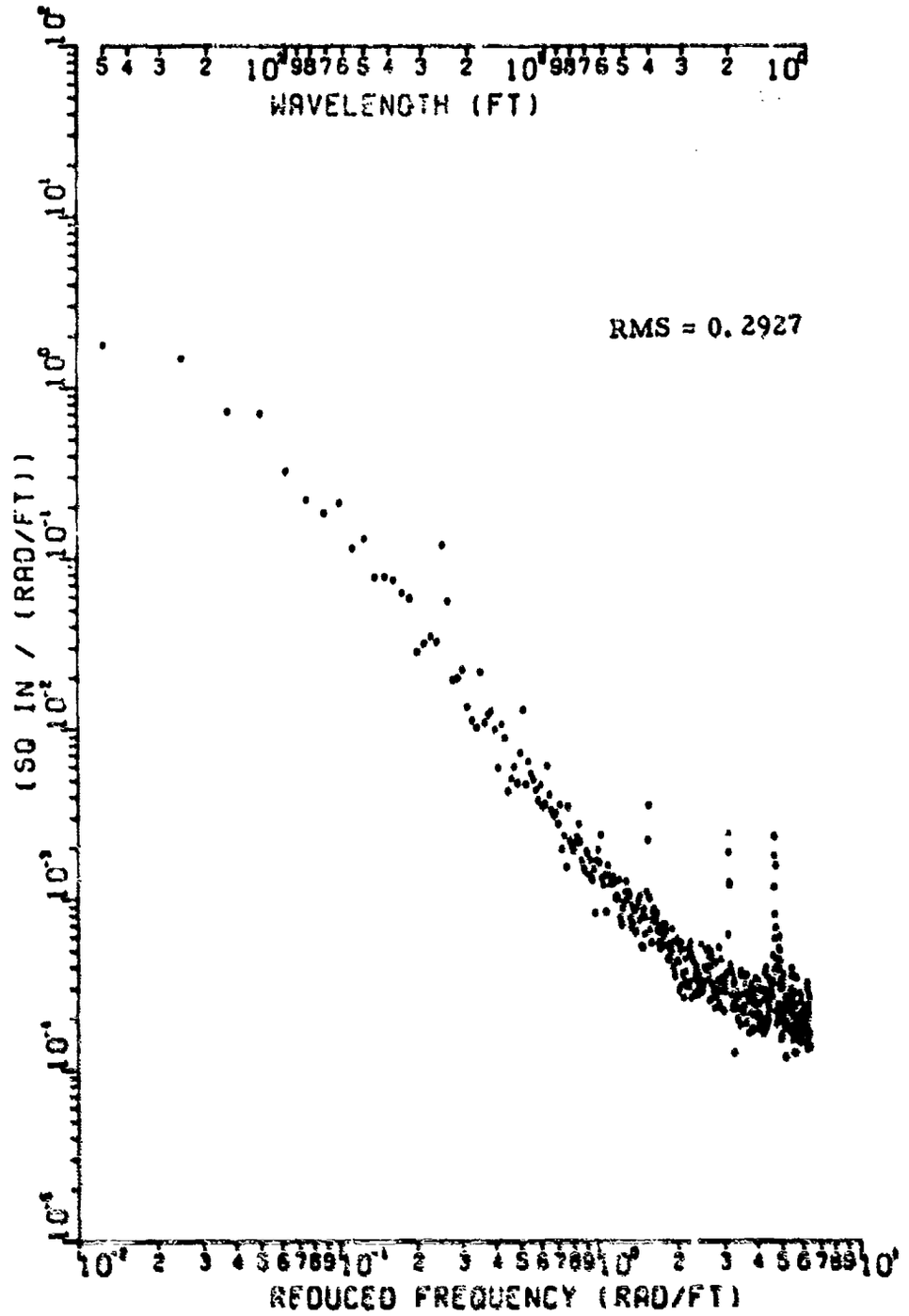

Figure 82 Power Spectral Density of Palmdale, 50L, filtered at 500 ft

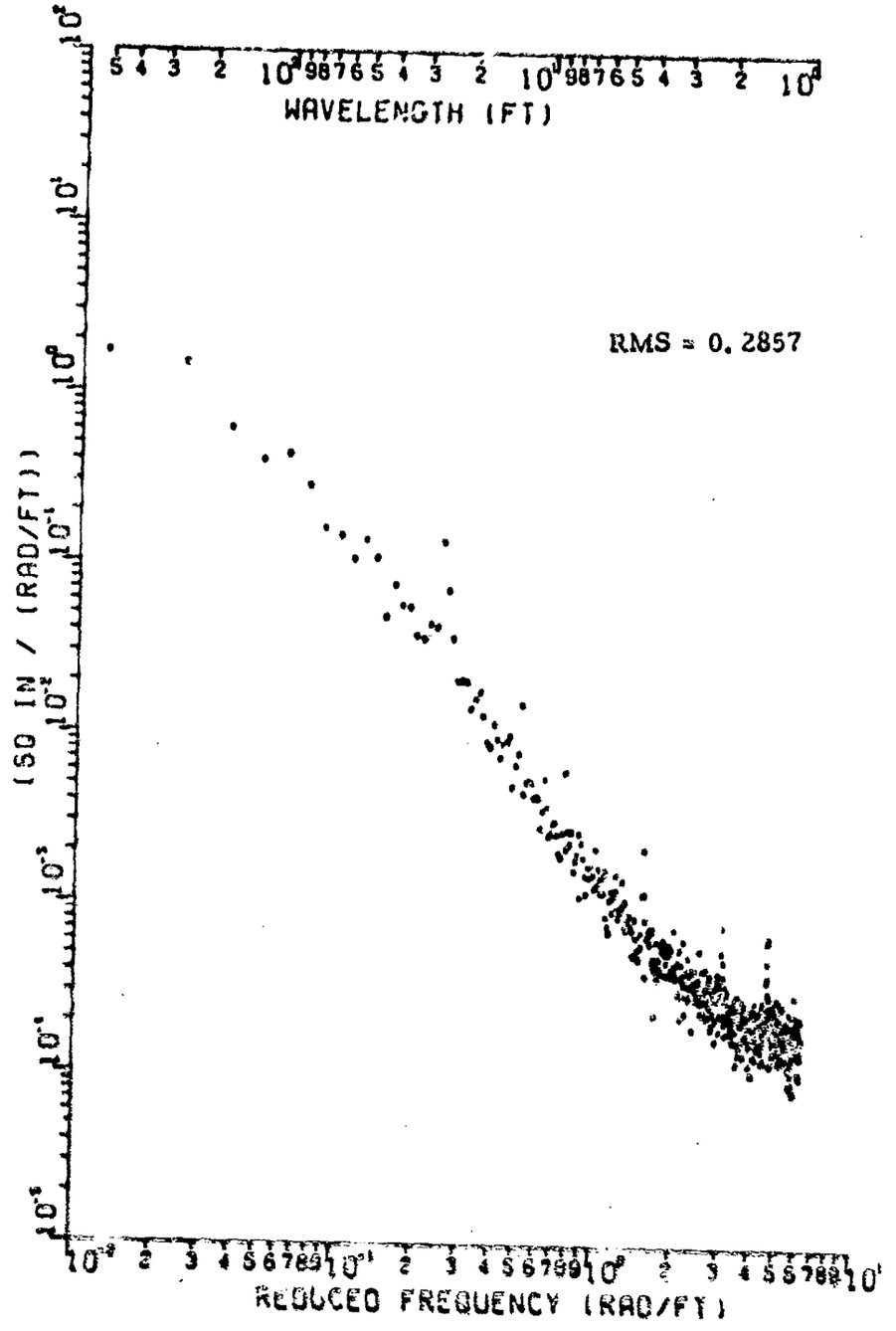

Figure 83 Power Spectral Density of Palmdale, Center, filtered at 500 ft

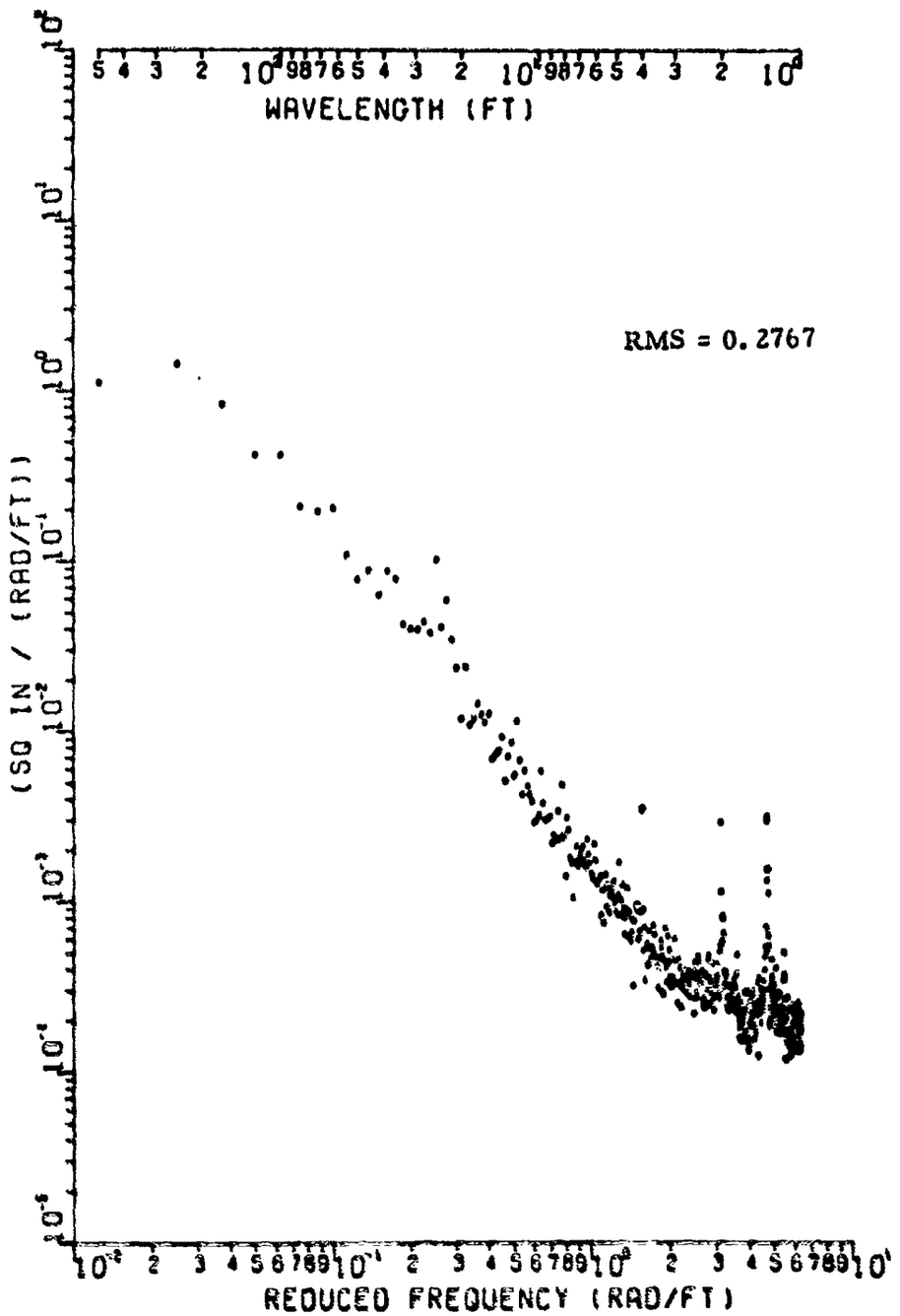

Figure 84 Power Spectral Density of Palmdale, 50R, filtered at 500 ft

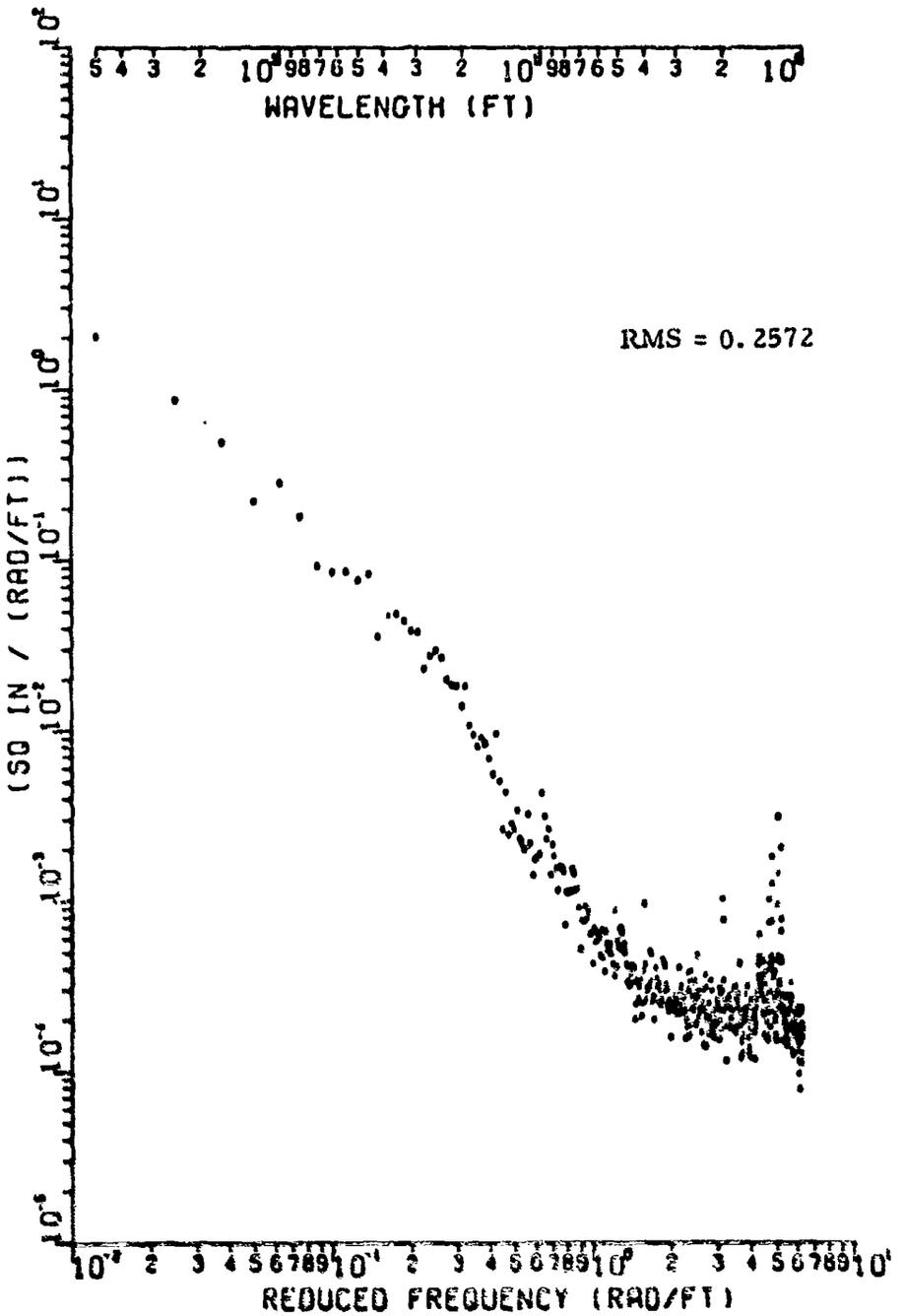

Figure 65 Power Spectral Density of Shaw, 50L, filtered at 500 ft

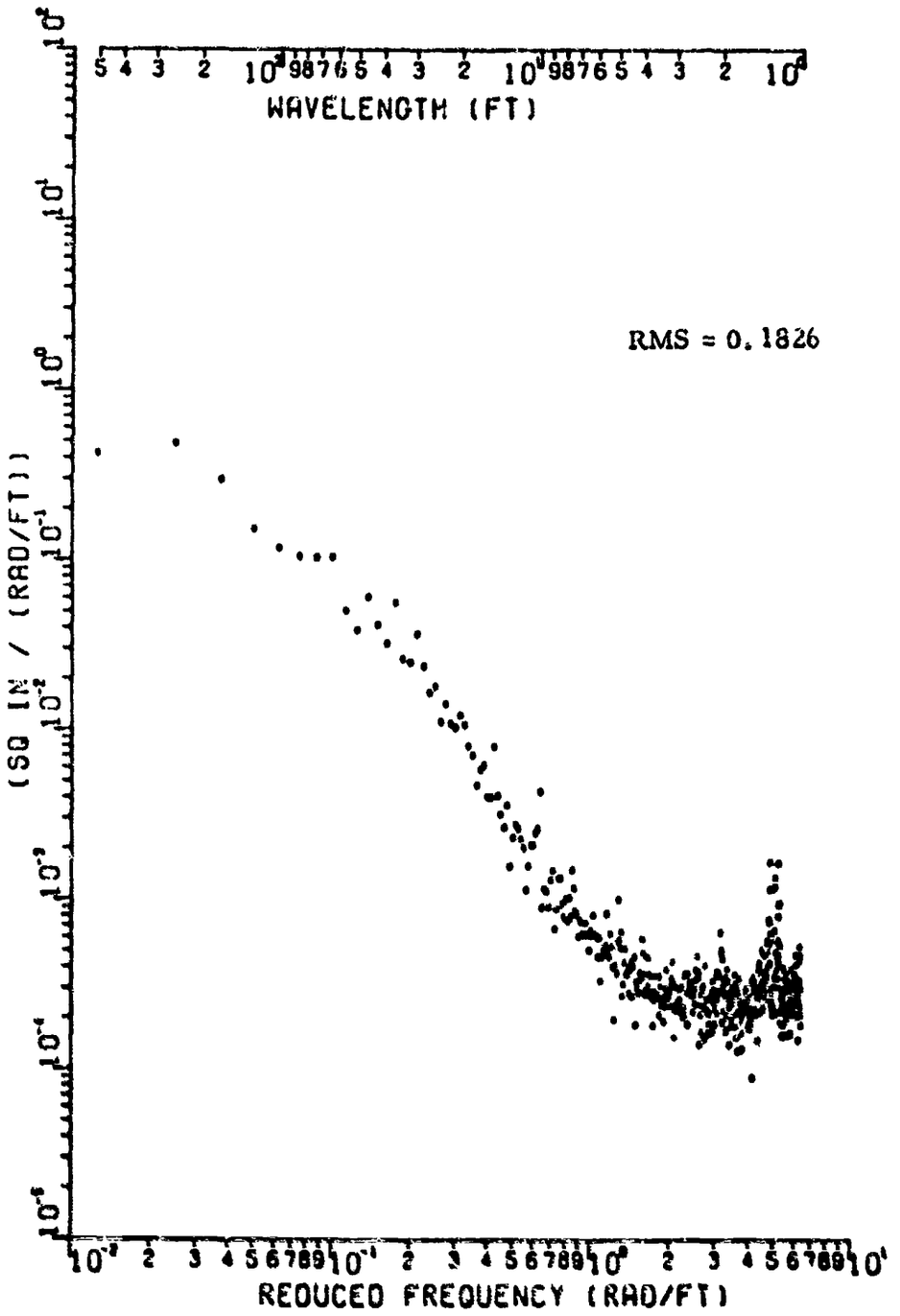

Figure 86 Power Spectral Density of Shaw, Center, filtered at 500 ft

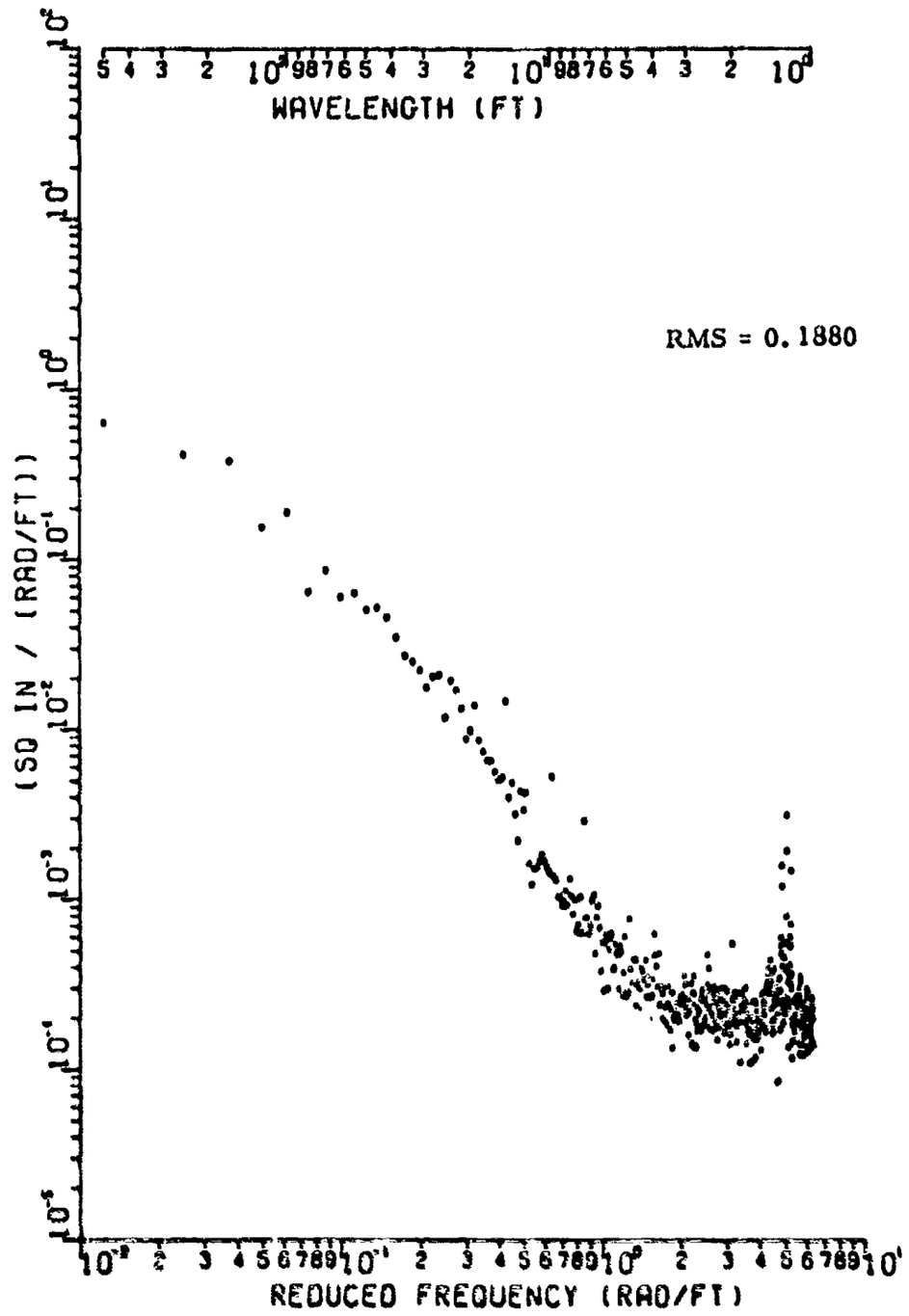

Figure 87 **Power Spectral Density of Shaw, 50R, filtered at 500 ft**

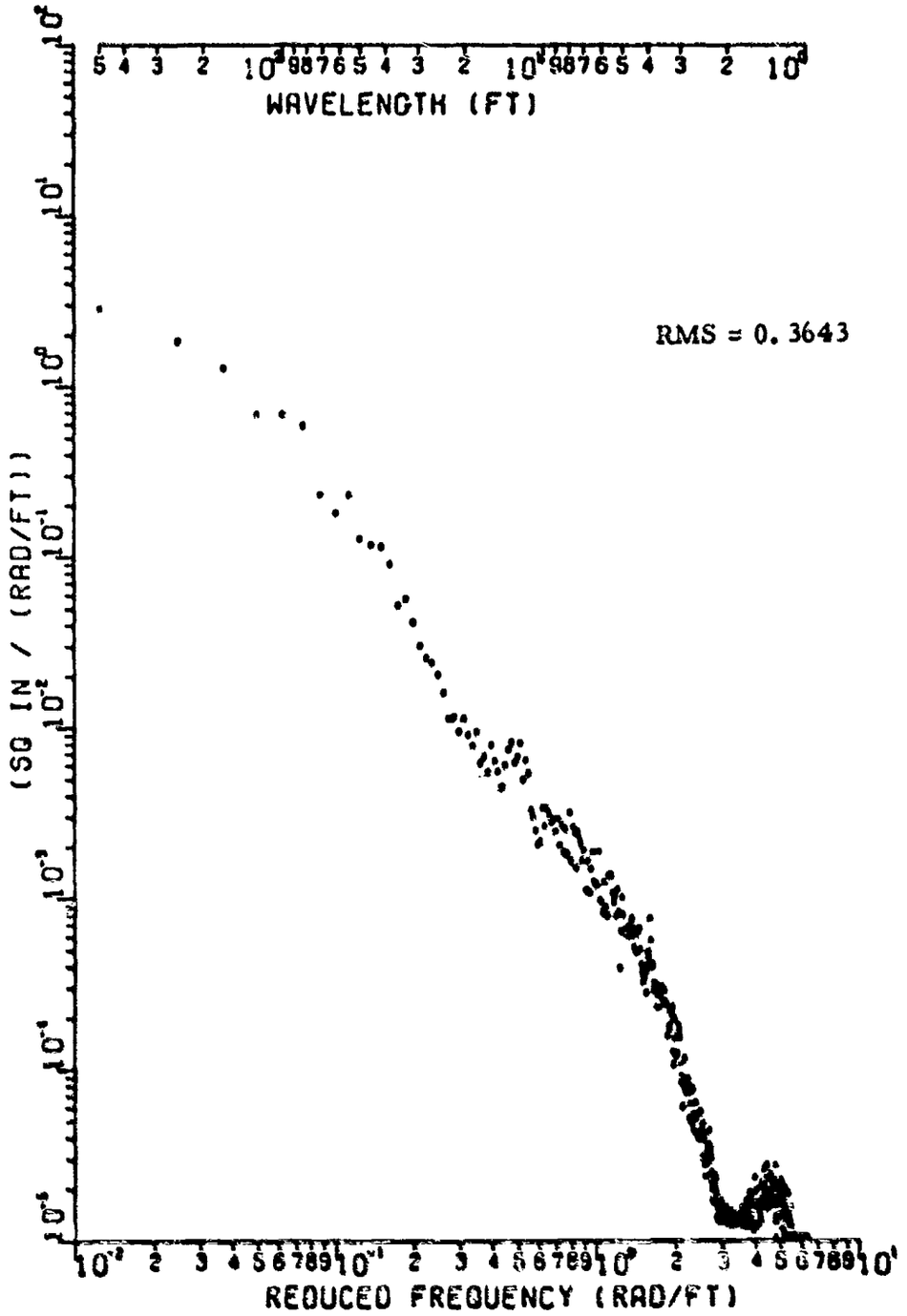

Figure 88 Power Spectral Density of Torrejon, Center, filtered at 500 ft

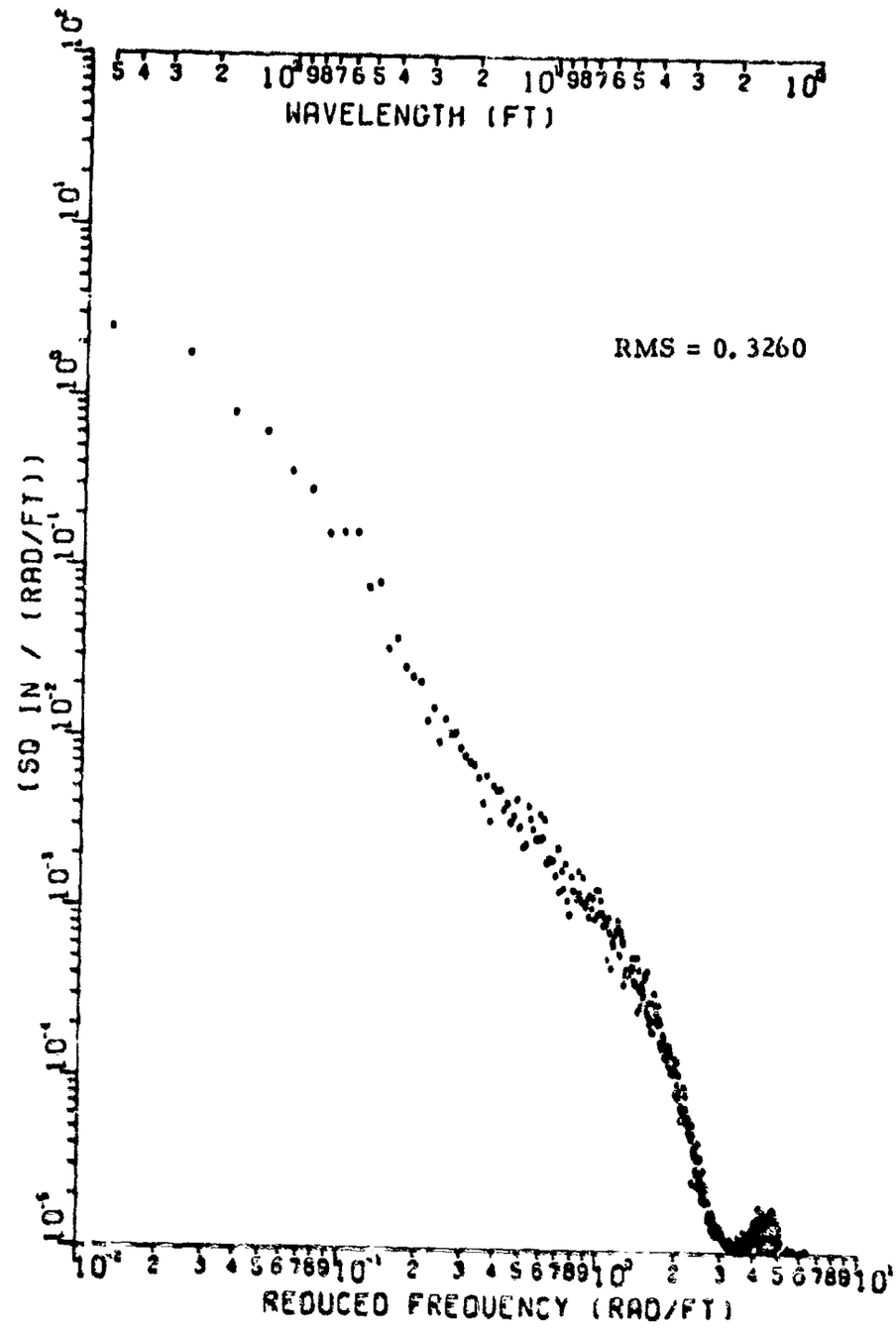

Figure 89 Power Spectral Density of Torrejon, 12L, filtered at 500 ft

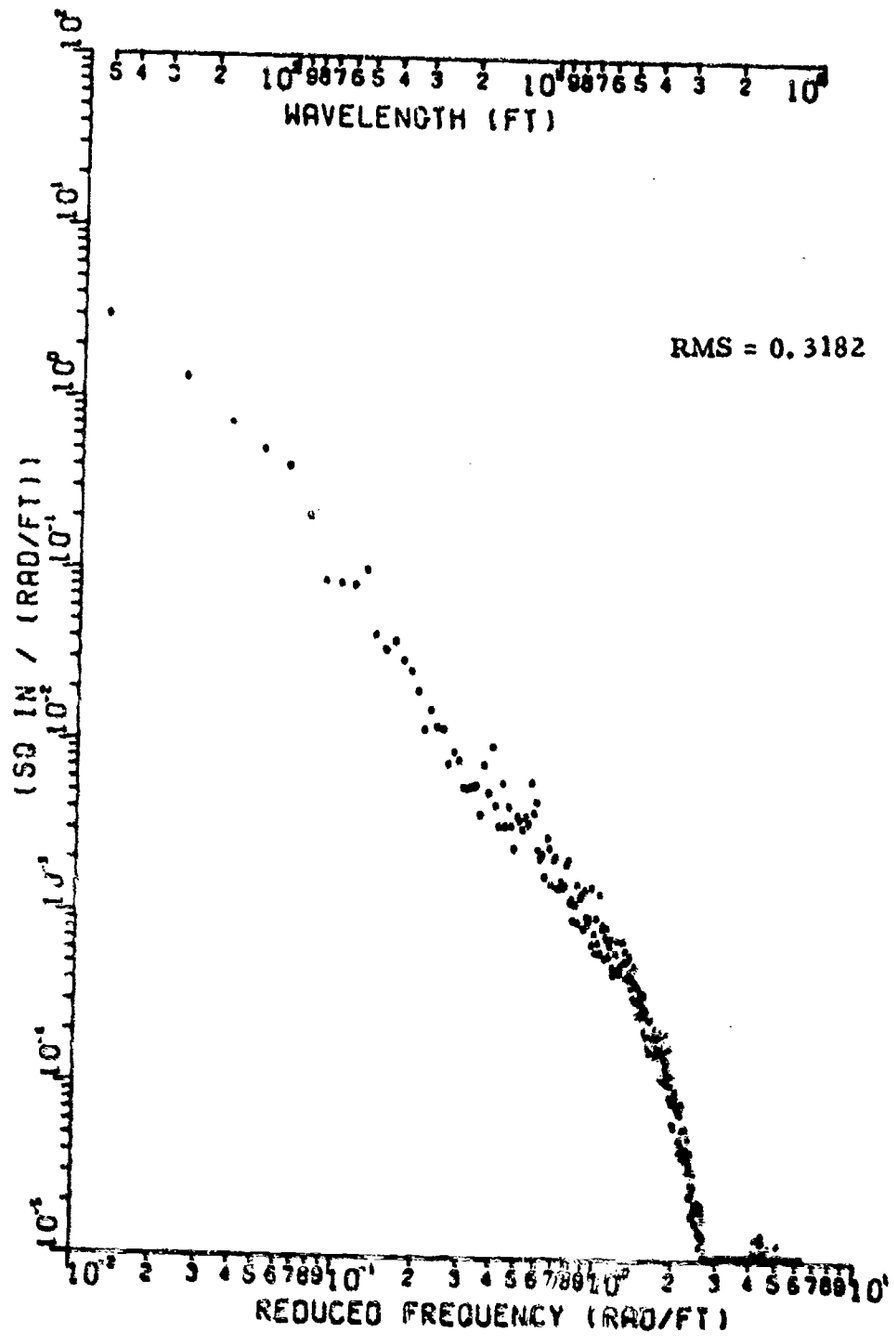

Figure 90 Power Spectral Density of Torrejon, 12R, filtered at 500 ft

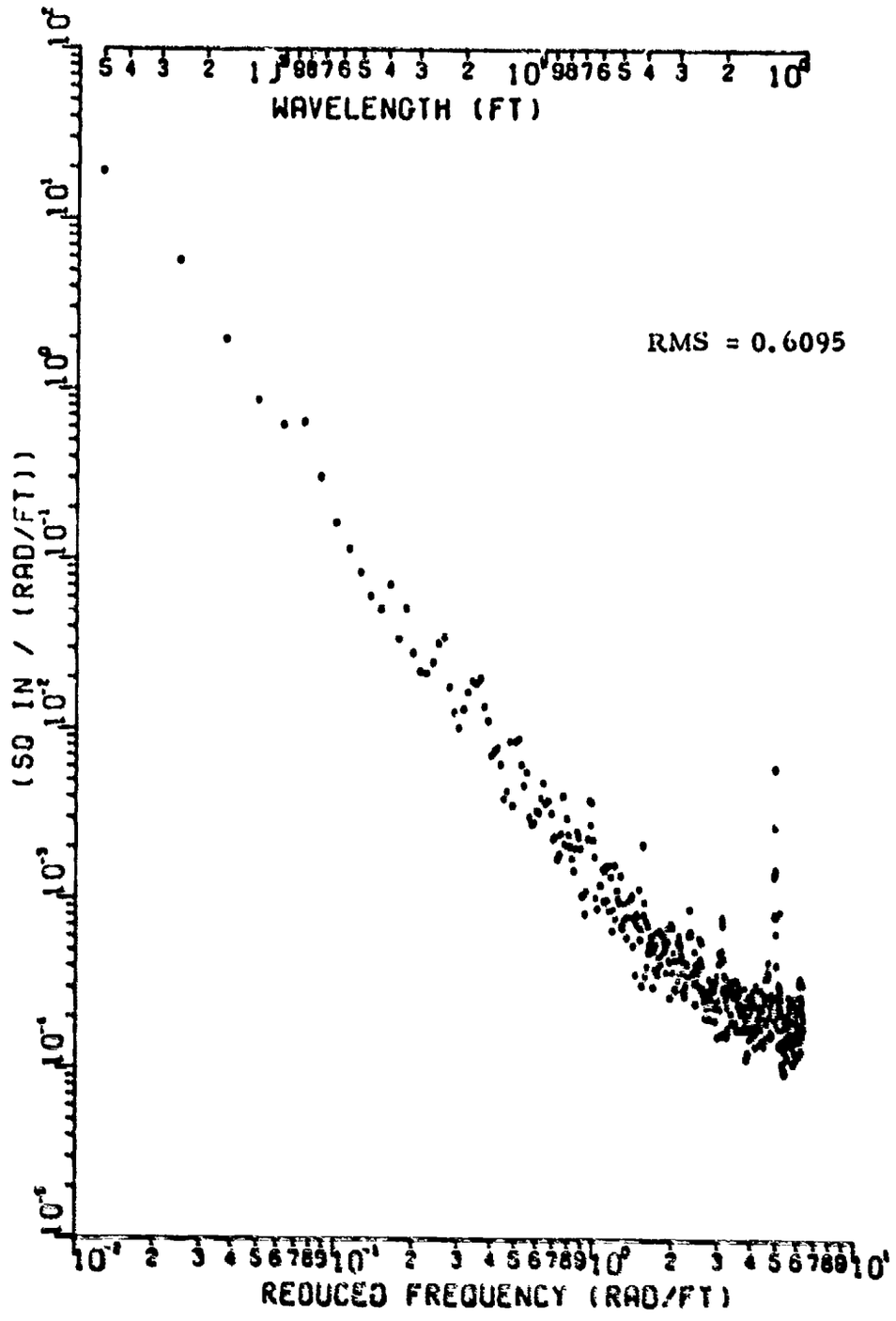

Figure 91 Power Spectral Density of Travis, 75L, filtered at 500 ft

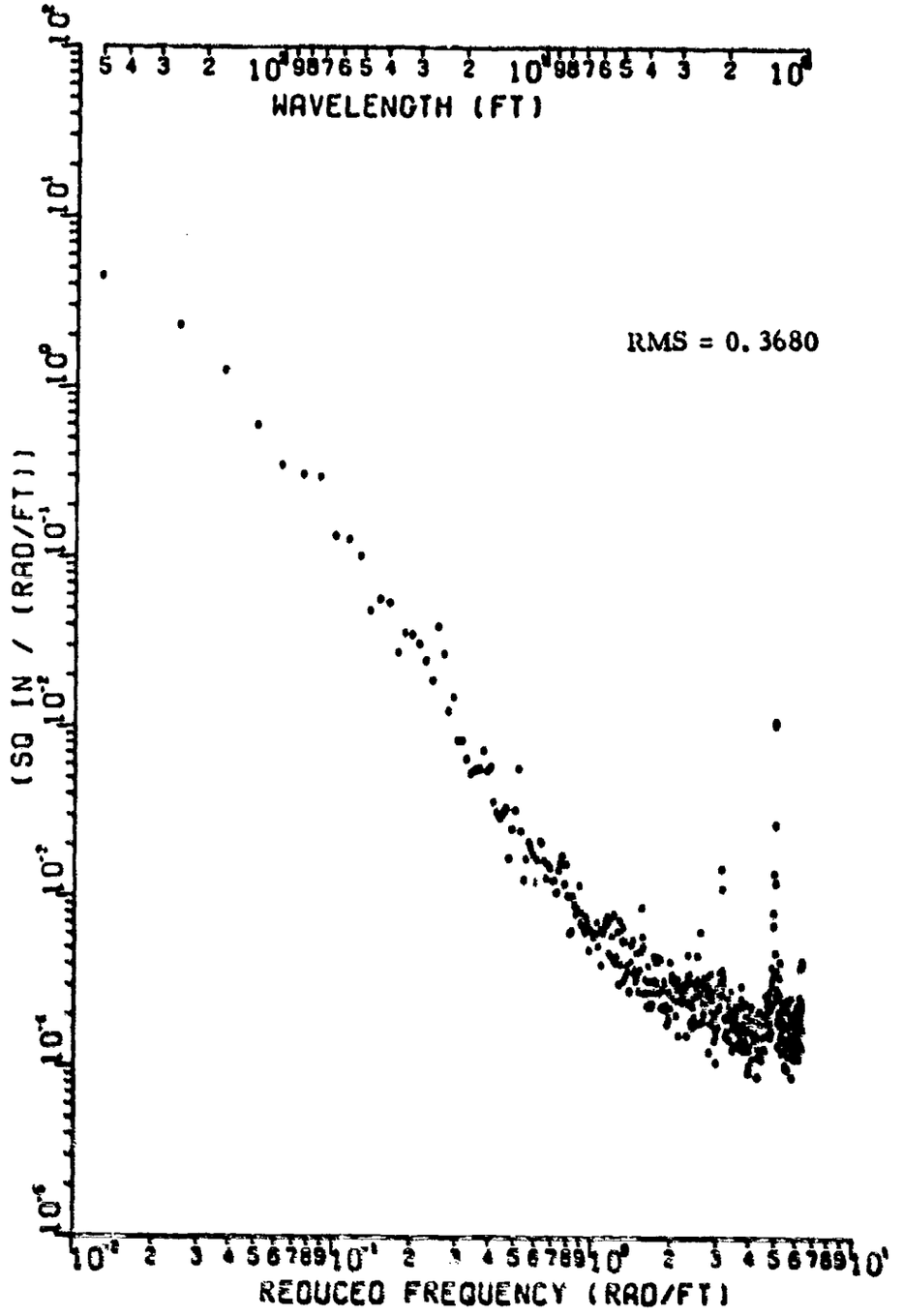

Figure 92 Power Spectral Density of Travis, Center, filtered at 500 ft

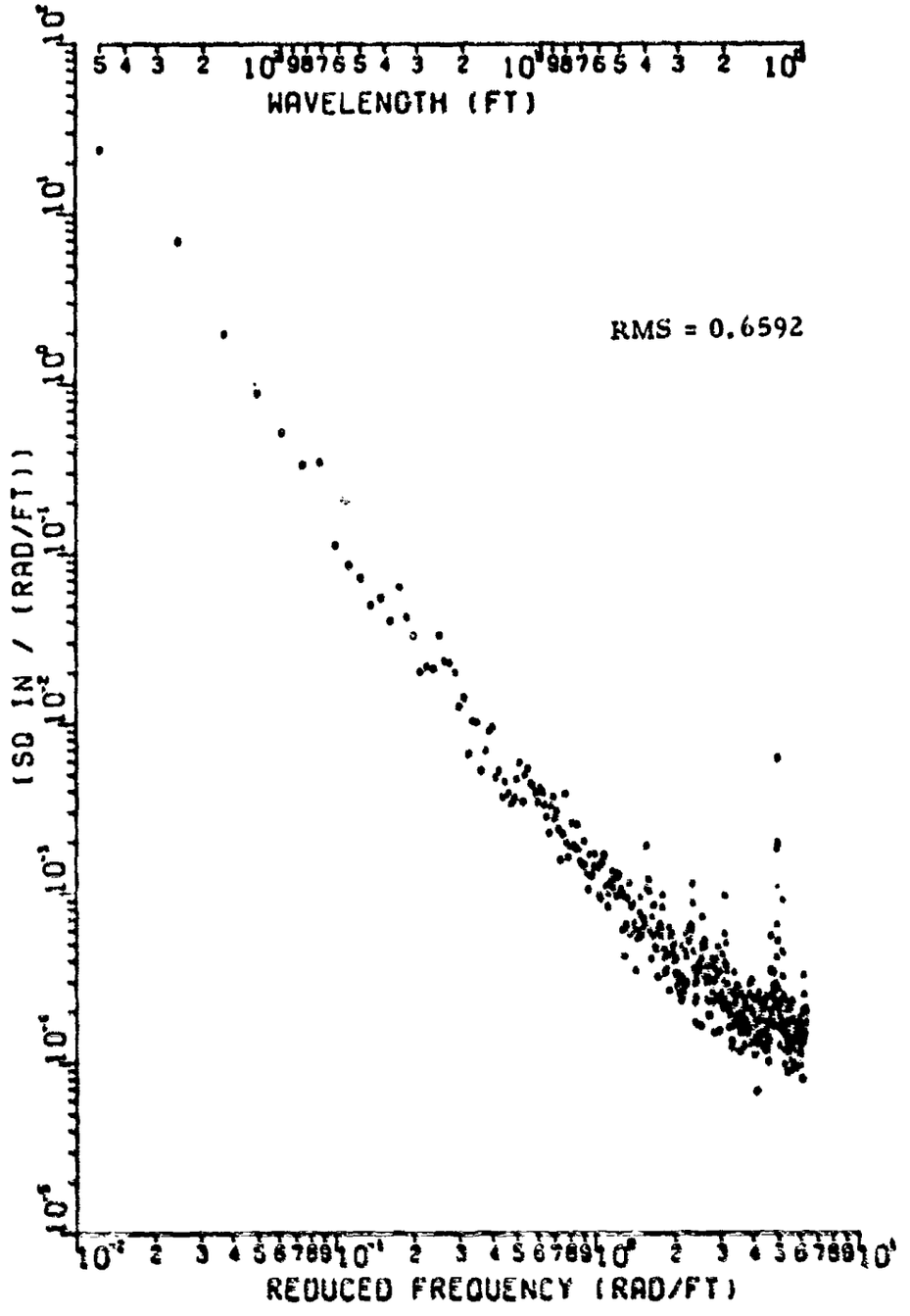

Figure 93 Power Spectral Density of Travis, 75L, filtered at 500 ft

APPENDIX IV

RMS HISTORIES FOR ALL LINES OF DATA FILTERED AT 500 FEET

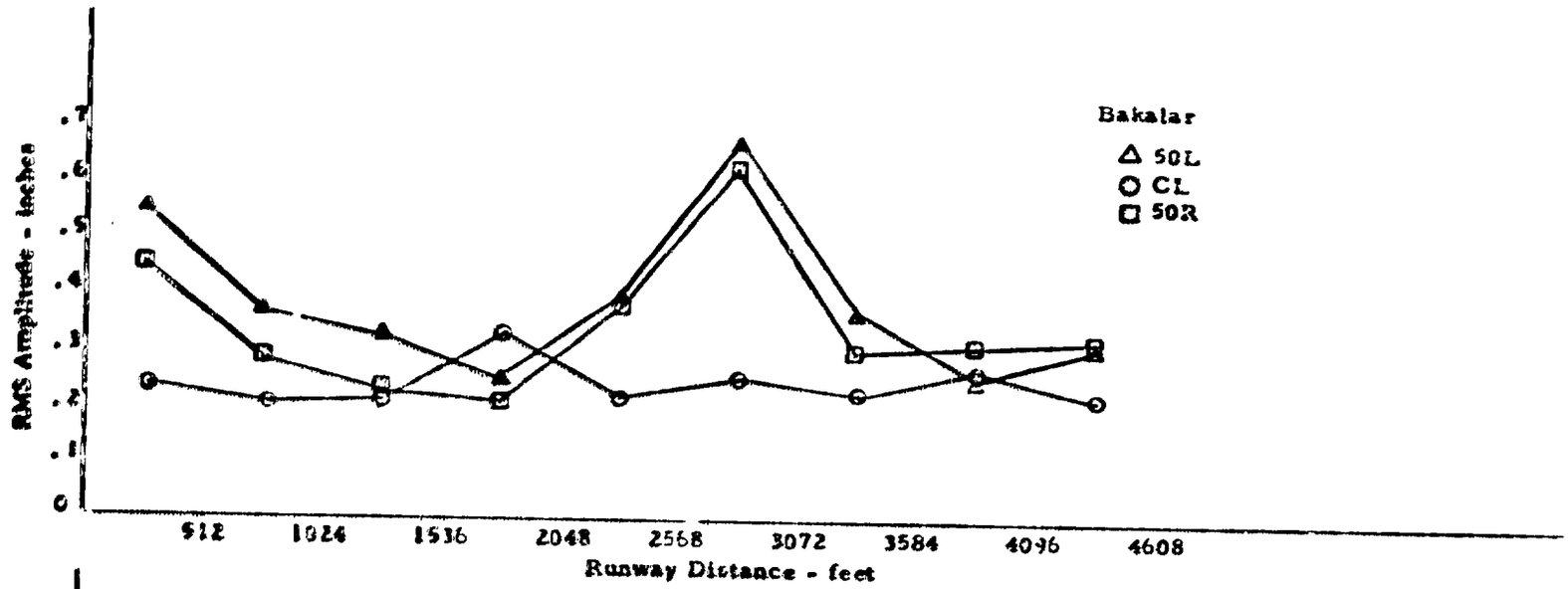

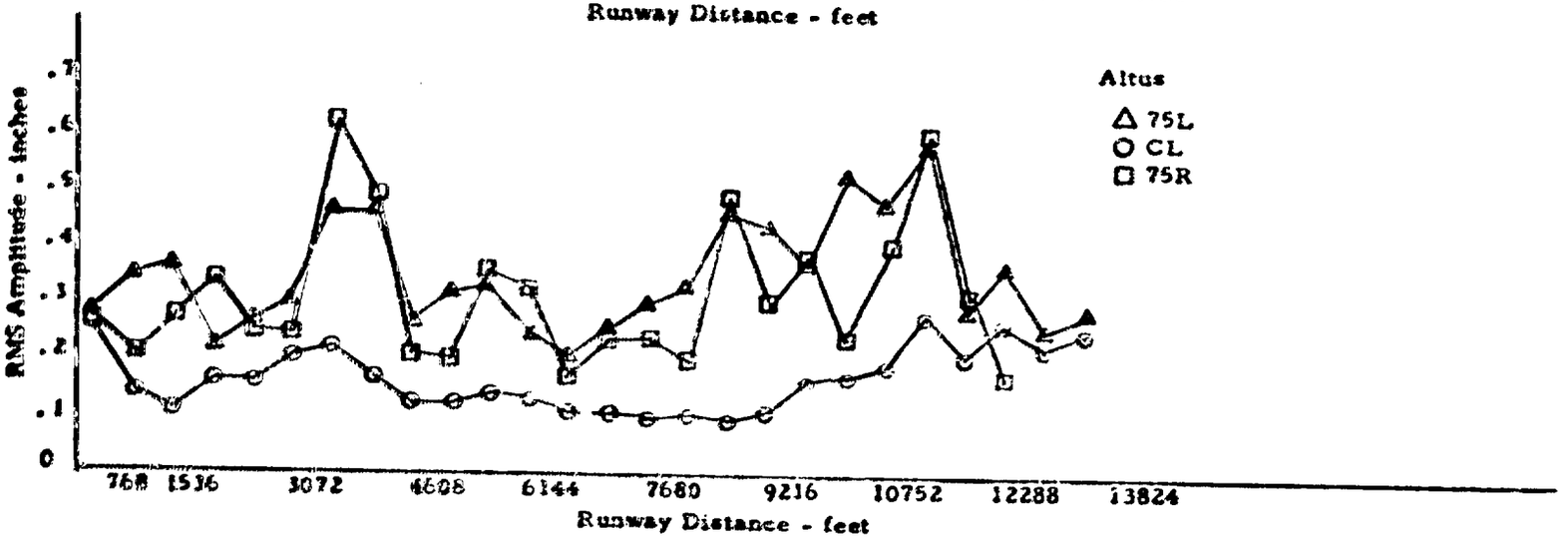

Figure 94 RMS Histories for Altus and Bakalar filtered at 500 ft

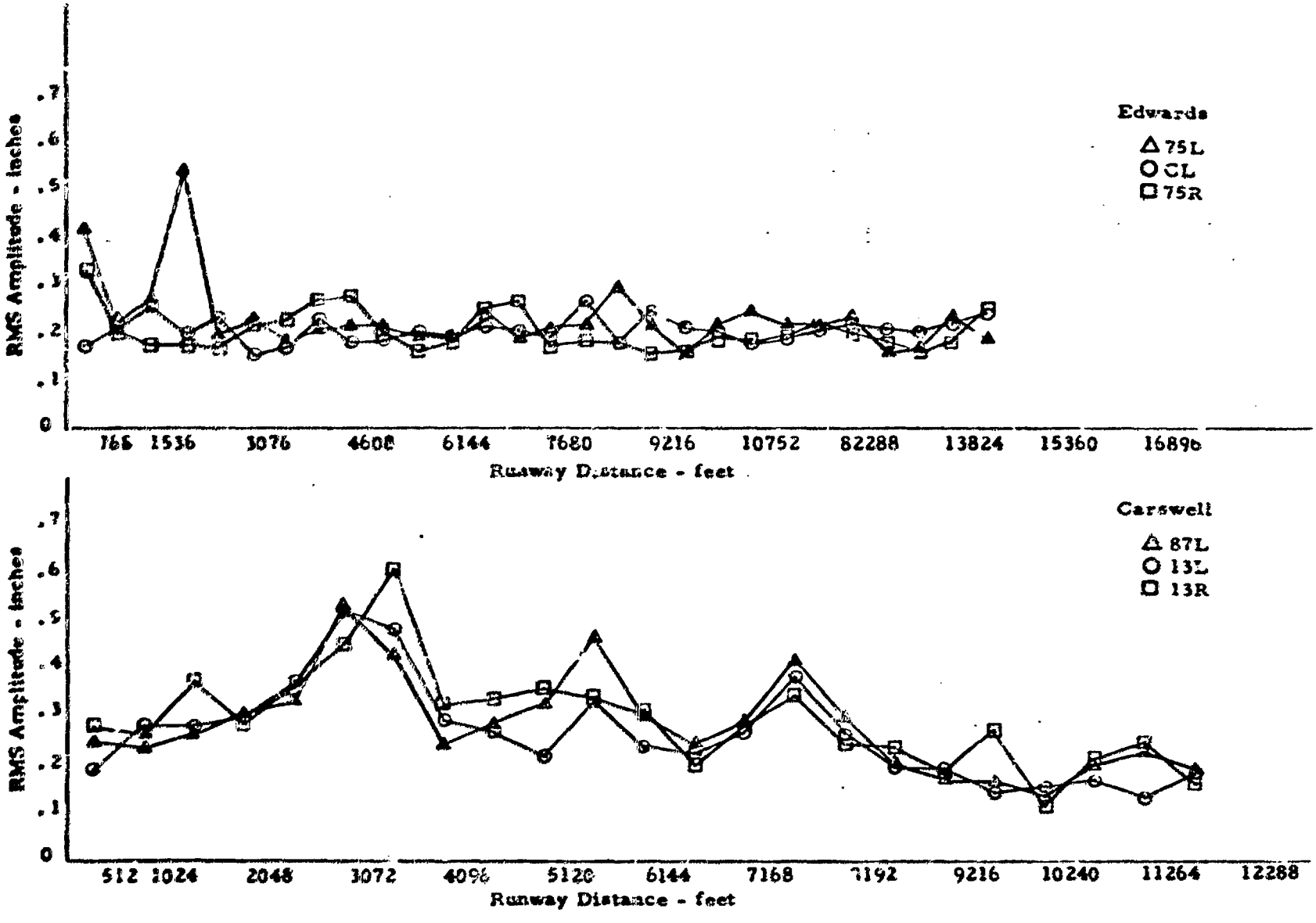

Figure 95 RMS Histories for Carswell and Edwards Filtered at 500 ft

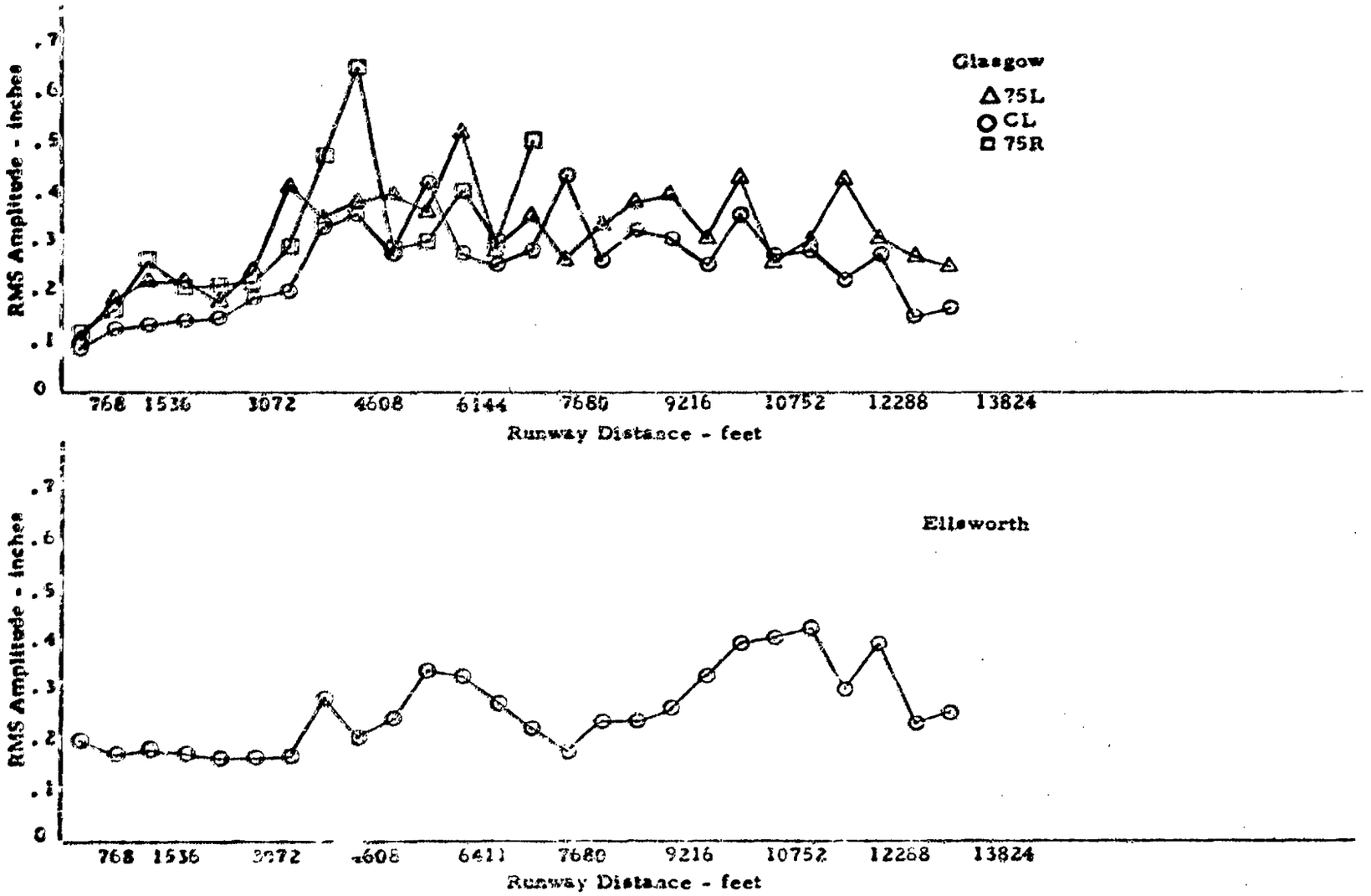

Figure 96 RMS Histories for Ellsworth and Glasgow filtered at 500 ft

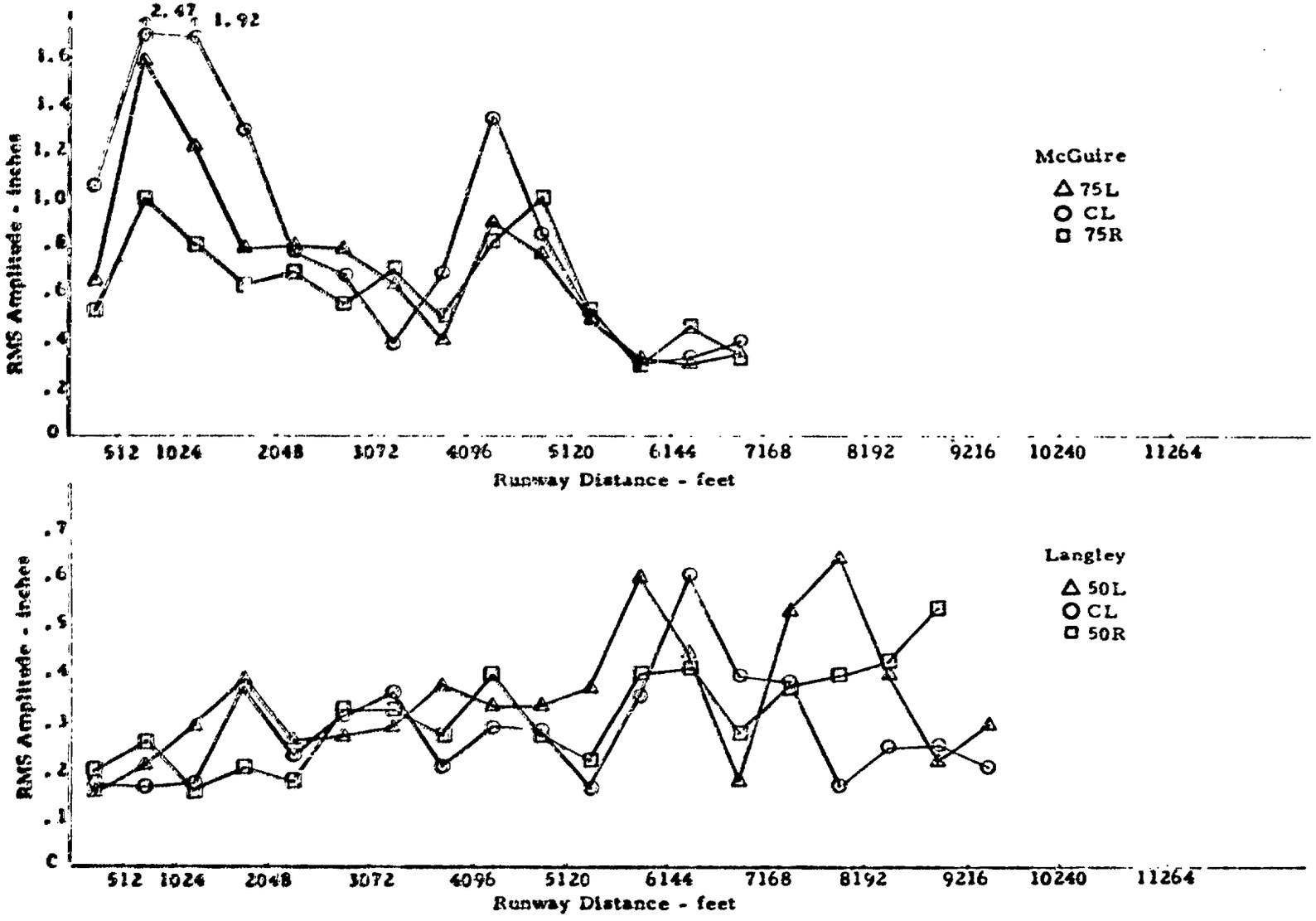

Figure 97 RMS Histories for Langley and McGuire Filtered at 500 ft

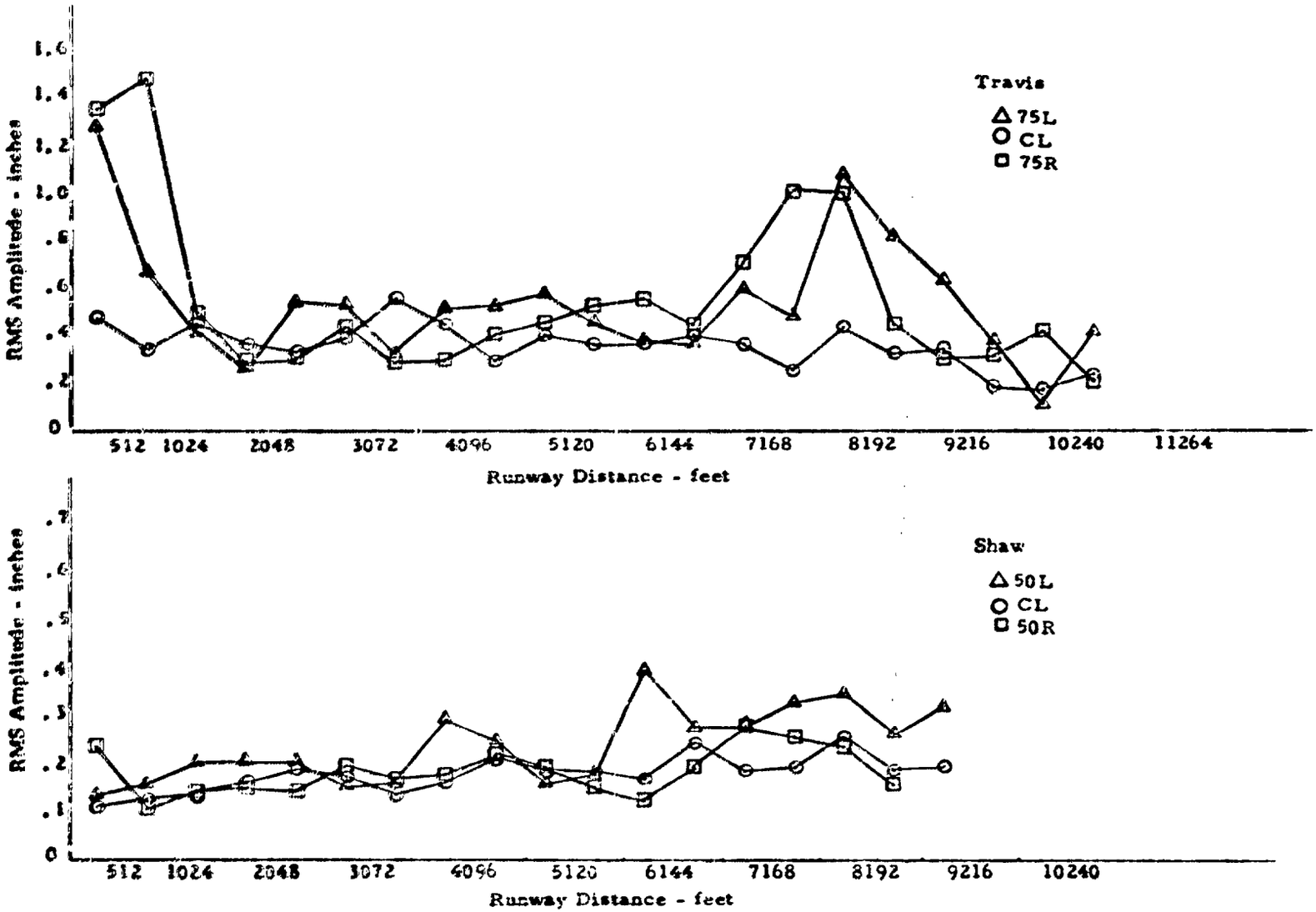

Figure 98 RMS Histories for Shaw and Travis Filtered at 500 ft

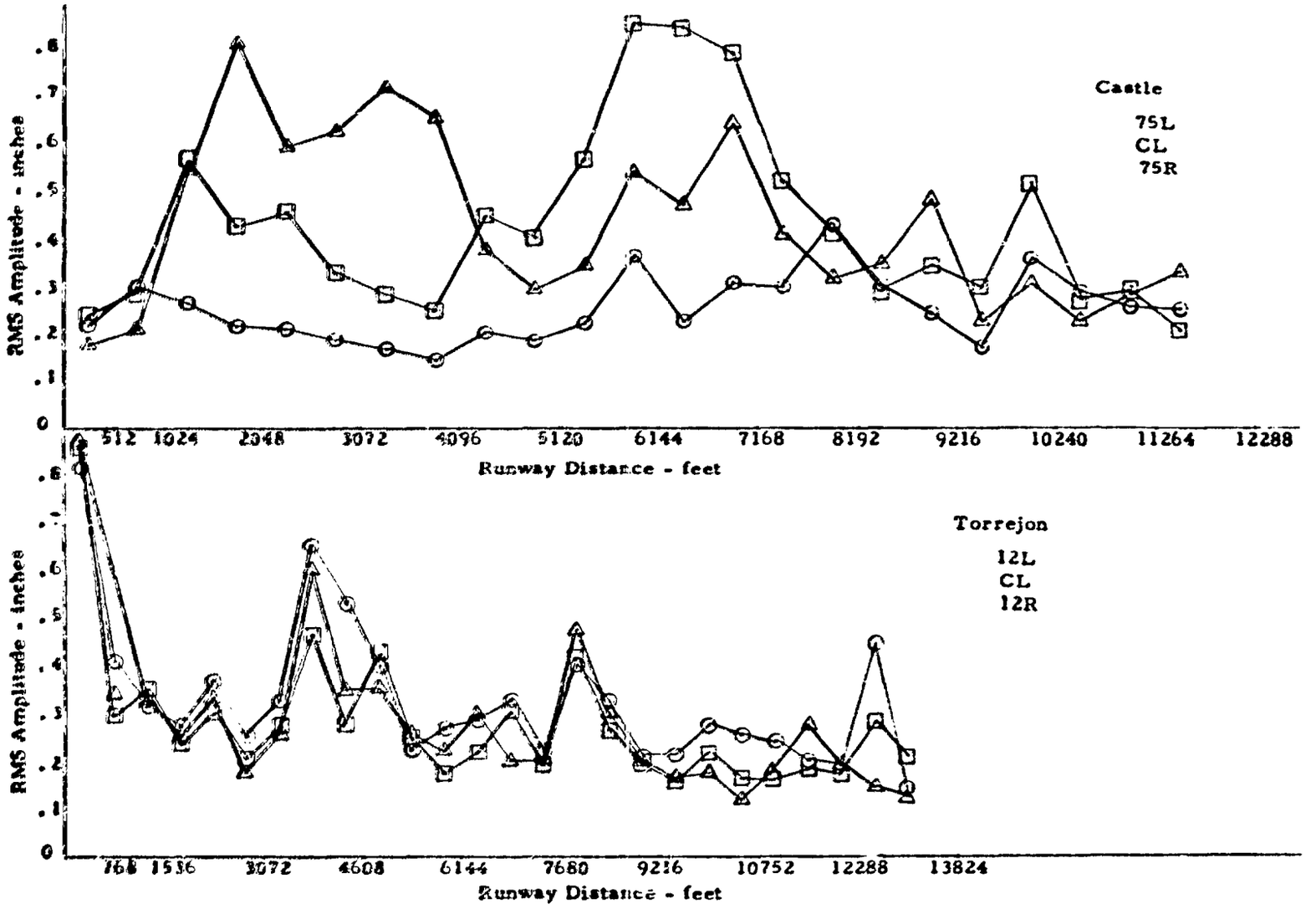

Figure 99 RMS Histories for Torrejon and Castle Filtered at 500 ft

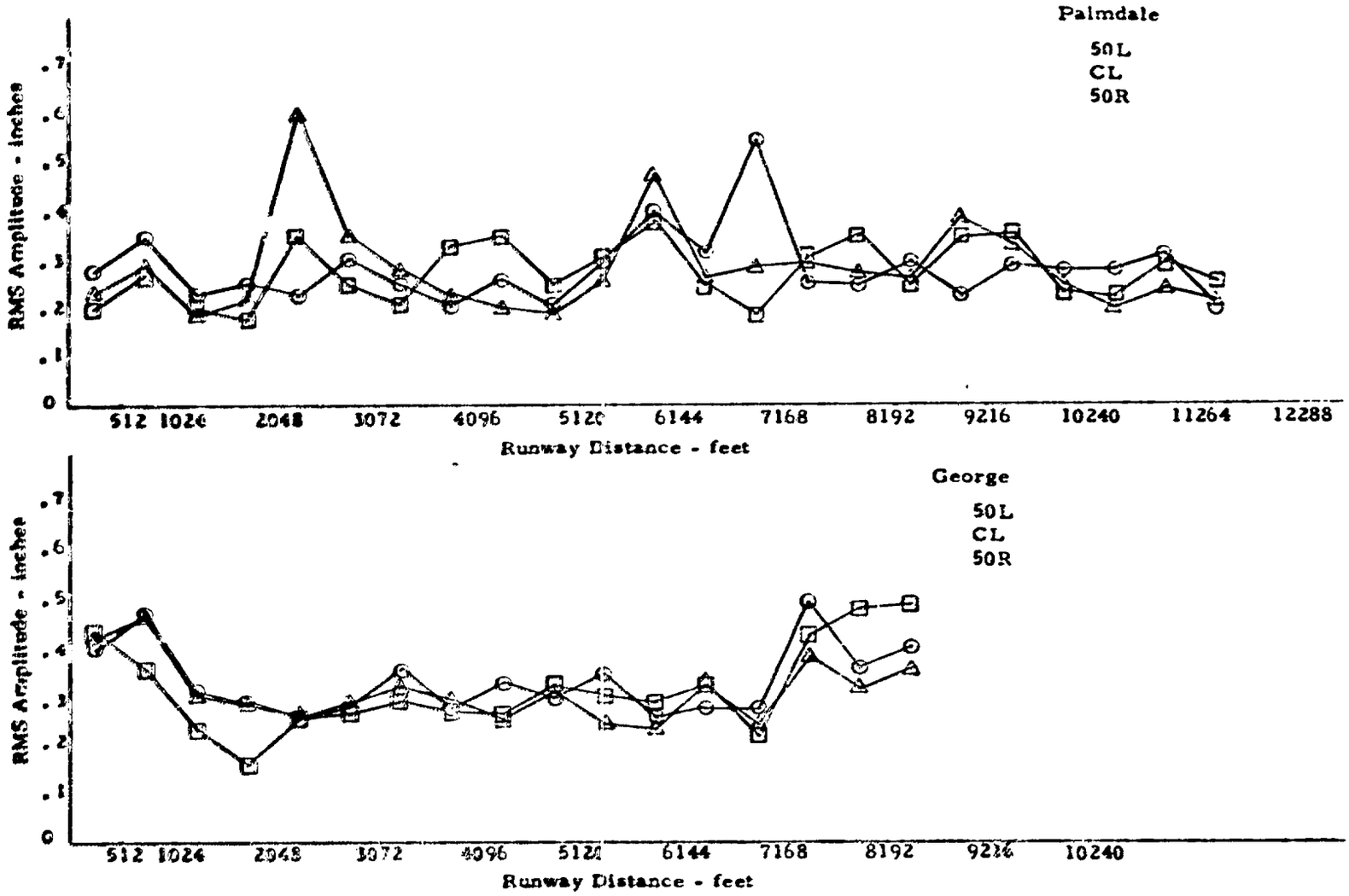

Figure 100 RMS Histories for George and Palmdale Filtered at 500 ft

APPENDIX V

CUMULATIVE DISTRIBUTIONS OF AMPLITUDES FOR ALL LINES OF DATA FILTERED AT 400 FEET

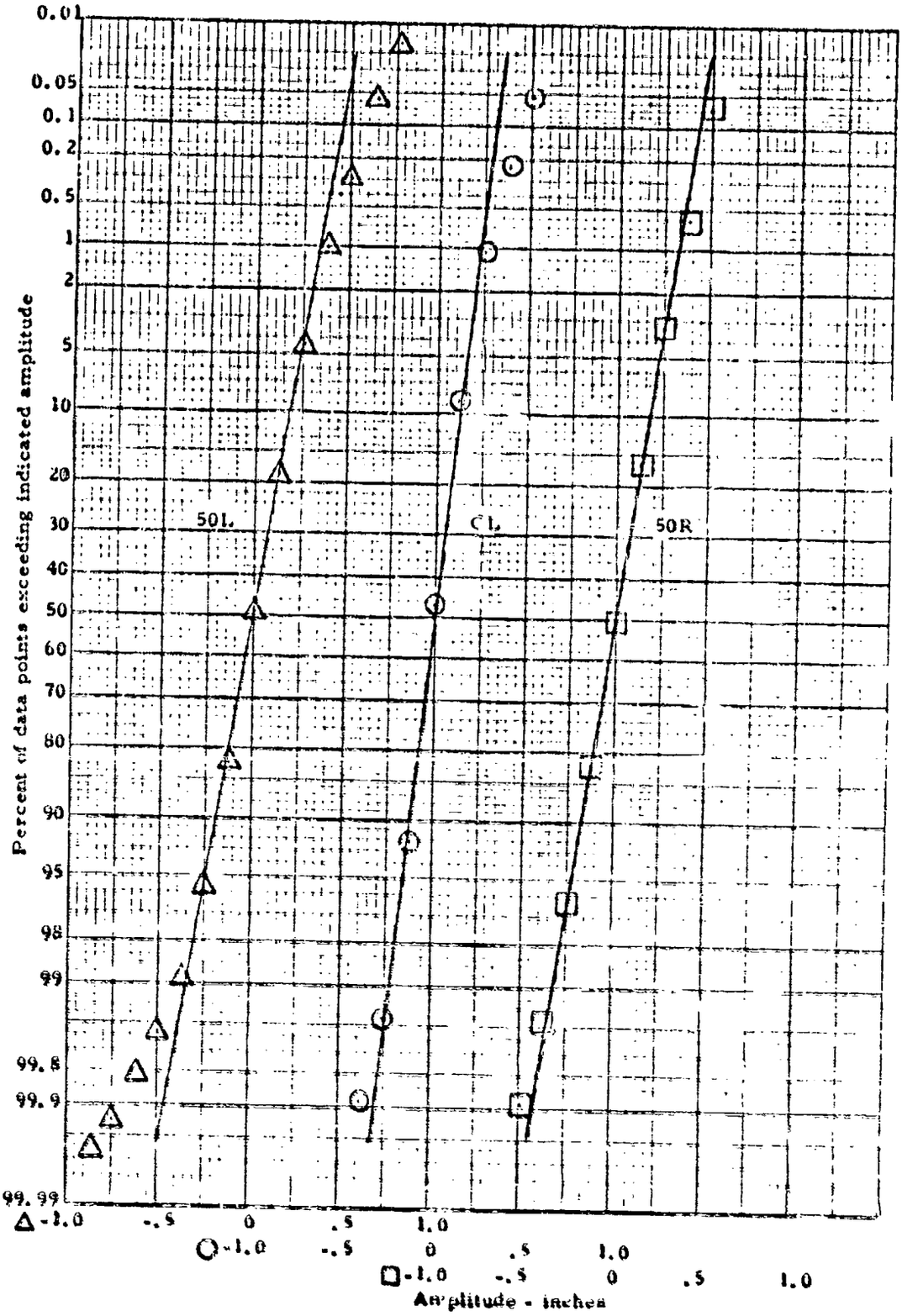

Figure 101 Cumulative Distribution of Amplitudes from Altus Filtered at 100 ft

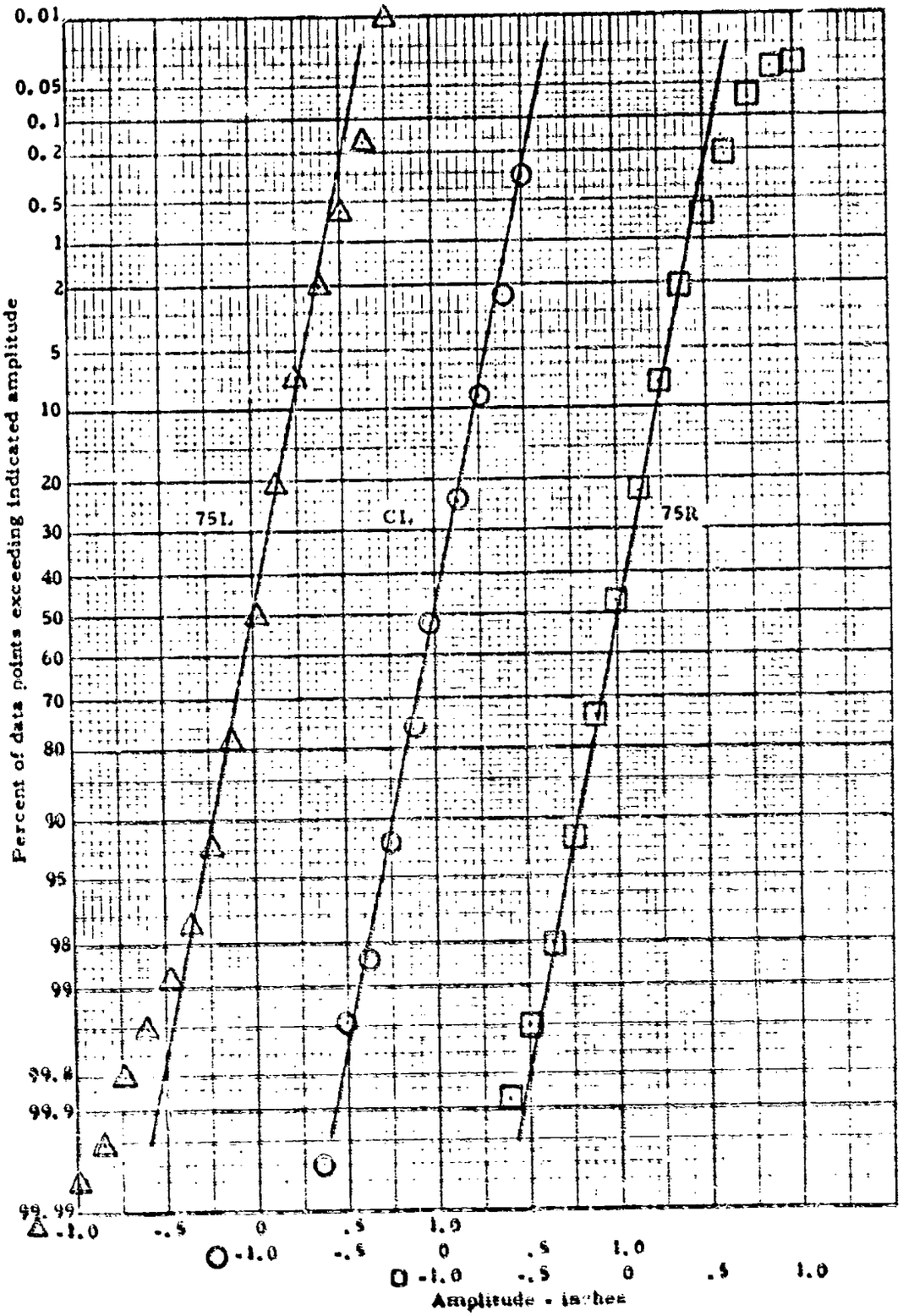

Figure 102 Cumulative Distribution of Amplitudes from Bakalar Filtered at 100 ft

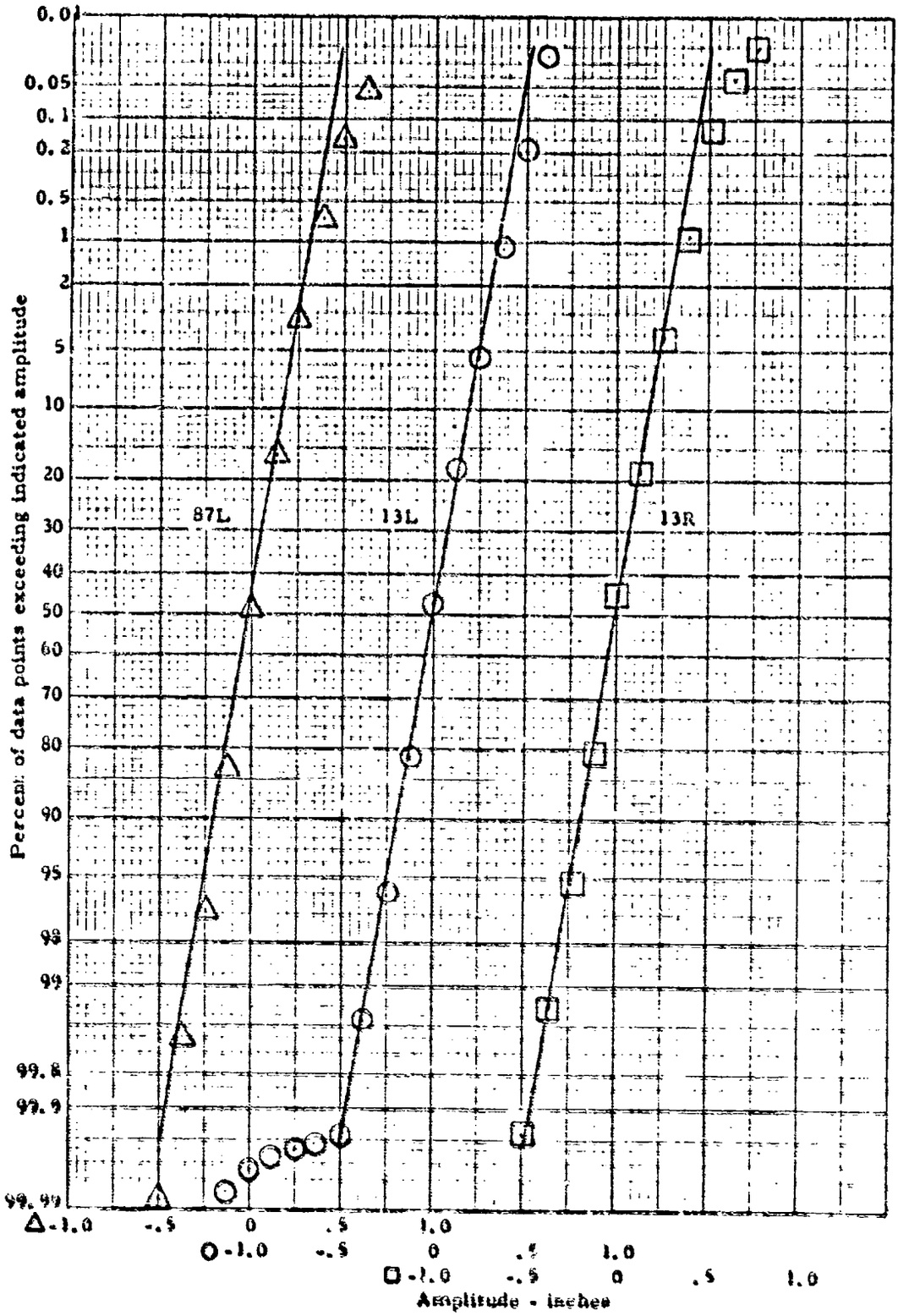

Figure 103 Cumulative Distribution of Amplitudes from Caswell Filtered at 100 ft

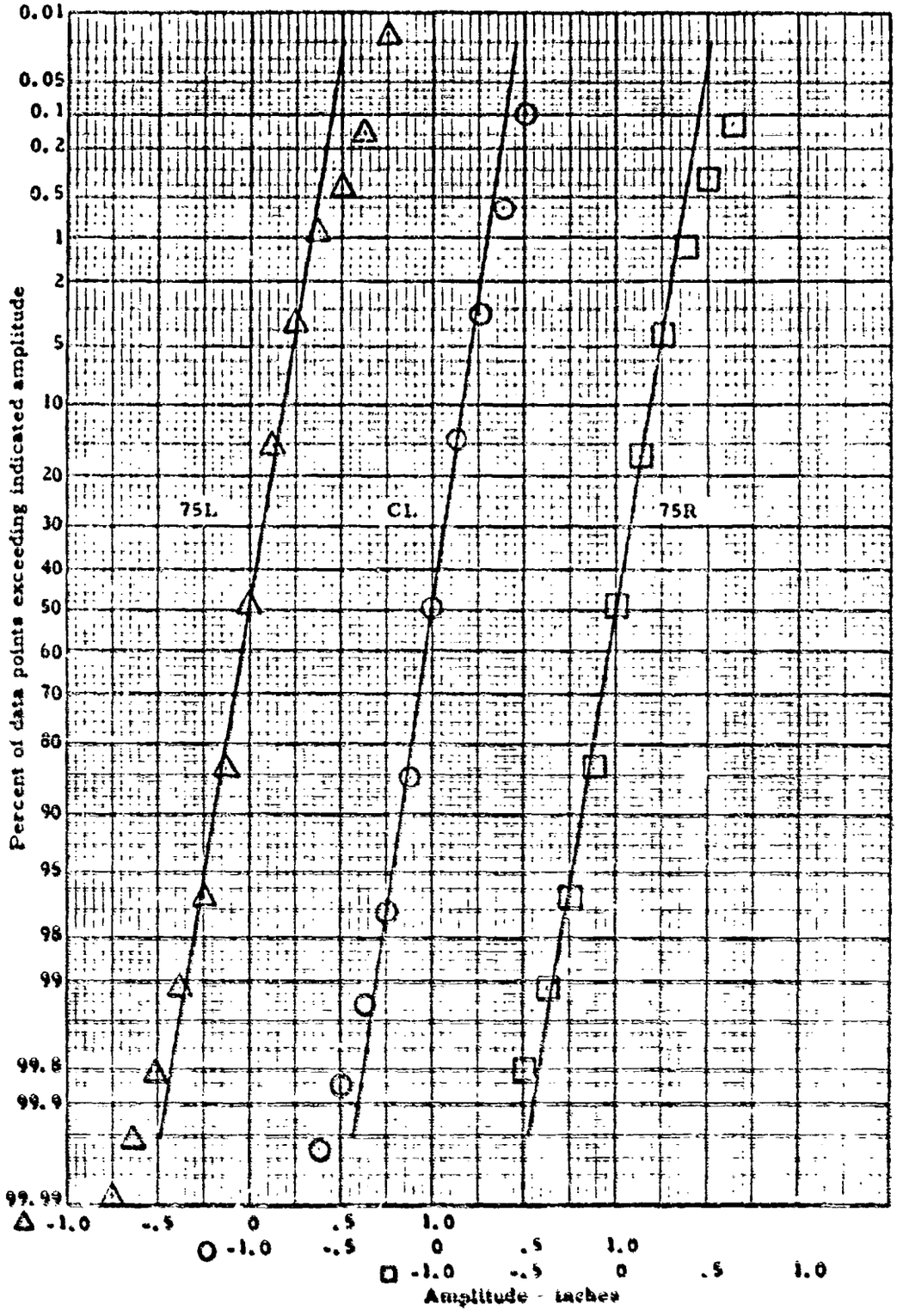

Figure 104 Cumulative Distribution of Amplitudes from Edwards Filtered at 100 ft

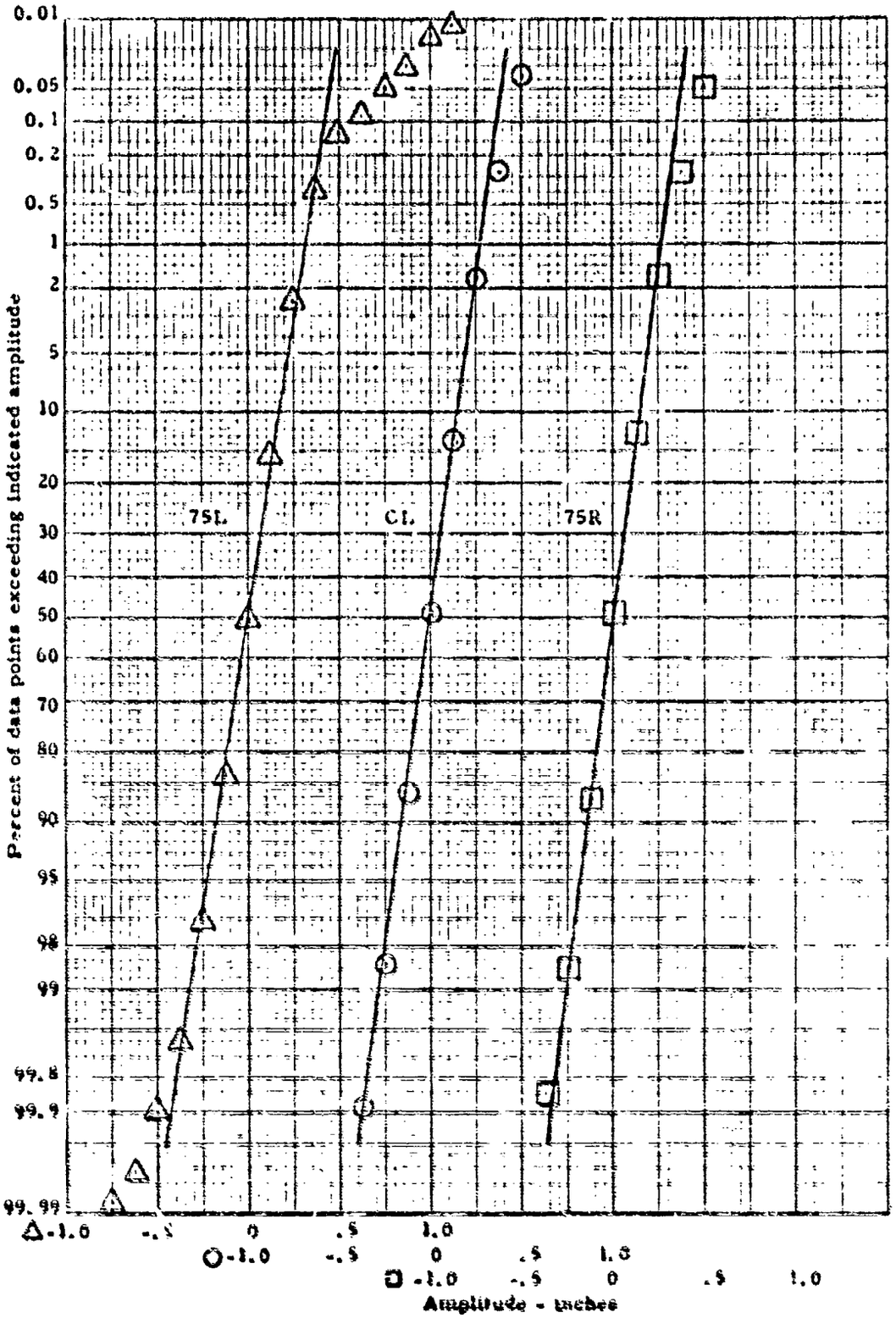

Figure 108 Cumulative Distribution of Amplitudes from Castle Filtered at 100 ft

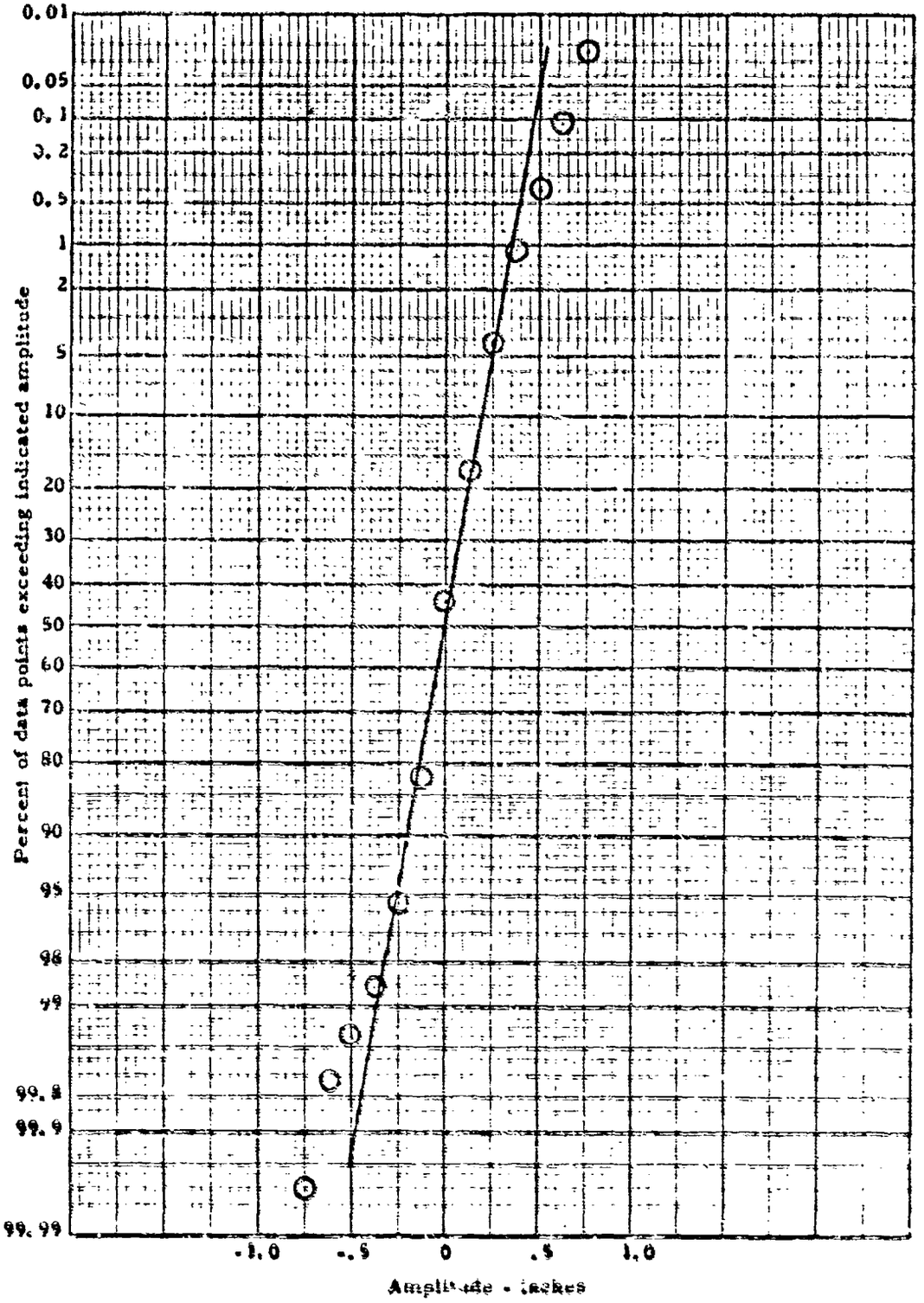

Figure 106 Cumulative Distribution of Amplitudes from Ellsworth Filtered at 100 ft

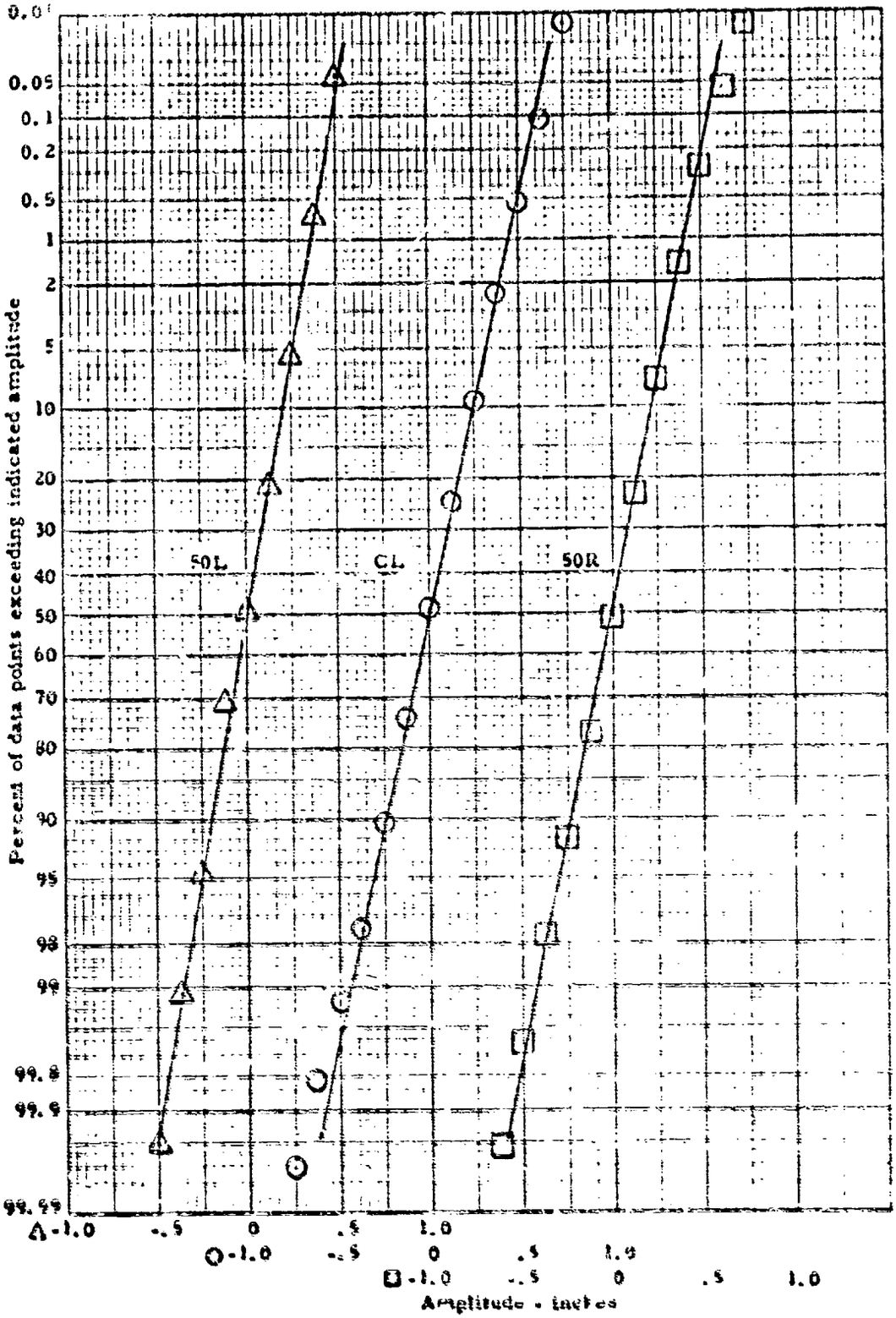

Figure 107 Cumulative Distribution of Amplitudes from George Filtered at 100 ft

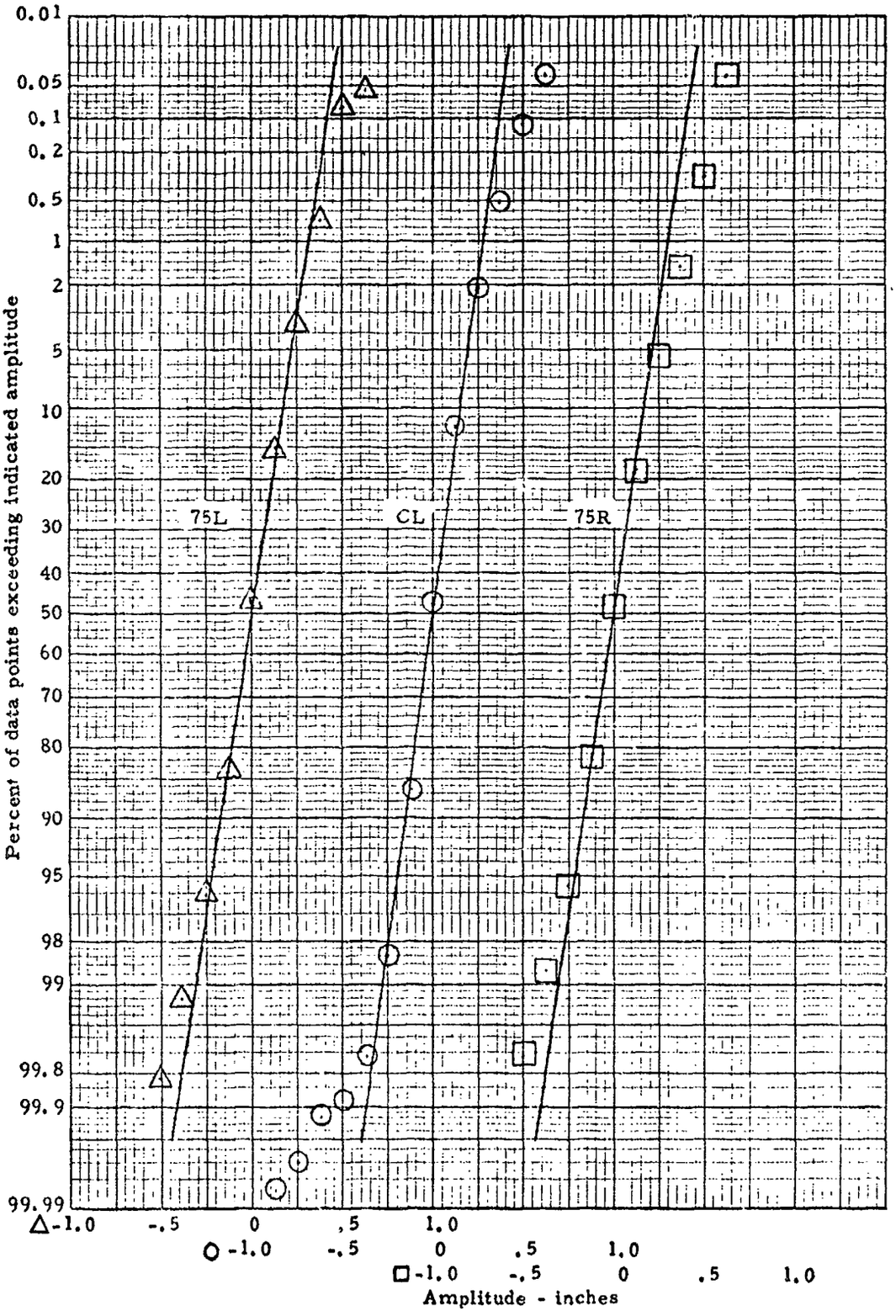

Figure 108 Cumulative Distribution of Amplitudes from Glasgow Filtered at 100 ft

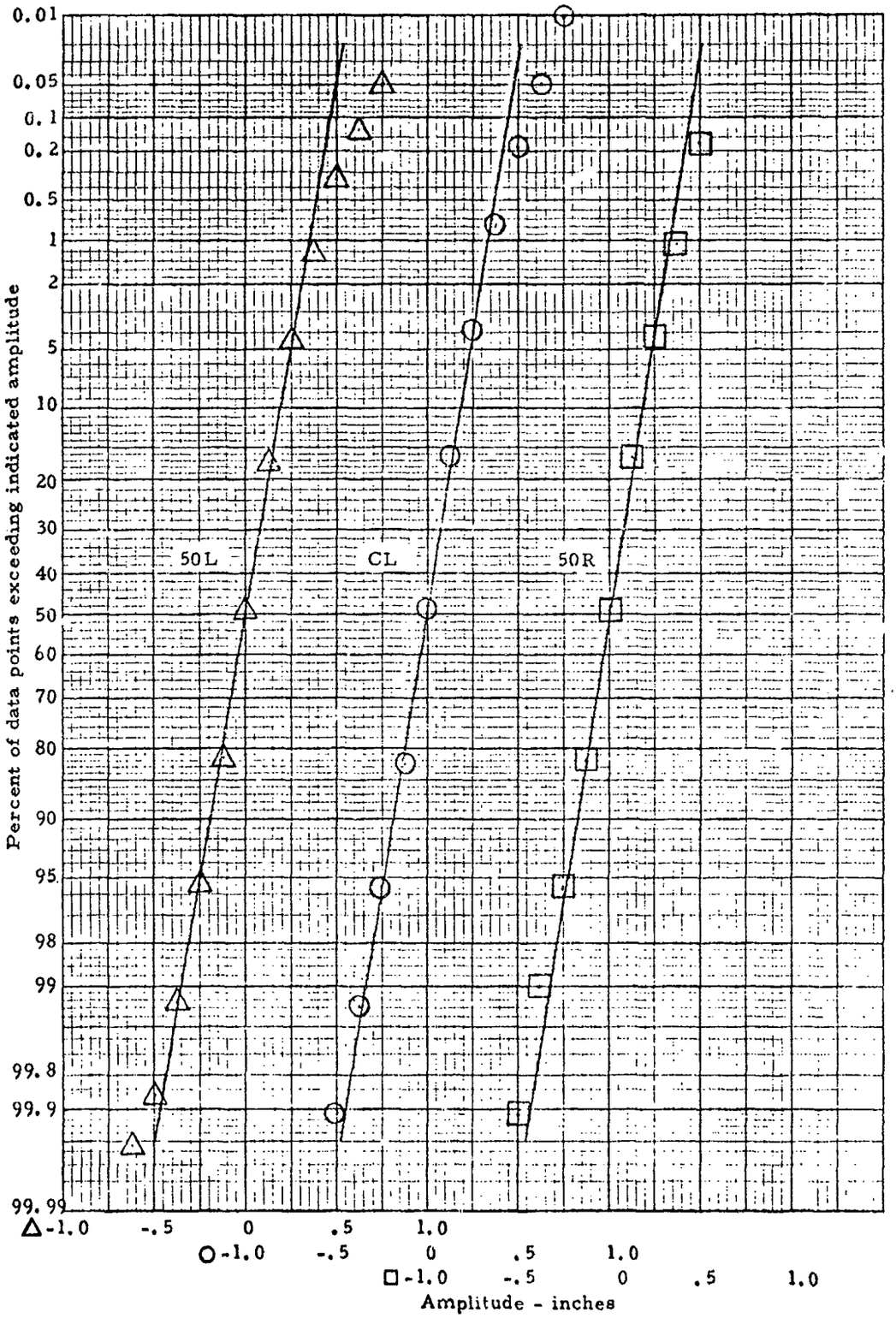

Figure 109 Cumulative Distribution of Amplitudes from Langley Filtered at 100 ft

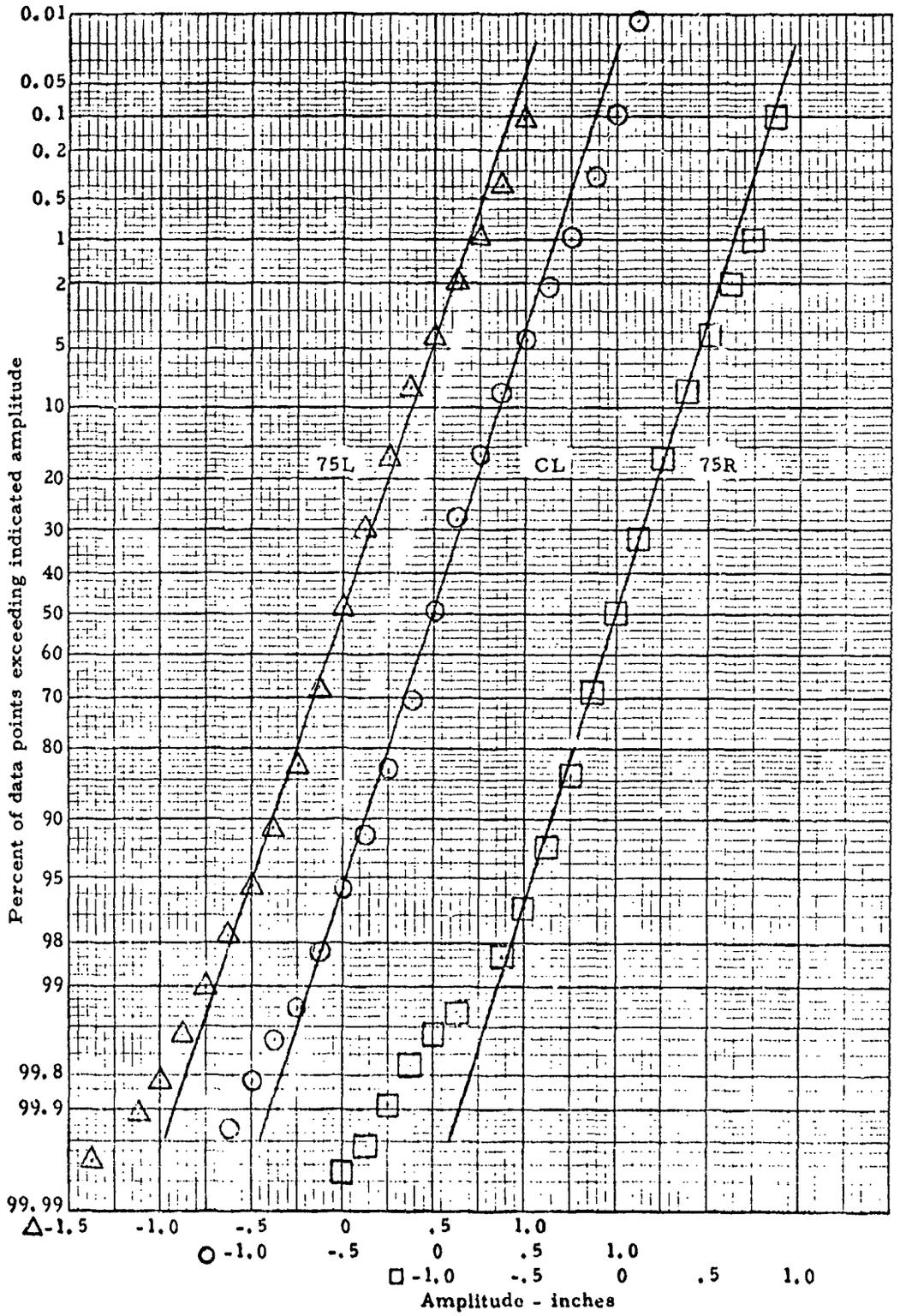

Figure 110 Cumulative Distribution of Amplitudes from McGuire Filtered at 100 ft

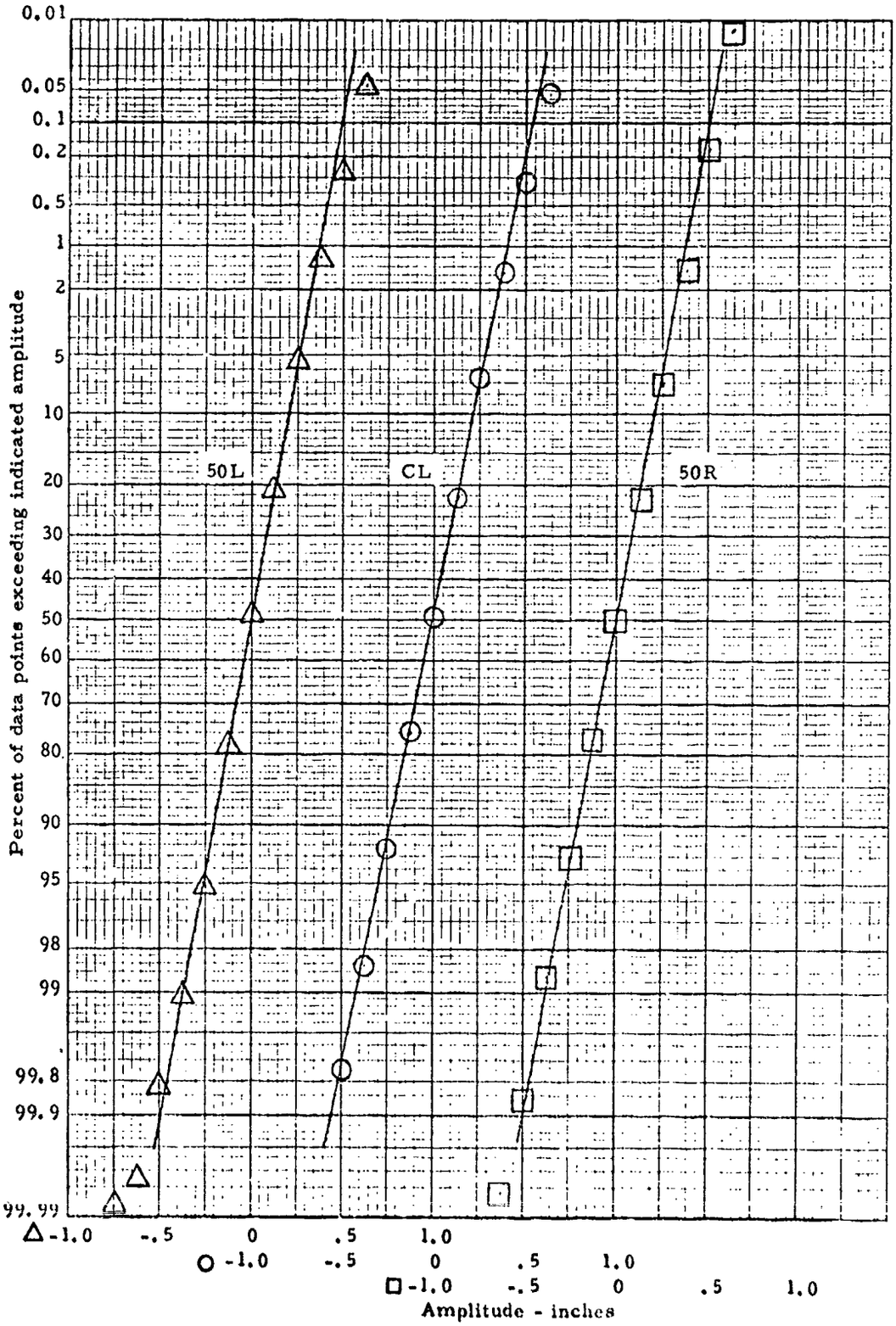

Figure 111 Cumulative Distribution of Amplitudes from Palmdale Filtered at 100 ft

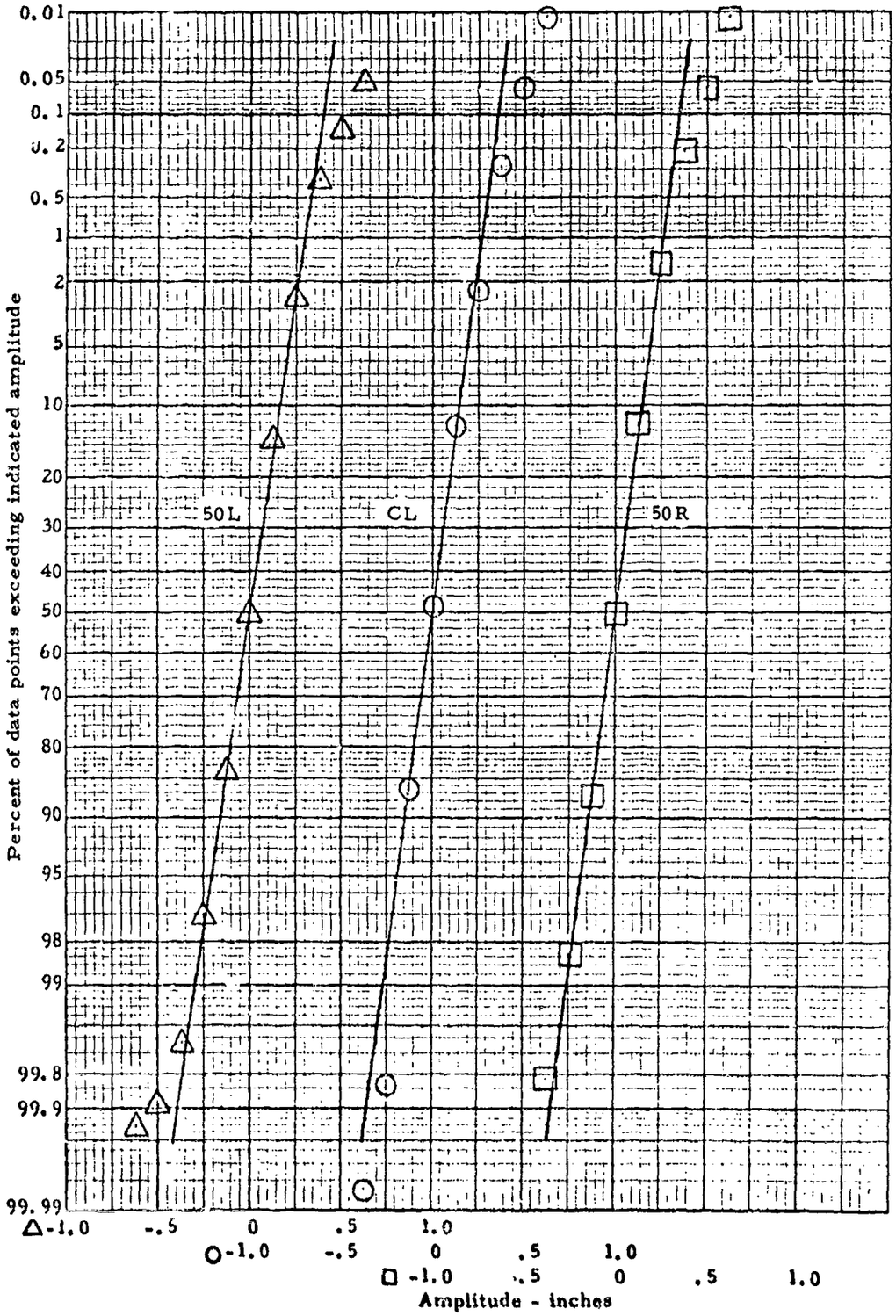

Figure 112 Cumulative Distribution of Amplitudes from Shaw Filtered at 100 ft

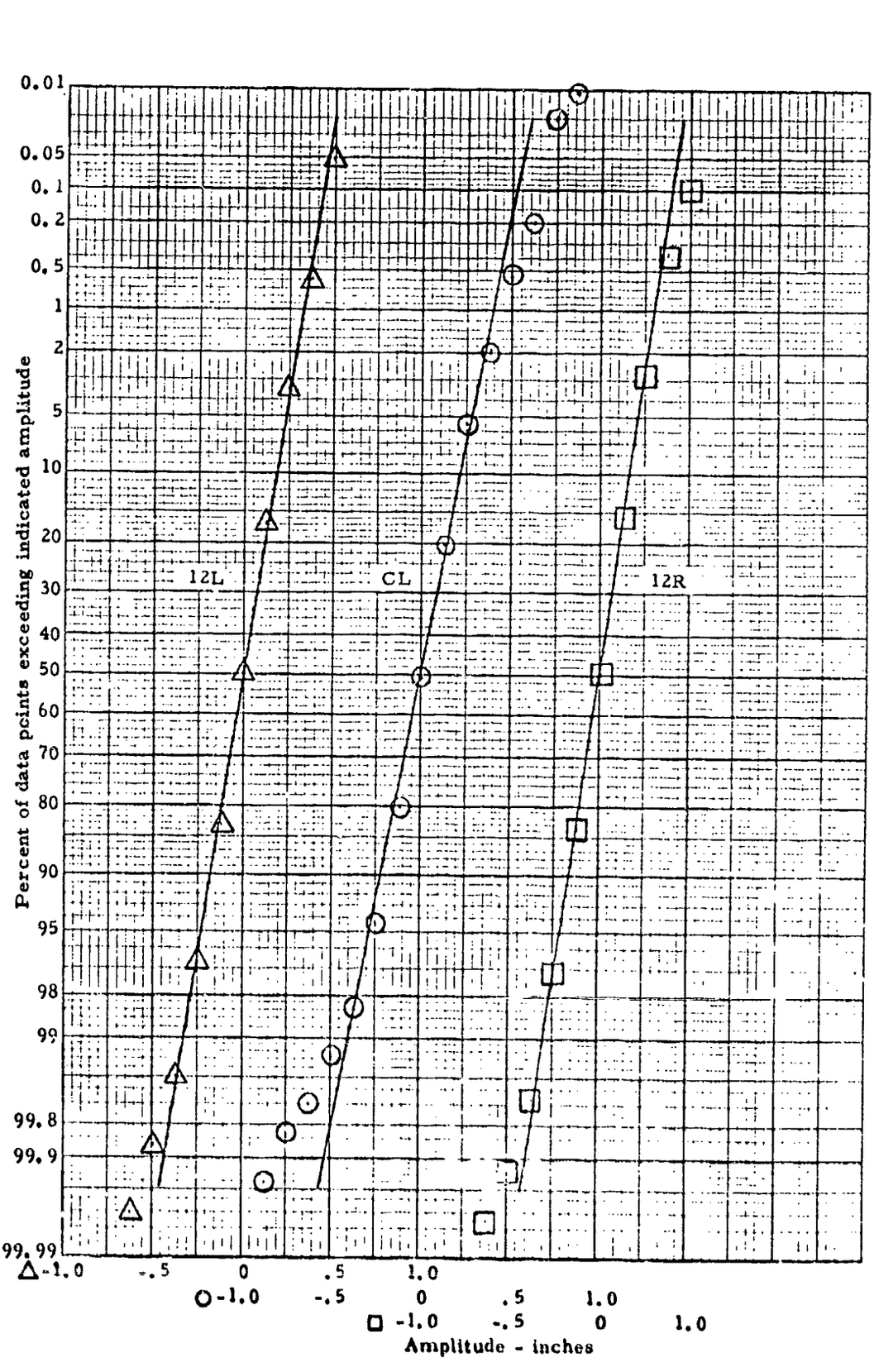

Figure 113 Cumulative Distribution of Amplitudes from Torrejon Filtered at 100 ft

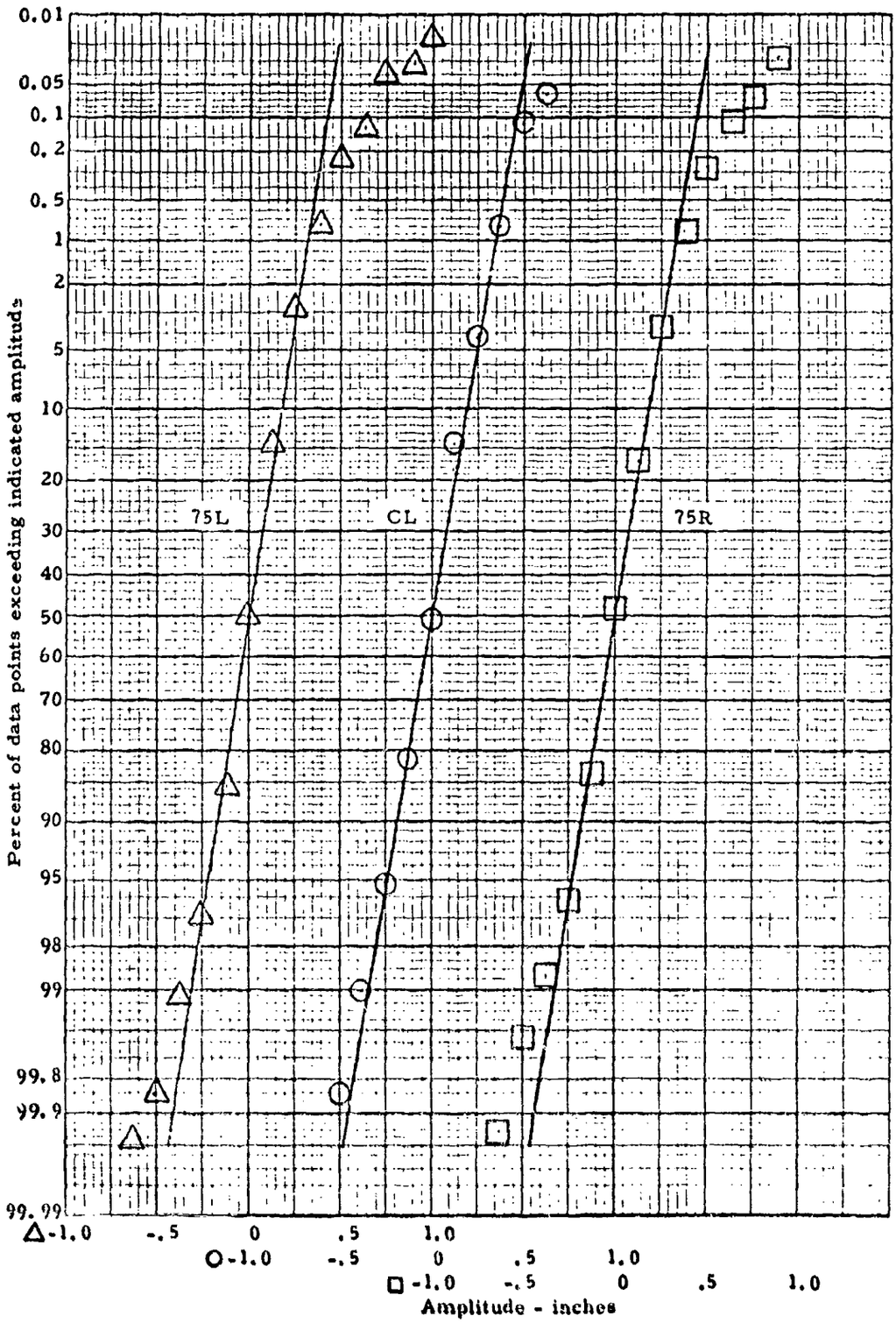

Figure 114 Cumulative Distribution of Amplitudes from Travis Filtered at 100 ft

APPENDIX VI

RMS HISTORIES FOR ALL LINES OF DATA FILTERED AT 100 FEET

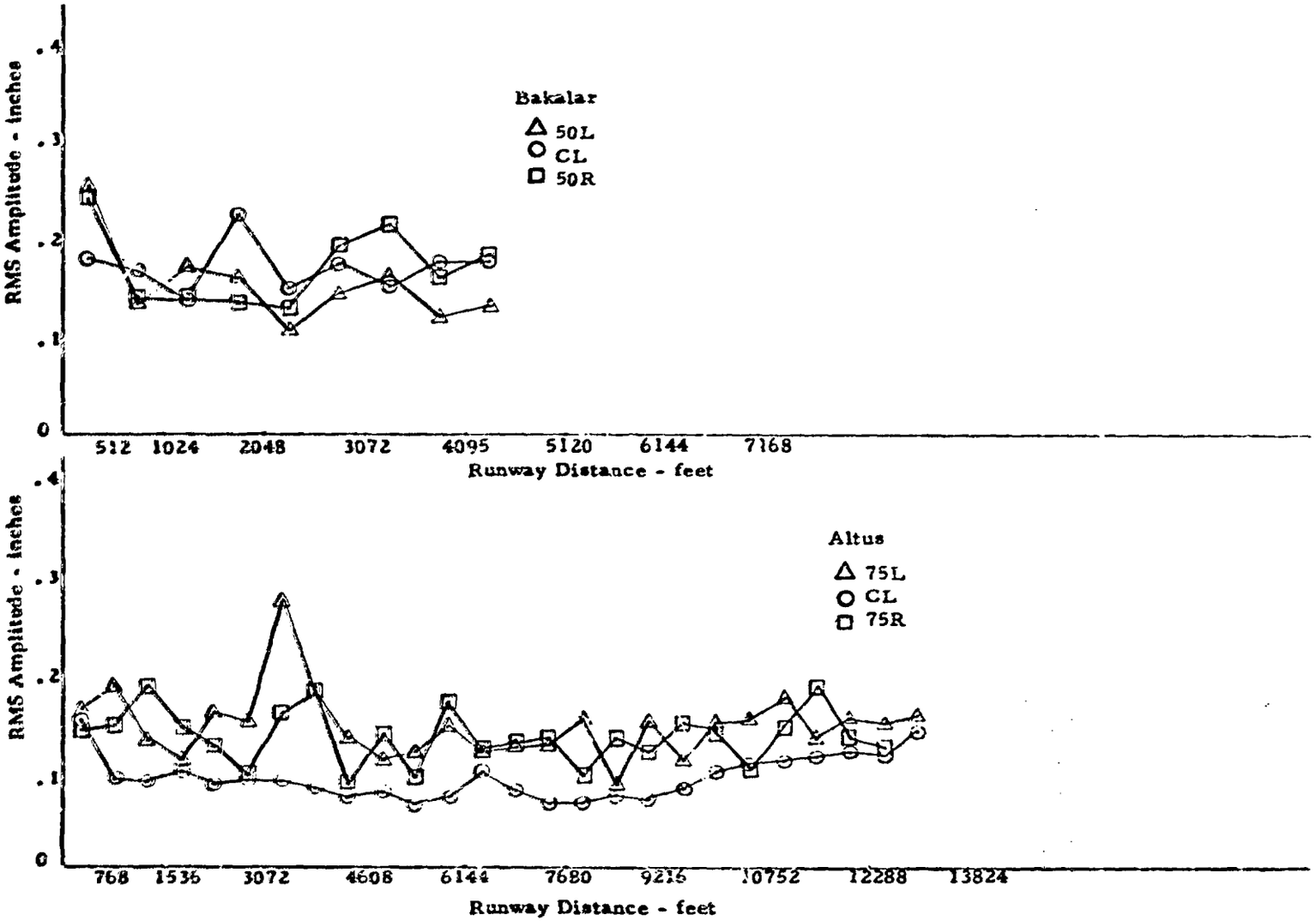

Figure 115 RMS Histories for Altus and Bakalar Filtered at 100 ft

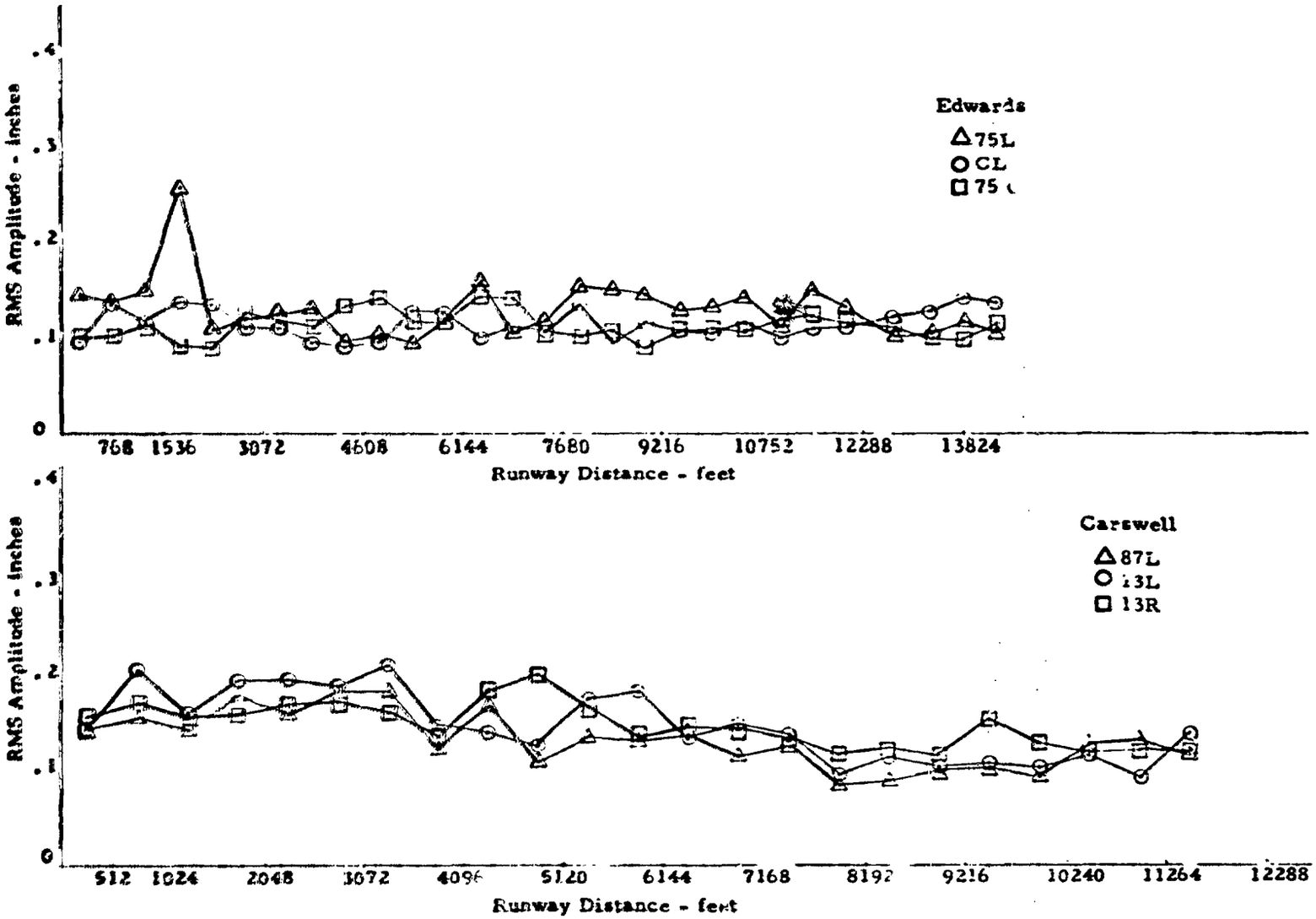

Figure 11. RMS Histories for Carswell and Edwards Filtered at 100 ft

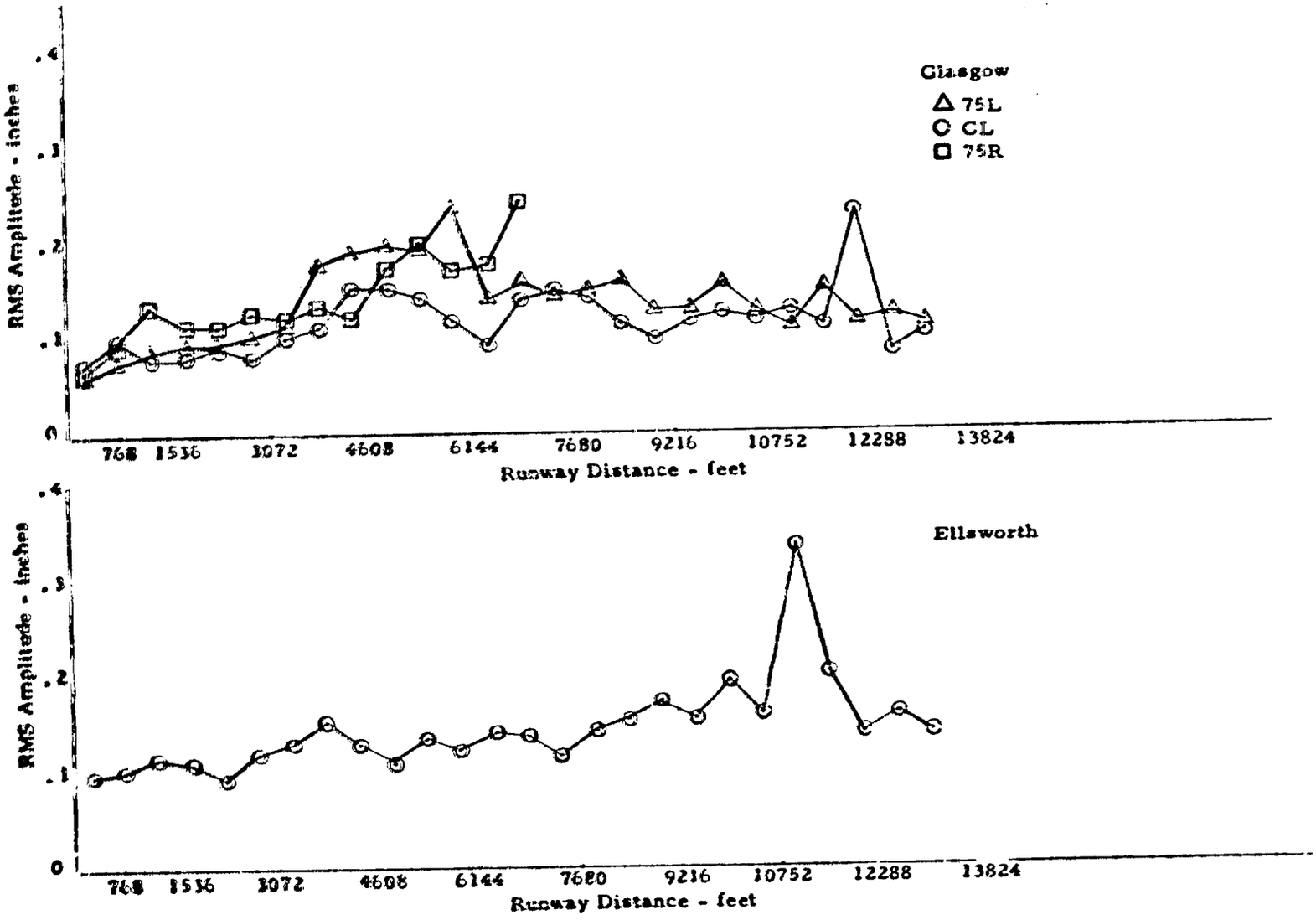

Figure 117 RMS Histories for Ellsworth and Glasgow Filtered at 100 ft

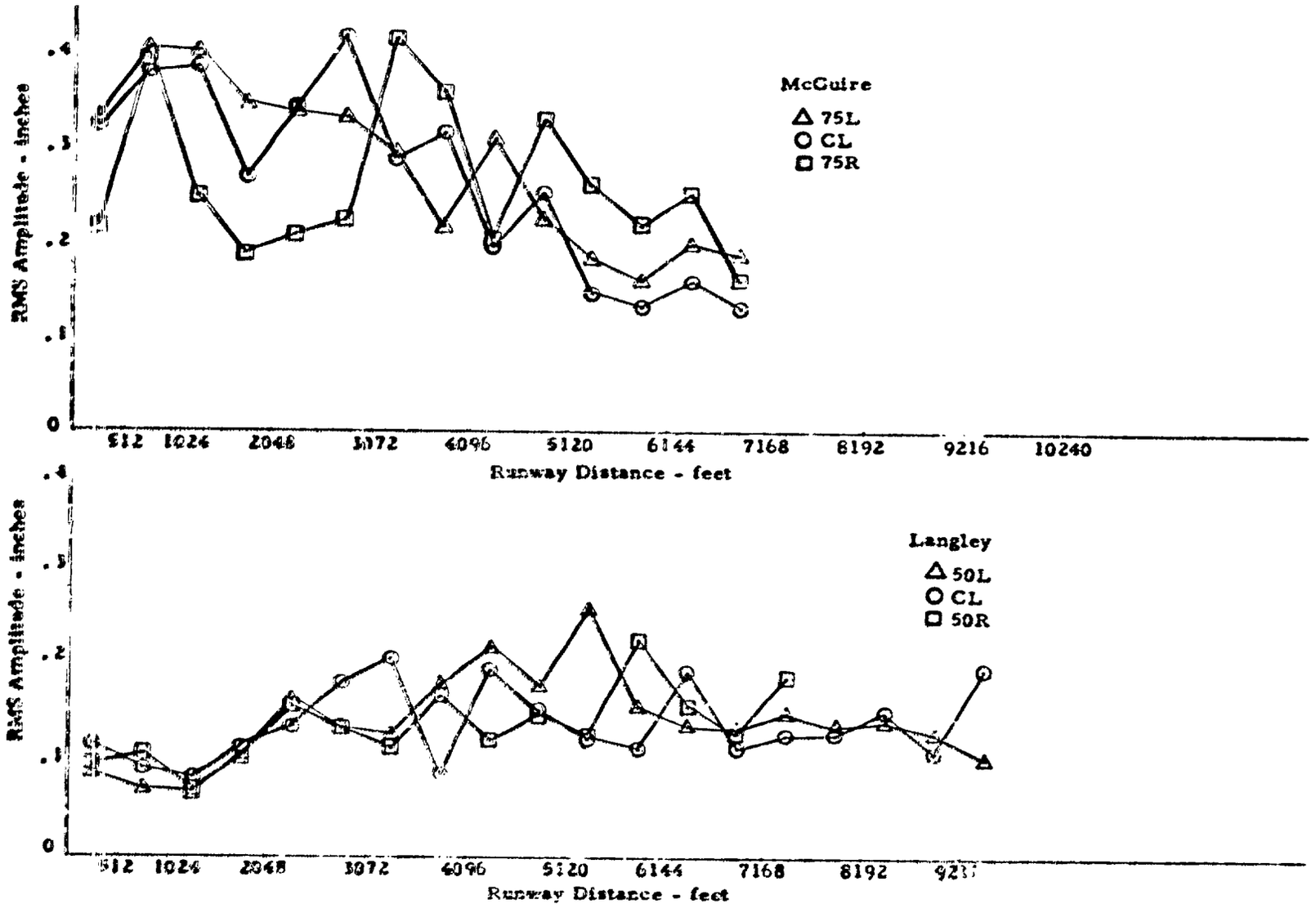

Figure 11[illegible] RMS Histories for Langley and McGuire Filtered at [illegible]

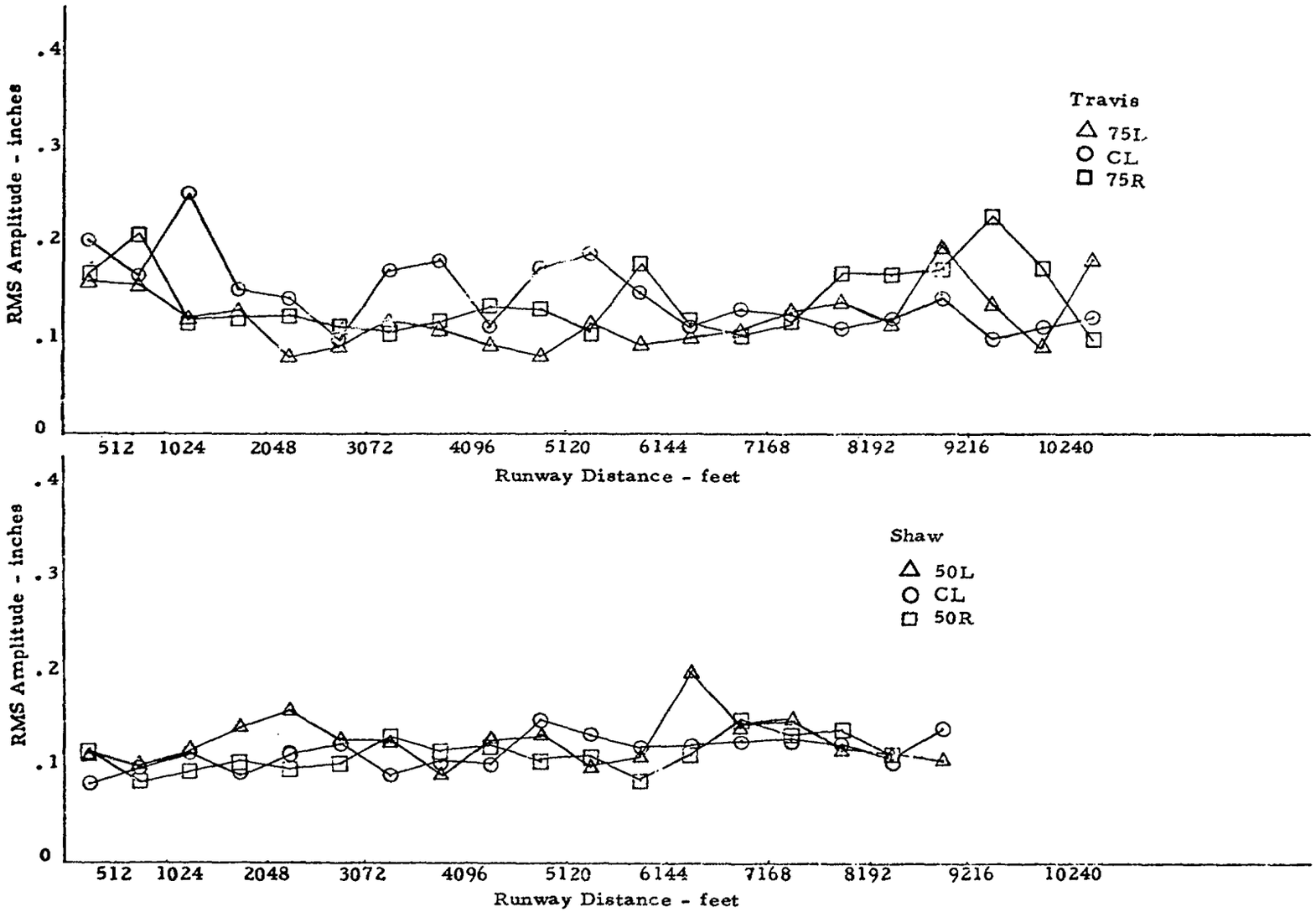

Figure 119 RMS Histories for Shaw and Travis Filtered at 100 ft

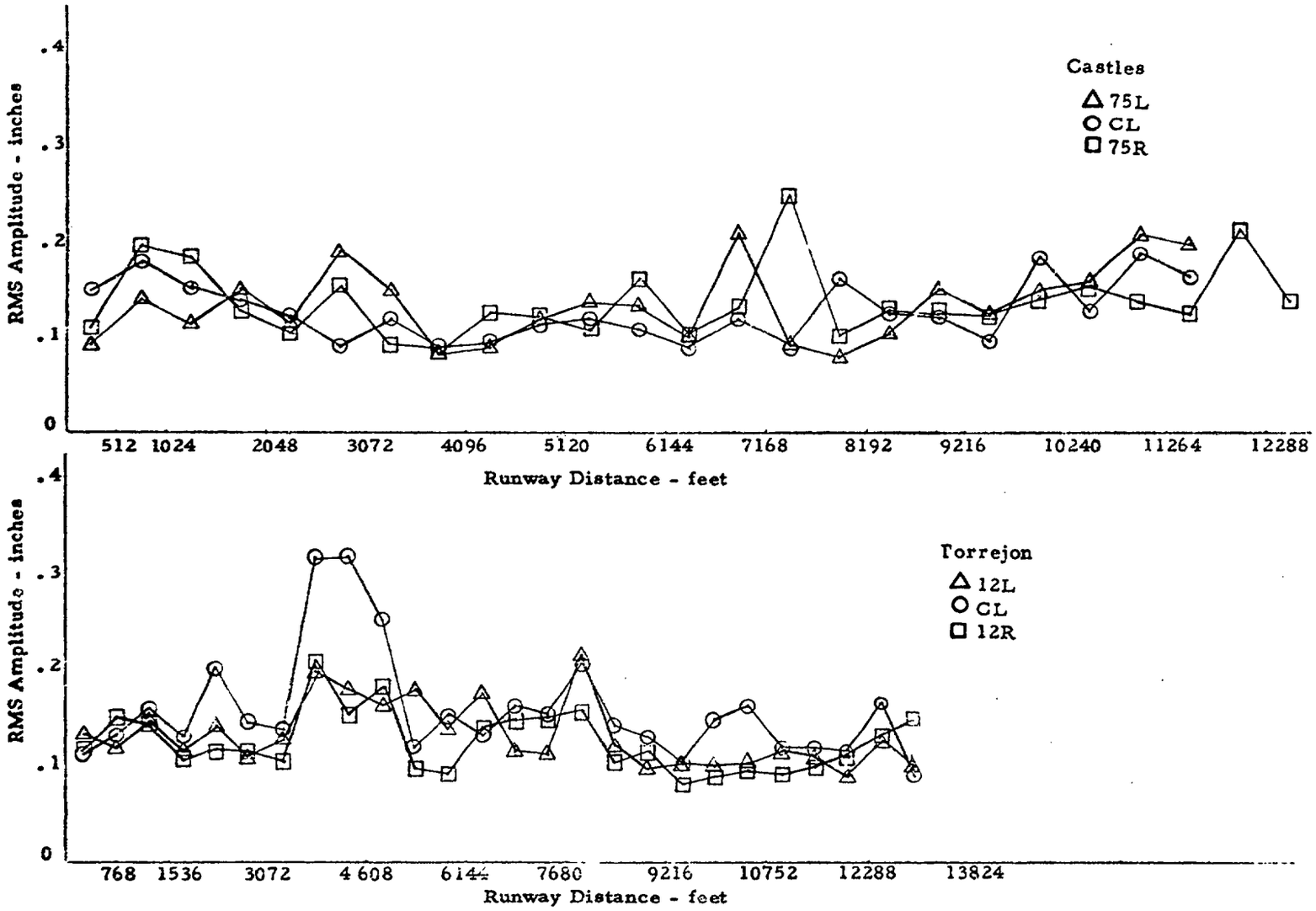

Figure 120 RMS Histories for Torrejon and Castles Filtered at 100 ft

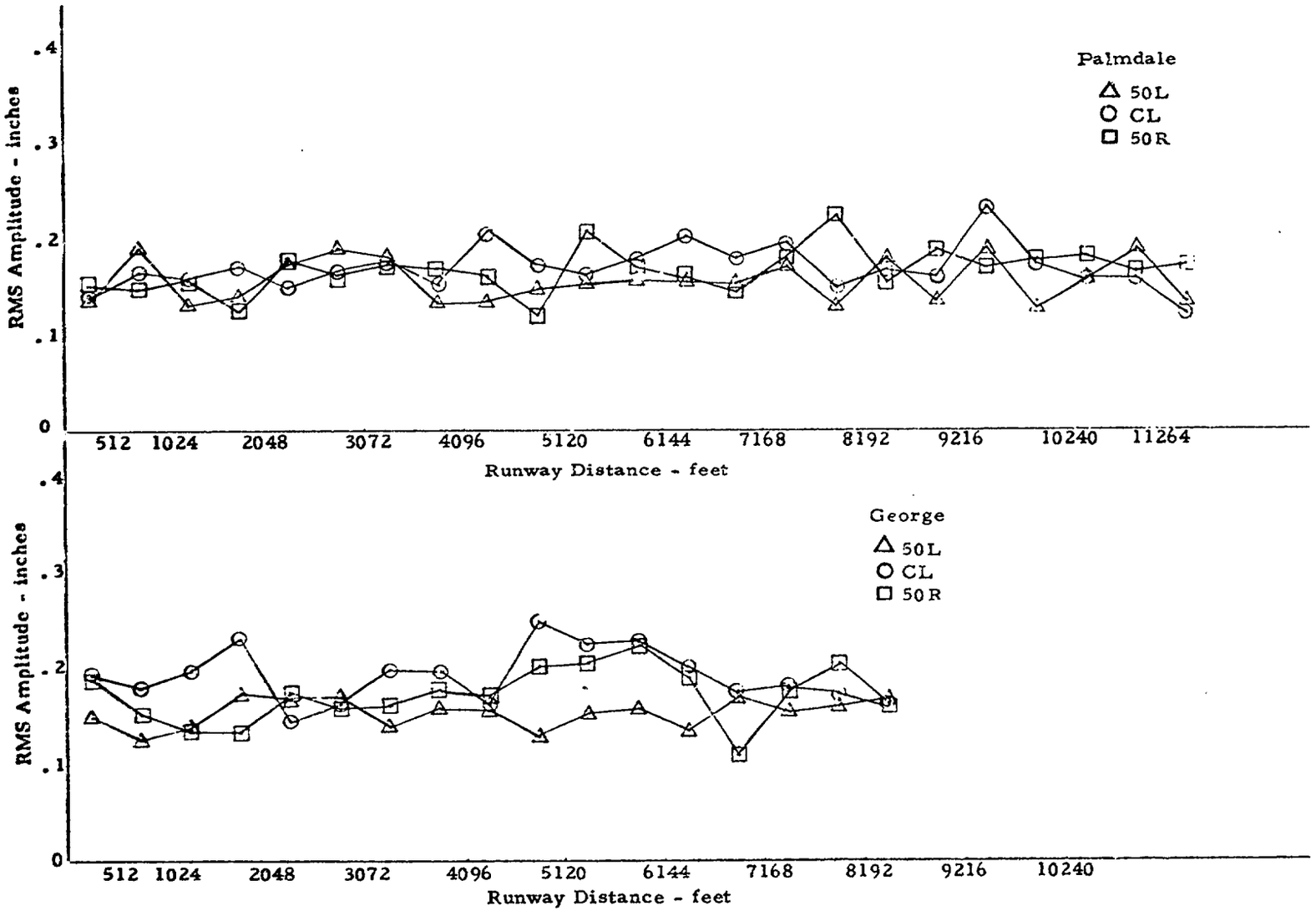

Figure 121 RMS Histories for George and Palmdale Filtered at 100 ft

REFERENCES

1. Turner, D. F., Automatic Runway Profile Measuring Instrumentation and Runway Properties, Part III, Base Surveys, WADD-TR-60-470, Part III, July 1963.

2. Shinozulsa, Masanobu, Monte Carlo Solution of Structural Dynamics, Computers and Structures, Vol. 2, pp. 855-874, Pergamon Press, 1972.

3. Martin, M. A., Digital Filters for Data Processing, G. E. Technical Information Series, 62SD484, October 1962.

4. Graham, R. J., Determination and Analysis of Numerical Smoothing Weights, NASA TR T-179, 1963.

UNCLASSIFIED

Security Classification

DOCUMENT CONTROL DATA - R & D

(Security classification of title, body of abstract and indexing annotation must be entered when the overall report is classified)

1. ORIGINATING ACTIVITY *(Corporate author)*
Air Force Flight Dynamics Laboratory
Air Force Systems Command
Wright-Patterson Air Force Base, Ohio 45433

2a. REPORT SECURITY CLASSIFICATION
UNCLASSIFIED

2b. GROUP

3. REPORT TITLE
ANALYSIS FOR THE DETERMINATION OF SIGNIFICANT CHARACTERISTICS OF RUNWAY ROUGHNESS

4. DESCRIPTIVE NOTES *(Type of report and inclusive dates)*
TECHNICAL REPORT

5. AUTHOR(S) *(First name, middle initial, last name)*
ALAN P. BERENS and RONALD K. NEWMAN

6. REPORT DATE	7a. TOTAL NO. OF PAGES	7b. NO. OF REFS
November 1973	206	4

8a. CONTRACT OR GRANT NO.	9a. ORIGINATOR'S REPORT NUMBER(S)
Contract F33615-72-C-1346	AFFDL-TR-73-109
b. PROJECT NO. 1370	
c. Task 137003	9b. OTHER REPORT NO(S) *(Any other numbers that may be assigned this report)*
d.	

10. DISTRIBUTION STATEMENT
Distribution limited to U.S. Government agencies only; test and evaluation; statement applied August 1973. Other requests for this document must be referred to Air Force Flight Dynamics Laboratory (FY), Wright-Patterson AFB, Ohio 45433.

11. SUPPLEMENTARY NOTES	12. SPONSORING MILITARY ACTIVITY
	Air Force Flight Dynamics Laboratory Wright-Patterson AFB, Ohio 45433

13. ABSTRACT

To determine and evaluate significant characteristics of runway roughness, 40 runway elevation profiles from 14 runways were analyzed. Grade effects were removed by high-pass filtering at a maximum cutoff wavelength of 500 ft and the resulting profiles were shown to be both nonstationary and nongaussian. Since nonstationarity was caused by the long wavelength undulations, the profiles were again filtered at a maximum cutoff wavelength of 100 ft. These short wavelength profiles are shown to be sufficiently stationary for a compound characterization. The short wavelength components are modeled in the frequency domain while the long wavelength components are modeled by the distribution of relative maxima and minima per 1000 ft and the joint distribution of wavelength and amplitude of the maxima and minima. A method is presented for generating a simulated runway which has the characteristics of the real profiles used in the analysis.

DD FORM 1 NOV 1473

UNCLASSIFIED

Security Classification

14. KEY WORDS	LINK A		LINK B		LINK C	
	ROLE	WT	ROLE	WT	ROLE	WT
Concrete runways						
Runway pr files						
Surface properties						
Roughness						
Statistical properties						
Simulated runways						

U.S. Government Printing Office: 1973 — 758-430/346